ABSTRACT

Title of Document: ECOLOGICALLY INSPIRED DESIGN OF GREEN ROOF RETROFIT

Laura M. Schumann, Master of Science, 2007

Directed By: Associate Professor David Tilley, Department of Environmental Science and Technology

Green roofs are becoming popular in the United States for their runoff and energy reduction abilities. However, current designs have high installation costs, heavy load-bearing requirements, and restrictions to low-sloped roofs. We designed a novel retrofit technology, the *green cloak*, which uses fast-growing vine species and a trellis to suspend vegetation above a roof. We conducted field experiments, prototype testing, and mathematical modeling to determine the effect of the green cloak on stormwater runoff and indoor summertime building temperature reduction. We assessed energy and monetary cost-benefits. The green cloak reduced July indoor building temperature by 11.3°C which saved 73% of cooling energy costs. The green cloak delayed the peak storm runoff from a 0.15mm/min storm by 100 minutes. The green cloak costs 38% less than a green roof. The green cloak demonstrated great potential for mitigating runoff impacts of impervious surfaces, reducing summer temperatures of buildings, and creating urban greenery.

ECOLOGICALLY INSPIRED DESIGN OF GREEN ROOF RETROFIT

By

Laura M. Schumann

Thesis submitted to the Faculty of the Graduate School of the
University of Maryland, College Park, in partial fulfillment
of the requirements for the degree of
Master of Science
2007

Advisory Committee:
Associate Professor David Tilley, Chair
Michael Furbish
Associate Professor Patrick Kangas

Dedication

I would like to dedicate this thesis to my friends and family, particularly to those that have passed on teaching me to embrace and value life's precious opportunities with open eyes, energy, and creative thoughts.

Acknowledgements

I would like to thank my committee, Michael Furbish, Dr. Patrick Kangas, and Dr. David Tilley, for their everlasting guidance, encouragement, and excitement for this project.

I'd also like to thank the guys in the ENST Project Development Center, the folks at the University of Maryland Research Greenhouse Complex, Undergraduate Research Assistants Vera Jaffe and Alex Macleod, and my brother Andrew Schumann for making it all happen.

Table of Contents

Chapter 1: Introduction

Problem Statement

Both global and local environmental problems arise as land is rapidly developed for industry, government, and homes. Along with global climate change, unfortunate local effects include resource depletion, increased waste generation, and the creation of urban heat islands (Wong, 2002). Specifically, as land is cleared for the construction of new buildings, cities no longer dissipate heat through evapotranspiration like their forested counterparts. Differences in temperatures could be as high as 15 ºC between a dense urban area and its cool rural surroundings (Ferrante and Mihalakakou, 2001).

To avoid the ecological drawbacks of land development, smart urban planning techniques are created to promote the use of energy conscious natural and passive structures, increase permeable surfaces, and use plants to absorb excess carbon dioxide. Specifically, the abilities of natural ecosystems are recognized as being important tools of man. The use of ecosystems to solve man's problems also helps to promote green space in urban areas leading to less harmful environmental impact. Habitat is created or conserved. Additionally, by using ecosystems over conventionally engineered systems, money can be saved with naturally occurring ecosystem services rather than machines that require electricity and maintenance.

To enhance the beauty of a building and to provide energy savings, passive solar architecture, strategic placement of trees in the landscape, façade greening, and green roofs are examples of eco-friendly practices. Passive solar houses are built with south facing overhangs that shade out the high summer sun, but capture the low winter sun's energy.

Landscape managers can retain large shade trees and plant young trees to keep building temperatures cool, but to also moderate urban temperatures and prevent environmental degradation (Ferrante and Mihalakakou, 2001). Deciduous trees planted on the south side of a building provide shade during the summer while allowing warming solar energy in the winter after leaves have fallen. Landscapers plant coniferous trees on the north side of buildings to block out frigid winter winds.

On sites where there is not enough space for trees, landscapers may cover building walls with vines. Called façade greening, this practice first showed extensive popularity in the early 20th century during the Art Nouveau movement in Germany and the arts-and-crafts movement in the United States (Dunnett and Kingsbury, 2004). Today, the destructive effects of vines on building materials are avoided by the use of a trellis system to hold climbers away from the surface. Greenscreen, a California based landscape supply company, sells sturdy metal mesh in several prefabricated sizes and shapes so that it can be used on any building front (Greenscreen, 2007). A variety of vine species are grown on the forms both enhancing the aesthetics of the building and providing insulating effects.

Architects also use green roofs to provide habitat, runoff reduction, and insulation on the top of a building. Green roofs are simply vegetated roof tops that have shown high success in Europe, specifically in Germany where it is estimated that 10% of flat roofs are green (Rowe, 2007). Green roofs are slowly becoming popular in many American cities, such as Chicago, IL, Baltimore, MD, Portland, OR, and Washington, DC. The designs of green roofs vary with many different plant varieties; some even have wetland vegetation.

There are two types of green roofs: intensive and extensive. Intensive green roofs have a thick soil layer which is usually greater than 30 cm. The rooftop system is comprised of engineered materials layered one on top of another with each layer serving a specific duty in the successful implementation of the green roof. Starting at the roof, the layers include structural support, a waterproofing membrane to prevent building leaks, insulation to keep cool (or warm) air inside the building, drainage cups to provide aeration, water, and a barrier to roots, an engineered growing medium specified by vegetation requirements, and lastly vegetation which may include small trees, bushes, perennials, or succulents. When larger plants are used in the green roof, they are often termed “intensive” green roofs due to the increased substrate depth required by the larger plants. Since these deep green roofs require more structural support for the larger plants and increased substrate load, people are also supported and are able to congregate on decks or patios.

“Extensive” green roofs have soil layers which are only a few centimeters thick. Hardy succulents, which grow horizontally, rather than vertically, are planted on these surfaces. Succulents are able to withstand both drought and high rainfall. Extensive green roofs are designed only for occasional maintenance foot traffic (Bengtsson et al. 2005).

Green Roof Benefits

Whether they were called green roofs or not, vegetated roofs were common hundreds of years ago in wet climates as an additional way to insulate homes from cold weather. Today, green roofs are viewed as ways to primarily control stormwater runoff, to moderate indoor building temperature, to enhance the aesthetics of buildings, and as a method to extend the life of expensive conventional roofs. On a city scale, green roofs help to limit the intensity of the urban heat island, add green space to concrete urban environments, and increase natural habitats (Bengtsson et al. 2005).

Current Maryland land development law allows only 15-25% of land cover to be impervious (Owens, 1999). This limits the amount of total land surface for driveways, patios, and roof tops impermeable to rainwater. Green roofs, with pervious soil surfaces, function to limit (and delay) runoff to the surrounding environment (Figure 1). Additionally, plant evapotranspiration sends a large fraction of the rainfall back into the atmosphere as water vapor rather than over land surfaces as damaging runoff. Measured during a rain event of an average intensity of 0.22 mm/min, a 3 cm deep sedum-moss roof in southern Sweden had runoff values that were half of precipitation volumes (9 to 10 mm), showing that runoff volume was halved compared to a traditional impervious roof (Bengtsson et al. 2005).

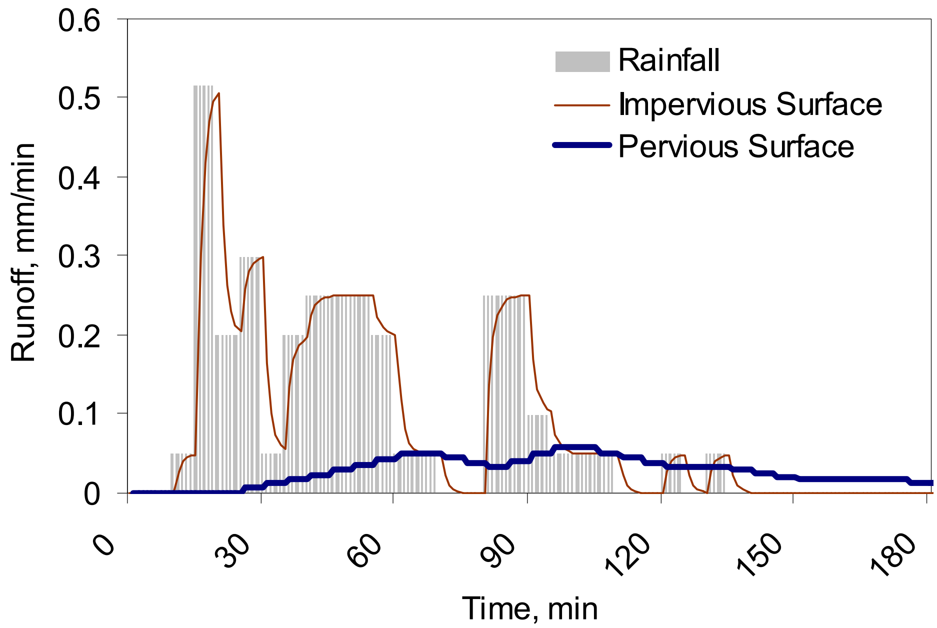

Figure 1. Hydrograph comparing delayed and reduced peak discharge of pervious surfaces compared to impervious surfaces.

To understand hydrologic function of green roofs, researchers compared both rainfall retention and the runoff intensity reduction of green roofs to traditional roofs. Based on rainfall depths of 1514 and 314 mm, Goldsboro and Raleigh, North Carolina green roofs retained 63 and 55% of rainfall, respectively. Runoff rates from the green roofs were 87 and 57% less than the actual rainfall intensity (36 and 44 mm/h) (Moran et al. 2005).

Green roofs are used to control the temperature of a building with the result of reducing heating and cooling energy costs. In summer months, green roofs shade the building's roof from solar radiation. In winter months, green roofs provide an extra layer of insulation to the building's roofing system. A computer simulation program has been used to examine the indoor air temperatures of buildings with and without green roofs during both the summer and winter. For example, in July at 3:00 pm, indoor air temperature was reduced by at least 10 ºC in a building with a green roof compared to a building with a traditional non-vegetated roof (Ferrante and Mihalakakou, 2001). A similar test was run in January at 2:00 pm. This time the indoor air temperature of a building with a green roof was approximately 1 ºC warmer than a building with a traditional roof (Ferrante and Mihalakakou, 2001). These results suggested that green roofs may work better in the summer to shade buildings than in the winter to insulate them.

Wong et al. (2002) conducted a field study to understand the thermal properties of a green roof located in Singapore. He found a maximum roof surface temperature reduction of 30 ºC compared to the surface temperature of a traditional roof. Temperature reduction varied with plant type and density. Leaf area index (LAI), a ratio of leaf area to ground area, was used to quantify these differences. Wong recommended denser plants, like trees and shrubs, for lower indoor temperatures but warned about since they require more soil and thus a stronger roof (Wong et al. 2002). The planted roof showed less heat transfer than the traditional roof and the soil-only roof (Wong et al. 2002).

Since green roofs are more expensive to install than traditional roofs, Wong et al. (2003) conducted life cycle cost analyses to determine their benefit. In his study, green roof installation costs ranged from three to six times the cost of a conventional roof system, but a green roof system was projected to outlive traditional roofs three-fold. Initial costs, maintenance and replacement costs, service life, inflation rates, discount rates, structural costs, and energy costs were all considered. Wong et al. (2003) found that green roofs saved \$4,773 per year, which during its lifetime would save \$190,936 (Wong et al. 2003).

Green Roof Limitations

The widespread use of green roofs is limited by high installation costs, extra structural load requirements, and low applicability to most roof slopes which are at high angles. In addition, green roofs may add nutrients to the environment. Green roofs are an excellent way to save money on summer energy costs and to lengthen the lifetime of expensive roofing replacements, but in the short term, they are costly. Installation of conventional roofs costs between \$43 and \$91/m^2 (\$4 and \$8.50/ft^2) while extensive green roofs cost between \$108 and \$215/m^2 (\$10 to \$20/ft^2) (Dunnett and Kingsbury, 2004).

Around the world, each political boundary has its own building codes that dictate the minimum load bearing of the roof. The code will take into consideration both the dead load (i.e., roofing materials) and the live load (e.g., snow and ice accumulation). For green roofs to be applicable on existing buildings, their load must be equal or less than the roof's dead load maximum. In Ontario, Canada, for instance, roofs are built to sustain loads of 195 kg/m^2. This allows for 107 kg/m^2 of snow (liveload), and 88 kg/m^2 for roofing materials (deadload) (Dunnett and Kingsbury, 2004). Typical loadings of the lighter extensive green roof range from 80 to 150 kg/m^2, meaning many extensive retrofits are not possible without expensive roof support added to the building by a structural engineer (Dunnett and Kingsbury, 2004).

In one study along the Mediterranean, the soil layer, which is often thought of as an important insulating property, showed no significant affect on the green roof's ability to cool. Also, insulation, such as root and leak barriers were found to be a drawback in the modeled green roof's summer performance as they limited hot interior air to escape through the roof to the cooler canopy area (Theodosiou, 2003).

Roof slope can also be a problem for retrofit projects. Flat roofs are not ideal for green roofs because it requires an additional drainage layer to remove water from the root zone. Roof slopes ranging from 5 degrees (1:12) and 20 degrees (4:12) work best to naturally drain water via gravity. Roofs with slopes greater than 20 degrees require wooden lath grids to hold squares of soil substrate in place until a thick vegetative mat forms (Scholz-Barth, 2001).

It is still uncertain whether or not green roofs improve or degrade local runoff water quality. Nutrients leaching from the rooftop soil to the environment must be further explored. In one study, total nitrogen concentration was higher in green roof runoff than on traditional roof top runoff (Moran, 2005).

Green Cloak Design and Justification

We designed the green cloak to overcome many of the limitations identified for extensive green roof designs. First, the green cloak was lightweight and designed to not necessarily add any load to the building's roof. Second, it was designed to maximize vegetated cover to minimize the solar-forced heat load. Third, the design was less expensive to install than extensive green roofs. Fourth, the green cloak could be used for buildings with flat or highly sloped roofs. Fifth, green cloaks did not require the roof to be covered in soil-media, which decreased the need for man-made materials and the chances of emitting nutrients into receiving waters.

Our green cloak design consisted of a vine canopy suspended above the roof surface on a lightweight trellis system (Figure 2). During our experiments we placed the canopy approximately 20 cm above the roof, but we believe a larger gap of as much as 200 cm would provide the same storm water and heat reduction benefits, while reducing the chances for the vines to attach to the roof surface.

(a)

(b)

Figure 2. Experimental green cloaks without scaled buildings underneath at (a) one month of growth and (b) seven months of growth.

Experimental Green Cloak Description

Experimental green cloaks were built by suspending a wire trellis from a frame made of ¾ inch polyvinyl chloride (PVC) tubing, which was contoured to form to the roof angle of scaled buildings we constructed (Figure 3). Two scaled wood-frame, plywood-covered buildings (1.75 m x 1.5 m x 1 m) with a door, three plexiglass windows, black asphalt shingles, and fiberglass insulation were built for the experiment (Figure 3). Over the course of a year, nine vine species were grown on eleven different trellis systems in the University of Maryland greenhouse. The species were: black-eyed Susan vine (*Thunbergia alata*), Chinese trumpet creeper (*Campsis grandiflora)*, cross vine (*Bignonia capreolata*), kudzu (*Pueraria lobata*), Japanese honeysuckle (*Lonicera japonica*), moonflower (*Ipomoea alba*), morning glory (*Ipomoea tricolor*), porcelain berry (*Ampelopsis brevipedunculata*), and Virginia creeper (*Parthenocissus quinquefolia*). Vines were grown in 8 liter (2-gallon) pots with organic potting soil (Sun Gro Horticulture, Bellevue, WA).

Figure 3. Scaled, wood-frame, plywood-covered model buildings used during heat and runoff experiments with the green cloak.

Objectives

Our objectives stemmed from our goal to develop a novel green roof design that could be applied to many existing building types, while reducing indoor building temperatures and slowing down storm runoff. Other design considerations included minimizing structural loads, installation costs, and maintenance costs. Our specific objectives were to:

1. Compare vine growth rates on our experimental green cloaks to that of a natural analog, which we defined as abandoned barns with extensive vine communities growing on their sides.

2. Determine the effect of the green cloak on indoor building temperatures considering various vine species and amounts of leaf surface area.
3. Develop a mathematical model of the green cloak's effect on indoor building temperature so effects on full-scale buildings can be predicted.
4. Determine the effect of the green cloak on stormwater runoff from a roof for various vine species and amounts of leaf surface area.
5. Develop a mathematical model of the green cloak's effect on stormwater runoff to predict its effect during various storms of various size and duration.
6. Determine the installation and maintenance costs for the green cloak and compare its energy and cost savings to those of a traditional extensive green roof.

Plan of Study

1. To understand vine growth characteristics, we observed vines growing on trellises at the University of Maryland Research Greenhouse Complex and vines growing naturally on rundown tobacco barns in Southern Maryland. We assumed the barn vine ecosystems to be mature vine ecosystems. We compared barn data to trellis data to determine optimum green cloak growth scenarios.
2. To determine the ability of the green cloak to moderate indoor air temperature, we conducted time-series studies under both simulated and real summertime conditions measuring indoor building temperatures of model houses with and without green cloaks.
3. To determine the temperature effects of the green cloak on indoor building temperature of a full scale building, we used data gathered from the temperature

moderation experiments as inputs in a mathematical model determining green cloak temperature moderation of an expected canopy leaf area index (gathered from the natural vine ecosystems mentioned in Objective 1).

4. To understand the ability of the green cloak to limit runoff quantity by leaf interception, we conducted an experiment using a rainfall simulator to measure the intensity of canopy throughfall compared to control roof runoff rates.

5. To understand the facility of the green cloak to moderate rainfall runoff under various storm and canopy density scenarios, we created a mathematical model predicting runoff reduction and retention for a cloak of reasonable LAI (also from Objective 1). Model results were compared to empirical extensive green roof data.

6. To quantify the economic benefits of the green cloak, we compared the cost of materials, installation, and maintenance to projected energy savings. Green cloak costs and benefits were compared to extensive green roof costs and benefits.

Chapter 2: Vine Growth on an Ecological Analog to the Green Cloak

Abstract

Designing and understanding the long-term behavior of ecologically engineered green roof covers, such as our green cloak, can be informed from natural vine communities. Specifically, our objective was to compare growth characteristics of vines cultivated on engineered PVC trellises (our green cloak) with natural vine communities colonizing dilapidated tobacco barns. The growth characteristics of eleven cloaks were examined weekly for approximately one year and nine vine-covered barns were sampled as an ecological analogue to the green cloak. Several of the cloaks achieved 100% trellis coverage in less than one year of growth. With these growth results, we believe that the barns' maximum leaf area index of 5 is an achievable green cloak leaf area index. Barn ecosystems typically had higher species diversity and leaf area indices than green cloaks. Trumpet creeper and Virginia creeper were species found on barns with high leaf area indices. Leaf area index regression results suggested that relatively high leaf area indices can be achieved in immature ecosystems without extensive woody material growth as found in mature barn vines. Additionally, green cloaks had lower light transmission for equivalent barn LAI indicating the benefit of even an immature green cloak. Several of the findings from this ecological comparison will be used to guide the following chapters on indoor temperature control and rainfall runoff reduction as well as enlighten future pilot scale green cloak design.

Introduction

Ecological engineering is an emerging field that couples the ecosystem services of natural systems with engineering design to benefit both man and nature. The ecological engineer can save his client money and energy by replacing costly and potentially environmentally harmful energy-intensive solutions with living systems that can adapt to various operating conditions. The success of the field is shown by wetland ecosystems that treat wastewater, microorganisms that cleanup contaminated soils and groundwater, and riparian tree species that stabilize stream banks and prevent erosion (Kangas, 2004).

We can see how an ecological engineer operates by looking back at Walter Adey's work on coral reefs leading to the development of his natural water purification system called the turf scrubber. Figure 2.1 lists some of Adey's published work. By looking at the titles in the top box of the figure it is seen that Adey was an ecologist studying algae of Caribbean reefs in the 1970s. In the bottom box, Adey's 1990s research is listed. His publication titles indicate that Adey became an engineer using what he had learned about the nutrient removal abilities of Caribbean algae for the treatment of human sewage, something that probably was not on his mind when studying the intricacies of the reef system. This example is ecological engineering; it uses a biological system in an application in which it was not designed or naturally found, but with careful design the system ends up working beautifully.

Adey, W.H. and R. Burke, 1976. Holocene bioherms (algal ridges and bank barrier reefs) of the eastern Caribbean. *Geol. Soc. of Am. Bull.*, 87:95-109.

Connor, J.L. and W.H. Adey, 1977. The benthic algal composition, standing crop, and productivity of a Caribbean algal ridge. *Atoll Res. Bull.*, 211.

Adey, W.H., 1978. Algal ridges of the Caribbean Sea and West Indies. *Phycologia*, 17:361-367.

This jump is the essence of ecological engineering

Adey, W.H., C. Luckett, and K. Jenson, 1993. Phosphorus removal from natural waters using controlled algal production. *Restor. Eco.*, 1:29-39.

Adey, W.H., C. Luckett, and M. Smith, 1996. Purification of industrially contaminated groundwaters using controlled ecosystems. *Ecolog. Eng.*, 7:191-212.

Craggs, R.J., W.H. Adey, B.K. Jessup, and W.J. Oswald, 1996. A controlled stream mesocosm for teriary treatment of sewage. *Ecol. Eng.*, 6:149-169.

Figure 2.1. Walter Adey's development of the turf scrubber started with studying coral reef algae.

Walter Adey studied ecology, which then inspired and informed his ecological design. An ecological engineer can also work in the opposite direction by first having a design idea and then seeking out nature's analogue to increase his understanding of the system. This gives the engineer insight into the future design's operation requirements and performance.

We conducted our green cloak research using ecological engineering theory. First the engineering problem was identified as the need for an alternative green roof design. The idea of using a vine cloak system was born and model trellises were built and vines were grown on them. We monitored the vine cloak growth for a period of one year to understand cloak coverage time, vine species growth rates, and canopy dimensions. Additionally, we conducted experiments on the vine cloaks to determine their ability to reduce runoff and building heat gain. With these engineered experiments, we decided we needed an ecological analogue of the green cloak to understand how vines grow naturally because we want the green cloak to function as naturally as possible, alleviating the need for energy intensive human input. With this, we chose abandoned, vine-covered tobacco barns as an inspirational analogue for our engineered green cloaks. We compared the growth characteristics of our engineered green cloaks to the barn vine communities by collecting the same data on LAI, canopy thickness, light interception, and species diversity. This chapter presents the methods and results of our comparative study.

Objectives

The specific objectives of this chapter were to:

1. Monitor several green cloaks over a one year growing season in greenhouse during cooler months and outside during warmer months to determine how vines grow on trellises.
2. Study the vine covered tobacco barn as an ecological analogue to the green cloak system to learn how vines grow in nature.
3. Compare green cloak growth characteristics to barn vine ecosystems for information on full scale build up and design considerations.

Materials and Methods

Experimental Design

This experiment was designed so that vine growth on the manmade cloak vine systems could be compared to the vines in the barn ecosystems. To this end, the eleven cloaks mentioned in Chapter 1 were measured weekly for growth for a period of approximately one year from September 2005 through August 2006. Source location of the vine material and date each cloak was started are in Table 2.1.

Table 2.1. Cloak information including start date and plant material source.

Cloak	Date Planted Clipping or Seed	Date Started on Cloak	Source
Porcelain berry	1-Jul-05	17-Aug-05	Clipping from College Park, MD
Virginia creeper 1	1-Jul-05	17-Aug-05	Clipping from College Park, MD
Virginia creeper 2	1-Jul-05	17-Aug-05	Clipping from College Park, MD
Kudzu 1	15-Jul-05	22-Sep-05	Purchased seed
Kudzu 2	15-Jul-05	10-Jan-06	Purchased seed
Japanese honeysuckle	11-Nov-05	15-Feb-06	Clipping from Silver Spring, MD
Trumpet vine	11-Nov-05	14-Mar-06	Clipping from Silver Spring, MD
Cross vine	11-Nov-05	11-May-06	Clipping from Silver Spring, MD
Morning glory	14-Mar-06	11-May-06	Purchased seed
Black eyed Susan vine	14-Mar-06	6-Jul-06	Purchased seed
Moonflower	14-Mar-06	6-Jul-06	Purchased seed

As Table 2.1 indicates, as plants became large enough, they were started on cloaks. The cloaks were grown in the University of Maryland Research Greenhouse Complex under light, temperature, and relative humidity conditions experienced during summer months. Cloaks were watered three times per week and fertilized (Jack's 20-10-20, Allentown, PA) once per week. On May 12, 2006 cloaks were taken outside of the greenhouse and kept there until September of the same year when cloaks were harvested for biomass. Cloaks were watered daily and fertilized (Nutricote 18-6-8, Bellevue, WA) once every 180 days while outside.

In summer 2006, vines on nine tobacco barns were studied. The barns were in Friendship, MD located in southern Anne Arundel County. Figure 2.2 is a map of Friendship (shown by large arrow) relative to Washington, DC, Annapolis, MD, and the Chesapeake Bay. Three 0.25 m^2 plots were made on each barn. Growth characteristic measurements were made at each plot.

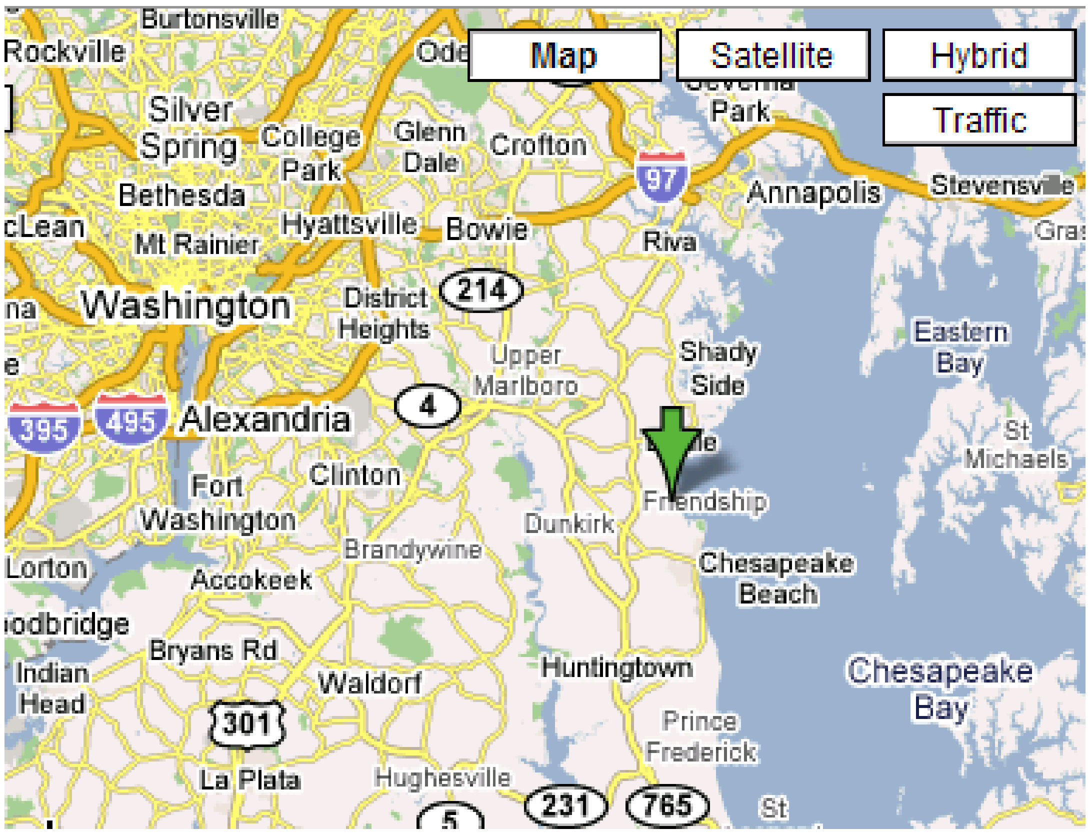

Figure 2.2. Map of Friendship, MD. Map from Google.com.

Two to three barns were analyzed during each trip to Friendship, MD. Table 2.2 lists the dates of each barn analysis.

Table 2.2. Date each barn was analyzed.

Barn	Date Analyzed
1	July 14, 2006
2	July 14, 2006
3	July 21, 2006
4	July 21, 2006
5	July 21, 2006
6	August 4, 2006
7	August 4, 2006
8	August 25, 2006
9	August 25, 2006

Data Collection

Each week, cloaks were observed for growth. Leaf area index (LAI) was recorded using a LAI-2000 Plant Canopy Analyzer (Li-Cor, Lincoln, NE) or the point-intercept method. We were forced to use both LAI measurement techniques because midway through our experiment the LAI malfunctioned and had to be sent out for repairs. With the LAI-2000, three subsample measurements were averaged to represent the LAI of a cloak. With the point-intercept method six subsample measurements were averaged to represent the LAI of a cloak.

Average thickness for each cloak was measured as the average distance between the cloak wire and the top of the vine canopy. Maximum thickness was measured similarly except it was the distance between the cloak wire and the tallest vine leaf.

Percent cover was estimated as the percentage of the cloak trellis that was covered with vines. Percent dead was estimated as the total percentage of leaves that were yellow or brown.

At the start of each measurement, time of day and sky conditions were recorded. A photograph of each cloak was also taken to examine growth (Figures 2.3a and 2.3b).

(a)

(b)

Figure 2.3. Photographs of vine cloaks at the beginning and the end of summer 2006.

At the end of the growing season, we measured photosynthetically active radiation (PAR), number of species per cloak, and biomass. We measured photosynthetically active radiation (PAR) using Apogee Instruments, Inc. Quantum Meter Model QMSW-SS (Roseville, CA) on the University of Maryland campus in College Park on September 22, 2006 at 3:00 pm. We used the side of the cloak with the densest canopy for each PAR measurement. Using a compass, the chosen side of each cloak was oriented at 146 degrees relative to north (the average orientation of all vine covered barns). The PAR meter was held perpendicular to the canopy surface for each measurement. We made rapid measurements to avoid changing sky conditions first taking one measurement above the canopy, five measurements under the canopy in an "X" formation, and then one measurement above the canopy. For each cloak, we found an average above canopy and below canopy measurement. The average below canopy measurement was divided by the above canopy measurement to find percent PAR transmitted through the canopy.

We called the number of vine species growing on each cloak the system species count, which we measured.

We harvested 0.25 m^2 of biomass of each cloak using a 0.25 m^2 quadrat. To determine the dry mass of each sample, we dried a representative subsample of each cloak in a drying oven for about 24 hours to eliminate all water weight. The mass of each dry subsample was taken and a ratio of the green to wet subsample weights was made. Using the subsample ratio, we predicted the dry sample weight.

Additionally on September 22, 2006 at 3:00 pm prior to harvest, we measured solar radiation, reflectance, and transmittance on Virginia Creeper 1 using a hyperspectral radiometer (ASD Handheld SpectroRadiometer, Analytical Spectral Devices, Boulder, CO) with a spectral range of 330 to 1075 nm and 1 nm waveband resolution.

We made similar growth measurements at each of the nine vine covered barns in summer 2006. Figures 2.4 and 2.5 show three plots on one barn where biomass had been harvested.

Figure 2.4. Three 0.25 m^2 plots at barn 8 after we harvested biomass.

Figure 2.5. Close-up photograph of a $0.25m^2$ plot delineated by the quadrat.

For each of the three plots at each barn, five subsample measurements of LAI were made using the point intercept method. We averaged the five subsample measurements into one LAI sample measurement for each plot.

On each plot, three subsample measurements of canopy thickness were made. Canopy thickness was the perpendicular distance from the surface of the barn to the outer edge of vine canopy. We averaged the three subsample measurements into one thickness sample measurement for each plot.

Using a compass, we found the orientation relative to north that the vegetated wall faced. Using a meter stick, we measured the height of each plot off the ground.

Called the system species count, the number of vine species growing on each barn was counted.

Using a 0.25 m^2 quadrat, we harvested the biomass from each plot on each barn. We separated each plot's biomass into "woody" and "nonwoody" biomass for comparison to cloak biomass numbers. Woody biomass was vegetation with stems of diameter greater than 0.6 cm while nonwoody biomass was all vegetation with stems less than 0.6 cm. We chose this diameter because there were no stems on the cloaks larger than 0.5 cm. This meant that nonwoody biomass measurements could be compared to the total biomass measurements of the cloaks. We made representative subsamples of the woody and nonwoody biomass samples and dried them for 24 hours in a drying oven. A ratio of the green to dry subsample weight was found for each sample and was used with the green sample weights to predict their dry weight.

All barns were revisited on September 29, 2006 and PAR was measured for each plot using the same methods described for the cloaks.

Data Analysis

For the one year cloak growing period, we made time series plots of each species' LAI, average thickness, maximum thickness, percent cover, and percent dead. Assuming that the barn vine communities were mature ecosystems, we plotted the times series data against the average value of the barn growth characteristics. This allowed us to quantify the growth rate of the vines.

When we harvested the cloaks, the minimum, average, and maximum values of biomass, thickness, leaf area index, light transmission, and system species count, were found. We computed the minimum, average, and maximum values of biomass, thickness, leaf area index, light transmission, and system species count for the barns also.

A t-test was performed using with a significance level of 0.05 to determine if the values for the barns and cloaks were significantly different. Again, we assumed that the cloaks were immature ecosystems and the barns were mature ecosystems. We compared the minimum, average, and maximum values of the cloaks and barns to determine the potential for growth of the cloaks if allowed to grow naturally without maintenance like the barn ecosystems. This comparison would give us insight into how the cloaks would develop over time and how we should design a pilot scale green cloak given the barn ecosystems biomass, canopy thickness, species diversity, etc.

Since we assumed that best cloak runoff and energy performance would be achieved with a maximum leaf area index, we used regression analysis to test for relationships between leaf area and biomass, average thickness, light transmission, system species count, cover, and dead cover. A best fit line, R^2, and p-value were found for each comparison. A significance level of 0.05 was used. We compared barn and cloak regression metrics to determine differences in how immature and mature ecosystems grow and function.

Results

Cloak Vine Growth

The following sets of Figures 2.6 through 2.8 show each species' trellis coverage, canopy thickness, and leaf area index growth over a one year growing period. In each figure, the x-axis represents days of growth for that particular species. Since species were collected at different times in the one year growing period, each figure's days of growth do not represent the same calendar days for all cloaks, but rather represent the elapsed time of growth unique to that cloak's plants.

Specifically, Day 0 represents the day in which the plant material was collected from clipping or seed and potted. The solid square on the x-axis represents the day when vines were placed on the cloak trellis. The open diamond represents the first measurement (taken on May 18, 2006) after we moved cloaks from inside to outside of the greenhouse on May 12, 2006.

May 18, 2006 is not plotted on the black eyed Susan vine, cross vine, moonflower, or morning glory covered cloaks because we had not placed these plants on their trellises yet. Instead, we started these four cloaks on trellises outside after we moved all other cloaks outside.

All canopies that were started inside the greenhouse and then moved outside (except for porcelainberry) show a temporary decrease in coverage, thickness, or leaf area index after the move. Once the cloaks acclimated to the outdoor conditions, the canopies returned back to a pattern of growth. Porcelainberry shows a rapid decrease in coverage, thickness, and leaf area index after Day 324 due to pruning. We cut back the cloak significantly after it became infested by insects during temperature testing in the environmental chamber.

Figures 2.6a through 2.6k depict the growth in trellis cover of each cloak species over the one year growing period. Coverage reached 100% by at least Day 253 for Japanese honeysuckle, porcelainberry, Virginia creeper 1, and Virginia creeper 2. Kudzu 1 reached 97% coverage by Day 272. Chinese trumpet creeper also grew quickly, but only reached 85% by Day 265. We were unable to observe a full year of growth for vines acquired later in the one year study period, but these species, particularly black eyed Susan vine, moonflower, and morning glory showed potential for similar trellis coverage given their comparable growth in the first few days of being on a trellis. Cross vine grew slowly on the trellis reaching only 55% coverage in 313 days.

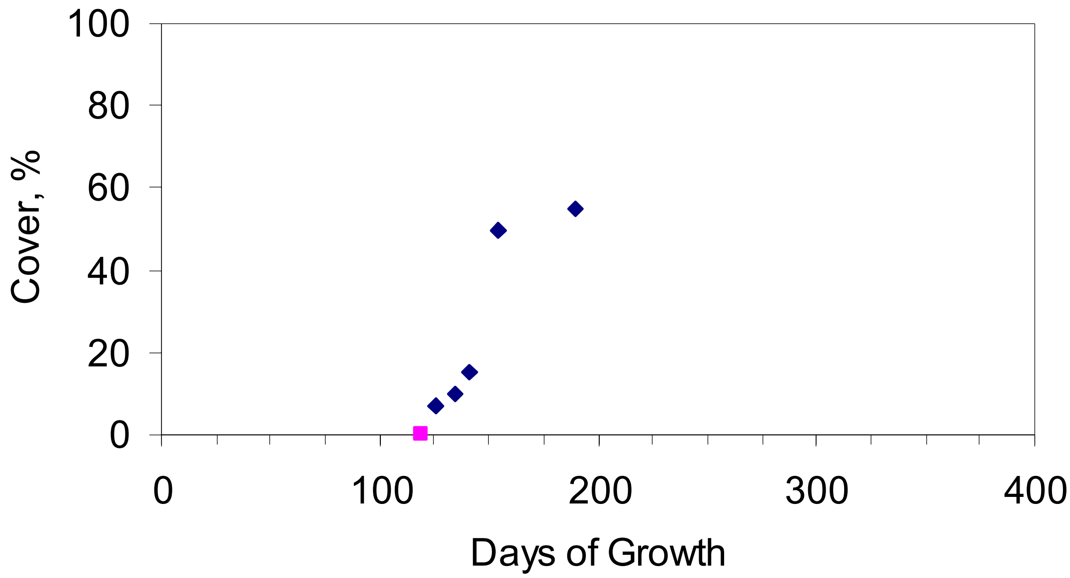

(a) Black Eyed Susan Vine

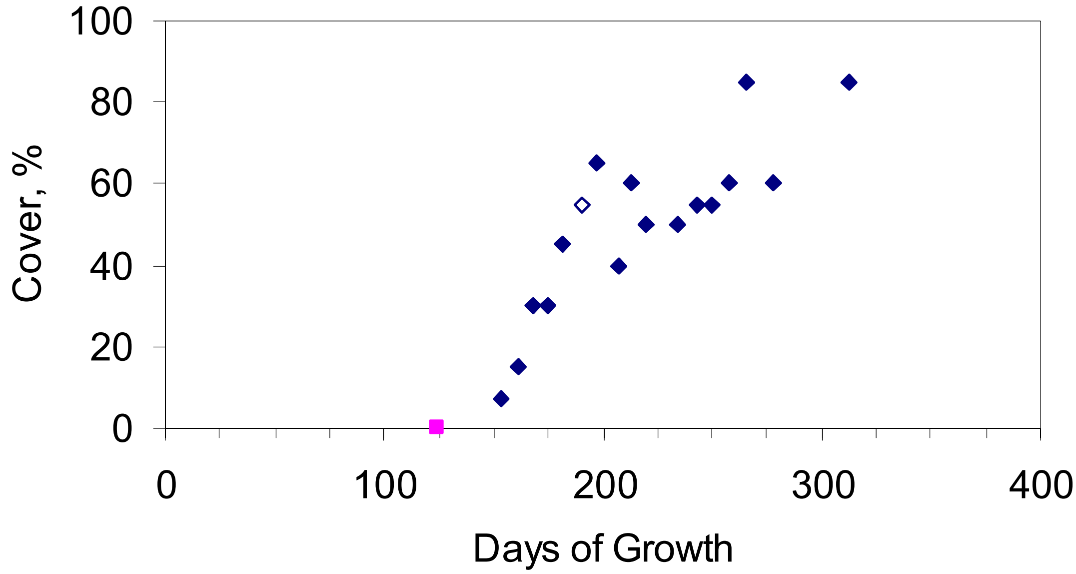

(b) Chinese Trumpet Creeper

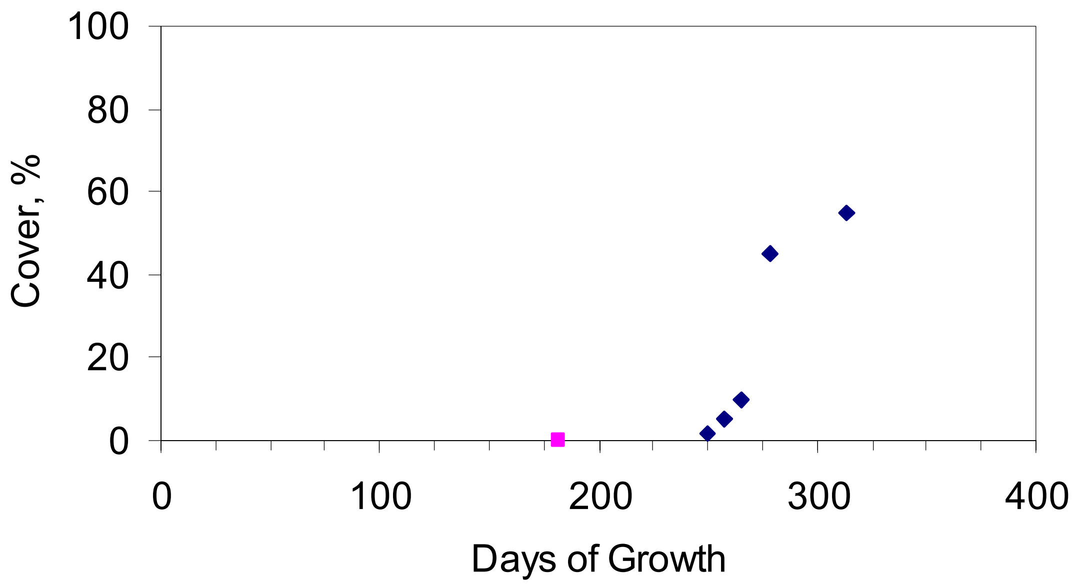

(c) Cross Vine

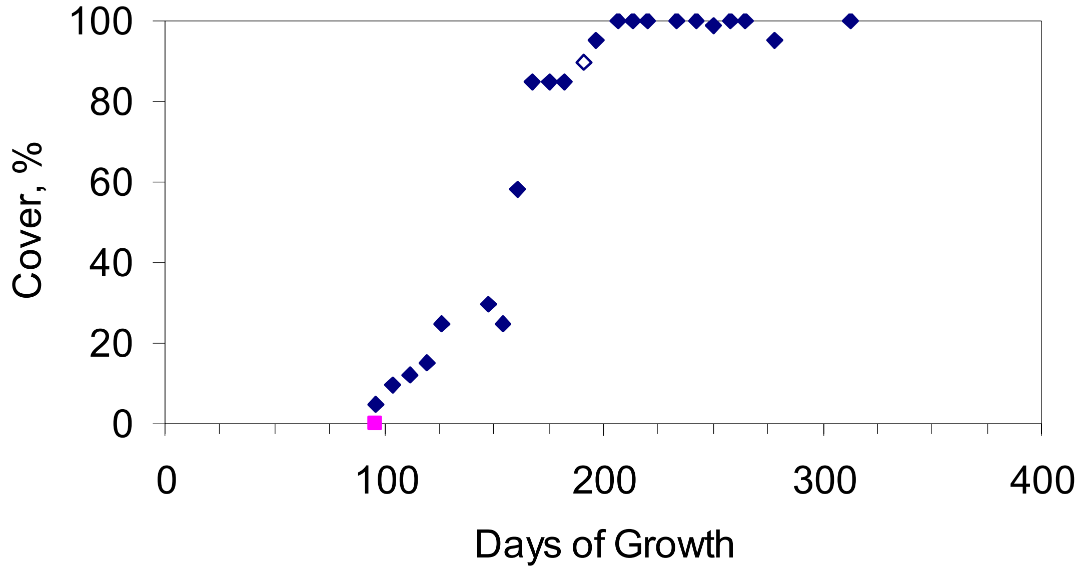

(d) Japanese Honeysuckle

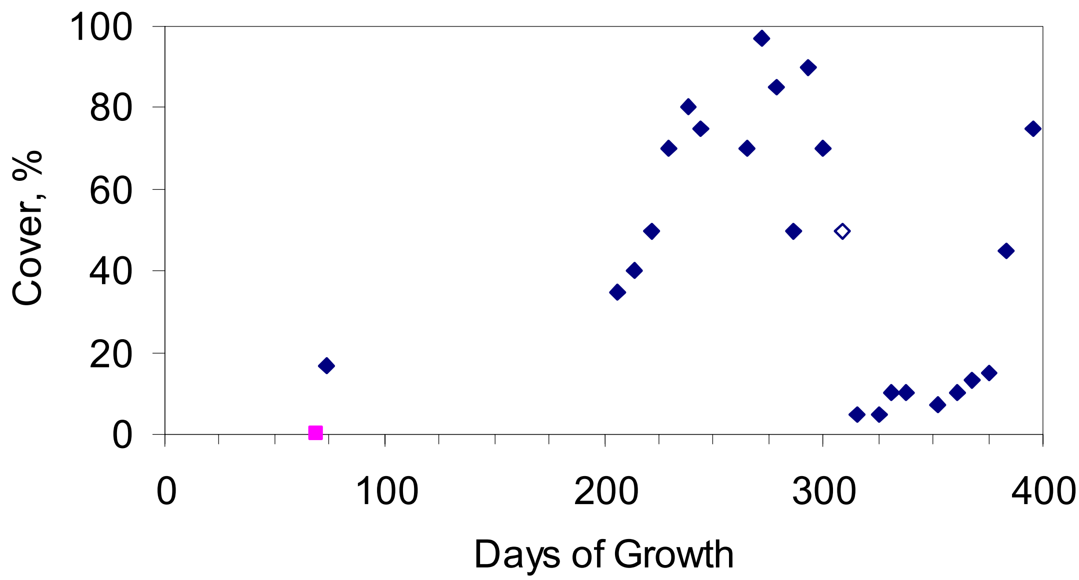

(e) Kudzu 1

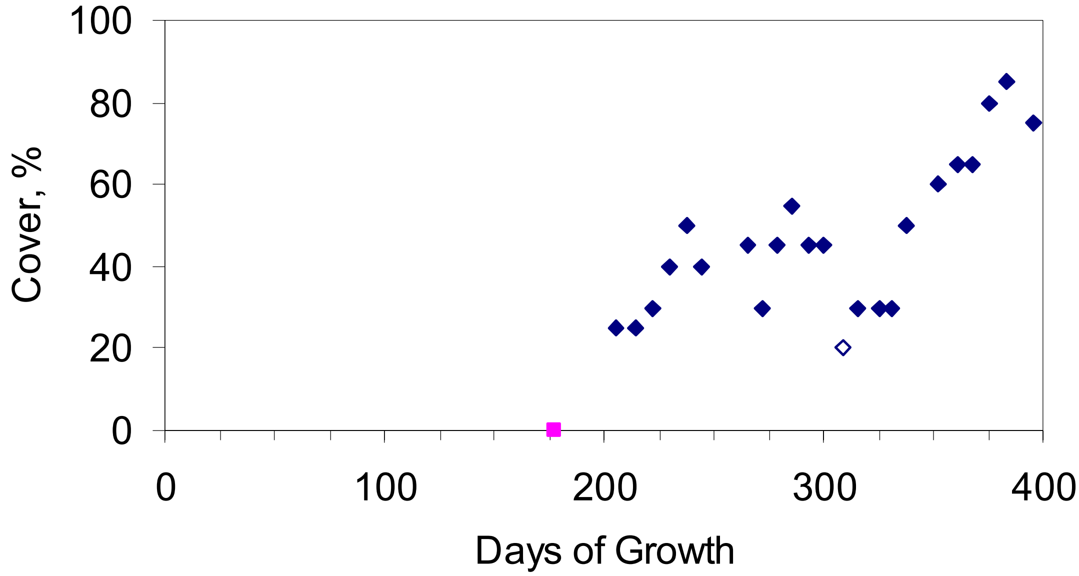

(f) **Kudzu 2**

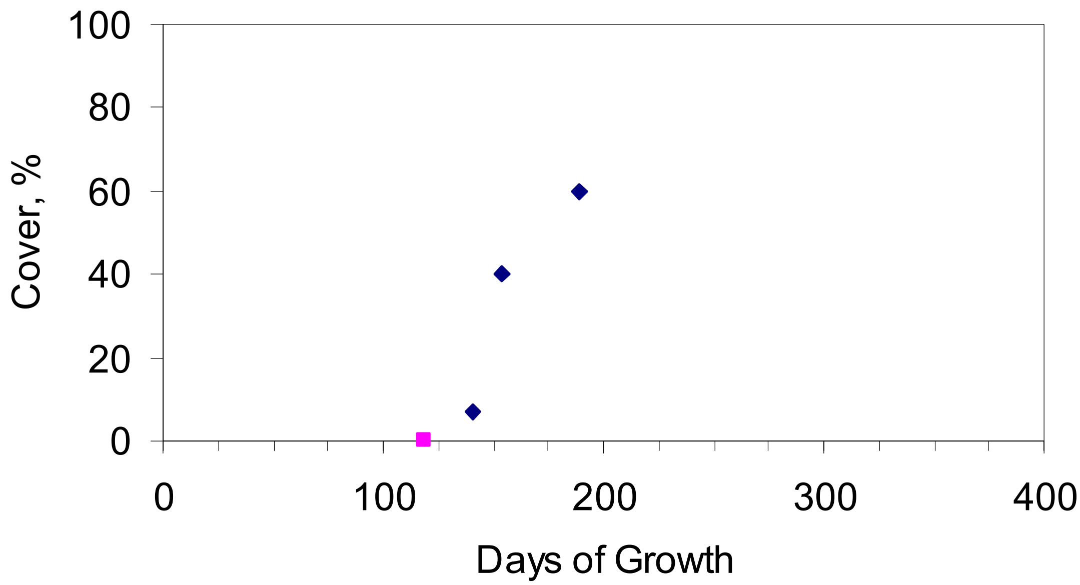

(g) **Moonflower**

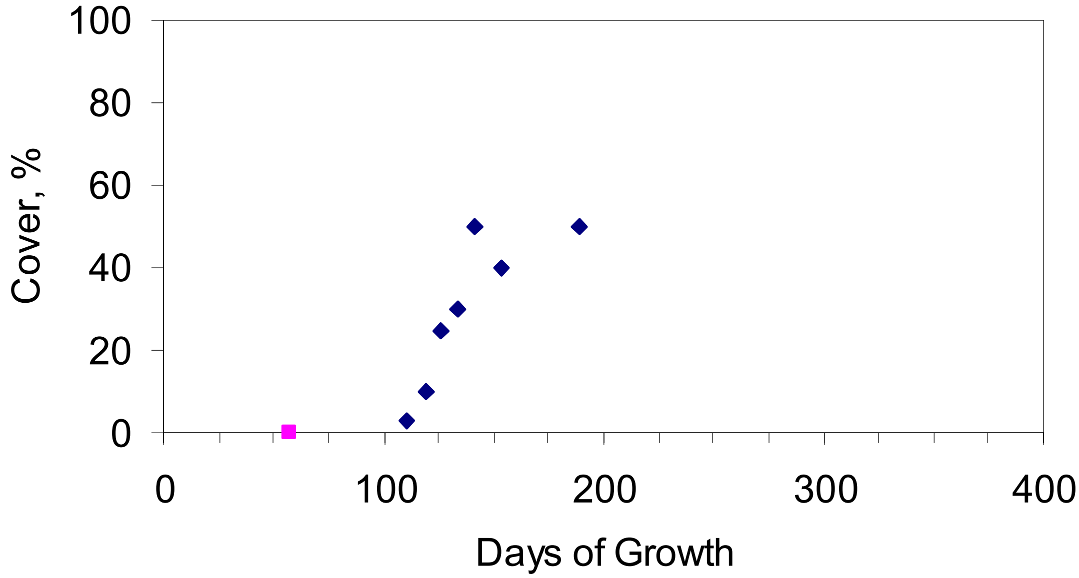

(h) Morning Glory

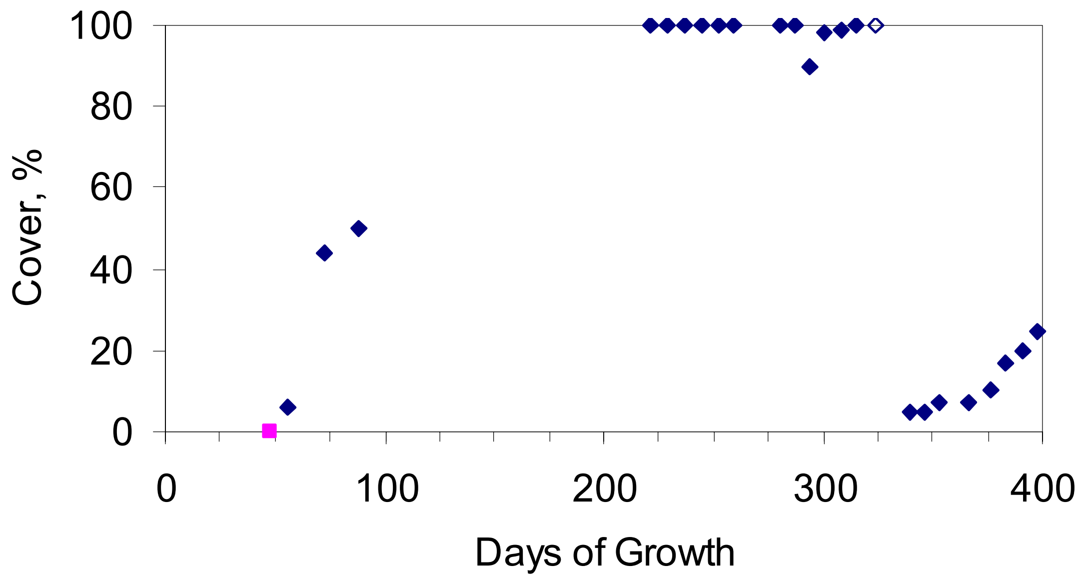

(i) Porcelainberry

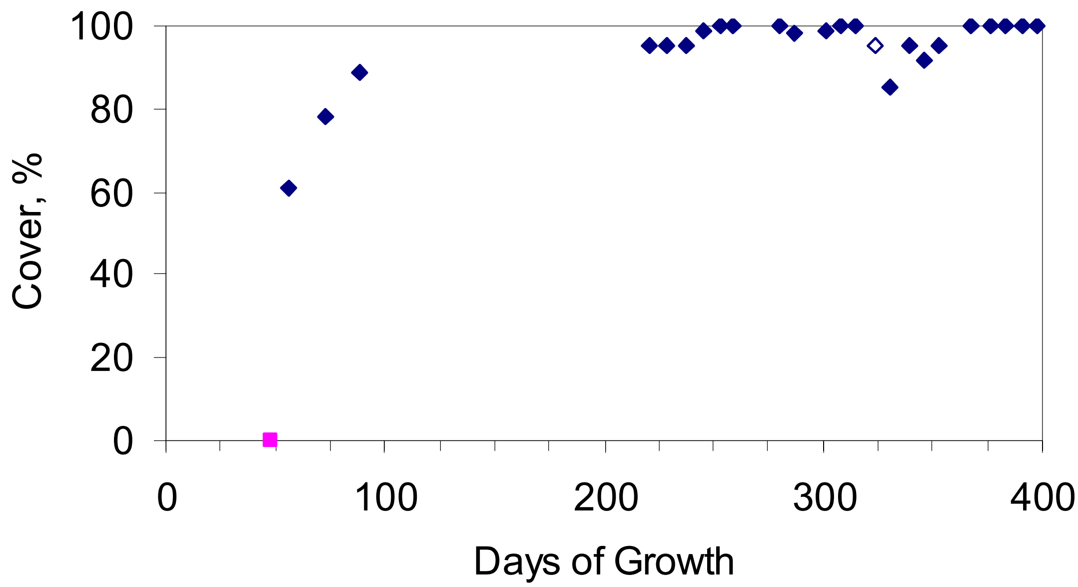

(j) Virginia Creeper 1

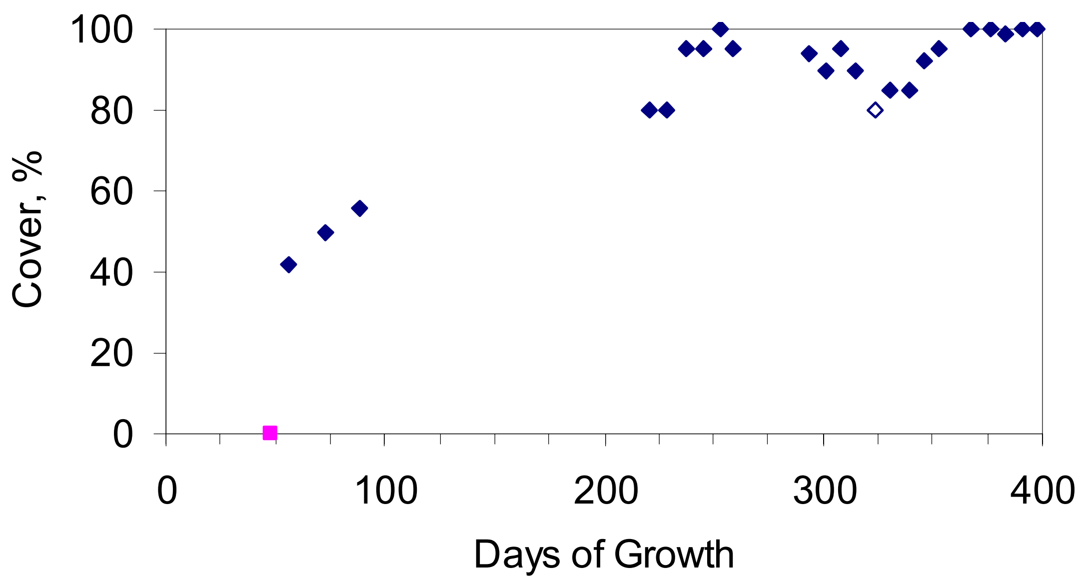

(k) Virginia Creeper 2

Figures 2.6. Growth in canopy cover of eleven vine covered cloaks.

Figures 2.7a through 2.7k depict the growth in average canopy thickness of each cloak species over the one year growing period. Average canopy thickness reached 27.6

cm for Chinese trumpet creeper, Japanese honeysuckle, Kudzu 1, Kudzu 2, porcelainberry, Virginia creeper 1, and Virginia creeper 2 by at least Day 340. Black eyed Susan vine, moonflower, and morning glory average canopy thickness maximums were an average of 16.2 cm within 190 days of growth. The cross vine average thickness was only 14.5 cm after 313 days of growth.

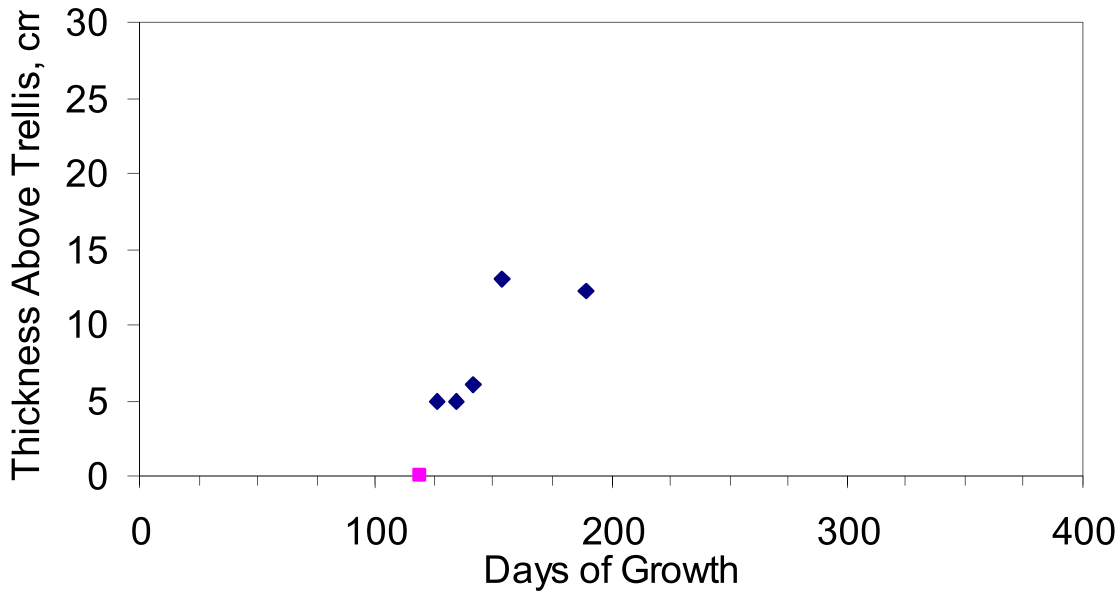

(a) Black Eyed Susan Vine

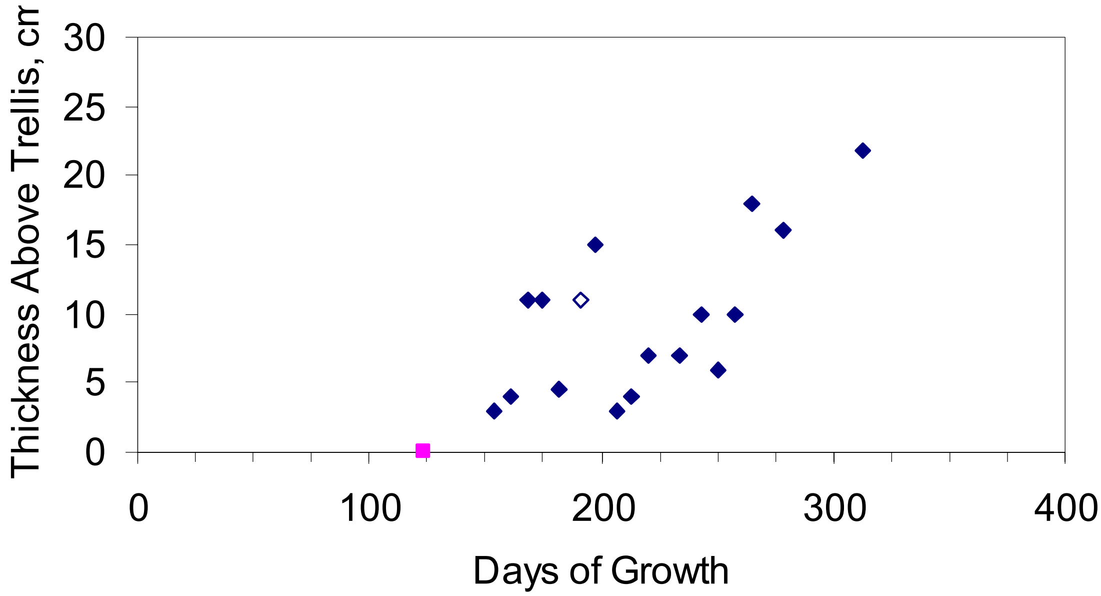

(b) Chinese Trumpet Creeper

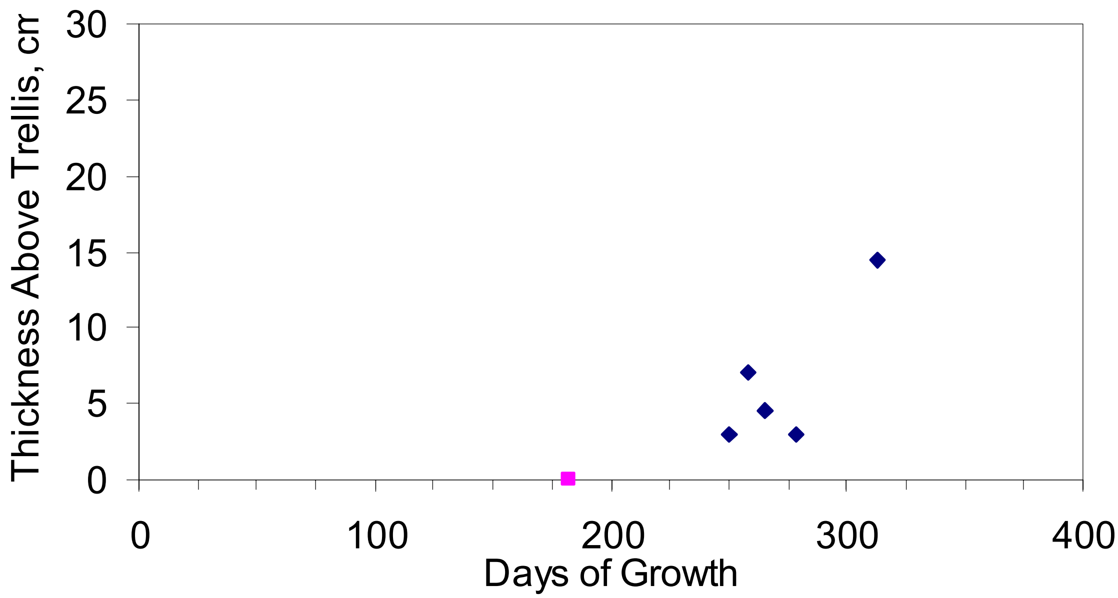

(c) Cross Vine

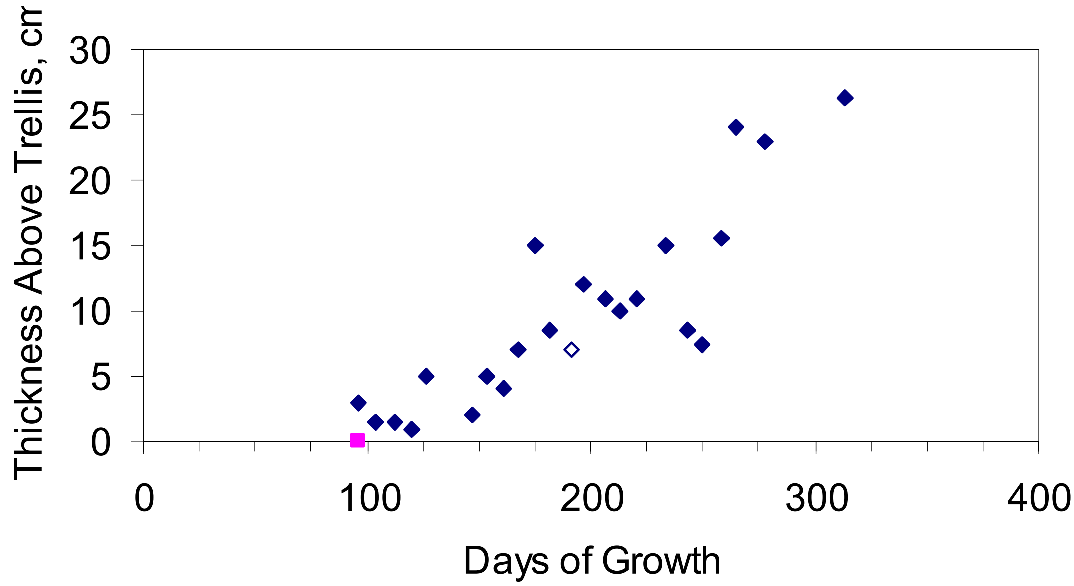

(d) Japanese Honeysuckle

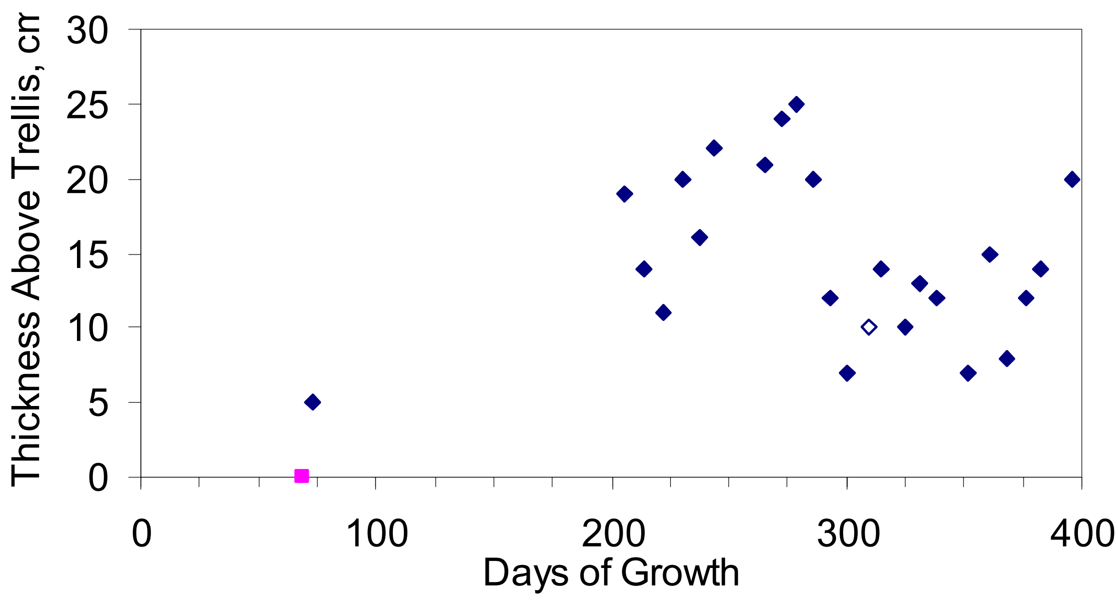

(e) Kudzu 1

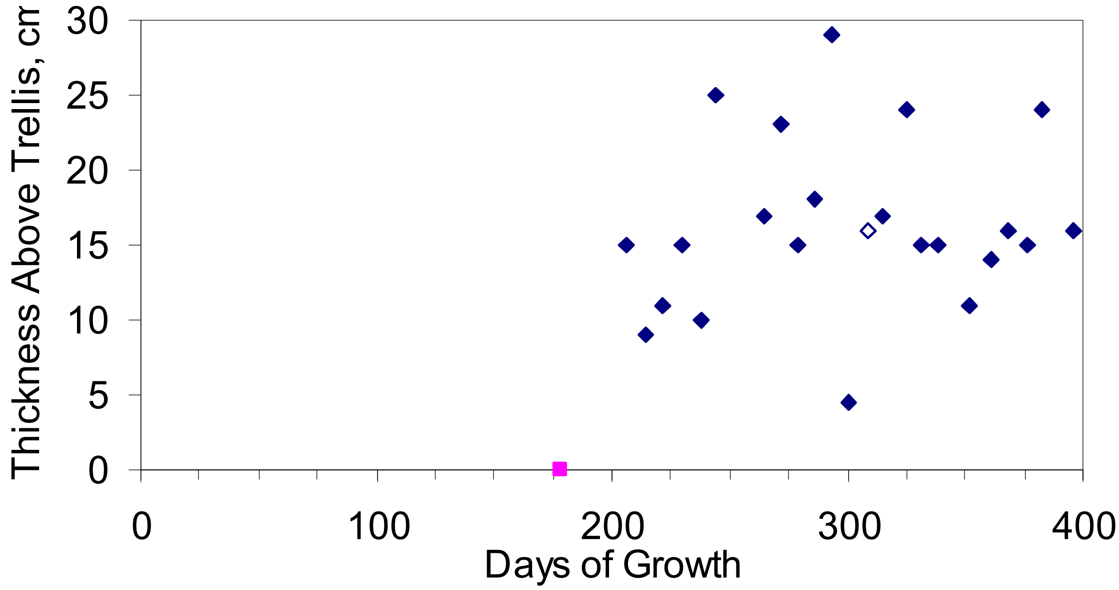

(f) Kudzu 2

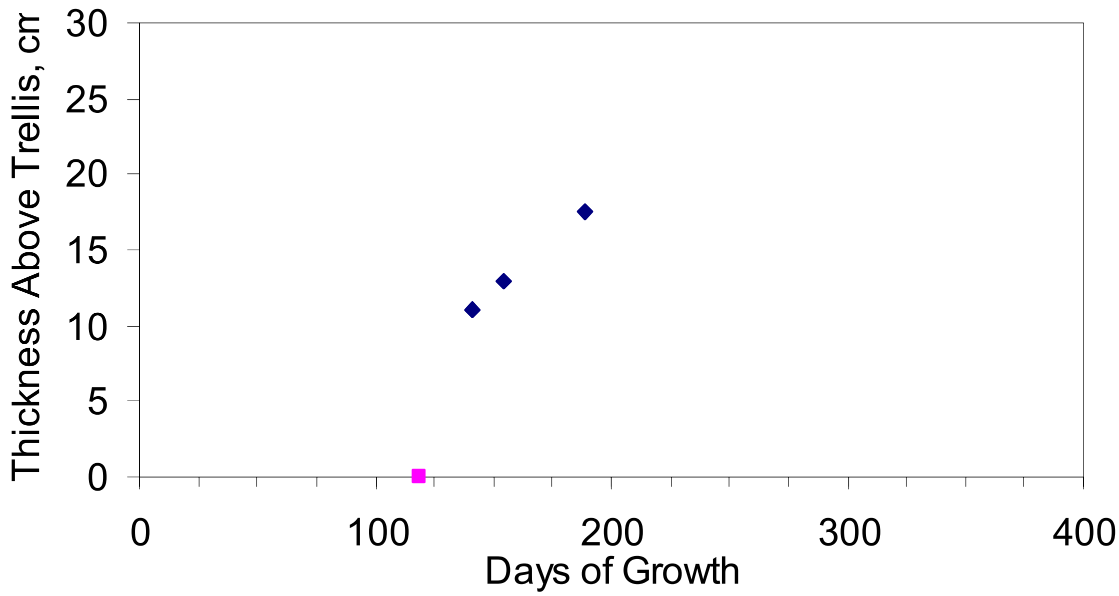

(g) Moonflower

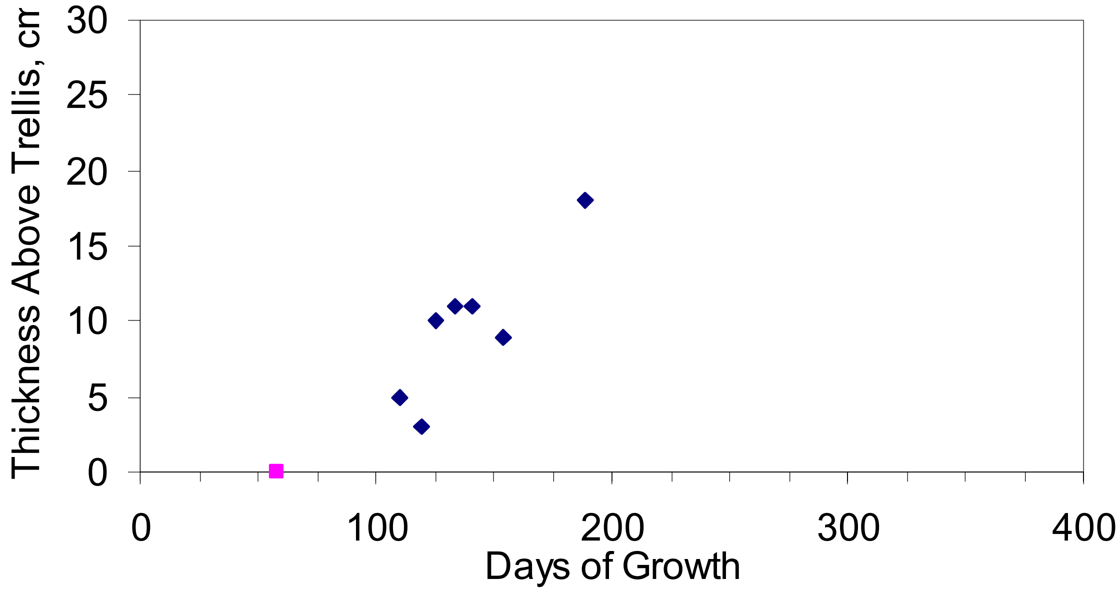

(h) Morning Glory

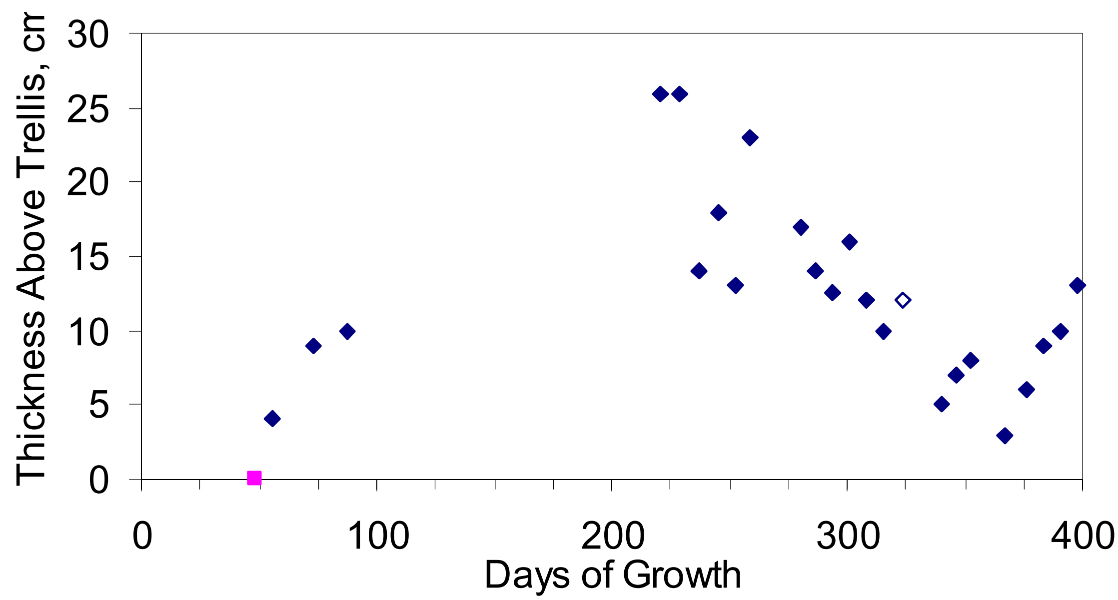

(i) Porcelainberry

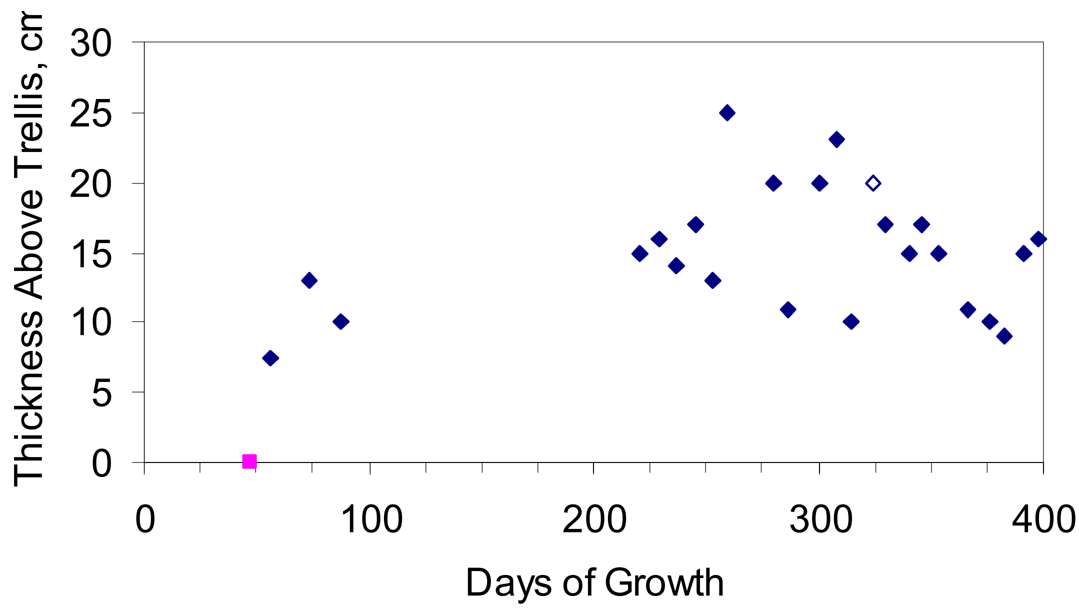

(j) Virginia Creeper 1

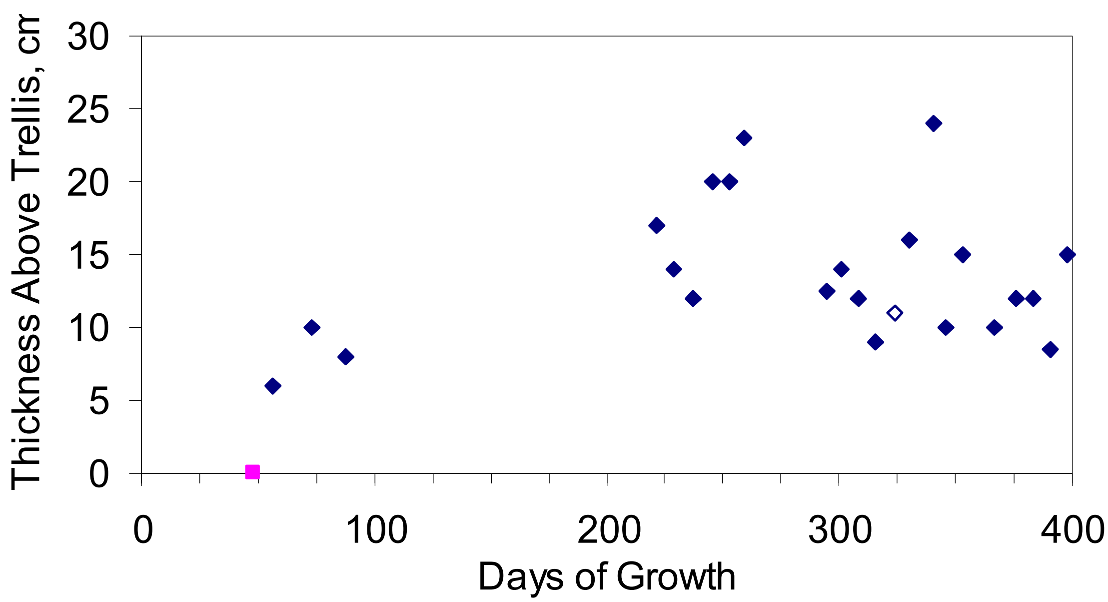

(k) Virginia Creeper 2

Figures 2.7. Growth in average canopy thickness of eleven vine covered cloaks.

Figures 2.8a through 2.8k depict the growth in leaf area index of each cloak species over the one year growing period. We showed the average barn LAI of 3.14 as a solid reference line for comparison to the cloak canopy thicknesses. Maximum LAI were greater than the barn average for Japanese honeysuckle, porcelainberry, Virginia creeper 1, and Virginia creeper 2 by at least Day 398. Porcelainberry had a maximum leaf area index of 4.33 by Day 237 and surpassed the barn average by Day 221 with an LAI of 3.78. Chinese trumpet creeper also had a dense canopy with a leaf area index of 2.5 by Day 265. Kudzu 1 and 2 had limited maximum leaf area indices of 2.44 and 2.33, respectively, due to repeated aphid infestations and related insecticide and pruning treatments. Black eyed Susan vine, moonflower, and morning glory canopy maximum leaf area indices were an average of 1.5 within 154 days of growth. The cross vine leaf area index was only 1.17 after 313 days of growth.

Increases and decreases in leaf area index are often seen in these measurements especially during the first few measurements. This is measurement variability in the LAI-2000. Fluctuations in the leaf area index in Virginia creeper 1 and 2 are observed while the cloaks were in the environmental chamber for the temperature control experiment (Chapter 3). The cloaks were taken from spring-like conditions in the greenhouse and put into summer-like conditions where temperatures and solar radiation were higher.

Additionally, we made the last three leaf area index using the point intercept method explaining some of the fluctuations in the last data points for each cloak.

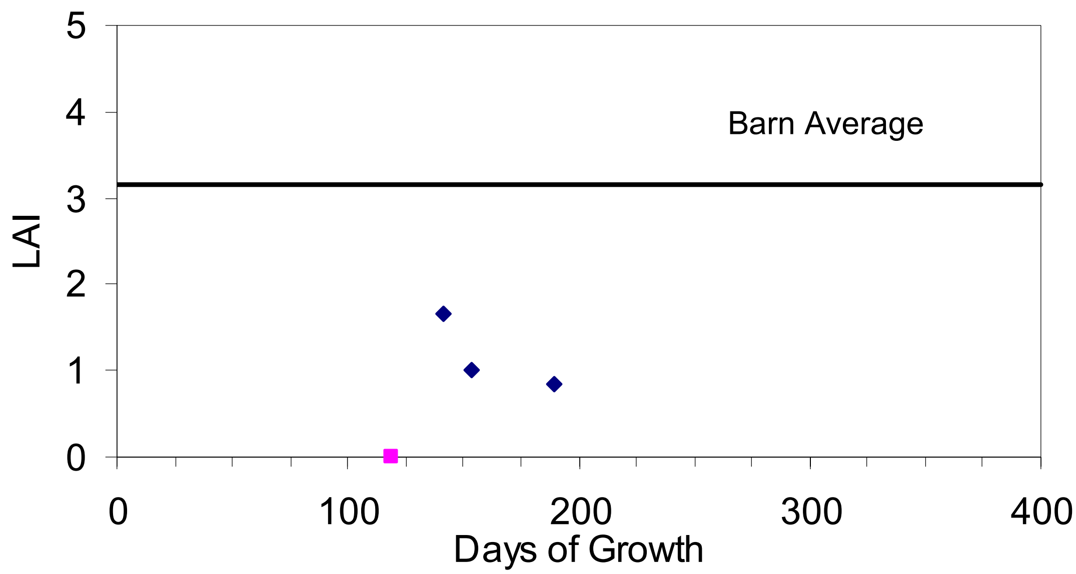

(a) Black Eyed Susan Vine

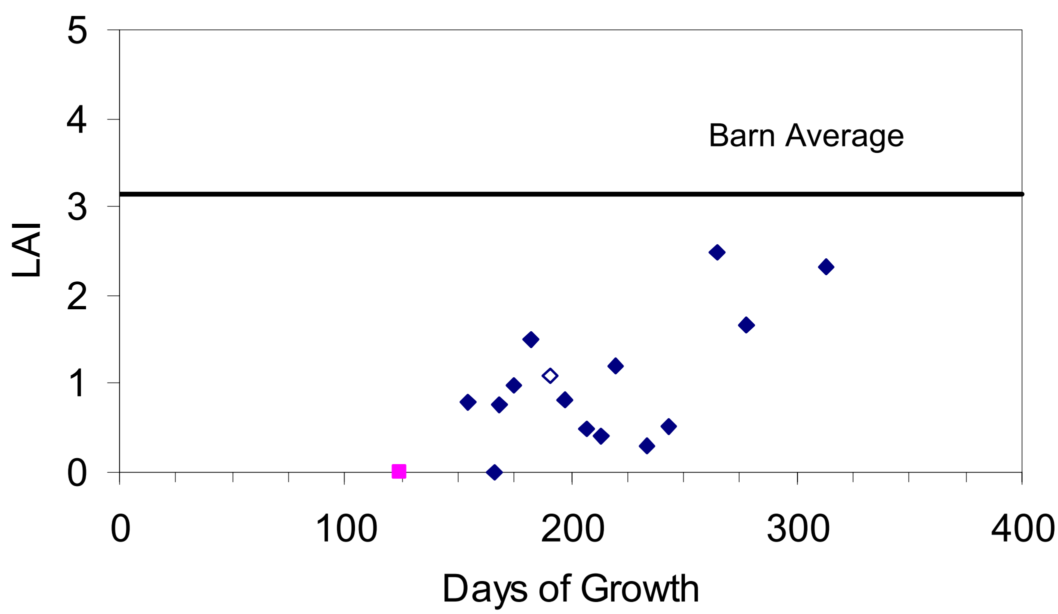

(b) Chinese Trumpet Creeper

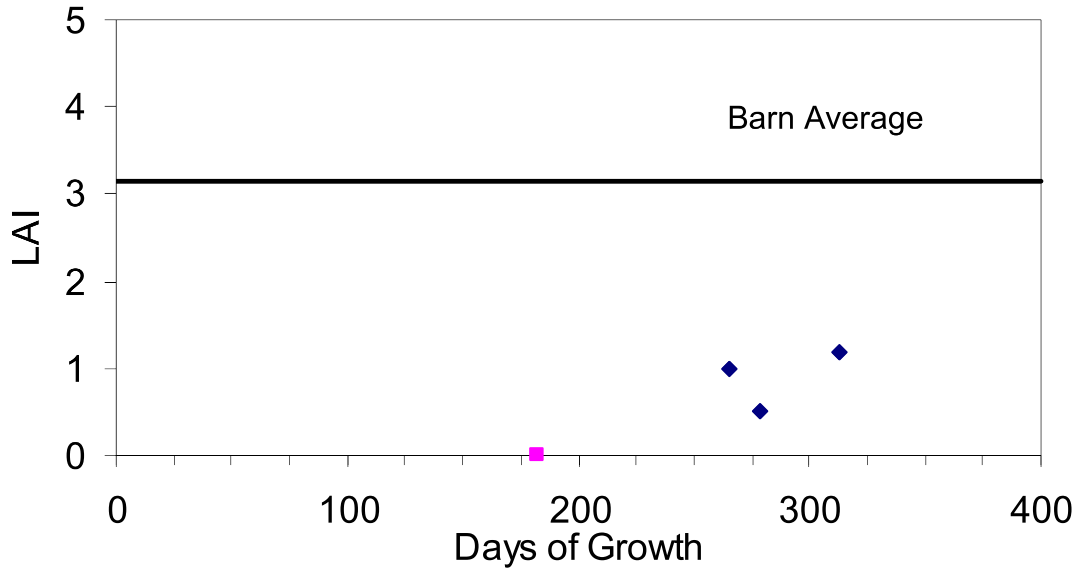

(c) Cross Vine

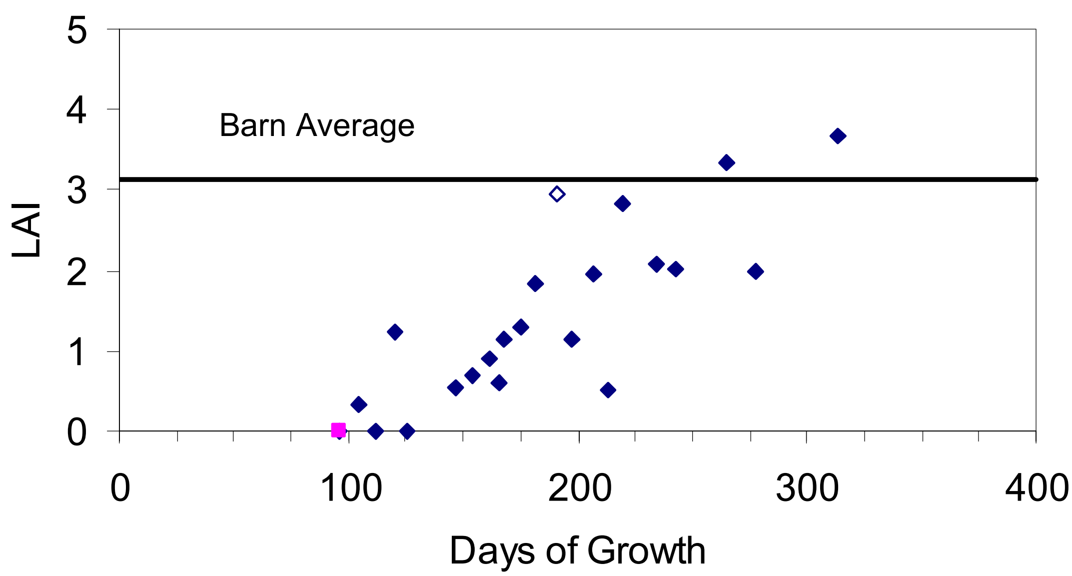

(d) Japanese Honeysuckle

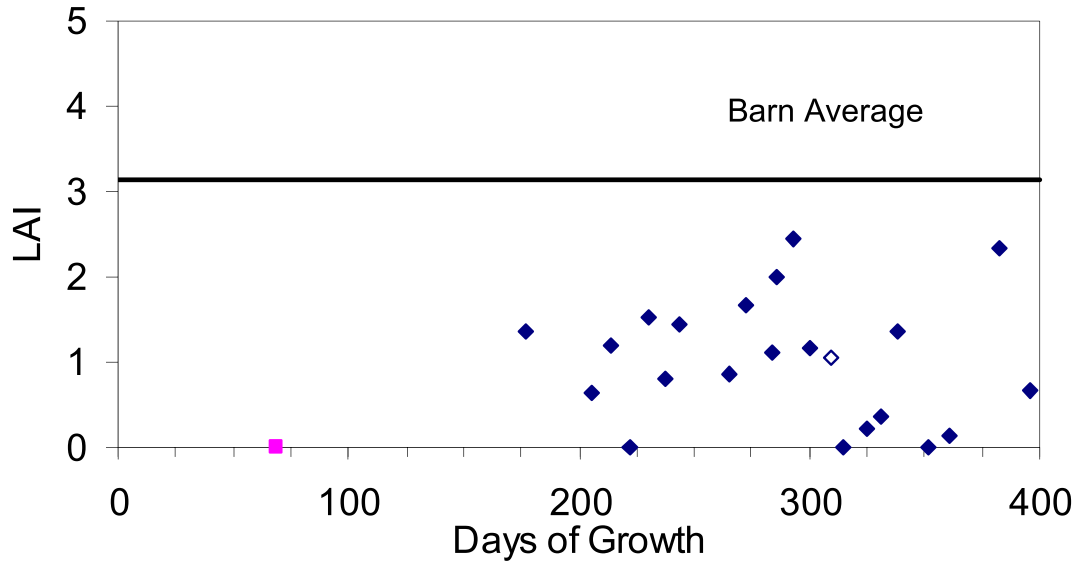

(e) Kudzu 1

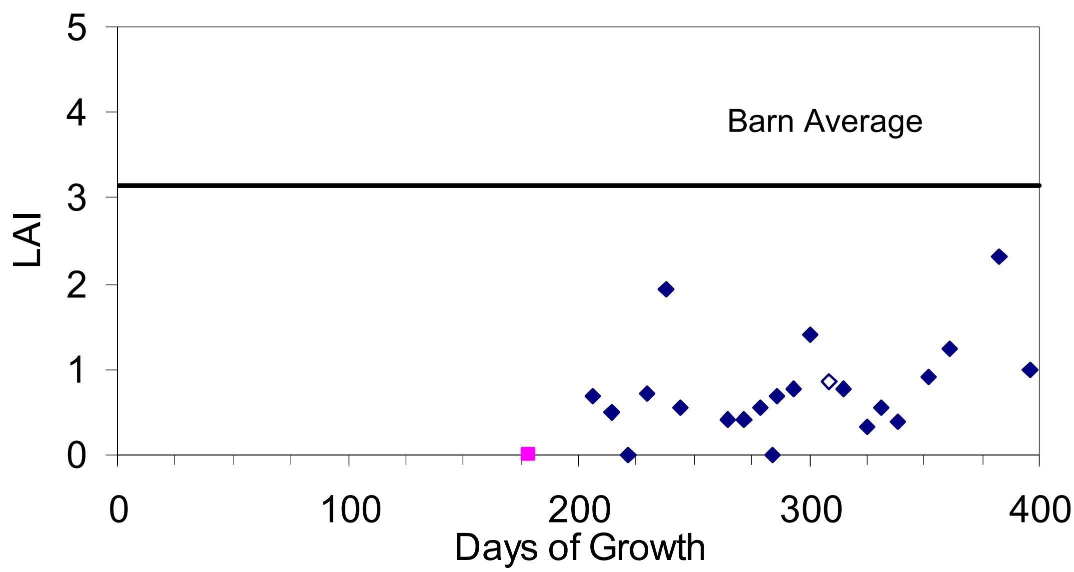

(f) Kudzu 2

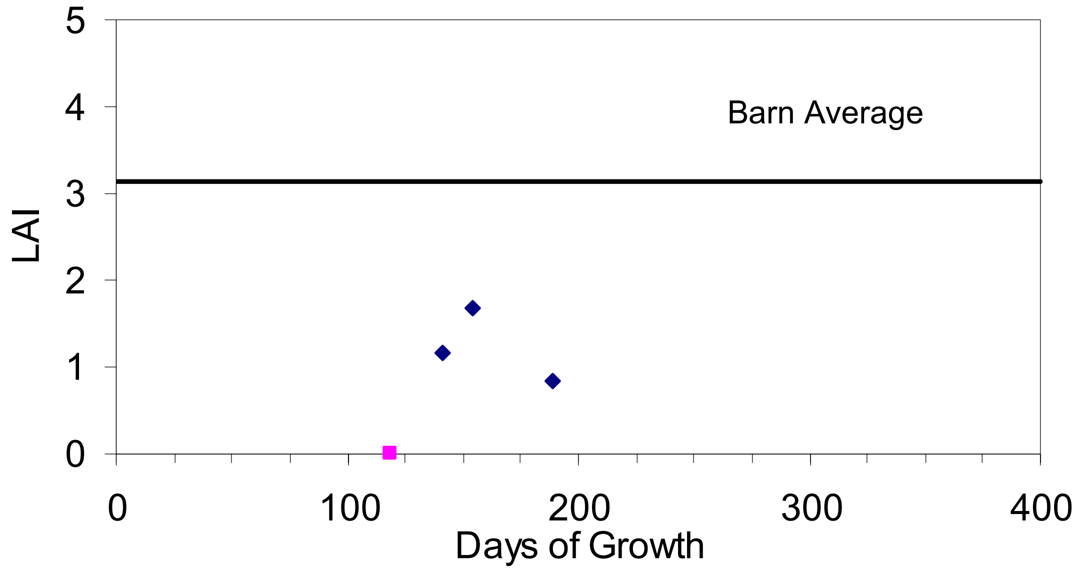

(g) Moonflower

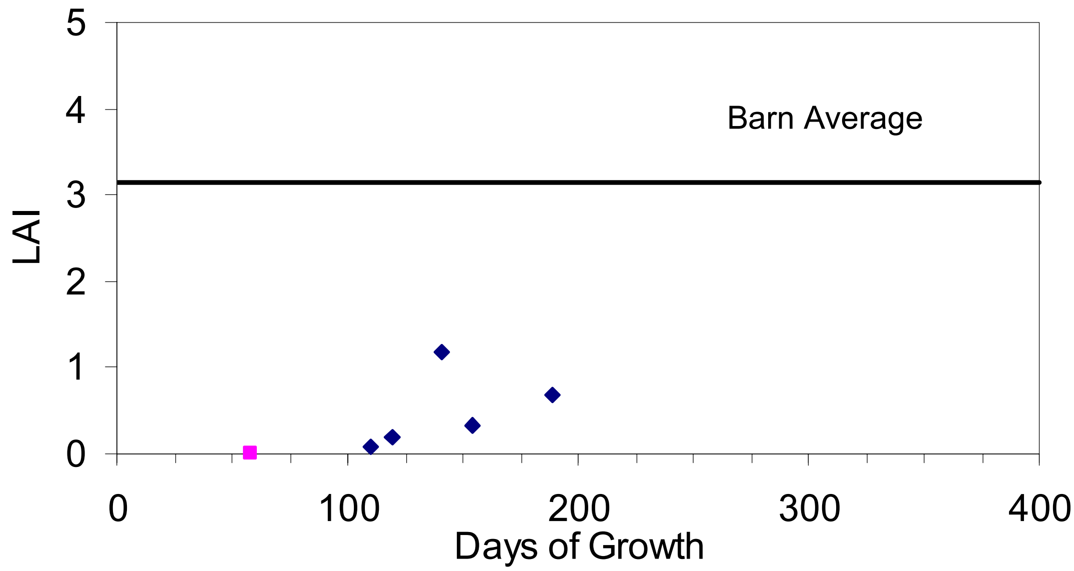

(h) Morning Glory

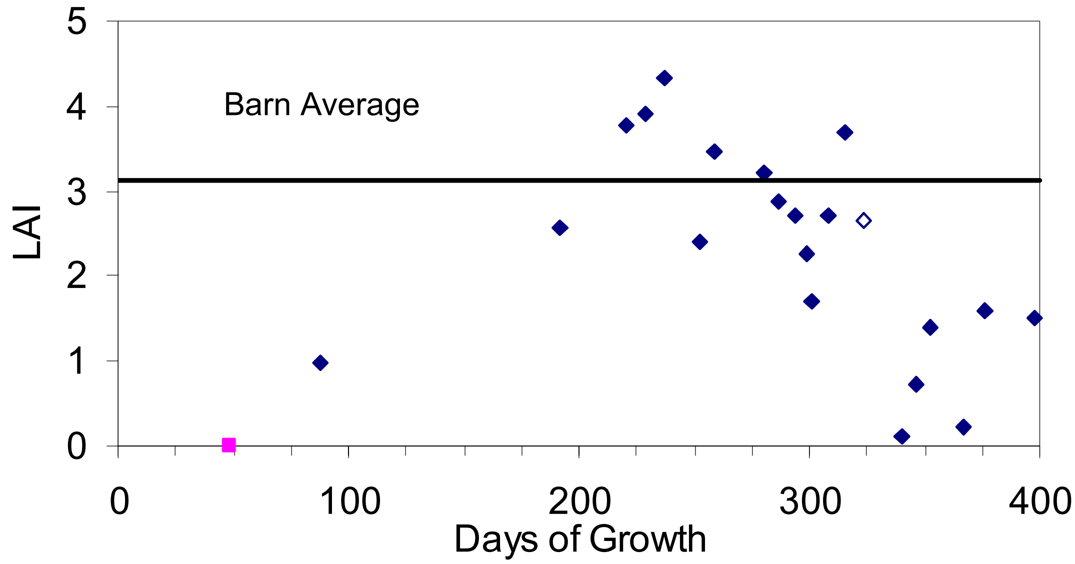

(i) Porcelainberry

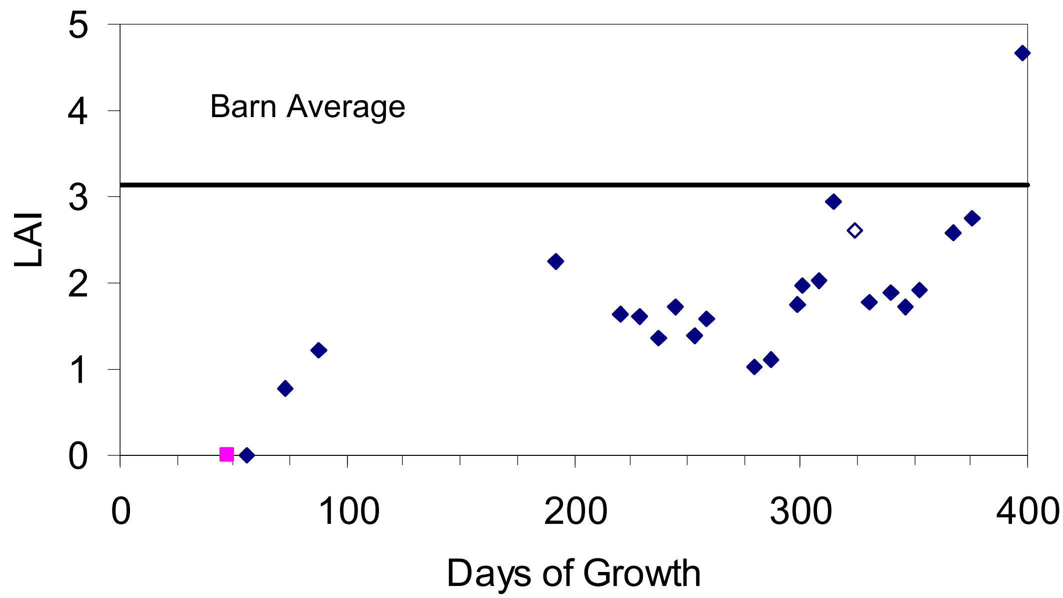

(j) Virginia Creeper 1

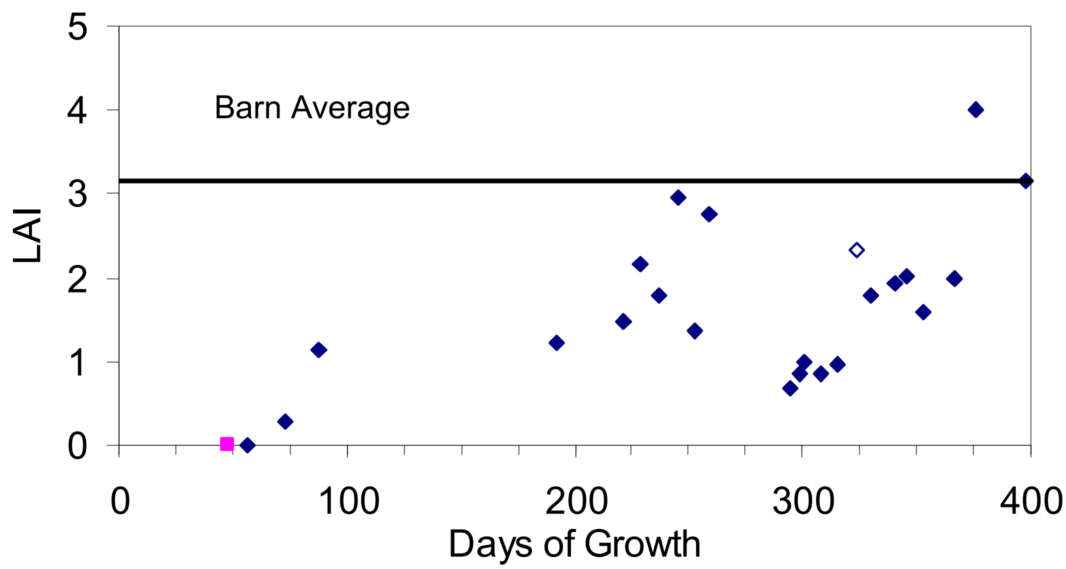

(k) Virginia Creeper 2

Figures 2.8. Growth in canopy leaf area index of eleven vine covered cloaks relative to average barn leaf area index of 3.14.

Barn Leaf Area Index

Figure 2.9 shows that leaf area indices for barn plots ranged from 1.2 to 6.2 showing wide variability in vine community growth.

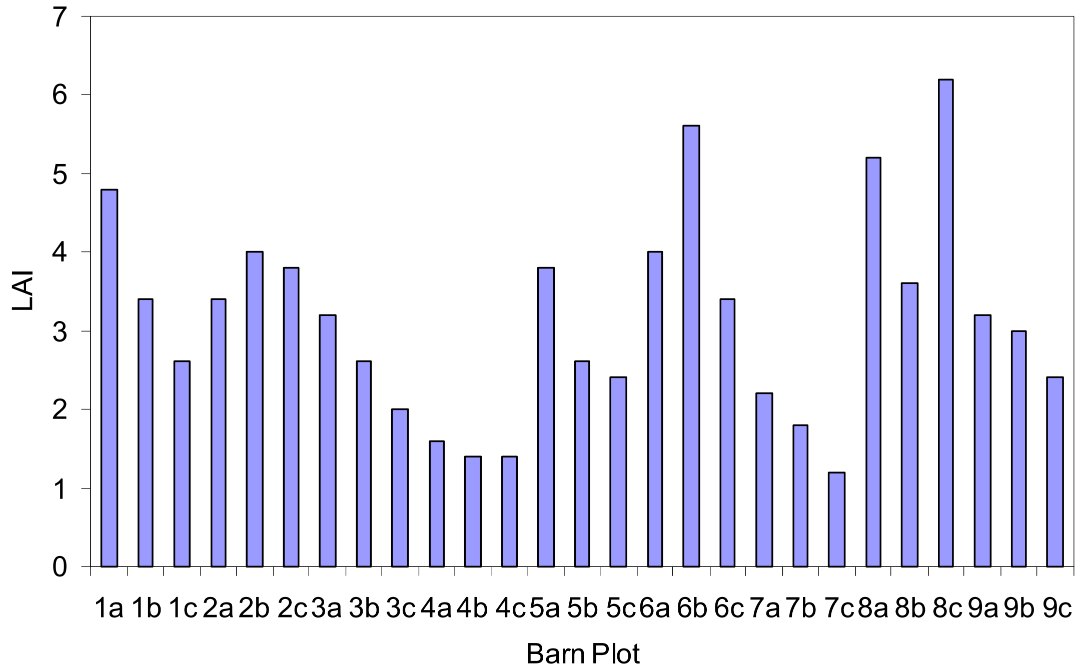

Figure 2.9. Leaf area index of each of the three plots on each of the nine barns.

Characteristic Comparison

Table 2.3 compares the minimum, average, and maximum values of biomass, canopy thickness, LAI, light transmission, and number of species per system for the barns and cloaks at time of harvest. For each of the barn characteristics, we averaged the three plot sample values into one average value for each barn. Of the nine barns, we found the minimum, average, and maximum of each value. Similarly, at harvest, we found the minimum, average, and maximum for the eleven cloaks.

Table 2.3. Minimum, average, and maximum growth characteristic comparison of barn vines and green cloak trellis vines. Values in parenthesis are standard deviations of the averages.

	Barn Vine Community			Green Cloak		
Measurement	**Minimum**	**Average**	**Maximum**	**Minimum**	**Average**	**Maximum**
Biomass (g/m^2)						
Total	345.2	1250.9 (945.6)	3647.6	96.8	546.6 (464.1)	1685.6
Woody*	47.2	513.6 (511.5)	1727.2	0	0 (0)	0
Nonwoody	269.6	769.1 (473.8)	1920.4	96.8	546.6 (464.1)	1685.6
Canopy Thickness (cm)*	38	69.7 (31.3)	121.7	12.3	21.7 (6.68)	31.5
Leaf Area Index*	1.47	3.14 (1.09)	5	0.67	1.73 (1.04)	3.67
Light Transmission, %	4.5	17.3 (11.0)	37.0	3.4	26.8 (20.1)	72.5
# Species per System*	1	2.33 (1.05)	4	1	1 (1)	1

*Indicates barn and cloak average characteristic values are significantly different.

For minimum, average, and maximum cloak light transmission, the three control readings (LAI = 0) were omitted since there were no controls for biomass, canopy thickness, leaf area index, or number of species. There were no barns or cloaks with an LAI of 0.

The number of species per system is the total number of species found in the three plots. Additionally, there was only one species growing on each cloak.

We averaged the three LAIs of the barn plots for each barn to get a maximum barn LAI of 5. Figure 2.9 described each plot's leaf area index. The maximum LAI on the cloaks was 3.67 at time of harvest. The average biomass of each cloak was 547 g/m^2 and the average for each barn was 1251 g/m^2.

The t-test results show that the total biomass, nonwoody biomass, and light transmission were not significantly different for cloaks and barns. Longer growing time did not make the barns have different values for these characteristics. Woody biomass, canopy thickness, leaf area index, and number of species per system were significantly different. These results indicate that cloaks left to overwinter for several seasons may not have significantly greater biomass, but would have a higher leaf area index and thickness.

Barn and Cloak Regression Comparison

Figures 2.10 through 2.14 are linear regressions comparing the nine barns' and eleven cloaks' leaf area index to total biomass, nonwoody biomass, thickness, light transmission, and system species count. Line of best fit, R^2, and p-values are given in each figure.

Barn Regression　　　　　　　　　　Cloak Regression

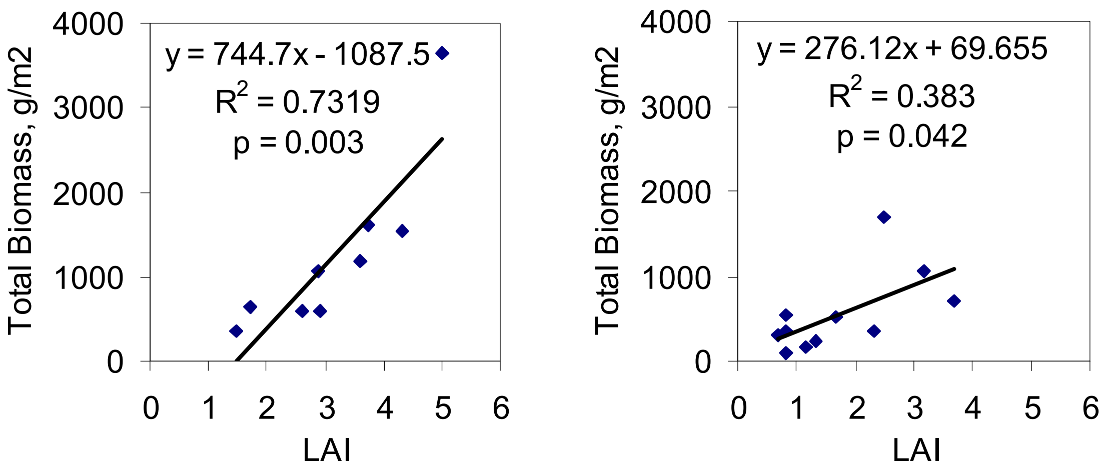

Figure 2.10. Total biomass as function of leaf area (LAI).

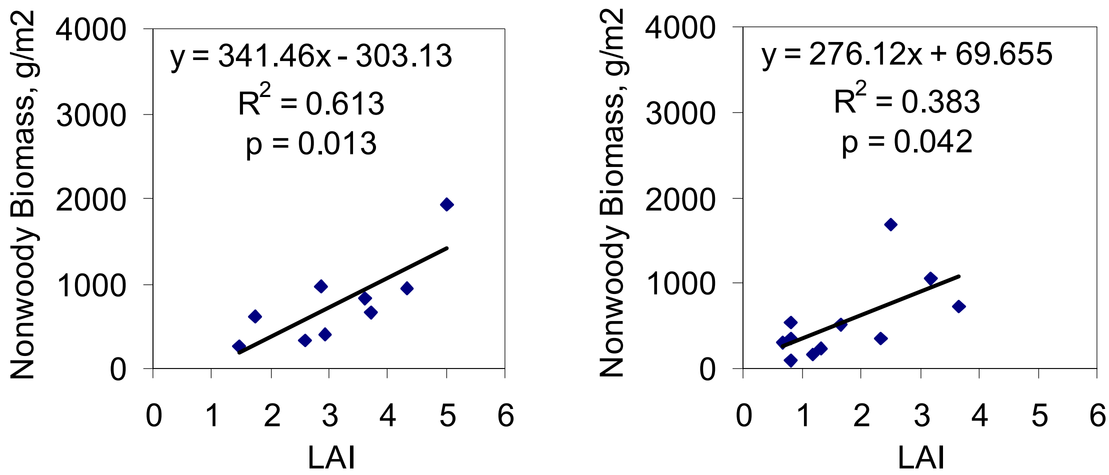

Figure 2.11. Nonwoody biomass as function of leaf area (LAI).

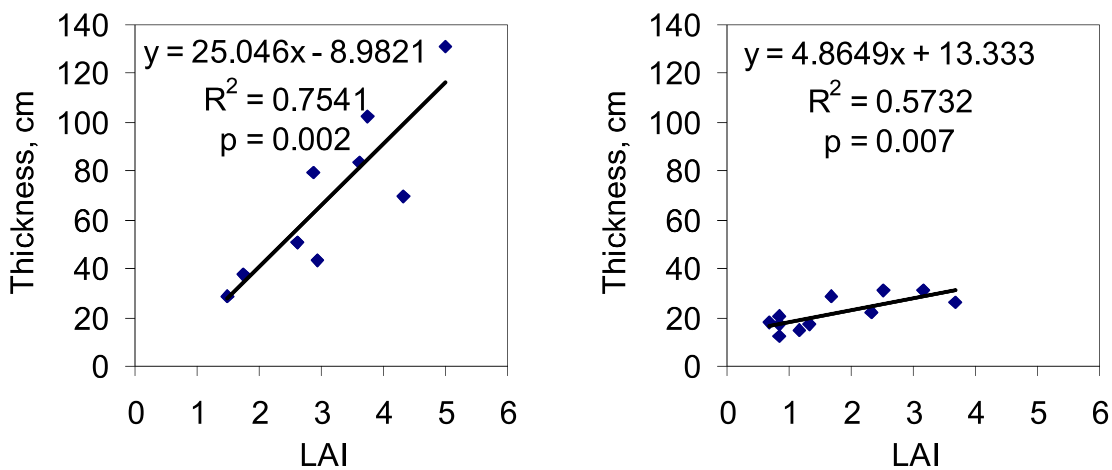

Figure 2.12. Canopy thickness as function of leaf area (LAI).

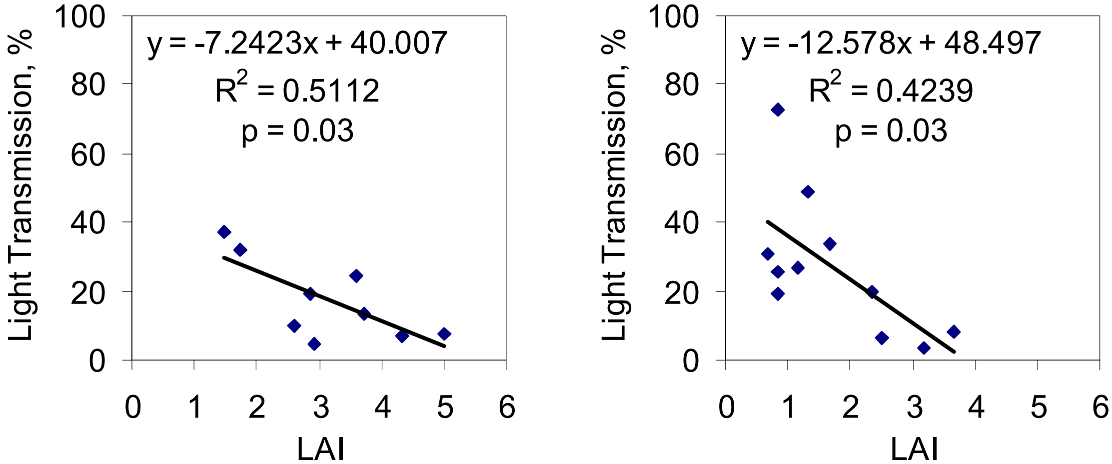

Figure 2.13. Light transmission through canopy as function of leaf area (LAI).

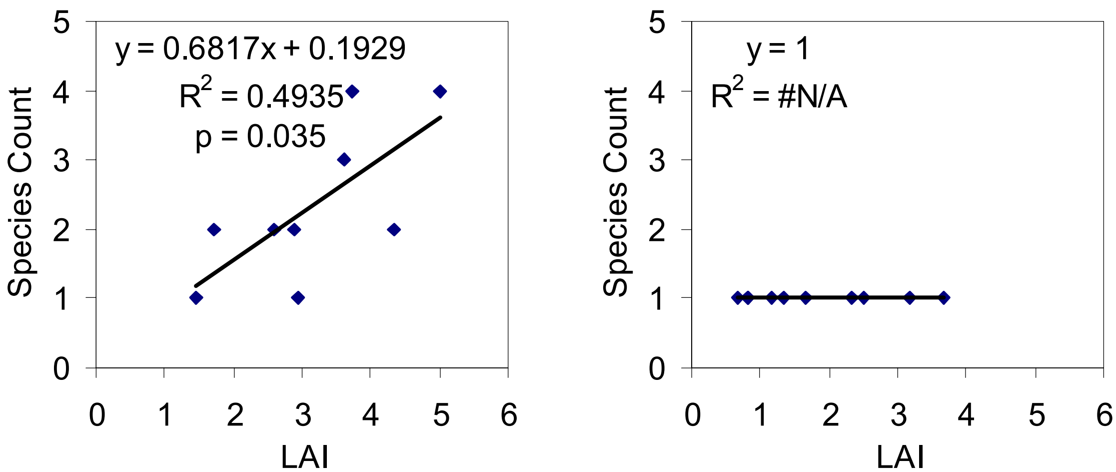

Figure 2.14. Species count as function of leaf area (LAI).

Leaf area was always positively related to biomass, nonwoody biomass, and canopy thickness (Figure 2.10 – 2.14) for both barns and cloaks. The number of species was also positively related to LAI, but only for the barns. Interestingly, slopes for the barns was always greater than for the cloaks possibly indicating that the relationships between LAI and growth measurements changes as vine communities mature.

Light transmission for both barn and cloak decreased with leaf area (Figure 2.13) with the cloak exhibiting more sensitivity to leaf area. The lower amount of light transmitted through the immature canopy of the cloak indicated that a young cloak with a low leaf area could moderate solar heating loads substantially.

Canopy Reflectance and Transmittance

Solar radiation above and below Virginia Creeper 1 (LAI 3.17) and percent transmission are shown in Figure 2.15. We determined percent transmission by dividing below canopy radiance by above canopy radiance for each wavelength. The canopy of the cloak transmitted 4% of the ultraviolet (325 to 400 nm) and visible (400 to 700 nm) radiation. The cloak vines transmitted 18% of the near-infrared radiation (700 to 1075 nm). For the entire UV/VIS/NIR spectrum measured, which is a major portion of the solar spectrum, the canopy only transmitted 9.3% of solar power.

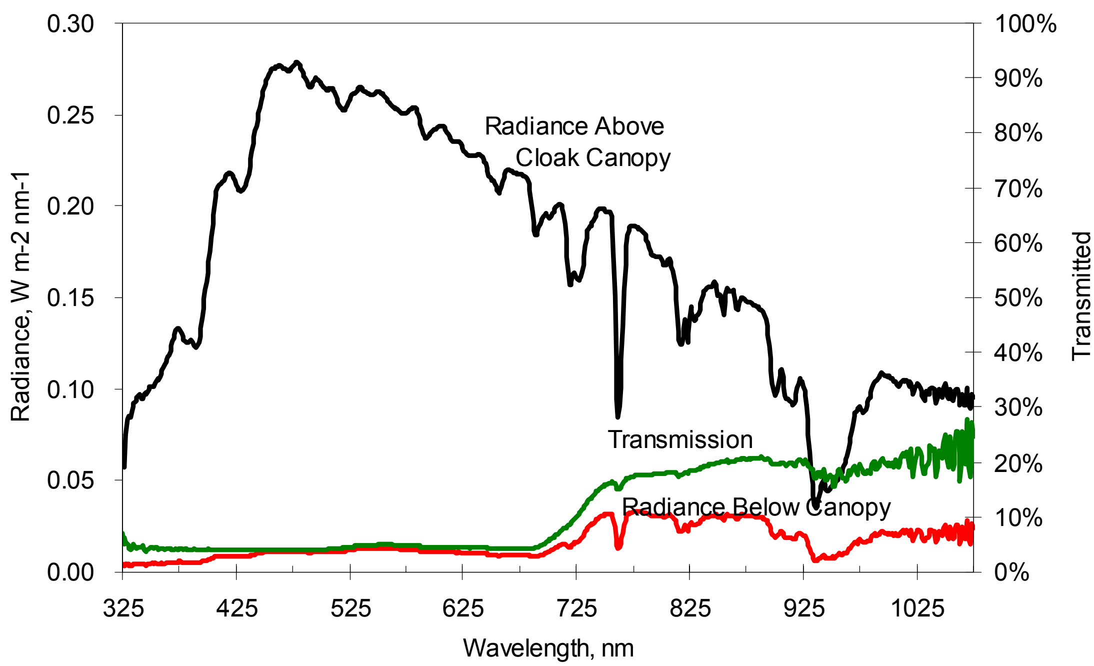

Figure 2.15. Radiance above and below the canopy of a green cloak with Virginia creeper and the percentage of light transmitted through the canopy.

Species Comparison

Table 2.4 is a list of some of the most common vine species in the mid-Atlantic U.S. The species are organized by species both grown on cloaks and observed on barns, species grown only on cloaks, species observed only on barns, and species neither grown on cloaks nor observed on barns. Only two species, Japanese honeysuckle and Virginia creeper, were grown on cloaks and observed on barns meaning several of the species grown on cloaks were not observed on barns. For green cloak design, some of the species studied are not of interest to due to their human irritant (poison ivy and porcelainberry) and invasive properties (Japanese honeysuckle and kudzu).

Table 2.4. Common mid-Atlantic vine species and their relative growth on cloaks and barns.

Species	Cloaks	Barns
Japanese honeysuckle (*Lonicera japonica*)	X	X
Virginia creeper (*Parthenocissus quinquefolia*)	X	X
Black-eyed susan vine (*Thunbergia alata*)	X	
Chinese trumpet vine (*Campsis grandiflora*)	X	
Cross vine (*Bignonia capreolata*)	X	
Kudzu (*Pueraria lobata*)	X	
Moonflower (*Ipomoea alba*)	X	
Morning glory (*Ipomoea tricolor*)	X	
Porcelainberry (*Ampelopsis brevipedunculata*)	X	
Blackberry (*Rubus argutus*)		X
Common greenbrier (*Smilax rotundifolia*)		X
Grapevine (*Vitis* sp.)		X
Poison ivy (*Toxicus radicans*)		X
Trumpet creeper (Campsis radicans)		X
Wild hydrangea (*Hydrangea arborescens*)		X
Creeping euonymus (*Euonymus fortunei*)		
Five-leaved akebia (*Akebia quinata*)		
Louis' swallowwort (*Cynanchum louis*eae)		
Mile-a-minute (*Polygonum perfoliatum*)		
Oriental bittersweet (*Celastrus orbiculatus*)		
Periwinkle (*Vinca minor*)		
Small red morning glory (*Ipomoea coccinea*)		
Wisterias, exotic (*Wisteria sinensis*, *W. floribunda*)		

Table 2.5 lists the system species count along with the individual species found on each barn relative to the barn canopy's LAI. Trumpet creeper was found on the barns with the two highest leaf area indices (Barn 6 and 8). Virginia creeper was found on

barns with moderately high leaf area indices (Barns 1 and 2). Barns with the higher leaf area indices also had higher species count of 3 and 4 (Barns 1, 2, and 8).

Table 2.5. Description of barn leaf area indices, system species count, and species.

Barn	LAI	System Species Count	Species
1	3.6	3	Poison ivy, **Virginia creeper**, Common greenbrier
2	3.73	4	Common greenbrier, Grapevine, Poison ivy, **Virginia Creeper**
3	2.6	2	Grapevine, Trumpet creeper
4	1.47	1	Poison ivy
5	2.93	1	Trumpet creeper
6	4.33	2	Blackberry, **Trumpet creeper**
7	1.73	2	Poison ivy, Virginia creeper
8	5	4	Hydrangea, Japanese honeysuckle, Poison ivy, **Trumpet creeper**
9	2.87	2	Grapevine, Poison ivy

Discussion

Ecological Comparison

The difference in how mature ecosystems and immature ecosystems grow was observed in the linear leaf area index regressions of the barn and cloak ecosystems. We believe the evolution of woody biomass may explain the greater slopes of the barn total biomass, nonwoody biomass, and thickness regression lines compared to the cloak regression lines. The greater barn slopes indicate a greater increase in biomass and canopy thickness with a relatively small increase in LAI. This is explained well by the emergence of woody biomass in the mature barn ecosystems—instead of energy resources being put into making leaves for LAI increase, ecosystems invest energy in making branches dense and woody. As the green cloak matures, significant increases in canopy growth may occur without significant increases in LAI.

In addition to barns having greater regression slopes than cloaks, barns also had greater leaf area indices and species count. We believe higher leaf area indices are achieved when multiple species are used because diverse species have diverse leaf shapes and sizes allowing species with small leaves to grow in gaps left by species with larger leaves. When the gaps are filled the canopies become more dense increasing leaf area index.

With increased LAI, light transmission decreased. Since low R^2 values were achieved for linear regression of barn and cloak light transmission, we tested logarithmic and exponential regression models. Figure 2.16a and 2.16b show improved R^2 values using logarithmic and exponential regression models for barn and cloak light transmission, respectively. The improved models have greater R^2 values and lower p-values. The results of the nonlinear regression models show that there are diminishing returns in light transmission with increasing leaf area index. Particularly with the cloak results, we see that for building energy savings applications a cloak leaf area index of 4 or 5 is sufficient given the limited decrease in light transmission with increased canopy LAI.

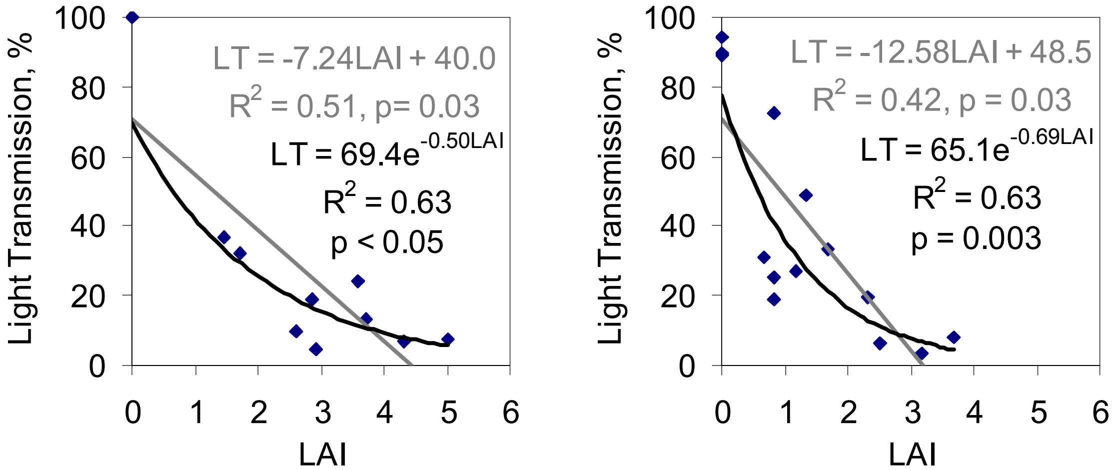

Figure 2.16. Curvilinear fit between leaf area and light transmission for barn (left) and cloak (right).

Design Implications for Green Cloak

We will use the trellis growth results and cloak barn ecosystem comparisons of this chapter to enlighten and improve our model scale green cloak design for future pilot scale application. Several of the cloaks achieved 100% coverage in less than one year of growth (Figures 2.6a-2.6k) leading us to believe that given the correct plant spacing and building size, a functioning cloak with approximately 100% trellis coverage would exist within two to three years given fall-winter dieback.

Along with recommending the use of a fairly tight wire mesh in the cloak trellis, we can use the thickness findings of this experiment to estimate a reasonable cloak-building spacing to protect the building surface. Since the barns' average and maximum canopy thicknesses were 69.7 cm and 121.7 cm, respectively, and given our observations of the cloak thickness measurements, we can assume that approximately one-third of the cloak vine canopy will hang below the wire mesh. One-third of the average and maximum barn thicknesses were 23.1 and 39.6 cm. Using a safety factor of 3 we recommend that the distance between the trellis and buildings roof be at least 1.2 m. In

Chapter 6, we have designed a pilot scale cloak with a 1.2 m (3.9 ft) cloak-building spacing.

The LAI time series results indicate that cloak vines will most likely surpass the barn average of 3.14 in 400 days (Figures 2.8a-2.8k). Of all the barns, Barn 8 had the maximum leaf area index of 5 and system species count of 4 (Tables 2.3 and 2.5). Extrapolating LAI increase in Figures 2.6a-2.6k, a leaf area index of 5 seems achievable within two to three growing seasons. We predict that with the use of multiple species, perhaps trumpet creeper and Virginia creeper, the high LAI would occur sooner when grown on a pilot scale cloak. We will use a leaf area index of 5 as an expected green cloak LAI in our indoor building temperature and runoff model application in Chapters 3 and 4.

Given that leaf area index correlated well with building temperature control (Chapter 3) and runoff reduction (Chapter 4) and biomass, thickness, and species count positively correlated with leaf area index, we learned that in future green cloak design and operation we should enable increases in these characteristics to maximize leaf area index to maximize green cloak function. Importantly, steeper barn biomass, thickness, and species count regression lines signified that as vine cloaks mature, less increase in leaf area index will occur with increased canopy growth. With this, we learn that an immature cloak may be able to function comparably to a mature cloak with similar LAI while having less biomass and canopy thickness.

Conclusion

Using ecological engineering techniques, we investigated the growth characteristics of an engineered vine community called the green cloak and its natural ecological analogue vine covered barns to learn about how vines grow in nature. We compared the growth rates of vines on trellises to the averages of the vines on barns. Using the data we collected, we estimated that a green cloak with a leaf area index of 5 (the maximum of the barns) could grow within two to three years. We recommend the use of two to three vines species to achieve high leaf areas and using a 1.2 m spacing between building roofs and the cloak's trellis. Finding that cloaks had slightly low leaf area indices with less biomass and canopy thickness, we believed that even a young green cloak could offer energy savings and runoff reduction benefits.

Chapter 3: Effect of Green Cloak on July Building Temperatures

Abstract

We compared the ability of our novel green cloaks to reduce building temperatures to conventional extensive green roofs. Our specific objectives were to evaluate the reduction of building temperature in both simulated and real climatic conditions and to perform regression analysis to determine which cloak growth characteristic controlled building temperature reduction most. Using two model buildings and seven green cloaks, we measured the indoor building temperatures under typical Maryland summer temperature and relative humidity conditions. Additionally, we compared indoor temperature reduction for each cloak to its leaf area index, canopy thickness, canopy cover, dead canopy leaves, and shingle roof temperature reduction. We found that green cloaks reduced maximum daily temperatures by as much as 3.1 °C, reduced roof temperatures by 23 °C, and that canopy cover and LAI were strong predictors of indoor building temperature reduction. These results showed the potential of the green cloak to save energy on a buildings cooling load and to extend the lifetime of asphalt shingles.

Introduction

Whether they were called green roofs or not, vegetated roofs were common hundreds of years ago in wet climates as an additional way to insulate homes from cold weather. Today, green roofs' energy performance is being evaluated to determine their precise ability to insulate buildings, shade buildings from summer heat, and to extend the life of expensive roofs. On a city scale, green roofs are expected to provide even more impressive results by limiting the intensity of the urban heat island (Bengtsson, 2005). The properties of direct building shading by plants, evaporative cooling through plant transpiration and media moisture evaporation, additional insulation values of plants, and growing medium, and thermal mass effects of growing medium are what make green roofs unique (Liu and Baskaran, 2003).

Green roofs are used to control the temperature of a building with the result of reducing heating and cooling energy costs. In summer months, green roofs are used to shade the building's roof from the hot sun's rays. In winter months, green roofs are thought of as an extra layer of insulation of the building's roofing system. A computer simulation program was used to examine the indoor air temperatures of buildings with and without green roofs during both the summer and winter. For example, in July at three in the afternoon, indoor air temperature was reduced by at least 10 ºC in a building with a green roof compared to a building with a traditional non-vegetated roof. A similar test was run in January at two in the afternoon. This time the indoor air temperature of a building with a green roof was approximately 1 ºC warmer than a building with a traditional roof (Ferrante and Mihalakakou, 2001). These results suggest that green roofs may work better in the summer to shade buildings than in the winter to insulate them.

Peck et al. (1999) saw a 3 to 4 °C (6 to 8 °F) drop under a green roof compared to a building without a green roof when outdoor temperatures were 25 to 30 °C (77 to 86 °F) (1999). In Toronto, Canada, it is estimated that with every 0.56 °C (1 °F) degree drop, air conditioning demand will drop 8% indicating that there could be a 48% to 64% drop in energy demand. Similarly in Maryland, a local power company predicts a 5% summertime energy demand decrease with each 0.56 °C (1 °F) increase in thermostat

(Pepco, 2005). In a one story Canadian building with a grass roof of 10 cm (4 in.), there was a 25% reduction in summer cooling needs (Peck et al., 2003).

Similar interior building temperature effects have been seen in other studies. Conducted in Rock Springs, Pennsylvania, six inches below the ceiling on a non-green roof building, the temperature exceeded 42 °C during the heat of the day when ambient temperatures reached 30 °C. Room temperatures in building with a green roof reached only 35 °C (Berghage, 2006).

This summertime room temperature decrease led to a decrease in air conditioning energy demand. The model buildings with extensive green roofs demanded 10% less electricity than buildings with flat black roofs (Berghage, 2006). These changes in energy demand will of course vary with location, season, and climate, and savings will increase in areas with higher cooling requirements.

Using Indian green roof building temperature data, a model was produced showing that a green roof of leaf area index 4.5 would reduce indoor air temperatures by an average of 5.1 °C over a 24 hour period. This translated to a 3.02 kWh reduction in energy demand per day. Additionally, air temperatures were most reduced in the green roof building during 1200 to 1500 hours when solar radiation peaked (Kumar and Kaushik, 2005).

Several studies have examined the benefits of green roofs on roofing membranes. With vegetation and substrate coverage, roof tops are protected from extreme high and low temperatures, diurnal temperature swing, UV rays, and freeze-thaw action that cause disintegration, cracking, and splitting of roofing materials (Dunnett and Kingsbury, 2004). Immediately above the waterproofing membrane, a non green roof reached 70 °C in June in Pennsylvania. On an extensive green roof, the temperature only reached 30 °C which was several degrees less than ambient air temperature (Berghage, 2006). This sort of surface temperature difference will lead to cooler indoor temperatures.

A field study was conducted to understand the thermal properties of an actual green roof located in Singapore. A maximum roof surface temperature reduction of 30 ºC was found compared to the surface temperature of a traditional roof. Temperature reduction varied with plant type and density. Leaf area index (LAI), a ratio of leaf area to ground area, was used to quantify these differences. Denser plants, like trees and shrubs, were recommended but warned about since they require more soil and thus a stronger roof (Wong, 2002). The planted roof showed less heat transfer than the traditional roof and the soil-only roof (Wong, 2002).

In Toronto, CA, conventional roof temperatures reached 70 °C (158 °F) while temperatures on the green roof membrane were only 25 °C (77 °F) (Liu and Baskaran, 2003).

Kolb and Schwartz (1986) saw diurnal temperature variations of up to 94% of daytime highs on conventional roofs. A rooftop of central European wildflower meadow diminished temperature extremes by 12 °C. Temperatures were overall 67% higher for the vegetated rooftop. Upon comparison of vegetation types, it was found that diversity in grasses was good because they provided greater height complexity trapping pockets of insulating air in the roof (Kolb and Schwartz, 1986).

In Singapore, a paved rooftop saw a daytime temperature peak of 57 °C (135 °F) and a maximum diurnal temperature fluctuation of 30 °C (86 °F). The green roof covered in *Raphis*, a palm, experienced a daytime high of 27 °C (81 °F) and only a 3 °C (6 °F) temperature fluctuation from day to night (Dunnett and Kingsbury, 2004).

At a talk by Robert Berghage (2006), Penn State Center for Green Roof Research leader, he said that in some climates, as in the eastern United States, there is a possibility that the summer insulation benefits could actually balance out with the winter insulation sun shielding drawbacks on the individual building scale. He professed that green roof benefits would be found on a city scale in which peak summer demand for a utility would be decreased when a significant majority of the buildings had green roofs. This would help alleviate peak demand and distribution problems that often arise in the summertime.

This benefit of green roofs has been realized in Tokyo where mitigation of their Urban Heat Island is a goal. In 2001, a law was passed requiring that all buildings over 1000 m^2 (10,760 ft^2) roof area must have at least 20% vegetation roof coverage. Their aim is to have 1200 ha of green roof by 2011 reducing the city air temperature by 1 °C (1.7 °F) (*Green Roofs Infrastructure Monitor*, 2001).

Reflective "cool" white roofs have also been used in an attempt to reduce energy needs. Roof materials are simply painted a reflective color reducing summertime energy needs by up to 40% (Dunnett and Kingsbury, 2004). A study in Nevada predicted only a 1% decrease in energy needs on cool roof buildings (Akbari, 2001).

Peck et al. (1999) calculated that 20 to 40 cm (8 to 16 in.) tall grass in 20 cm (8 in.) substrate is the insulation equivalent of 15 cm (6 in) mineral wool insulation. With this, green roofs and façade greening have a benefit that cool roofs do not have in the wintertime reducing building costs by not needing as much wool insulation.

Additionally, building costs can be reduced by decreasing the size of the air conditioning equipment needed (Peck et al., 1999).

Some thermal research has been done on the use of vines on walls as façade greening techniques. Again, vegetation is used to protect a building surface. The surface temperature fluctuation observed in Peck's study was a 50% decrease in temperature fluctuation (Peck et al., 1999). Specifically, temperature fluctuations at the wall have been decreased between 5 °C (9 °F) and 30 °C (54 °F) to 10 °C (18 °F) and 60 °C (108 °F) (Peck et al., 1999).

Of course this surface temperature decrease will lead to an indoor temperature decrease. It is estimated that a 5.5 °C (9.9 °F) temperature decrease immediately outside a building will reduce indoor air conditioning needs by 50 to 70% (Peck et al., 1999).

As species in green roofs can be explored for their thermal benefits, particular species can also be chosen for façade greening. It is recommended that in climates with cold winters, deciduous climbers should be placed on walls limiting summer solar radiation but welcoming warming winter radiation. Evergreen climbers should be placed on walls that do not get sun for all year benefits (Dunnett and Kingsbury, 2004).

Evergreen climbers provide winter insulation by maintaining an insulating air pocket between vegetation and wall and block chilling winter winds. It is estimated that 30% of a building's heating bill may be due to winter winds (Dunnett and Kingsbury, 2004). Limiting wind chill to a building by 75% can result in a 25% heat bill reduction (Dunnett and Kingsbury, 2004). Additionally, it is hypothesized that the insulating properties of deciduous climbers may not improve as a canopy gets older. For example, German research indicated that English ivy (*Hedera helix*) was most effective at a thickness of 20 to 40 cm (8 to 16 inches) while the canopy was still composed of dense insulating stems rather than large sparse woody branches (Dunnett and Kingsbury, 2004).

Due to plant evapotranspiration, green roofs are more thermally beneficial in the summer or in areas with year round heat. Additionally, deciduous vines have been shown to be productive in façade greening applications blocking summer sun, but permitting winter radiation.

Objectives

The objectives of this study were to:

1. Determine how much the green cloak reduced daily indoor building temperatures under simulated and real summer climatic conditions.
2. Determine whether the leaf area index, thickness, or percent cover of the green cloak's vine canopy had an effect on daily indoor building temperature.

Materials and Methods

System Description

The experimental system was designed so that we could measure how much a cloak can reduce indoor building temperature. We first measured house temperatures under simulated conditions in an environmental chamber. Second, we measured house temperatures under real temperature conditions outside during Summer 2006. To this end, we used two model plywood houses and seven model green cloaks of varying leaf area indices to individually measure indoor building temperature differences between the house with a cloak and the house without a cloak. We built the model houses (1.75 m x 1.5 m x 1 m) with 2” by 4” (5.1 cm by 10.2 cm) wood-framing and ¾” (1.9 cm) plywood floors, walls, and roofs. We covered the plywood roofs with standard black asphalt shingles (GAF Materials Corporation). Each house had three plexiglass covered windows and one door. We painted the outside of the houses white. We added fiberglass insulation (Owens Corning, R-13) to the ceilings and walls after the environmental chamber experiment, but prior to the outdoor experiment (Figure 3.1).

Figure 3.1. Scaled model plywood houses with shingled roof.

We built frames for the green cloaks from ¾ inch diameter polyvinylchloride (PVC) tubing (Charlotte Pipe and Foundry Company). Using 16-guage wire, we constructed a grid of 6 inch (15.2 cm) squares on each frame to serve as a trellis for vine attachment (Figure 3.2). Green cloaks were designed to fit over the top of the model houses with about a 20 cm gap between vegetation and the asphalt shingles (Figure 3.3).

Figure 3.2. Green cloak composed of PVC frames, wire trellis mesh, and potted vines.

Figure 3.3. Green cloak fit over model house with 20 cm gap.

For the vine growth experiment in Chapter 2, we grew eleven green cloaks with one vine species on each green cloak (Figures 3.4 and 3.5). Of the eleven cloaks, seven of them were available at the time of the temperature experiments. In the environmental chamber experiment, we used Kudzu 1 (K1), Porcelainberry (PB), Virginia Creeper 1 (VC1), and Virginia Creeper 2 (VC2). In the outdoor experiment, we used Cross Vine (CV), Japanese Honeysuckle (JH), Kudzu 2 (K2), Virginia Creeper 1 (VC1), and Virginia Creeper 2 (VC2).

Figure 3.4. Kudzu 2 green cloak.

Figure 3.5. Eleven green cloaks comprised of nine vine species.

Experimental Design

To determine how much the green cloak reduced indoor building temperatures under simulated summer climatic conditions, we placed the scaled buildings and the green cloak in environmental growth chambers (Environmental Growth Chambers, Chagrin Falls, OH), which were set to emulate an average July diurnal temperature curve (Figure 3.6). Chamber lights (incandescent and fluorescent) were set to represent the diurnal change in photosynthetically active radiation (PAR) with five stages: night, sunrise and sunset, morning and late afternoon, late morning and afternoon, and noon (Figure 3.6). Due to a mechanical problem with the heating and cooling units, we were forced to indirectly affect indoor temperature by controlling the lights. This produced a diurnal temperature curve closely resembling a July day in Maryland. Average temperature and humidity values were taken from five years of hourly raw July data recorded in Baltimore, MD. Temperatures were averaged to “typical” hourly July conditions (Local, 2006).

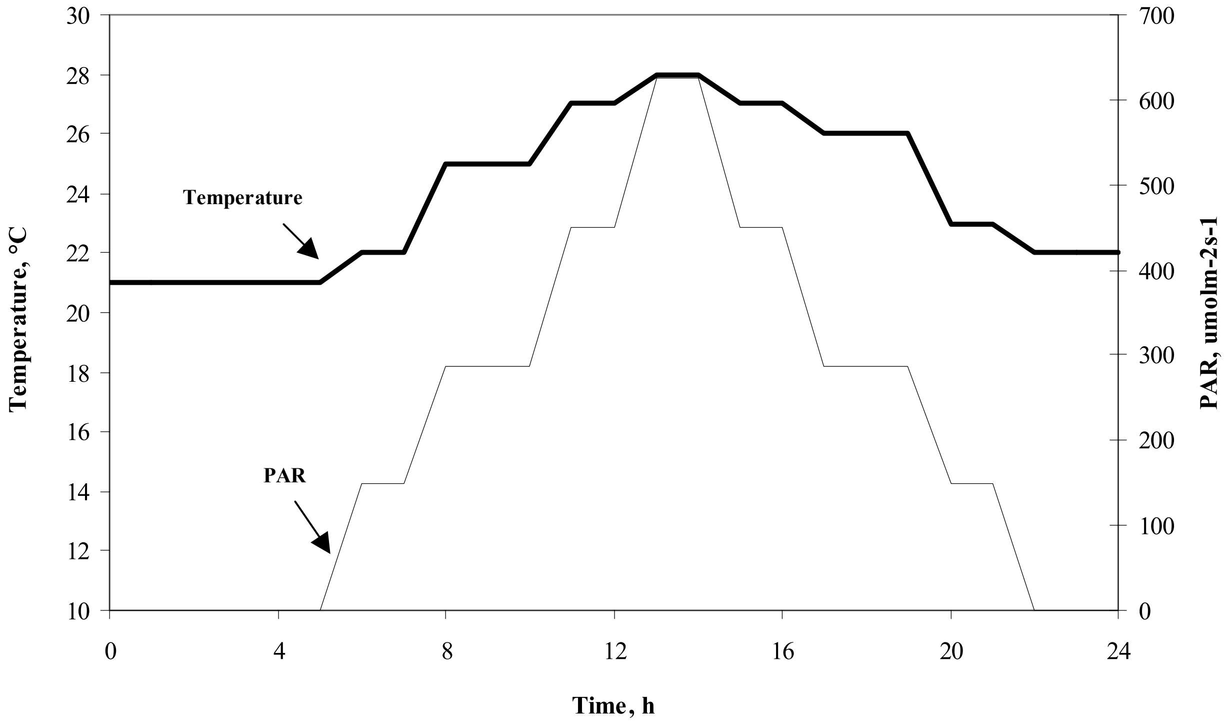

Figure 3.6. Temperature and photosynthetically active radiation (PAR) settings in environmental chamber.

House-models were placed in the environmental chamber and temperature and relative humidity of each building and the environmental chamber were recorded each minute (Figure 3.7). Before placing a green cloak over either house, we determined if there was any difference in daily temperature gain between the two houses. During the experiments a cloak was placed over one building (experimental building) while nothing was placed over the other (control building). The experiment proceeded for a period of three days as temperature and relative humidity values of each building were recorded every minute. At the end of the three day period, the cloak was placed over the other building and measurements were repeated for another 3 day period. Over a period of approximately 8 weeks, four cloaks with three different species and various leaf area indices were tested for a total of 24 days. Vines were watered every other day and fertilized (Jack's 20-10-20, Allentown, PA) once a week.

Figure 3.7. Virginia Creeper 2 shown in the environmental chamber during temperature experiment.

To determine how much the green cloak reduced hourly indoor building temperatures during real summer climatic conditions, we moved the houses and cloaks to an outside area near the greenhouse (Figure 3.8). We added fiberglass insulation (R-13) to the house walls and ceilings before conducting the outside temperature experiments. We conducted outside experiments during June, July, and August of 2006. House-models were placed outside in full sun. Similar to the indoor chamber experiment we tested whether there were differences in the diurnal temperature changes of each house.

During outside experiments a cloak was placed over one building (experimental building) while nothing was placed over the other (control building). After four days of temperature and humidity measurement the cloak was placed over the other building and measurements were continued for second four day period. Over a period of approximately 10 weeks, five cloaks with four different vine species and various LAIs were tested for a total of 40 average mid-summer day cycles. We watered cloaks daily and fertilized (Nutricote 18-6-8, Bellevue, WA) once every 180 days.

Figure 3.8. Model houses outside during the outdoor temperature experiment.

Data Collection

Model building and environmental chamber temperature and relative humidity measurements were taken using three Dickson TX120 data loggers (The Dickson Company, Addison, IL). Measurements were taken every minute for a period of 72 hours during indoor experiments and a period of 96 hours during the outside experiment. Control Net data logging software (Environmental Growth Chambers, Chagrin Falls, OH) was used to record PAR and to control chamber temperature and relative humidity.

Once during each cloak trial, we measured roof temperatures of the experimental and control buildings in the heat of the day using a UEi PDT550 Handheld Digital Thermometer (Beaverton, OR). We measured roof temperature in the middle of each roof wedged between shingles.

We measured percent cover and average and maximum canopy thickness once during each cloak trial. Plant health was also observed and quantified as a measure of percent senescent leaves.

Data Analysis

For both the environmental chamber and outdoor experiments, first the indoor temperatures of the model buildings without cloaks were compared to determine what temperature difference existed solely due to model building construction or solar orientation. For each minute of the preliminary house temperature trial, we subtracted the two house temperatures from one another. We averaged the building temperature differences into one 24-hour (1440-minute) temperature set so that at each minute of a day, we knew the average building temperature difference. Prior to experimental data analysis, we added the temperature difference of each minute to the indoor building temperature of the cooler building to make the buildings thermally equivalent. For example, if at 12:00 am House 1 was on average 0.5 °C warmer than House 2, we added 0.5 °C to House 2's temperature at 12:00 am on all cloak trial days. We repeated this for all 1440 minutes of the day so that all experimental indoor air temperatures were corrected.

To determine the ability of each cloak to control indoor building temperature, the temperature difference between the control and experimental buildings was determined. At each minute of the trial, we found the temperature difference between the control and experimental houses. We averaged the temperature differences into one 24-hour temperature difference data set. In particular, we found the average and maximum daily temperature decrease due to each cloak.

Next regression was performed on the maximum temperature decrease compared to cloak leaf area index, average thickness, maximum thickness, cover, dead (senescent leaves), and roof temperature difference. We also performed regression on roof temperature difference compared to cloak leaf area index and cover.

Results

Temperature Dynamics of Experimental Houses

The mean difference in temperature between the two experimental houses when neither had a cloak was less than 0.5 ºC while in the environmental growth chamber (Figure 3.9a). However, when the same houses were placed outdoors the low angle of the sun at 1800 h caused the temperature of one house to rapidly increase forcing a 4 ºC difference for about one hour (Figure 3.9b). Therefore, we did not use post-1800 h data for the outside experiments. This same data were excluded from model validation (Chapter 4).

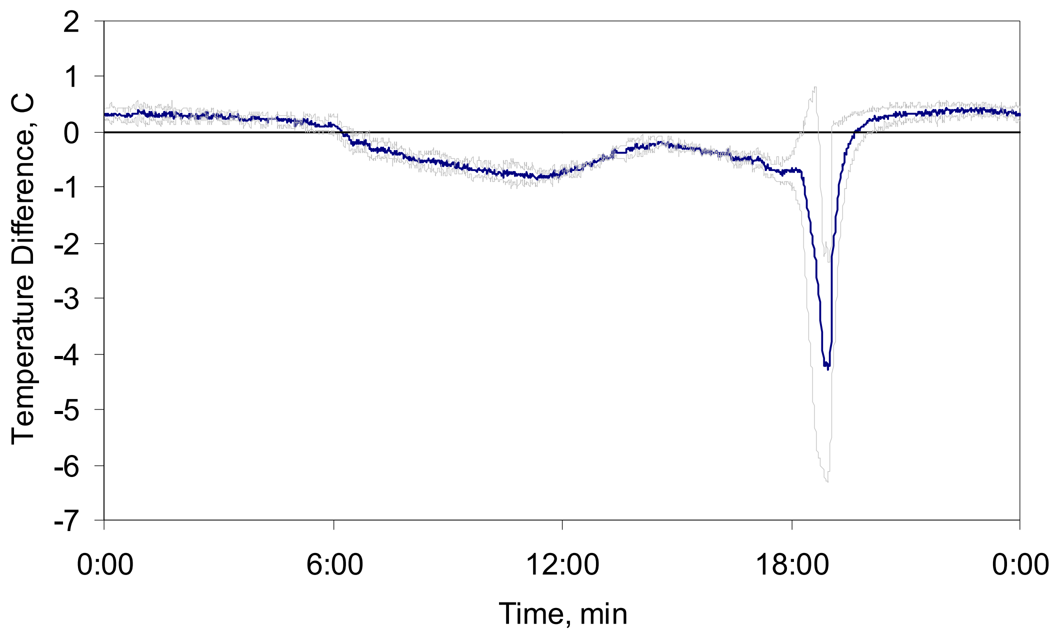

(a)

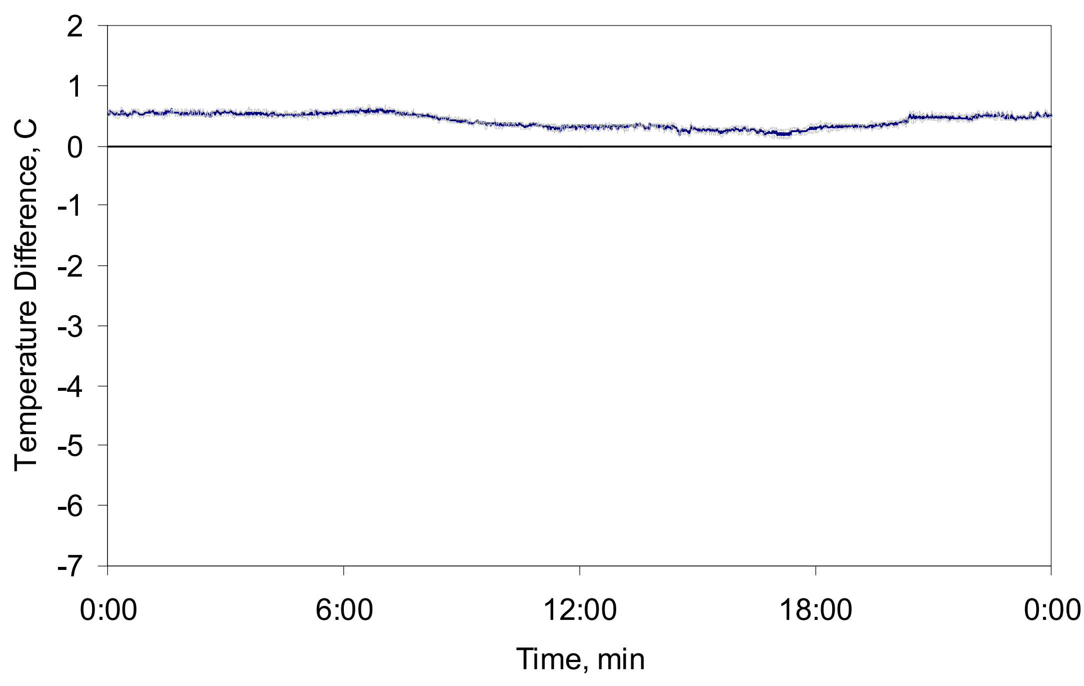

(b)

Figure 3.9a and b. Temperature difference between model buildings without cloaks in environmental chamber (a) and outdoor (b) temperature experiments. Standard deviation (light) shown above and below temperature difference (dark) curve.

Diurnal Temperature Reduction from Green Cloak

Houses with green cloaks had indoor temperatures reduced by as much as 3.1 °C during a simulated a 24-hour solar loading cycle compared to control houses (Figures 3.10a-3.10d). Temperature reduction was lowest during the night and greatest in mid-afternoon. Porcelainberry (PB) and Virginia creeper were the two species with the greatest temperature reduction.

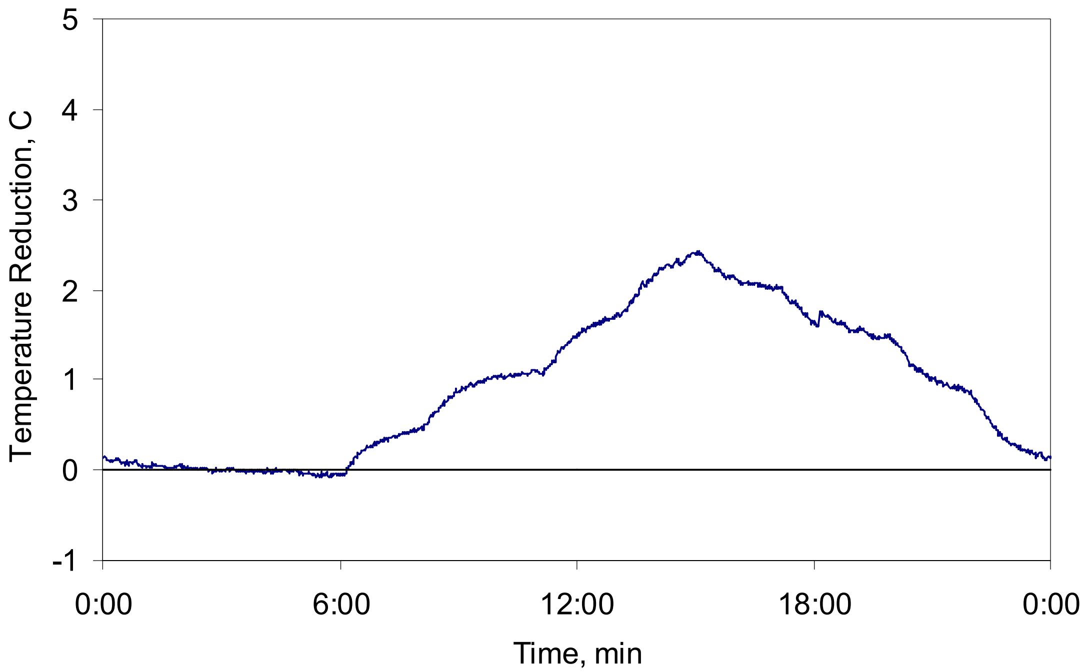

(a) Virginia creeper 2 (VC2)

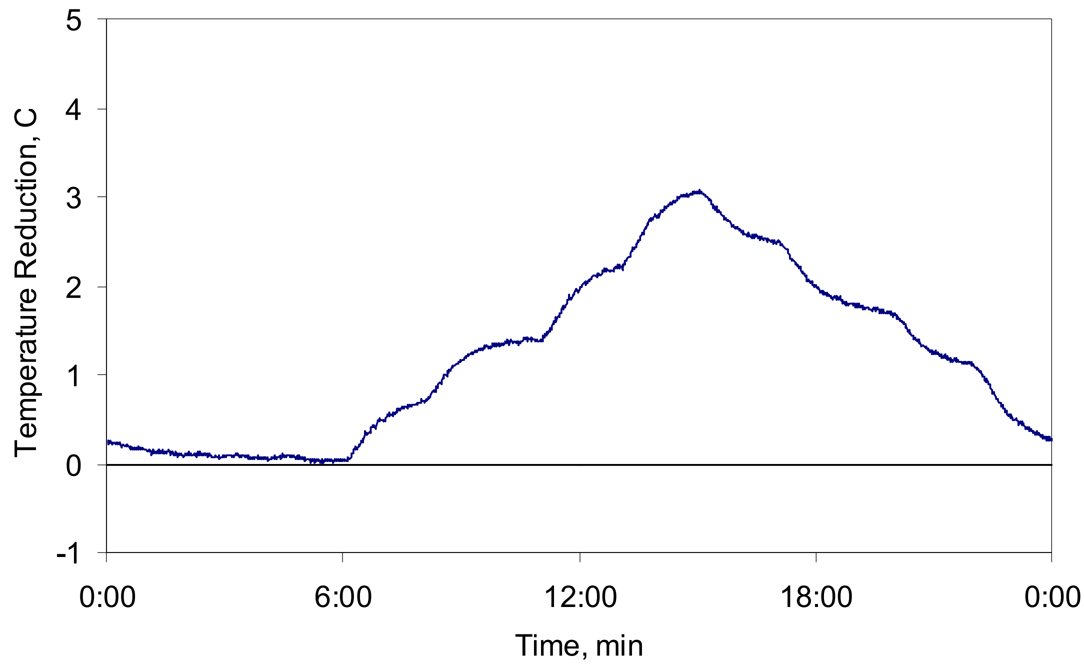

(b) Virginia creeper 1 (VC1)

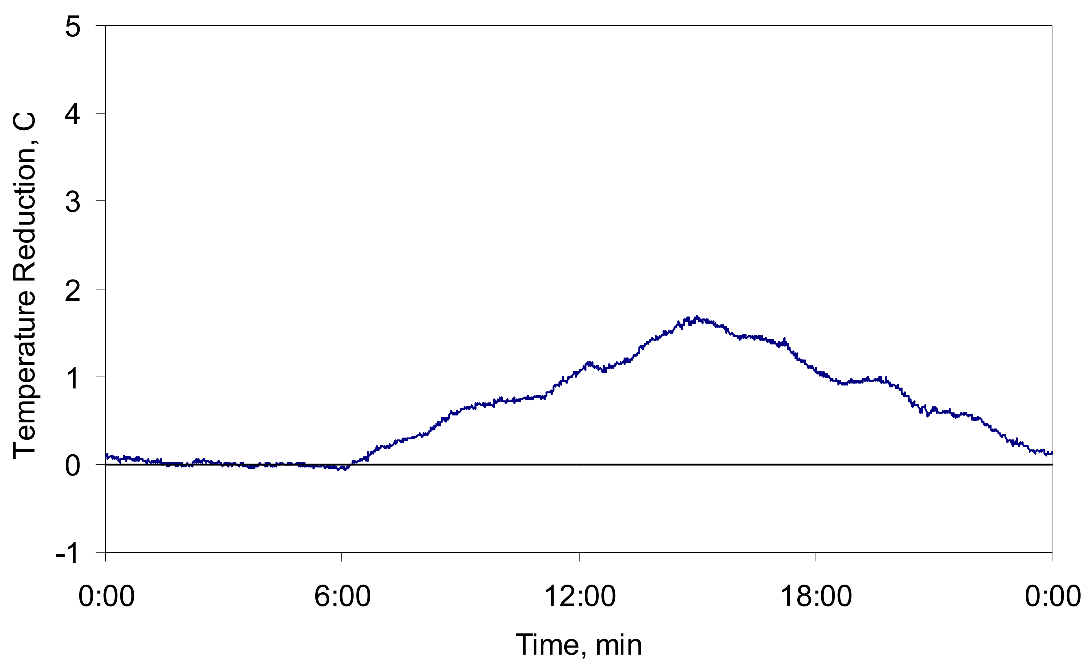

(c) Kudzu 1 (K1)

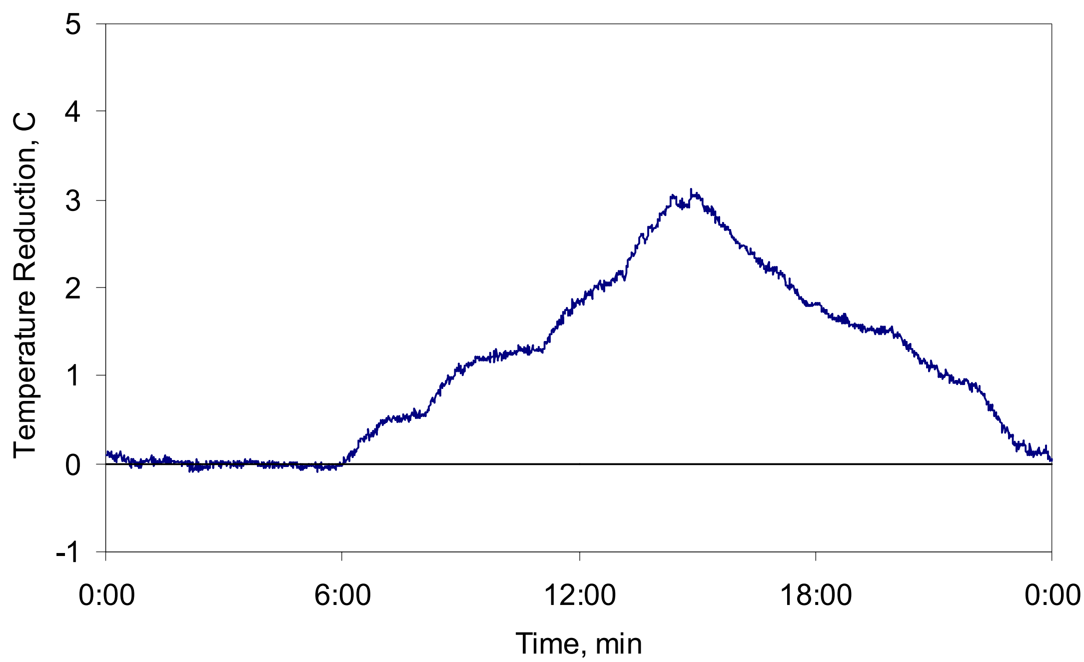

(d) Porcelainberry (PB)

Figures 3.10. House temperature differences during the experiment in the environmental chambers. The 24-hour temperature differences were found by subtracting the control house (without cloak) temperature from the experimental house (with cloak) temperature for each minute of the experiment. Temperature differences for each minute were averaged into one 24-hour data set and plotted.

Houses with green cloaks had indoor temperatures reduced by as much as 3 °C during the outdoor temperature experiment (Figures 3.11a-3.11e). Temperature reduction was lowest during the morning and late evening and greatest in mid-afternoon. Virginia creeper was the species with the greatest temperature reduction.

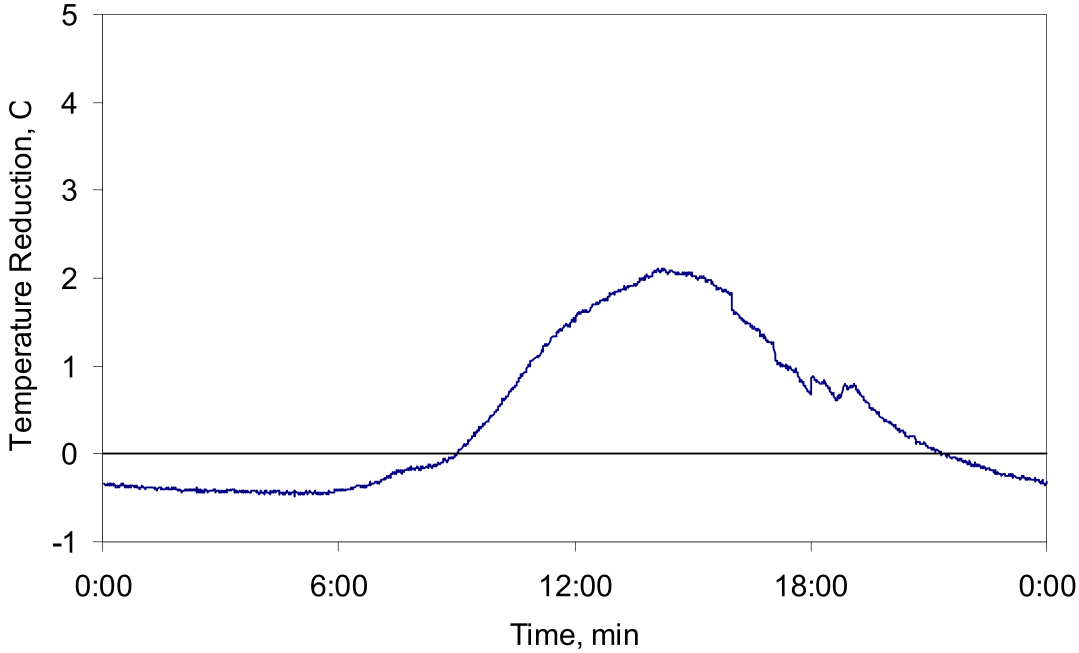

(a) Japanese honeysuckle (JH)

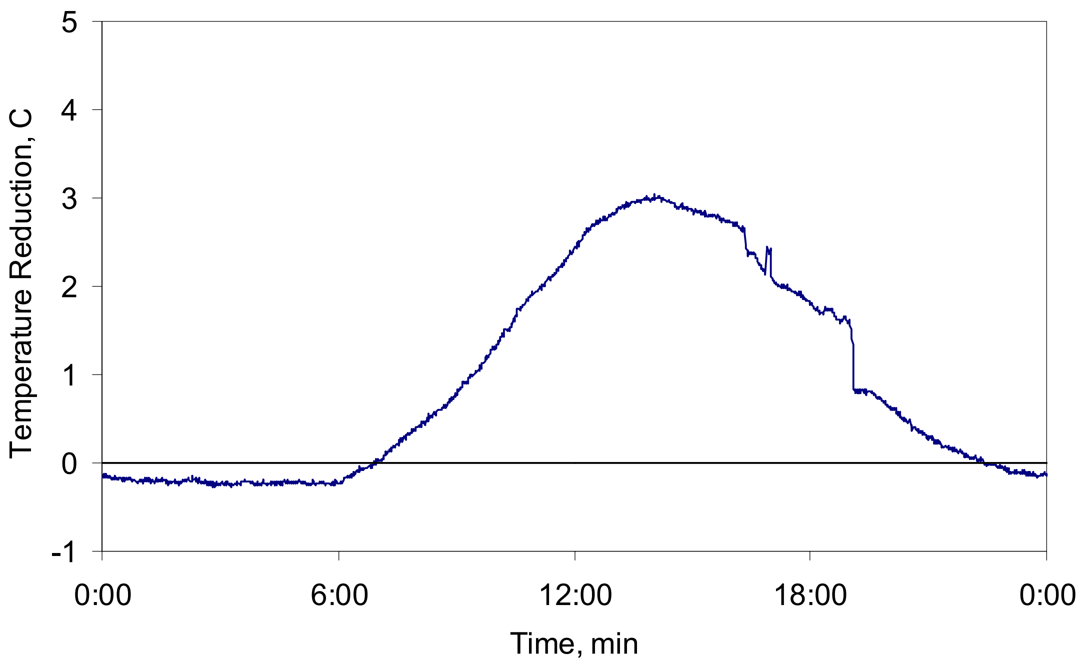

(b) Virginia creeper 1 (VC1)

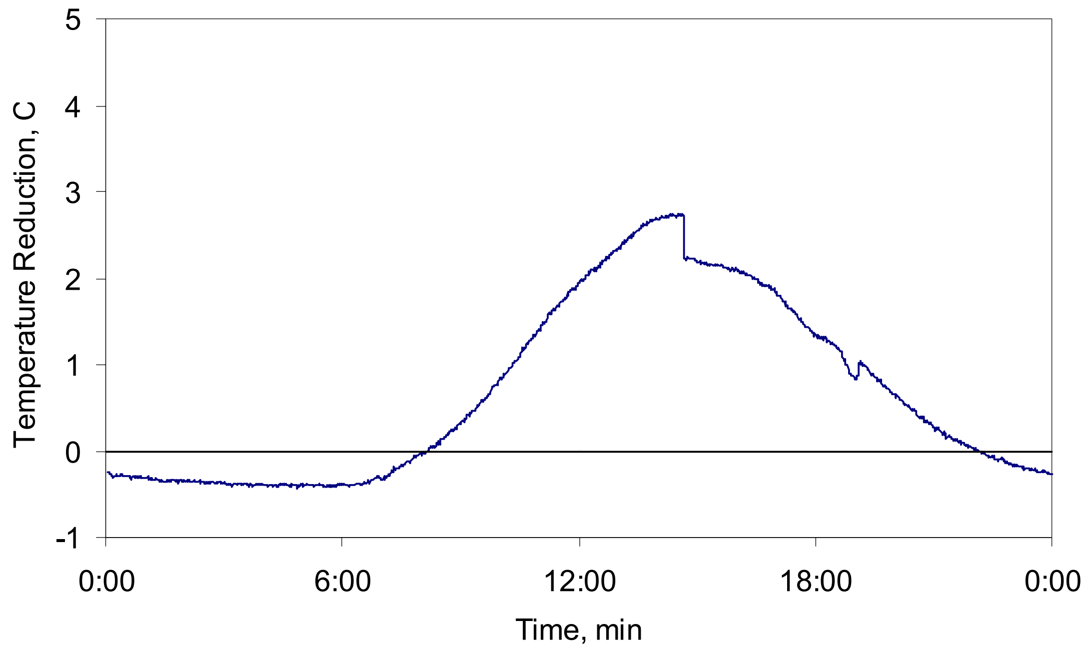

(c) Virginia creeper 2 (VC2)

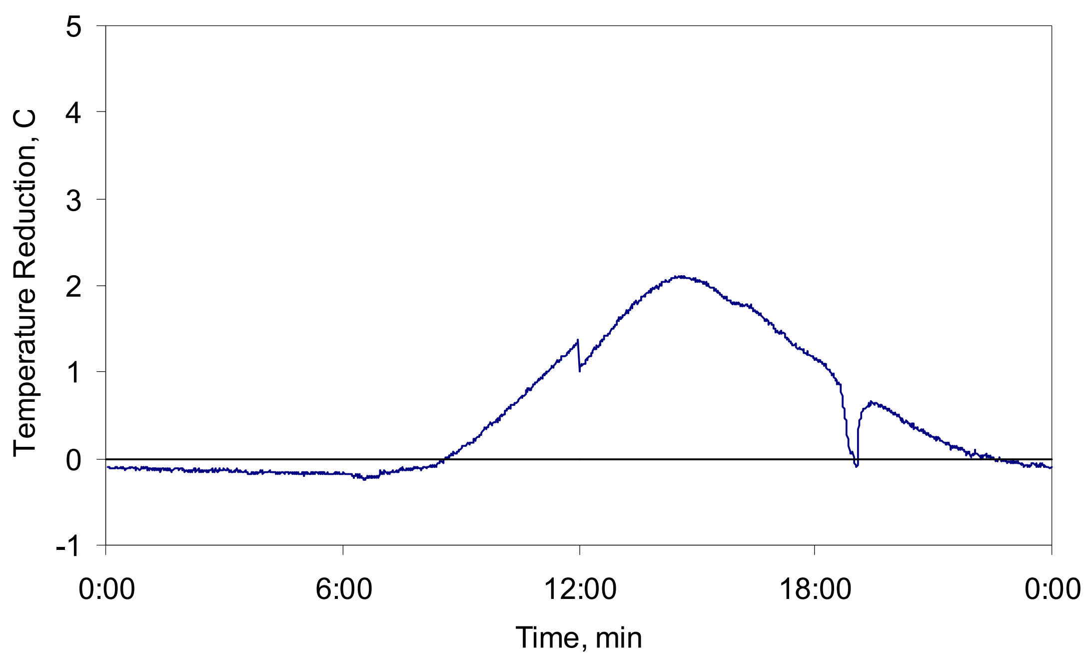

(d) Kudzu 2 (K2)

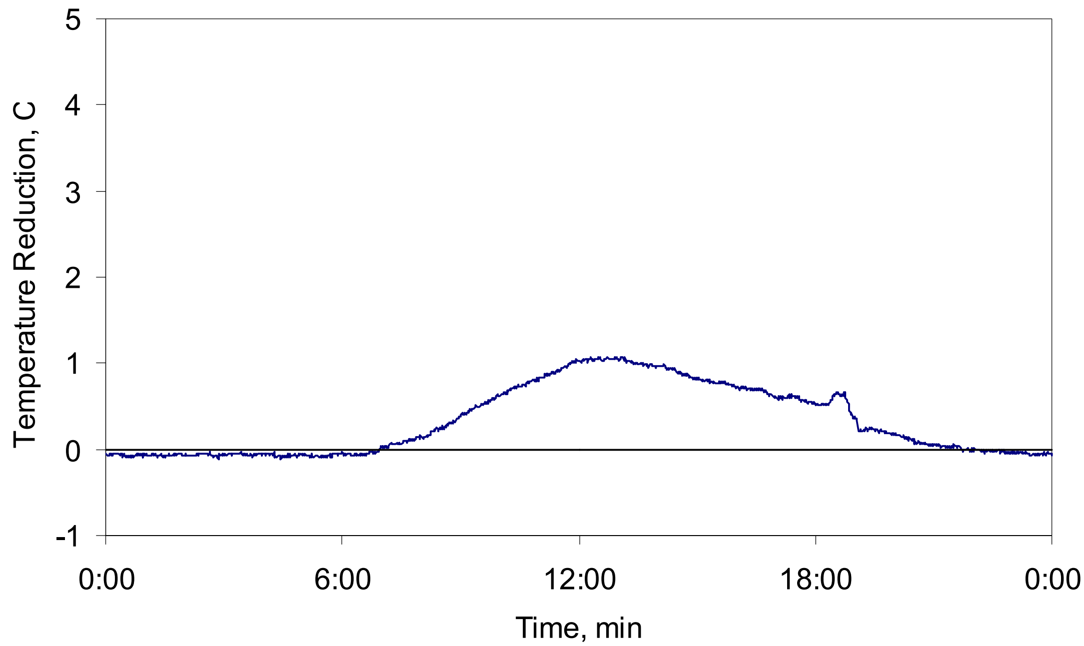

(e) Cross vine (CV)

Figures 3.11. House temperature differences during outdoor experiment.

Roof Temperature Reduction from Green Cloak

Houses with green cloaks had roof surface temperatures reduced by as much as 11 °C during the environmental chamber experiment and 23 °C during the outdoor temperature experiment (Table 3.1). Overall, both control and experimental roof temperatures were hotter during the outdoor temperature experiments.

Table 3.1. Roof temperature for control (without cloak) and experimental (with cloak) houses during the environmental chamber and outdoor experiments.

		Temperature, C		
	Cloak	**Control Roof**	**Experimental Roof**	**Reduction**
Chamber	**K1**	44	38	6
	PB	44	33	11
	VC1	42	31	11
	VC2	37	32	5
Outside	**CV**	61	57	4
	JH	53	38	15
	K2	62	50	12
	VC1	64	41	23
	VC2	54	31	23

Effects of Green Cloak Growth Characteristics on Building Temperature Reduction

We performed linear regression comparing indoor building and roof temperature reduction to several growth characteristics to find that leaf area index and vine canopy cover most strongly influenced building and roof temperature reduction. Tables 3.1 lists the cloaks tested along with their growth characteristics, and building and roof temperature reduction.

Table 3.2. Green cloak growth characteristics and maximum reductions in indoor temperature and roof surface temperature during experiments conducted in environmental chambers and outside. (LAI-leaf area index).

	Cloak	LAI	Cover, %	Dead, %	Average Thickness, mm	Maximum Thickness, mm	Maximum Temperature Reduction, C Indoors	Maximum Temperature Reduction, C Roof
Chamber	Control	0	0	0	0	0	0	0
	K1	1.2	70	90	70	120	1.7	6
	PB	3.7	100	5	100	170	3.1	11
	VC1	1.8	99	2	155	205	3.1	11
	VC2	1.4	100	0	200	240	2.4	5
Outside	Control	0	0	0	0	0	0	0
	CV	0.8	23	0	58	285	1.1	4
	JH	1.3	93	4	110	370	2.1	15
	K2	1.8	50	2	270	535	2.1	12
	VC1	2.3	90	1	160	230	3	23
	VC2	2	88	3	150	385	2.7	23

The indoor temperature of the house was strongly influenced by the LAI of the green cloak (Figures 3.12a and 3.12b). According to the regression equations, each additional unit of leaf area reduced indoor temperature by 1.0 to 1.3 °C.

The amount of vine cover also influenced indoor house temperature (Figure 3.13). The amount of senesced vegetation (dead) was not correlated to temperature reduction (Figure 3.14).

Average thickness of the green cloak's canopy moderately affected temperature reduction ($R^2 = 0.52$, $p = 0.013$). The weak correlation between maximum thickness and building temperature reduction was not significant ($R^2 = 0.28$, $p = 0.096$). (Figures 3.15 and 3.16).

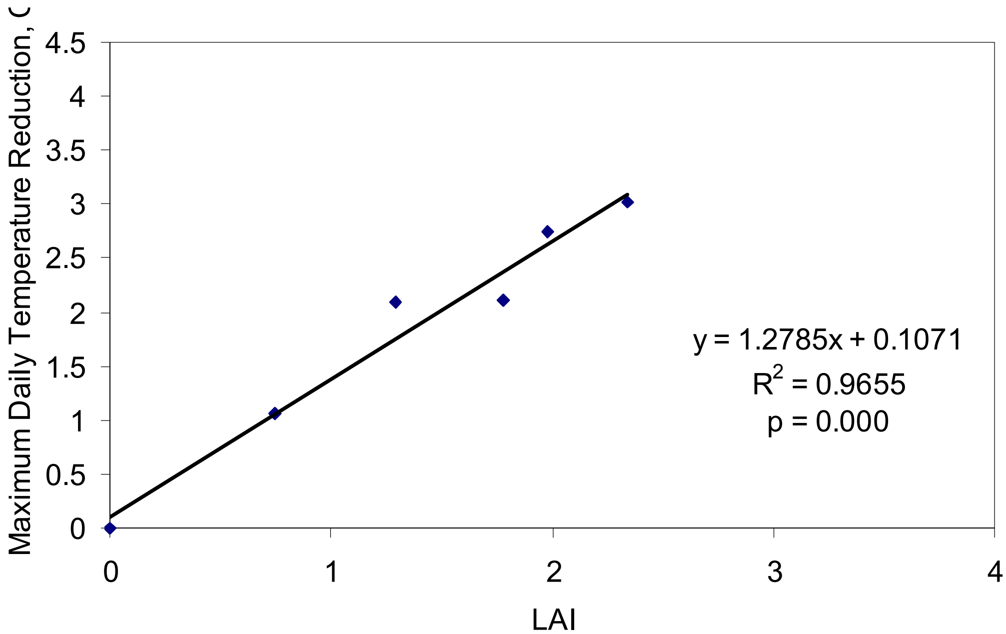

(a)

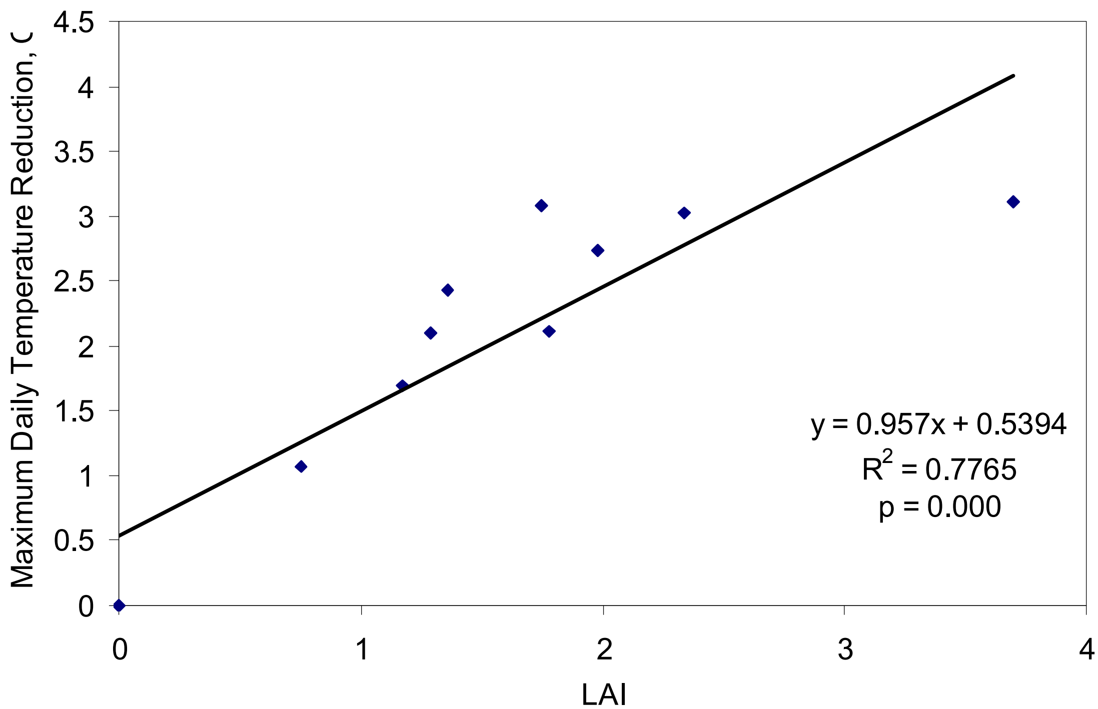

(b)

Figures 3.12. House indoor temperature reduction as a function of leaf area index (LAI) for data collected during (a) outside experiments and (b) both environmental chamber and outside experiments.

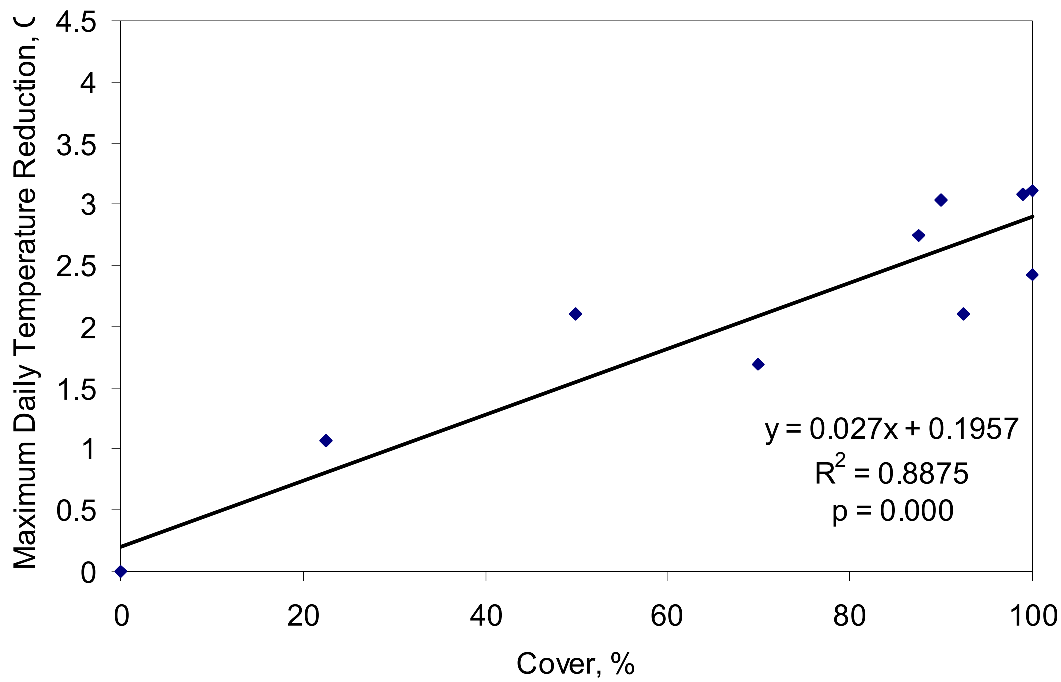

Figure 3.13. House indoor temperature reduction as a function of vine cover for data from environmental chamber and outdoor experiments combined.

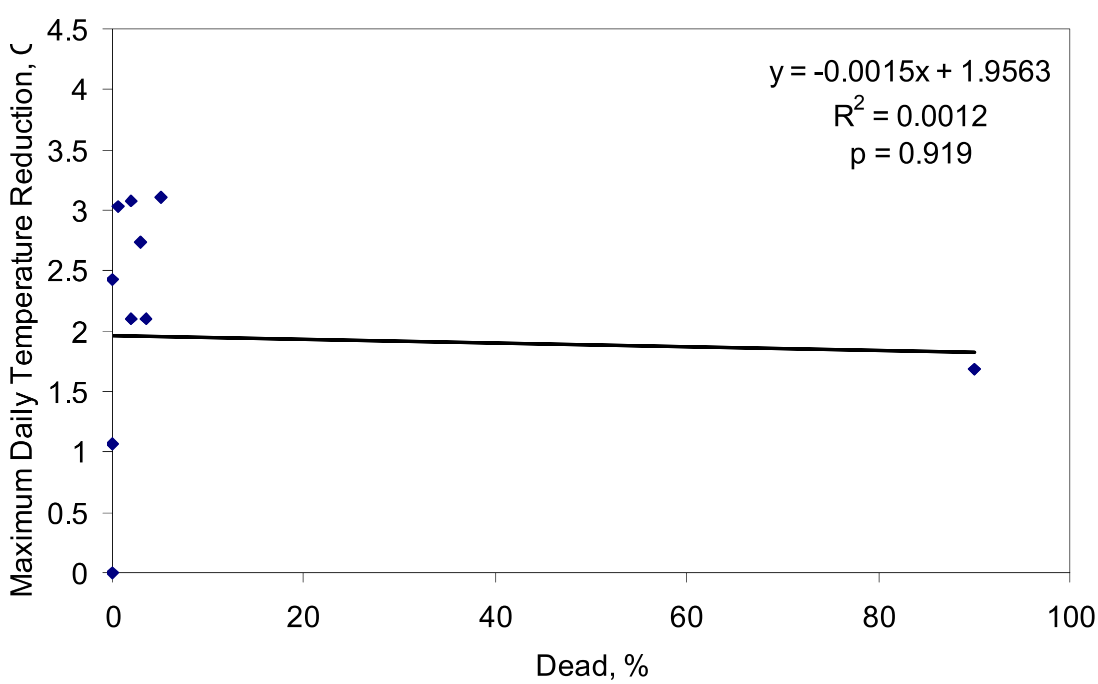

Figure 3.14. House indoor temperature reduction as a function of percentage of senescent (dead) canopy for data collected during environmental chamber and outdoor experiments combined.

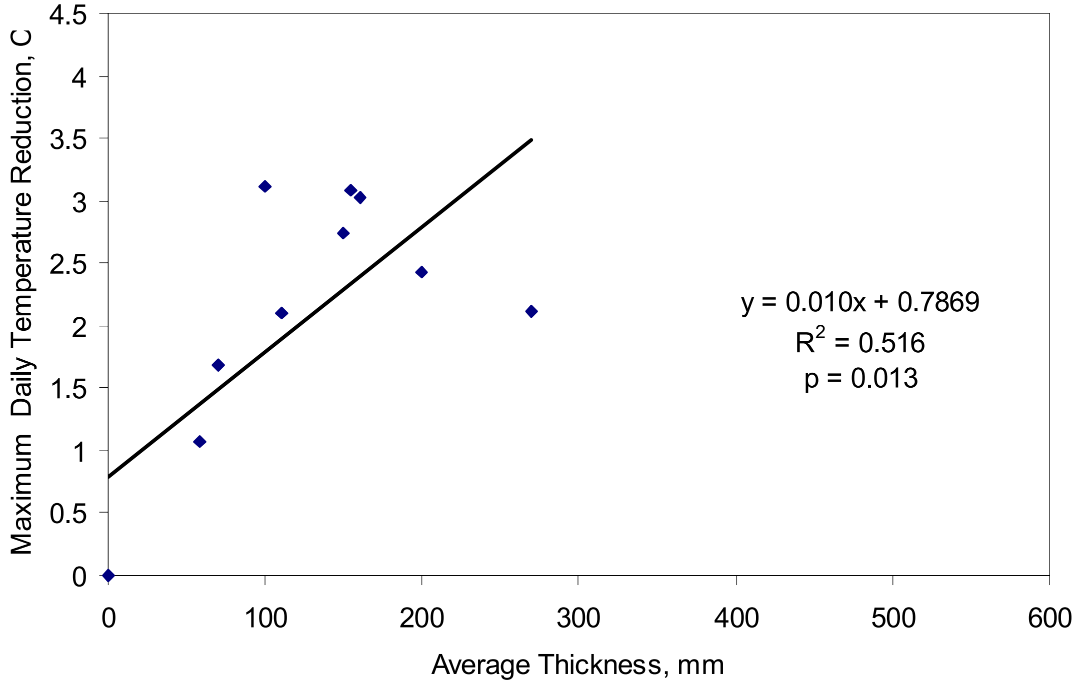

Figure 3.15. House indoor temperature reduction as a function of average canopy thickness for data collected during environmental chamber and outdoor experiments combined.

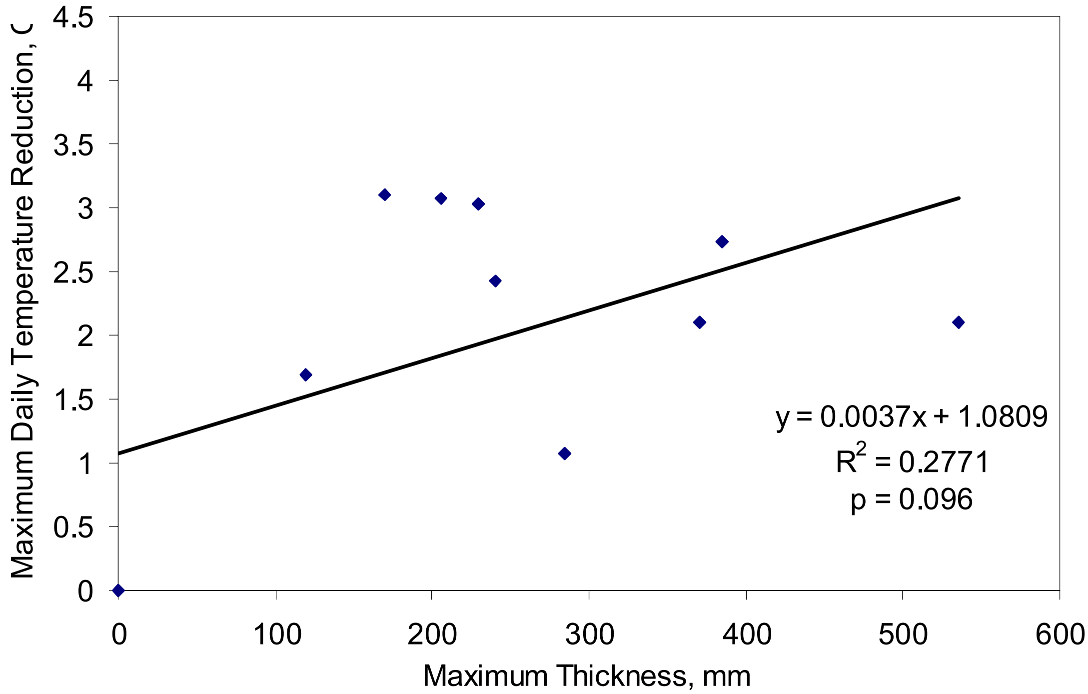

Figure 3.16. House indoor temperature reduction as a function of maximum canopy thickness for data collected during environmental chamber and outdoor experiments combined.

We found that roof temperature strongly influenced indoor building temperature (Figure 3.17). On at least two occasions the houses with the green cloak had roof temperatures that were nearly 25 °C less than the houses without the green cloak. This 25 °C difference corresponded to an indoor building temperature reduction of about 3 °C.

Higher leaf area index and more vine cover produced cooler roofs with $R^2 = 0.81$ and 0.78, respectively (Figures 3.18a and 3.18b).

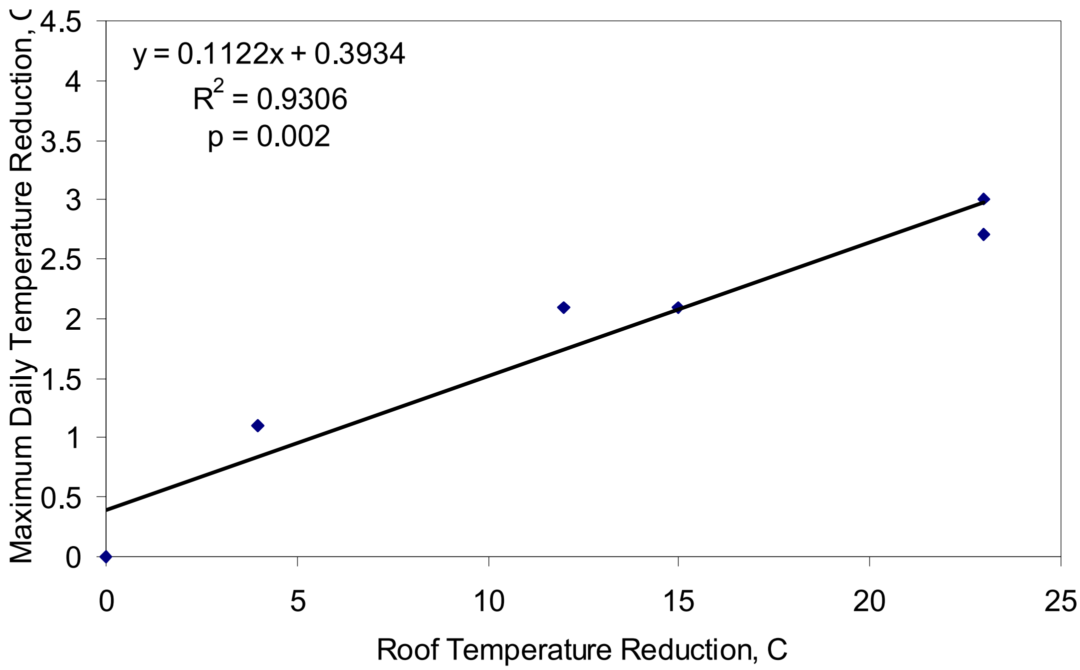

Figure 3.17. Temperature differences between cloak and no cloak house as a function of roof temperature reduction based on outside experiment only.

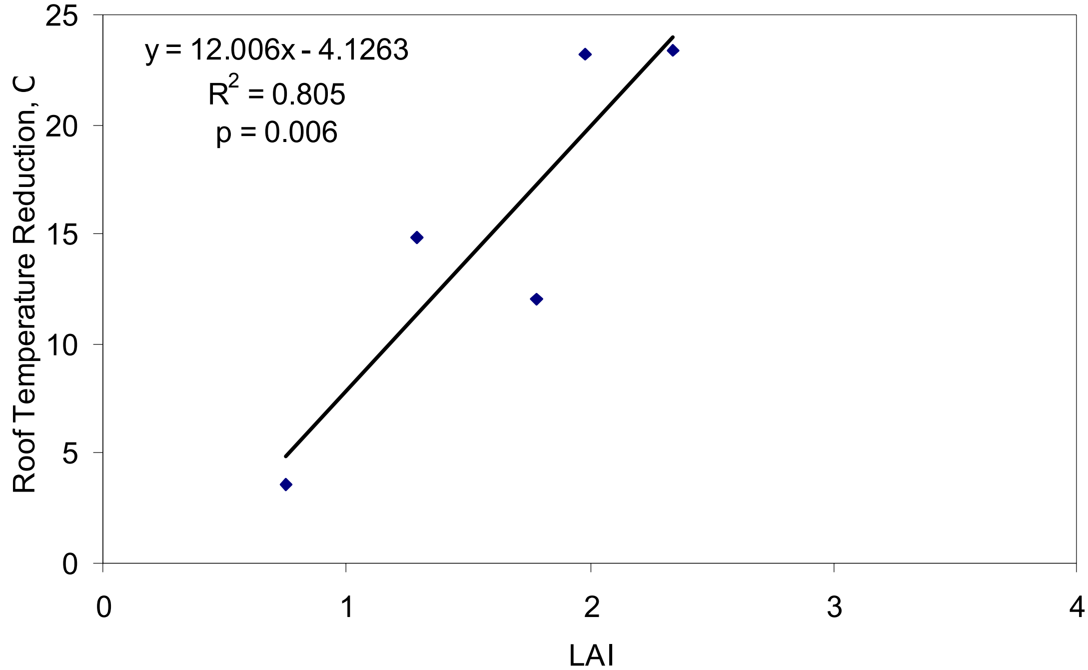

(a)

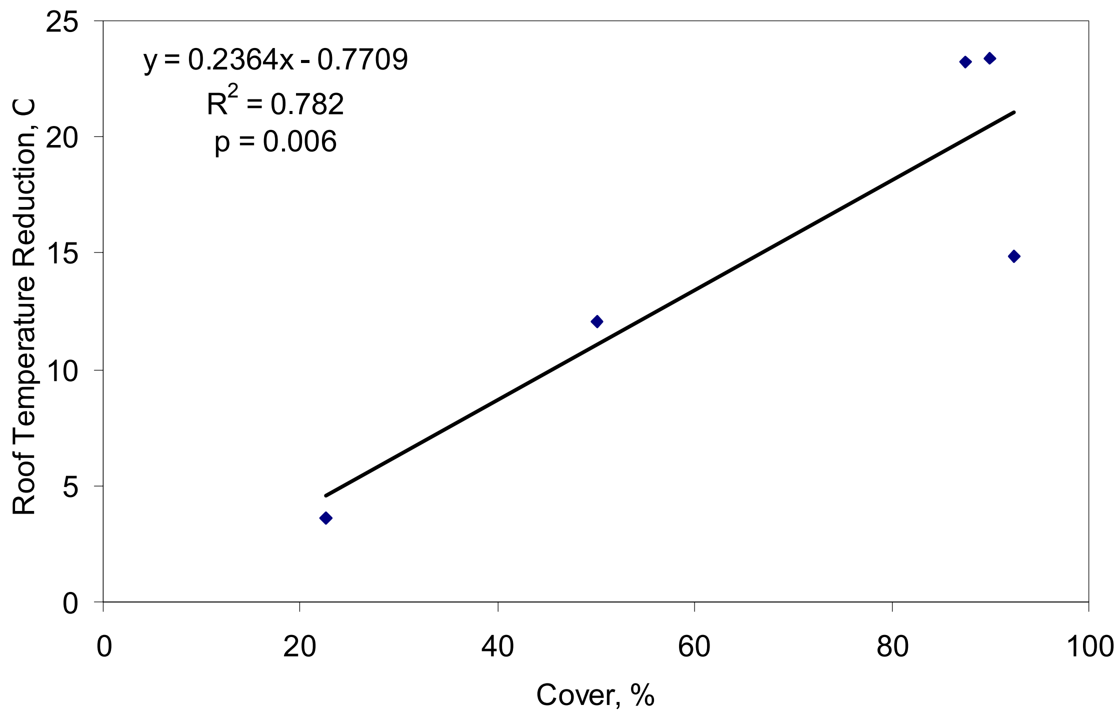

(b)

Figure 3.18a and 3,18b. Roof temperature difference between houses with and without a green cloak as a function of (a) leaf area index (LAI) and (b) vine cover based on data collected during outside experiment

Discussion

Indoor Temperature Reduction

It was seen that the maximum indoor temperature difference between control and experimental houses occurred during the day when temperature and solar radiation was greatest. During the environmental chamber experiment, the experimental houses always stayed cooler than the control houses with the exception of about one hour before chamber lights came on during the VC2 trial. During the outdoor experiment, the experimental houses were no more than 0.5 °C warmer at night than the control houses because the experimental houses could not dispel their energy as easily with the added cloak insulation. Of the environmental chamber and outdoor temperature experiments, the maximum indoor temperature difference occurred in the chamber with a 3.1 °C temperature reduction for the PB and VC1 cloaks. Indoor temperature reduction indicated that one-year old green cloaks can decrease indoor building air temperature. We developed a mathematical model that incorporated LAI to estimate the reduction in cooling load (Chapter 4).

Roof Temperature Reduction

The maximum roof temperature difference (23 °C) was experienced during the outdoor temperature experiment. We believe that roof temperatures differences were less in the environmental chamber because lighting was less intense in the chambers than outdoors to make up for malfunctioning chamber equipment. The roof temperature difference observed with the VC1 cloak of LAI 2.34, shows that a green cloak may have a significant ability to protect a roof from solar radiation prolonging the lifetime of the roof below. This finding will be used in the cost benefit analysis in Chapter 6.

LAI Predictive of Cover and Thickness

According to our linear regression, canopy cover and leaf area index most affected indoor house and roof temperature reduction. Leaf area index had the most control over roof temperature difference and roof temperature and indoor building temperature reduction positively correlated. We learned that to fully benefit from green cloak technology, we should design cloaks to optimize leaf growth and trellis coverage.

Chapter 4: Energy Model of Green Cloak Effect on Indoor Building Temperature

Abstract

We developed a mathematical model to predict indoor building temperature based on environmental air temperature, solar radiation, building dimensions, and cloak leaf area index so that we could determine the ability of the green cloak to lower temperature and energy consumption in a full-scale building. We calibrated and validated the model with temperature data recorded during the outdoor temperature experiments reported in Chapter 3. We applied the model to a one story 2000 ft^2 (185.8 m^2) house with a green cloak of LAI 2 to find a potential average daily building temperature decrease of 11.3 °C, a maximum temperature decrease of 13.1 °C, and an air conditioning energy consumption decrease of 72.9%. These results indicate that the green cloak is a comparable technology to green roofs from an energy savings standpoint and green cloak costs and benefits must be evaluated further.

Introduction

In our temperature experiments described in Chapter 3, we found a maximum reduction of 3.1 °C in the indoor air temperatures of a model house with a green cloak. This reduction was significant from an energy savings perspective and according to regression results, the reduction would have been more with a denser cloak. In this chapter we develop a mathematical model of indoor building temperature that includes environmental air temperature, solar loading, building dimensions, and cloak leaf area index. The model is used to estimate temperature decrease in an averaged sized home (2000 ft^2) for cloaks with various leaf areas. Furthermore, we used the model output to estimate building air conditioning energy reduction.

Objectives

Specifically, our objectives were to:

1. Develop a mathematical model that could simulate the hourly indoor temperature of a building covered by a green cloak based on solar loading, leaf area index of the green cloak, and ambient temperature.
2. Compare the temperature reduction and energy savings of the green cloak with the more established extensive green roof technology.

Model Development

We developed an energy systems-based model to simulate the temperature in model houses that were covered with green cloaks with various amounts of leaf area. In Chapter 3, both leaf area index and percent cover were highly correlated with indoor building temperature reduction. We chose to use leaf area index in the model because it was a more objective measurement and took into account both canopy thickness and coverage. Based on environmental air temperature, solar loading, canopy leaf area index, and building dimension, the model predicted changes in the amount of energy stored in the house (G).

Thermal energy in the house (G) was a balance between the solar load (S) that penetrated the green cloak canopy and convection of ambient heat into or out of the house (Eq. 1, Figure 4.1).

$$dG/dt = 60 \cdot S \cdot A \cdot k_1 \cdot \exp(-0.8802 \cdot LAI) + k_2(E - H)/R \qquad (1)$$

where dG/dt was the change in house thermal energy in J/min, S was the solar load in J/sec·m^2, A was the roof area of the building in m^2, k_1 was the solar loading coefficient (unitless), LAI was leaf area index, k_2 was the convective heat transfer coefficient from the environment to the house in min^{-1}, E was the environmental air temperature in °C, H was the house air temperature in °C, and R was thermal resistance of the house in °C·min/J.

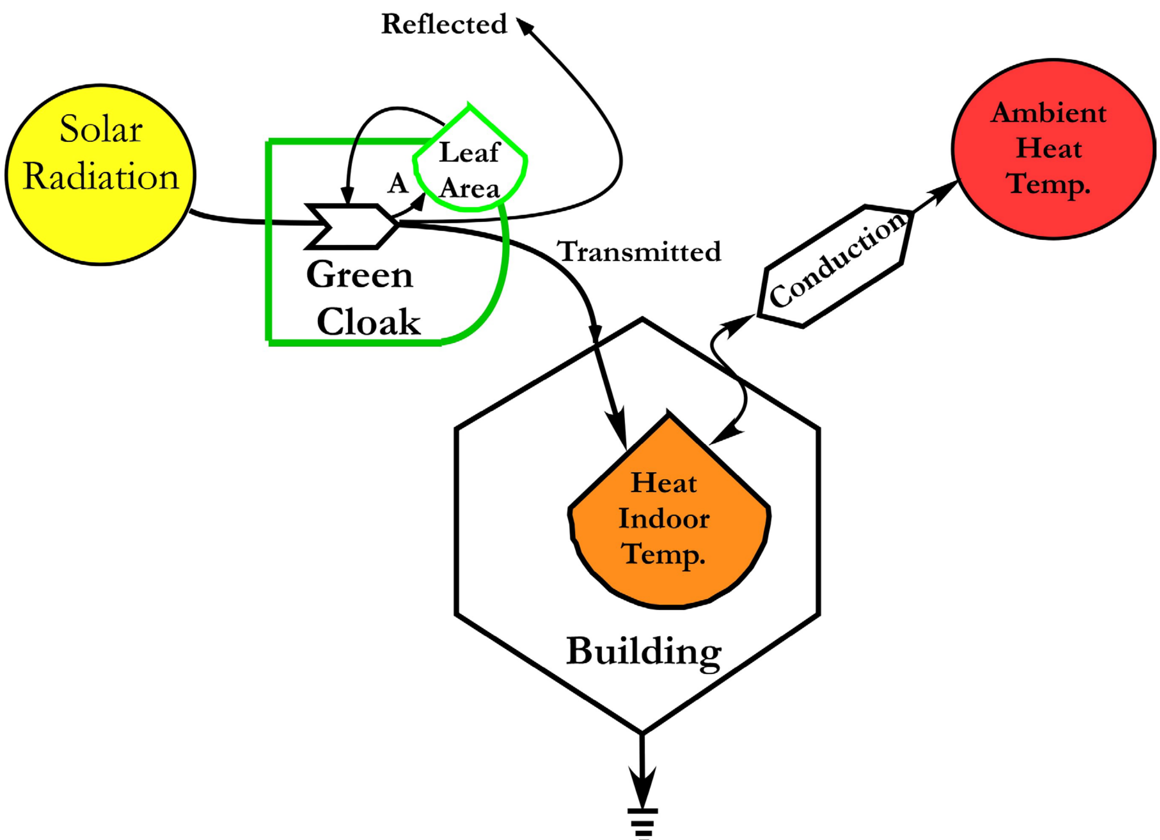

(a)

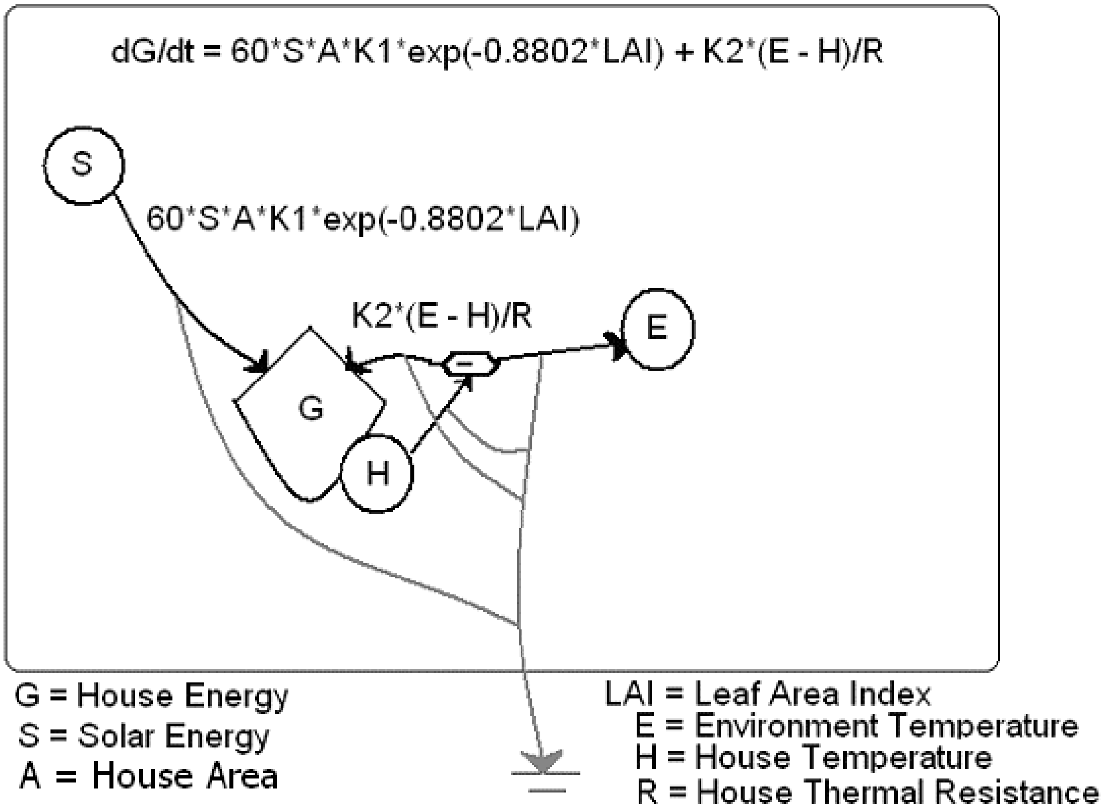

(b)

Figure 4.1. Energy systems diagram of the indoor heat balance (a) and the equations for the heat model.

The expression "60·S·A·k_1·exp(-0.8802·LAI)" represented energy loading of the house via solar radiation. S was the solar energy measured in units J/sec·m^2. Since the model's time step was in minutes, S was multiplied by both 60 sec/min and roof area in m^2 so that solar energy was in J/min. The cloak reduced solar energy entering the building from vine leaves reflecting solar radiation and heat absorption via evapotranspiration. Based on cloak leaf area index, the expression "exp(-0.8802·LAI)" represented the fraction of light transmitted through the green cloak and was derived from experimental data collected from the eleven green cloaks discussed in Chapter 2. There were also three control measurements made on a trellis with no canopy. Using Microsoft Excel, we fit an exponential curve to the data while forcing the y-intercept equal to 1.0 because with an LAI of zero there should be 100% transmission (Figure 4.2). In addition to the exponential curve, linear and logarithmic models were considered, but their R^2 values were not as high as for the exponential curve indicating it as the best-fit model.

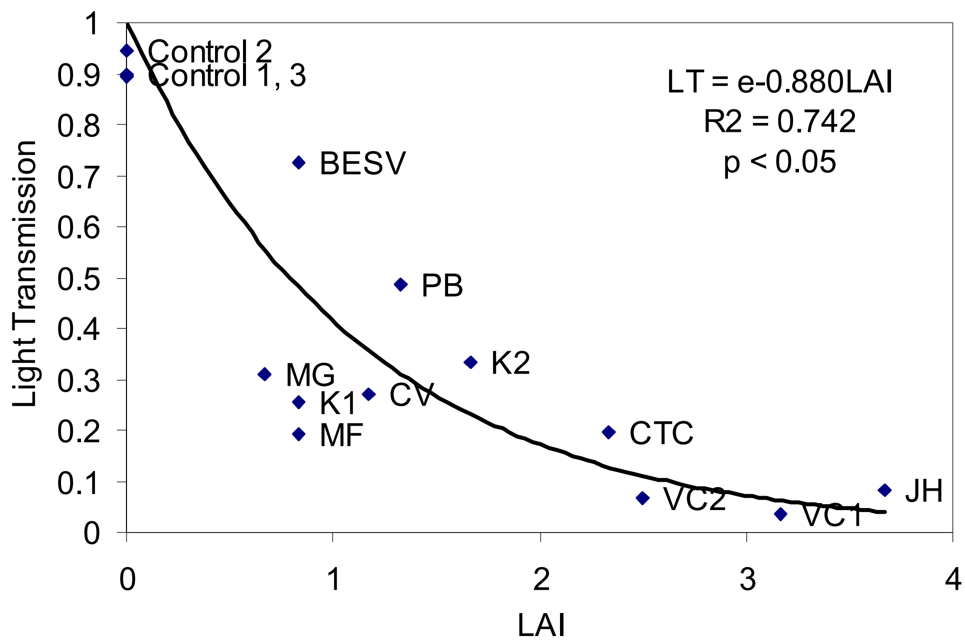

Figure 4.2. Effect of canopy leaf area index on canopy light transmission. Exponential curve was the best-fit model with $R^2 = 0.742$. Data points represent each cloak: Black Eyed Susan Vine (BESV), Porcelainberry (PB), Kudzu 2 (K2), Morning Glory (MG), Cross Vine (CV), Kudzu 1 (K1), Moonflower (MF), Chinese Trumpet Creeper (CTC), Japanese Honeysuckle (JH), Virginia Creeper 2 (VC2), and Virginia Creeper 1 (VC1).

The expression "$k_2(E – H)/R$" represented the flow of thermal energy into and out of the house through convection. Heat energy either flowed into or out of the house dependent upon the difference between the environmental air temperature (E) and the house air temperature (H). When the environmental temperature was greater than the house temperature, "E – H" was positive and energy flowed into the house making it warmer. Alternatively, when the house temperature was greater than the environmental temperature, “E – H” was negative and energy flowed out of the house making it cooler. The use of the insulating R value was based on building materials and dimensions to convert the temperature difference into energy terms conducive to use in the model.

Two values of k_2 were used in the model—one for when house temperature increased and one for when house temperature decreased. In the model, we used an if statement to automatically determine which value of k_2 to use. If the expression “E – H” was positive, “k_2-increasing” was used. If “E – H” was negative, “k_2-decreasing” was used.

Since we were more interested in the house air temperature rather than house energy, house energy (G) was converted to house temperature (H) by the equation

$$G = m \cdot C_p \cdot H \qquad (2)$$
$$H = G/m \cdot C_p$$

where G was the house energy in J, m was the mass of the air in kg, C_p was the specific heat capacity of the house air in J/kg·°C, and H was the house temp in °C. The mass of air was based on the volume of air in the house and the density of air. Volume of air in model house was 1.15 m^3, density of air was 1.201 kg/m^3 (assumed at 1 atm and 21 °C), giving a mass of 1.38 kg. C_p of air was 1005 J/kg·°C.

Determination of House Thermal Resistance

House thermal resistance, R, expressed the rate at which thermal energy flowed through the model house. Higher R values indicated a building with more insulation which caused thermal energy to flow more slowly into and out of the house. Specifically, R was a summation that described how thermal energy flowed into the house through the air surrounding of the house by convection (R_{conv}), then through the house materials by conduction (R_{cond}), and finally through the air in the house by convection (R_{conv}). We measured changes in thermal energy as temperature change on the dataloggers located inside the model houses (Ch. 3).

Since dataloggers were placed centrally in the model houses and thermal energy flowed radially into and out of the houses from the surrounding area, we used Incropera and DeWitt's (1990) equation for one dimensional radial heat transfer for a sphere to calculate R. Each of the R values were calculated and summed based on the house materials and properties of the air in and around the house.

For convective heat transfer through both the air around the house and inside the house

$$R_{conv} = 1/h \cdot D \tag{3}$$

where R_{conv} was convective heat transfer resistance in °C·min/J, h was the convection coefficient in N/(°C·min·m) based on the velocity of the air, and D was the surface area of the house in m^2.

For conductive heat transfer through the house materials

$$R_{cond} = L/k \cdot D \tag{4}$$

where R_{cond} was the conductive heat transfer resistance in °C·min/J, L was the material thickness in m, k was the thermal conductivity in N/°C·min, and D was the surface area of the house in m^2.

One dimensional conductive heat transfer was defined with

$$\dot{Z} = -k \cdot D \cdot dT/dx \tag{5}$$

where $\dot{Z}$ was thermal energy flow in J/min, k was thermal conductivity in N/°C·min, D was surface area in m^2, dT was temperature difference in °C, and dx was distance in m.

We rearranged and integrated Eq. 5 to indirectly find R_{cond}

$$dx = (-k \cdot D/ \dot{Z})dT \tag{6}$$

$$\int dx = (-k \cdot D/\dot{Z})\int dT \tag{7}$$

$$x_2 - x_1 = (-k \cdot D/\dot{Z})(T_2 - T_1) \tag{8}$$

$$x_2 - x_1 = (k \cdot D/\dot{Z})(T_1 - T_2) \tag{9}$$

where $x_2 - x_1 = L$ giving

$$L = (k \cdot D/\dot{Z})(T_1 - T_2) \tag{10}$$

$$\dot{Z} = (k \cdot D/L)(T_1 - T_2) \tag{11}$$

We rearranged Eq. 4

$$L = k \cdot D \cdot R_{cond} \tag{12}$$

We substituted L in Eq. 11

$$\dot{Z} = (1/R_{cond})(T_1 - T_2) \tag{13}$$

Since we modeled house heat transfer one dimensionally as a sphere, we integrated the heat transfer equation for a sphere and found R_{cond} based on Eq. 5.

$$\dot{Z} = -k \cdot D \cdot dT/dr \tag{14}$$

$$dr = (-k \cdot D/\dot{Z})dT \tag{15}$$

with the surface area of a sphere

$$D = 4 \cdot \pi \cdot r^2 \tag{16}$$

We substituted in Eq. 15

$$dr = (-4 \cdot k \cdot \pi \cdot r^2/\dot{Z})dT \tag{17}$$

$$(\dot{Z}/4 \cdot \pi)\int dr/r^2 = -k\int dT \tag{18}$$

We integrated both sides

$$(\dot{Z}/4\cdot\pi)*(-1/r_2 + 1/r_1) = -k(T_2 - T_1) \tag{19}$$

$$(\dot{Z}/4\cdot\pi)*(1/r_1 - 1/r_2) = k(T_1 - T_2) \tag{20}$$

$$\dot{Z} = 4\cdot\pi\cdot k(T_1 - T_2)/(1/r_1 - 1/r_2) \tag{21}$$

We rearranged Eq.21

$$1/\dot{Z} = (1/r_1 - 1/r_2)/(4\cdot\pi\cdot k(T_1 - T_2)) \tag{22}$$

We rearranged Eq. 13 and plugged in Eq. 22 to obtain R_{cond}

$$R_{cond} = (1/\dot{Z})(T_1 - T_2) \tag{23}$$

$$R_{cond} = (1/r_1 - 1/r_2)/4\cdot\pi\cdot k \tag{24}$$

for the house.

We found the R_{conv} value for the house by substituting the surface area of sphere in for the area D

$$R_{conv} = 1/h\cdot D \tag{25}$$

giving R_{conv}

$$R_{conv} = 1/h\cdot 4\cdot\pi\cdot r^2 \tag{26}$$

We found R_{total} by adding the R_{cond} of each house material to R_{conv} for the air inside and outside of the house. R values were added like resistors in series and parallel to take into account the different materials and thicknesses on each face of the house (Figure 4.3). An area factor was added in since the sides, roof, and floor of the model house were all made of different combinations of materials. For spheres

$$R_{cond} = (1/r_1 - 1/r_2)/4\cdot\pi\cdot k\cdot F_a \tag{27}$$

$$R_{conv} = 1/h\cdot 4\cdot\pi\cdot r^2\cdot F_a \tag{28}$$

where F_a equaled the area covered by the material divided by the total wall area. For example, windows did not cover the entire wall surface, so an area factor F_a was determined by dividing the total area taken up by windows on a single wall by the area of the wall.

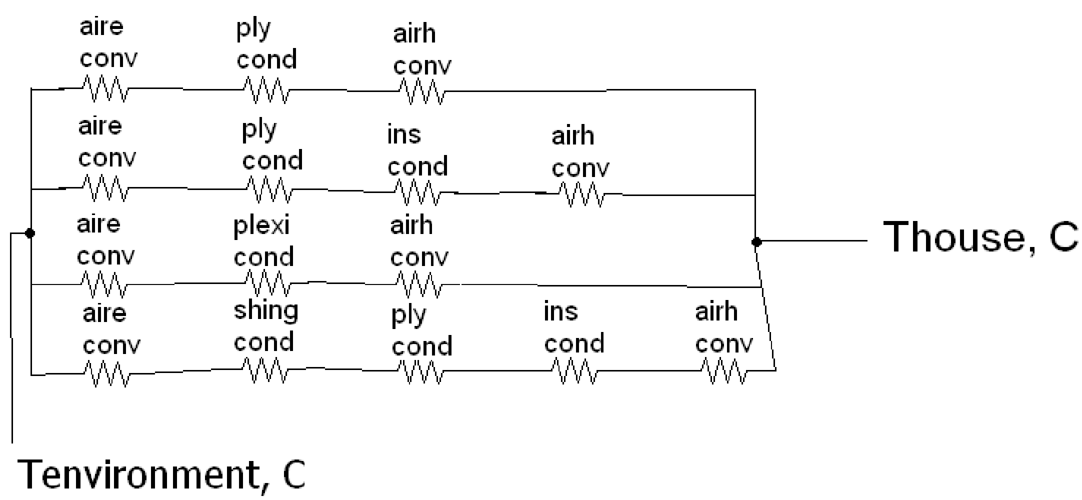

Figure 4.3. Total thermal resistance of model houses shown as a resistor diagram.

Figure 4.3 shows each pathway that energy will take to reach the center of the house (radial movement). Since energy flow was based on the temperature difference of the environmental air and air inside the house, the beginning and end of the pathways were these temperatures. Between the two temperatures was the resistance that the energy flow encountered as the system tried to come to equilibrium making the air temperatures inside and outside of the house equivalent. There were four different combinations of materials that energy went through to go into or out of the house. These were through the plywood floor, through the insulated wall, through one of the three windows, or through the insulated shingle roof. The top circuit pathway represented heat transfer through the plywood floor giving

$$R_{floor/environment,\ conv} + R_{floor/plywood,\ cond} + R_{floor/house,\ conv} \tag{29}$$

where the R subscript first described the thermal energy pathway, then the particular material through which energy traveled, and then the mode of heat transfer. For convection R values, either "environment" or "house" were listed as the particular material indicating heat transfer via convection through either air around the house or air in the house, respectively.

The second pathway from the top of the diagram represented heat transfer through the plywood walls giving

$$R_{walls/environment,\ conv} + R_{walls/plywood,\ cond} + R_{walls/insulation,\ cond} + R_{walls/house,\ conv} \tag{30}$$

The third pathway from the top of the diagram represented heat transfer through the windows giving

$$R_{windows/environment,\ conv} + R_{windows/plexiglass,\ cond} + R_{windows/house,\ conv} \tag{31}$$

The fourth and bottom pathway represented heat transfer through the roof giving

$$R_{roof/environment,\ conv} + R_{roof/shingle,\ cond} + R_{roof/plywood,\ cond} + R_{roof/insulation,\ cond} + R_{roof/house,\ conv} \tag{32}$$

We used the following equations to derive the specific resistances

$$R_{environment,\ conv} = 1/h_e \cdot 4 \cdot \pi \cdot r^2 \cdot F_a \tag{33}$$

where h_e was 138.85 N/°C·min·m based on the equation $h = 5.4 \cdot v^{0.466}$ when velocity v was less than 0.2 m/s. In a still room, the air velocity was taken to be 0.15 m/sec (Johnson, 1999). Additionally, r was the distance from the center of the house (where the datalogger was) to the outer most shingle. F_a was the area factor for that particular pathway of the resistor circuit, for example, if it was the roof pathway, the area factor was the roof surface area divided by the entire house surface area

$$R_{plywood,\ cond} = (1/r_1 - 1/r_2)/4 \cdot \pi \cdot k_{plywood} \cdot F_a \tag{34}$$

where r_1 and r_2 were the average of the minimum and maximum distances from the datalogger to the inner and outer edge of plywood, respectively.

$$R_{insulation,\ cond} = (1/r_1 - 1/r_2)/4 \cdot \pi \cdot k_{insulation} \cdot F_a \tag{35}$$

where r_1 and r_2 were the average of the minimum and maximum distances from the datalogger to the inner and outer edge of insulation, respectively.

$$R_{plexiglass,\ cond} = (1/r_1 - 1/r_2)/4 \cdot \pi \cdot k_{plexiglass} \cdot F_a \tag{36}$$

where r_1 and r_2 were the average of the minimum and maximum distances from the datalogger to the inner and outer edge of plexiglass, respectively.

$$R_{shingle,\ cond} = (1/r_1 - 1/r_2)/4 \cdot \pi \cdot k_{shingle} \cdot F_a \tag{37}$$

where r_1 and r_2 were the average of the minimum and maximum distances from the datalogger to the inner and outer edge of shingles, respectively.

$$R_{house,\ conv} = 1/h_h \cdot 4 \cdot \pi \cdot r^2 \cdot F_a \tag{38}$$

where h_h was 138.85 N/°C·min·m based on the equation $h = 5.4 \cdot v^{0.466}$ when velocity v was less than 0.2 m/s. In a still room, the air velocity was taken to be 0.15 m/sec. Additionally, r is the distance from the center of the house (where the datalogger was) to the closest inner most surface of the house, the plexiglass window.

After each pathway resistance was totaled, the total R value for the entire house was determined by adding up all the pathways like resistors in parallel.

$$R_{total} = (1/R_{floor} + 1/R_{walls} + 1/R_{windows} + 1/R_{roof})^{-1} \tag{39}$$

This gave an R_{total} for the house in the chamber (without insulation) of 0.0032 °C·min/J and an R_{total} for the house during outdoor experiment (with insulation) of 0.00411 °C·min/J. A larger R value existed for buildings with more insulation making the change in temperature due to building and environmental temperature differences less. We listed the values of the parameters we used to derive both R_{total} values in Tables 4.1 and 4.2.

Table 4.1. Parameters for R-value derivation for model house without insulation. Table has five horizontal sections listing in each section the parameters used to derive each R-value. The top section lists the inverse of the floor, sides, windows, and roof resistance used to determine R_{total}. Each of the four sections under the top section give the values used to derive R_{floor}, R_{sides}, $R_{windows}$, and R_{roof}. The bottom four sections of the table correlate with the four arms of the resistor diagram in Figure 4.3.

R_{total} **0.00321** **°C·min/J**	R_{floor}^{-1} 42.1 J/°C·min	R_{sides}^{-1} 182.2 J/°C·min	$R_{windows}^{-1}$ 12.5 J/°C·min	R_{roof}^{-1} 75.0 J/°C·min
R_{floor} 0.0238 °C·min/J	$R_{environment, conv}$ 0.00506 °C·min/J	$R_{plywood}$ 0.00186 °C·min/J	$R_{house, conv}$ 0.0168 °C·min/J	
	h_e 133.85 N/°C·min·m	r_1 0.653 m	h_h 133.85 N/°C·min·m	
	r 0.923 m	r_2 0.663 m	r 0.506 m	
	F_a 0.138	$k_{plywood}$ 7.2 N/°C·min	F_a 0.138	
		F_a 0.138		
R_{sides} 0.00549 °C·min/J	$R_{environment, conv}$ 0.00119 °C·min/J	$R_{plywood}$ 0.000337 °C·min/J	$R_{house, conv}$ 0.00396 °C·min/J	
	h_e 133.85 N/°C·min·m	r_1 0.743 m	h_h 133.85 N/°C·min·m	
	r 0.923 m	r_2 0.753 m	r 0.506 m	
	F_a 0.586	$k_{plywood}$ 7.2 N/°C·min	F_a 0.586	
		F_a 0.586		
$R_{windows}$ 0.0800 °C·min/J	$R_{environment, conv}$ 0.0181 °C·min/J	$R_{plexiglass}$ 0.00159 °C·min/J	$R_{house, conv}$ 0.0603 °C·min/J	
	h_e 133.85 N/°C·min·m	r_1 0.506 m	h_h 133.85 N/°C·min·m	
	r 0.923 m	r_2 0.509 m	r 0.506 m	
	F_a 0.0385	$k_{plexiglass}$ 12.6 N/°C·min	F_a 0.0385	
		F_a 0.0385		
R_{roof}	$R_{environment, conv}$	$R_{shingle}$	$R_{plywood}$	$R_{house, conv}$

0.0133 °C·min/J	0.00293 °C·min/J	0.000105 °C·min/J	0.000552 °C·min/J	0.00974 °C·min/J
	h_e 133.85 N/°C·min·m r 0.923 m	r_1 0.922 m r_2 0.923 m	r_1 0.912 m r_2 0.922 m	h_h 133.85 N/°C·min·m r 0.506 m
	F_a 0.0385	$k_{shingle}$ 3.72 N/°C·min	$k_{plywood}$ 7.2 N/°C·min	F_a 0.0385
		F_a 0.0385	F_a 0.0385	

Table 4.2. Parameters for R value derivation for model house with insulation. Table has five horizontal sections listing in each section the parameters used to derive each R-value. The top section lists the inverse of the floor, sides, windows, and roof resistance used to determine R_{total}. Each of the four sections under the top section give the values used to derive R_{floor}, R_{sides}, $R_{windows}$, and R_{roof}. The bottom four sections of the table correlate with the four arms of the resistor diagram in Figure 4.3.

R_{total} 0.00411 °C·min/J	R_{floor}^{-1} 42.1 J/°C·min	R_{sides}^{-1} 153.0 J/°C·min	$R_{windows}^{-1}$ 12.5 J/°C·min	R_{roof}^{-1} 35.6 J/°C·min	
R_{floor} 0.0238 °C·min/J	$R_{environment, conv}$ 0.00506 °C·min/J	$R_{plywood}$ 0.00186 °C·min/J	$R_{house, conv}$ 0.0168 °C·min/J		
	h_e 133.85 N/°C·min·m	r_1 0.653 m	h_h 133.85 N/°C·min·m		
	r 0.923 m	r_2 0.663 m	r 0.506 m		
	F_a 0.138	$k_{plywood}$ 7.2 N/°C·min	F_a 0.138		
		F_a 0.138			
R_{sides} 0.00653 °C·min/J	$R_{environment, conv}$ 0.00119 °C·min/J	$R_{plywood}$ 0.000337 °C·min/J	$R_{insulation}$ 0.00105 °C·min/J	$R_{house, conv}$ 0.00396 °C·min/J	
	h_e 133.85 N/°C·min·m	r_1 0.743 m	r_1 0.743 m	h_h 133.85 N/°C·min·m	
	r 0.923 m	r_2 0.753 m	r_2 0.733 m	r 0.506 m	
	F_a 0.586	$k_{plywood}$ 7.2 N/°C·min	$k_{insulation}$ 2.38 N/°C·min	F_a 0.586	
		F_a 0.586	F_a 0.586		
$R_{windows}$ 0.0800 °C·min/J	$R_{environment, conv}$ 0.0181 °C·min/J	$R_{plexiglass}$ 0.00159 °C·min/J	$R_{house, conv}$ 0.0603 °C·min/J		
	h_e 133.85 N/°C·min·m	r_1 0.506 m	h_h 133.85 N/°C·min·m		
	r 0.923 m	r_2 0.509 m	r 0.506 m		
	F_a 0.0385	$k_{plexiglass}$ 12.6 N/°C·min	F_a 0.0385		
		F_a 0.0385			
R_{roof}	$R_{environment, conv}$	$R_{shingle}$	$R_{plywood}$	$R_{insulation}$	$R_{house, conv}$

0.0281 °C·min/J	0.00293 °C·min/J	0.000105 °C·min/J	0.000552 °C·min/J	0.0148 °C·min/J	0.00974 °C·min/J
	h_e 133.85 N/°C·min·m r 0.923 m	r_1 0.922 m r_2 0.923 m	r_1 0.912 m r_2 0.922 m	r_1 0.912 m r_2 0.832 m	h_h 133.85 N/°C·min·m r 0.506 m
	F_a 0.0385	$k_{shingle}$ 3.72 N/°C·min	$k_{plywood}$ 7.2 N/°C·min	$k_{insulation}$ 2.38 N/°C·min	F_a 0.0385
		F_a 0.0385	F_a 0.0385	F_a 0.0385	

Model Calibration

To calibrate the model, we used the environmental temperatures, control house temperatures, experimental house temperatures, and solar data from VC1 and VC2 chamber experiments because they had similar environmental chamber light and temperature settings. Environmental temperatures, experimental and control house temperatures, and solar measurements were each averaged to a set of 24-hr (1440 minutes) temperatures for model calibration. Using the leaf area indices of the two green cloaks, a weighted experimental leaf area index was derived based on how many minutes each respective trellis was in chamber giving an average LAI of 1.34. For the control house temperatures a leaf area index of 0 was used. The averages from the two trials are shown in Figure 4.4.

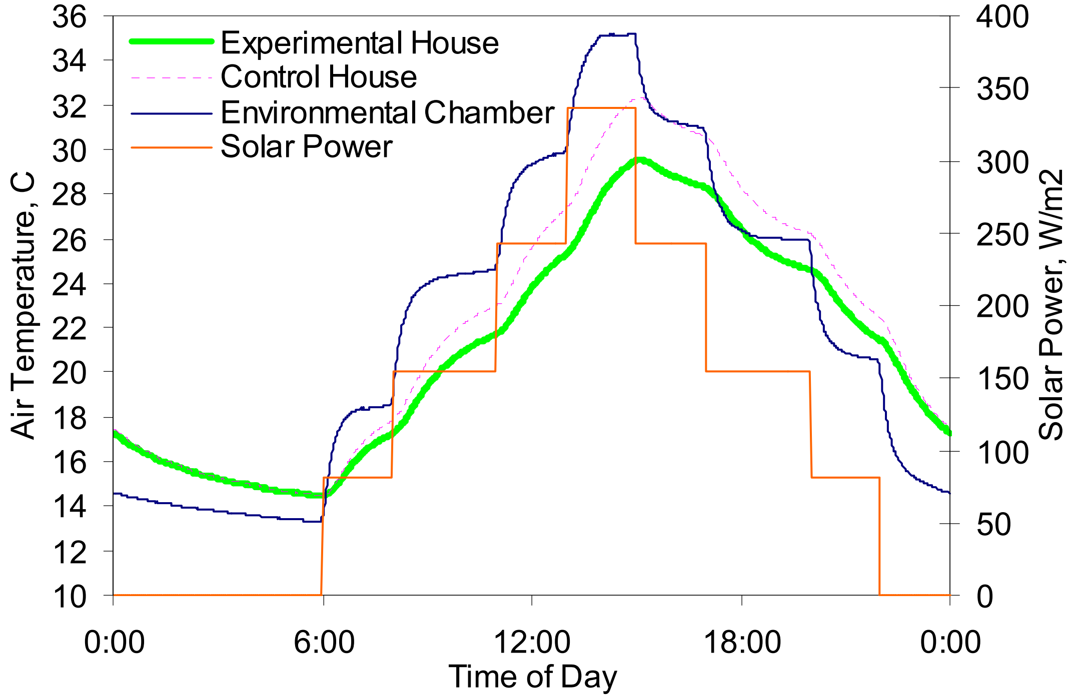

Figure 4.4. Twenty-four hour inside air temperatures for the experimental house with green cloak, the control house, the environmental temperatures, and the solar power load produced by a combination of fluorescent and metal halide lamps inside the environmental chambers.

The state equation for house energy, Eq. 1, was put into an Excel spreadsheet with the average temperature data, average solar data, and average leaf area index giving one 24-hour period of data for k_1 and k_2 coefficient calibration. The following model state equation was manipulated for the calibration.

$$dG/dt = 60 \cdot S \cdot A \cdot k_1 \cdot \exp(-0.8802 \cdot LAI) + k_2 \cdot (E - H)/R \quad (40)$$

To simplify the equation, an LAI of 0 was used only requiring the control house, environmental, and solar averages giving the following state equation

$$dG/dt = 60 \cdot S \cdot A \cdot k_1 + k_2 \cdot (E - H)/R \quad (41)$$

For k_1 calibration, the average environmental temperatures and control house temperatures were examined for a time when they were equivalent making the expression $k_2 \cdot (E - H)/R = 0$. This allowed us to approximate k_1 without needing to know k_2, but still allowing us to use the known values of dG/dt, S, A. This manipulation gave

$$dG/dt = 60 \cdot S \cdot A \cdot k_1 \quad (42)$$

$$k_1 = (dG/dt)/60 \cdot S \cdot A \quad (43)$$

Given that the house averages H were in temperature units, they were converted to energy units for use in dG/dt which is in J/min. The following transfer was made

$$dG/dt = (dH/dt) \cdot m \cdot C_p \quad (44)$$

where dH/dt was approximated as $(H_{n+1} – H_{n-1})/2$, m was mass of house air (1.38 kg), and C_p was specific heat of air in house (1005 N·m/kg·°C). This gave the following expression for dG/dt

$$dG/dt = ((H_{n+1} – H_{n-1})/2) \cdot m \cdot C_p \quad (45)$$

We plugged Eq. 45 into Eq. 43

$$k_1 = (((H_{n+1} – H_{n-1})/2) \cdot m \cdot C_p)/60 \cdot S \cdot A \quad (46)$$

The coefficient k_1 was calculated for each minute n that E – H was within 0.06 °C of 0 °C giving the results in Table 4.3 and A = 1.58 m^2. All values except for the 0605 h value of k_1 were negative. This value cannot be negative because solar loading $[60 \cdot S \cdot A \cdot k_1 \cdot \exp(-0.8802 \cdot LAI)]$ can only be positive. With this, the positive 0.00133 value of k_1 was chosen for the model.

Table 4.3. Calculated k_1 values for four temperature differences between environmental and house air.

Time of Day	E – H (°C)	k_1
0605 h	-0.056	0.00133
1520 h	0.011	-0.00138
1601 h	-0.008	-0.00117
1659 h	0.003	-0.00076

We determined the k_2 value next. The state equation with an LAI of 0 was used again substituting $((H_{n+1} – H_{n-1})/2) \cdot m \cdot Cp$ for dG/dt in Eq. 41

$$dG/dt = 60 \cdot S \cdot A \cdot k_1 + k_2 \cdot (E - H)/R \quad (47)$$

$$((H_{n+1} - H_{n-1})/2) \cdot m \cdot C_p = 60 \cdot S \cdot A \cdot k_1 + k_2 \cdot (E - H)/R \quad (48)$$

We solved for k_2

$$k_2 = (((H_{n+1} - H_{n-1})/2) \cdot m \cdot C_p - 60 \cdot S \cdot A \cdot k_1)/((E - H)/R) \quad (49)$$

The coefficient k_2 was calculated for each minute of the calibration data using the solar radiation at each minute S, area of roof A, k_1, environmental temperature E, control house temperature H, and the non-insulated model house R value (Figure 4.5).

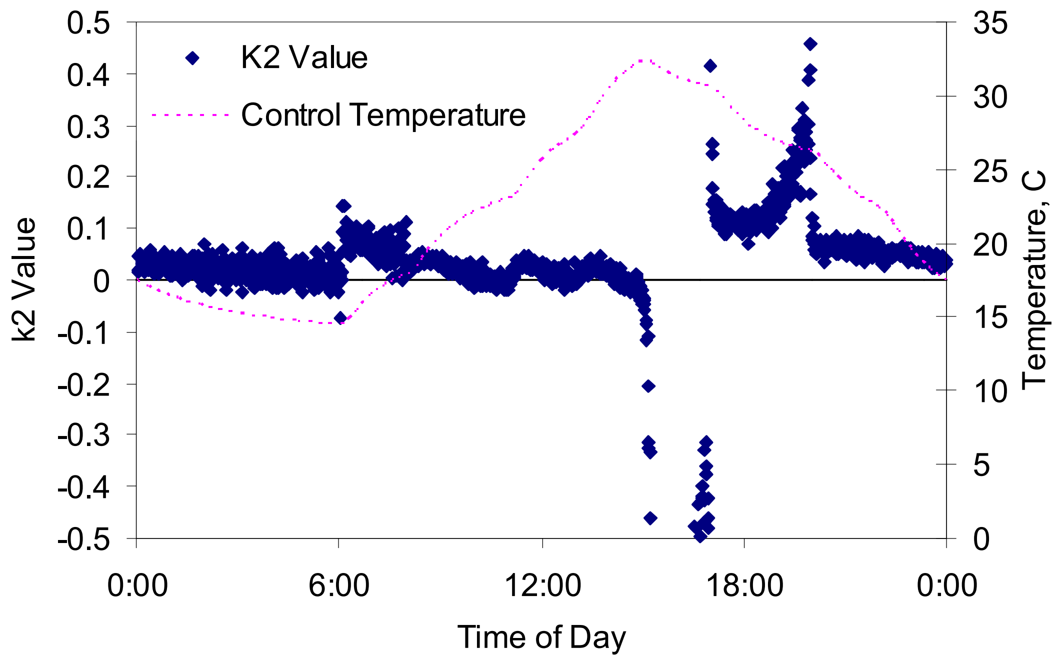

Figure 4.5. Calculated k_2 values and average control house temperatures used during calibration.

Given that k_2 values before 1500 h were generally less than k_2 values after 1700 h, we decided that two k_2 values were needed—one for when house temperatures increased and one for when house temperatures decreased, k_2-increasing and k_2-decreasing, respectively. We hypothesized that heat transfer into the house was different from transfer out of the house. The value for k_2-increasing was the mean during the 0700-1500 h period (0.0201), while k_2 decreasing was the mean during the 1500-2359 h period (0.121).

Using these calibration values, we made the following graphs showing the observed house temperatures and the modeled house temperatures. Control house temperatures (no cloak, LAI 0) and experimental house temperatures (cloak, LAI 1.34) are shown in Figures 4.6a and 4.6b, respectively.

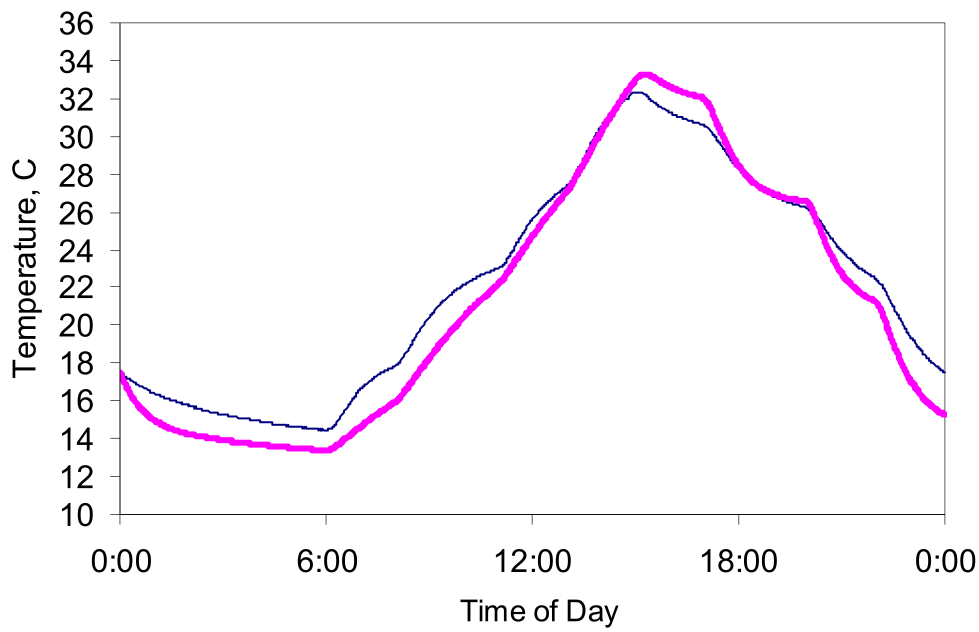

(a) no green cloak.

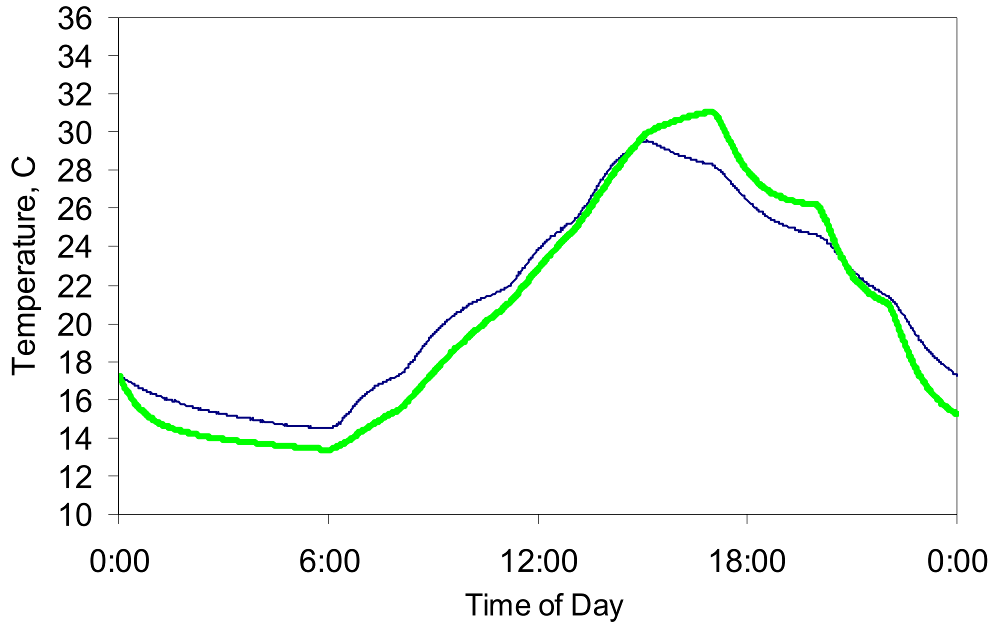

(b) with green cloak

Figure 4.6. Simulated (thick line) and observed (thin line) diurnal air temperatures inside model houses.

Since it was important to have average error low for both experimental and control house calibration, we calculated the total average error as the sum of the experimental and control average error. Total average percent error of each minute in the 24 hour period (1440 minutes) was calculated for the calibrated coefficients using the formula

$$\text{Total Average Error} = [(\Sigma(((C_o - C_p)^2)^{1/2})/C_o)/1440 + (\Sigma(((E_o - E_p)^2)^{1/2})/E_o)/1440)]*100 = 12.5\% \quad (50)$$

where C_o was observed control house temperature, C_p was predicted control house temperature, E_o was observed experimental cloak house temperature, and E_p was predicted experimental cloak house temperature for each minute of the 24 hour period. Individually, error of the control house model (no cloak) was calculated as

$$\text{Control Average Error} = [(\Sigma(((C_o - C_p)^2)^{1/2})/C_o)/1440]*100\% = 6.0\% \quad (51)$$

For the experimental house (with the cloak), experimental average error was calculated as

$$\text{Experimental Average Error} = [(\Sigma(((E_o - E_p)^2)^{1/2})/E_o)/1440]*100\% = 6.5\% \qquad (52)$$

To show that two k_2 values were needed, we used only k_2-increasing (0.0201) in the model to show that the coefficient worked well when house temperature increased, but a different coefficient was needed when house temperature decreased. Control house temperature is shown in Figure 4.7a and experimental house temperature is shown in Figure 4.7b.

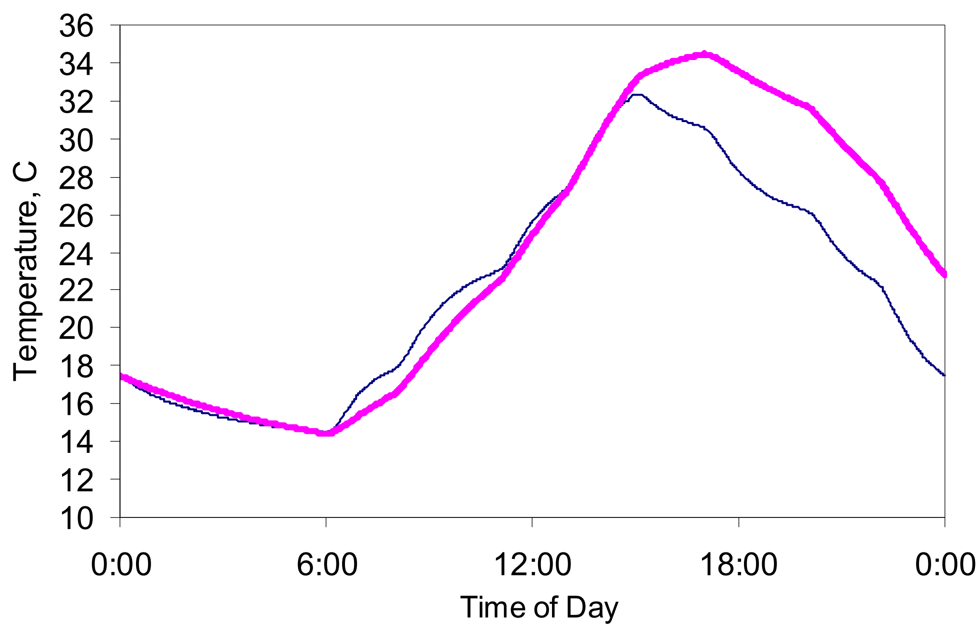

(a)

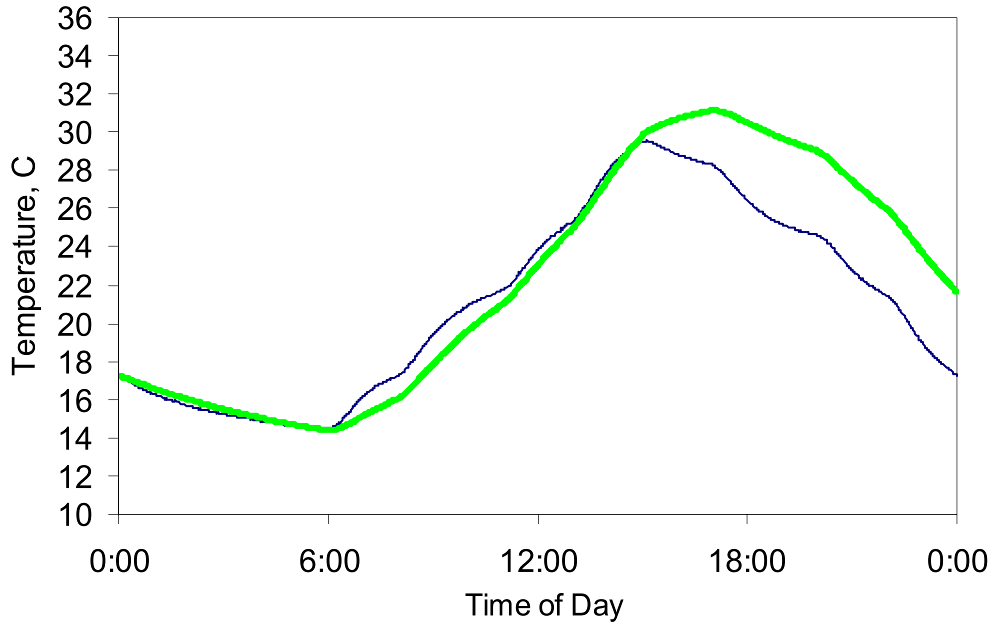

(b)

Figure 4.7. Simulated (thick line) and observed (thin line) diurnal air temperatures inside model house (a) without and (b) with green cloak. Mathematical model used only k_2 increasing.

With these values, total average error was 17.4%, control average error was 9.3%, and experimental average error was 8.1%. This was greater than the 12.5% when both k_2-increasing and k_2-decreasing were used.

Next, we altered the coefficients k_1, k_2-increasing, and k_2-decreasing to minimize the total error equation

$$\text{Total Average Error} = \min[(\Sigma(((C_o - C_p)^2)^{1/2})/C_o)/1440 + (\Sigma(((E_o - E_p)^2)^{1/2})/E_o)/1440]*100\% \quad (53)$$

which gave Figures 4.8a and 4.8b for the control and experimental houses, respectively.

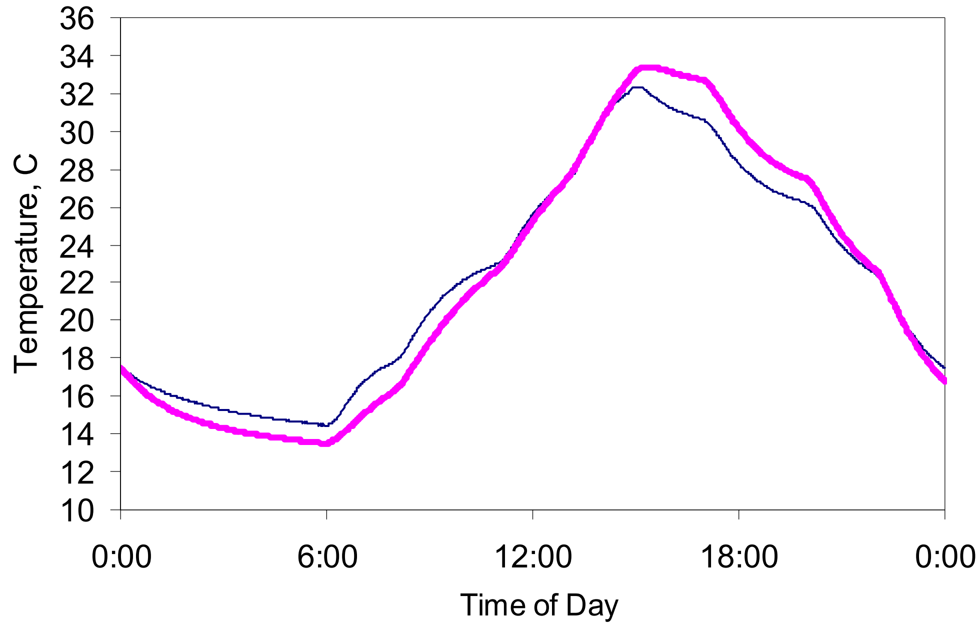

(a)

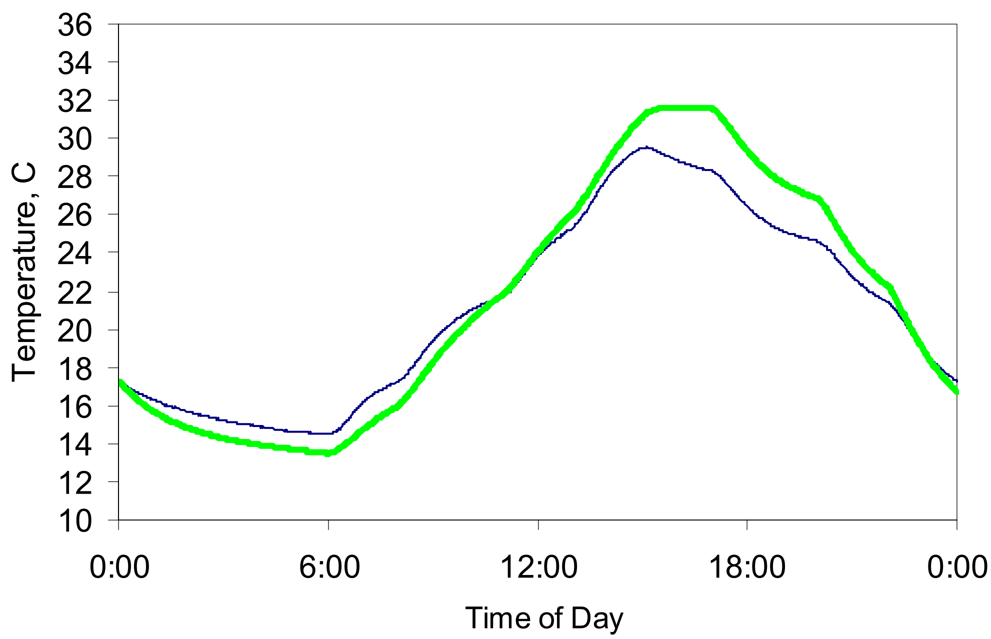

(b)

Figure 4.8. Simulated (thick line) and observed (thin line) diurnal air temperatures inside model house (a) without and (b) with green cloak.

The coefficients used were k_1 of 0.001, k_2-increasing of 0.028, and k_2-decreasing of 0.059. These values produced a total error of 10.2%, control error of 4.6%, and experimental error of 5.7%. Since these coefficients gave the least error, they were used to validate the model against outdoor temperature experiment data.

Model Validation

The model was validated using outside summer data. As reported in Chapter 3, five cloaks were tested outside for a total of 40 days. Both model houses were used on each day for control and experimental comparison. The leaf area indices of the cloaks tested are listed in Table 4.4.

Table 4.4. Leaf area indices of the cloaks used in model validation.

Cloak	LAI
Japanese Honeysuckle	1.29
Virginia Creeper 1	2.34
Virginia Creeper 2	1.98
Kudzu 2	1.78
Cross Vine	0.75

For each of the 40 days, the maximum daily temperature and solar radiation were graphed. Fifteen of the days (Figure 4.9) were chosen to represent the range in temperature and solar radiation load. This gave 30 days worth of validation data because of both control and experimental house temperature data.

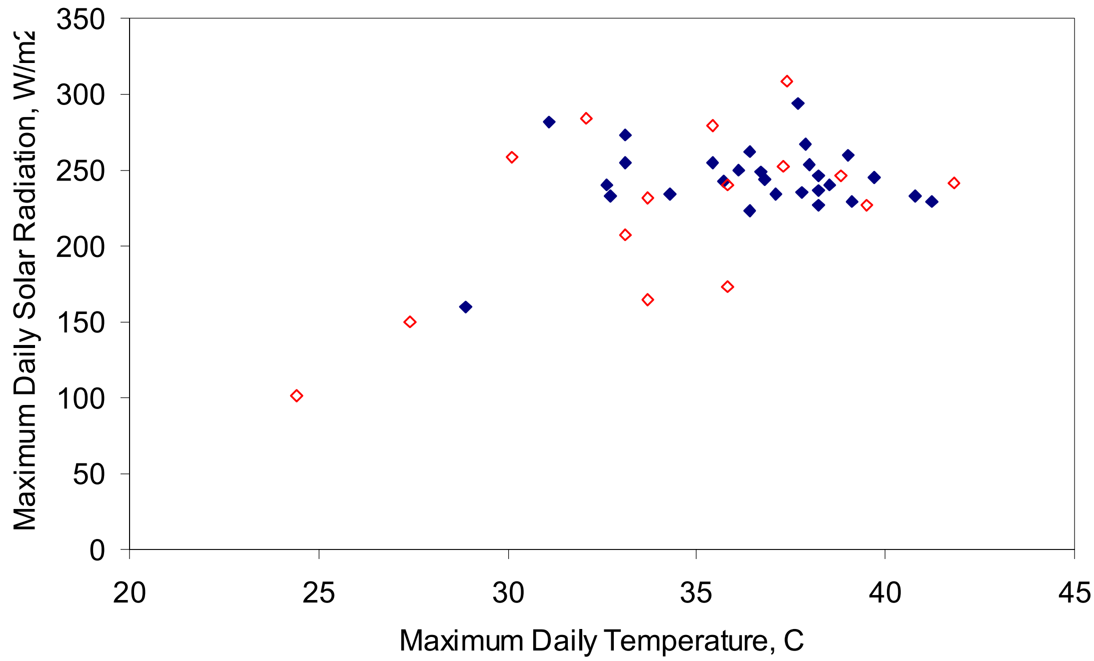

Figure 4.9. Maximum daily solar radiation and maximum daily temperature of outdoor temperature experiment trials. Open diamonds are the 15 data sets chosen for model validation.

For each validation, we input observed environmental temperatures, solar radiation, and leaf area index in the model to predict control and experimental indoor model house temperature. As stated in the model calibration section, the R value (0.00411 °C·min/J) for the house was recalculated to account for the roll insulation. The first data set validated in the model was temperatures recorded on June 14, 2006 during the Japanese honeysuckle trial. Figures 4.10a and 4.10b show the observed and model predicted indoor temperatures of the control and experimental houses. Total average error was 15.1%, control average error was 8.7%, and experimental average error was 6.4%.

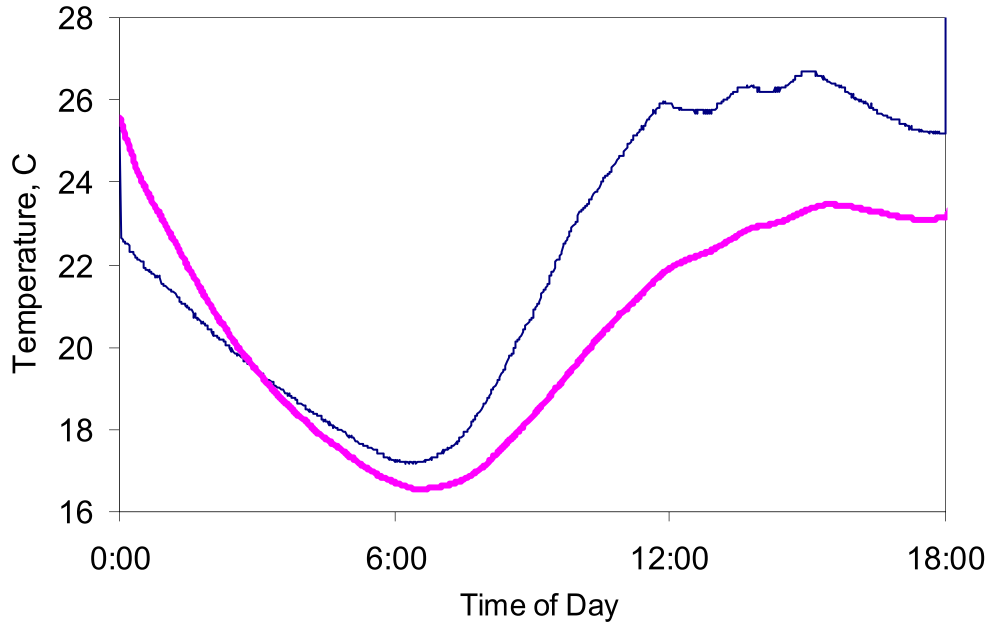

(a)

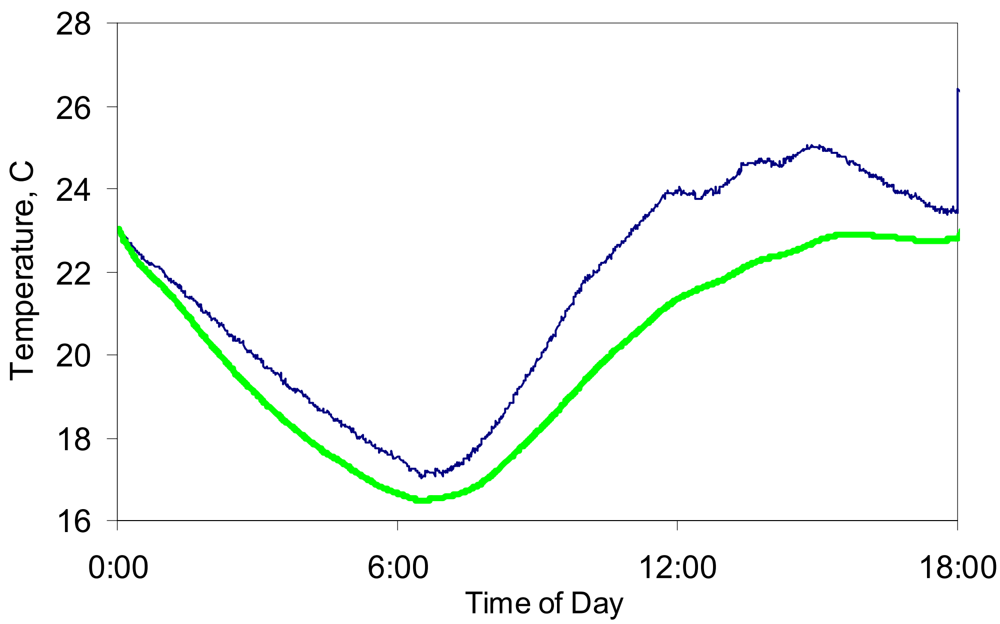

(b)

Figure 4.10. Simulated (thick line) and observed (thin line) diurnal air temperatures inside model house (a) without and (b) with green cloak.

Although we already calibrated coefficients with environmental chamber data, we recalibrated using the first validation day since error was still high. Upon recalibration with outdoor experiment data, all chamber-based calibration was disregarded. We altered coefficient values once again with this one day of outside data to minimize the total error. Coefficients k_1 of 0.005, k_2-increasing of 0.1 min^{-1}, and k_2-decreasing of 0.045 min^{-1} gave a minimum error. Figures 4.11a and 4.11b show a much better fit with these new values. Three reasons that new coefficients were needed might have been because of the difference in solar radiation values between in the chamber and outside, the added insulation in outside experiments, and outside winds. Total average error was 3.6%, control average error was 2.1%, and experimental average error of 1.5%.

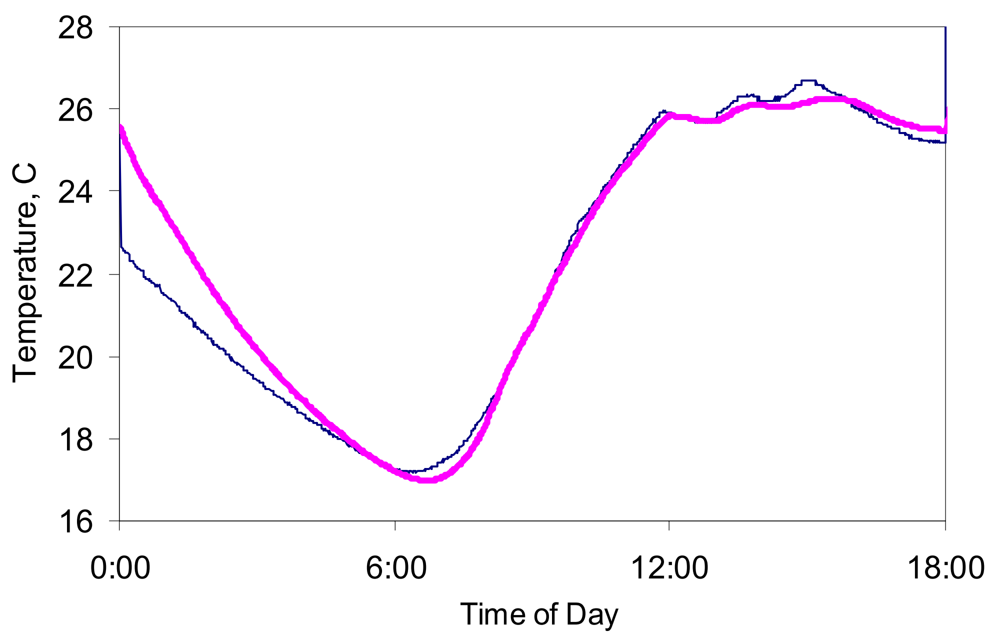

(a)

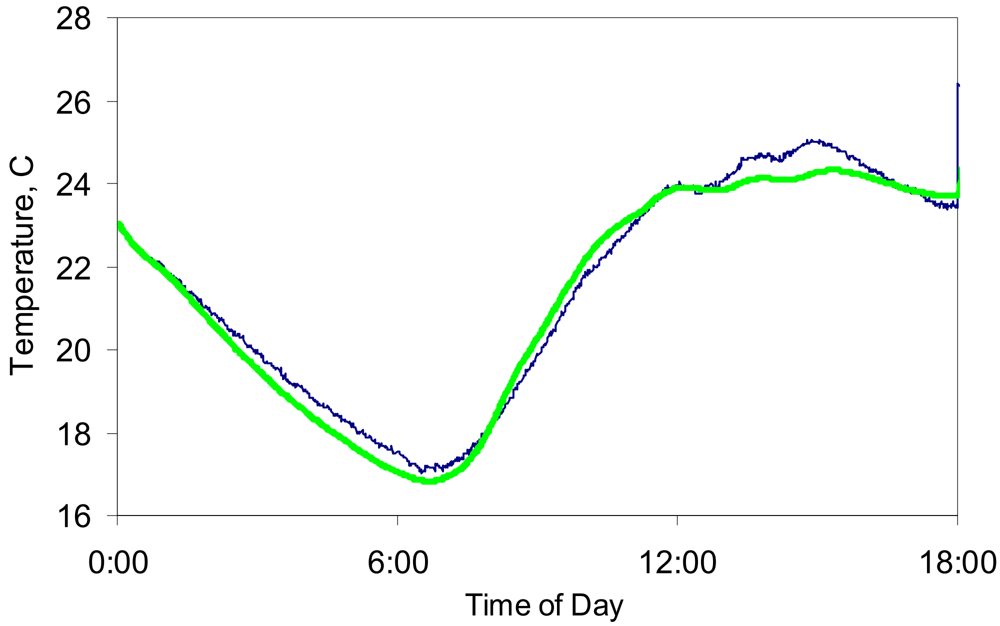

(b)

Figure 4.11. Simulated (thick line) and observed (thin line) diurnal air temperatures inside model house (a) without and (b) with green cloak.

The new coefficient values were used for validation of the other 14 days of outside data. Validation was only run to 1800 h because sun shined directly into the houses through the windows after this time and the model was not built to make this prediction. The validation data results are shown below in Figures 4.12a through 4.12o.

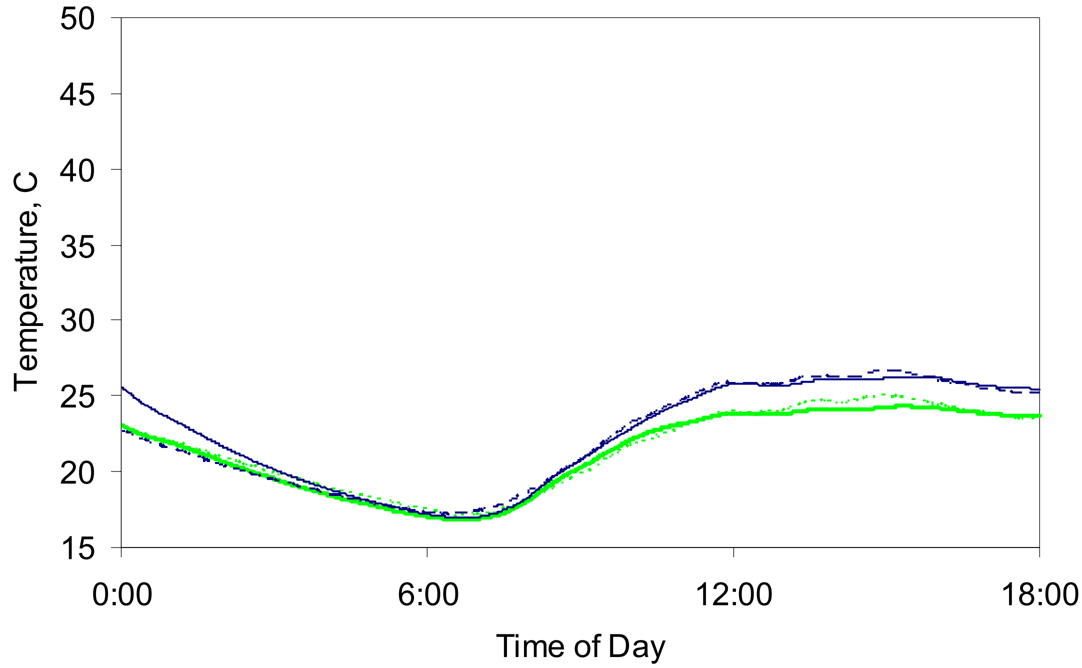

(a) Japanese honeysuckle, 6/14, LAI = 1.29

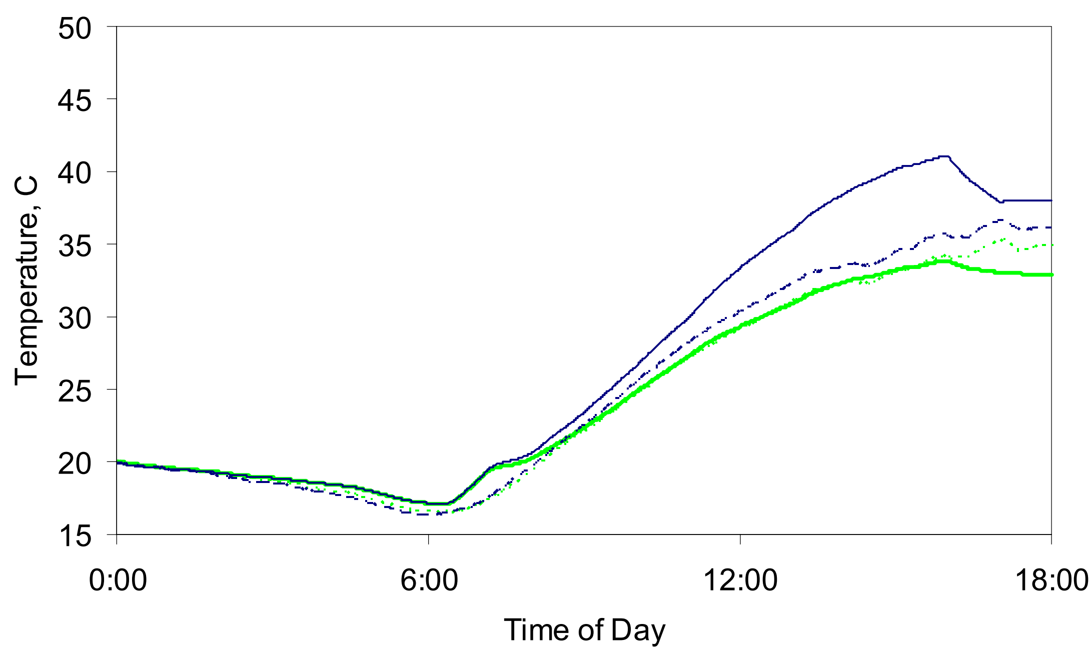

(b) Japanese honeysuckle, 6/15, LAI = 1.29

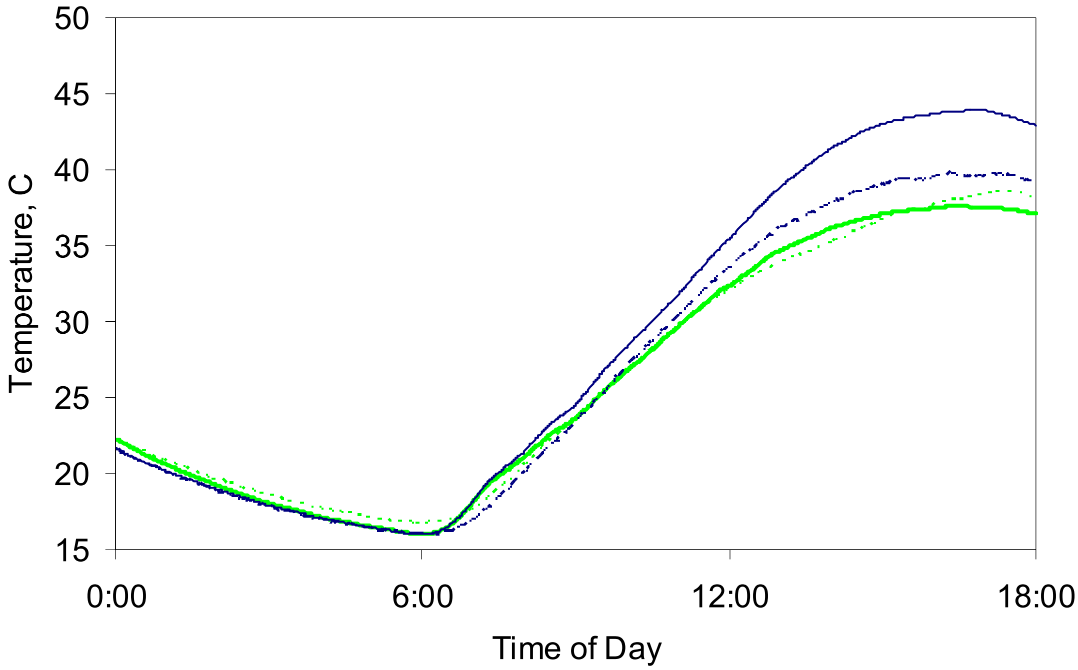

(c) Japanese honeysuckle, 6/17, LAI = 1.29

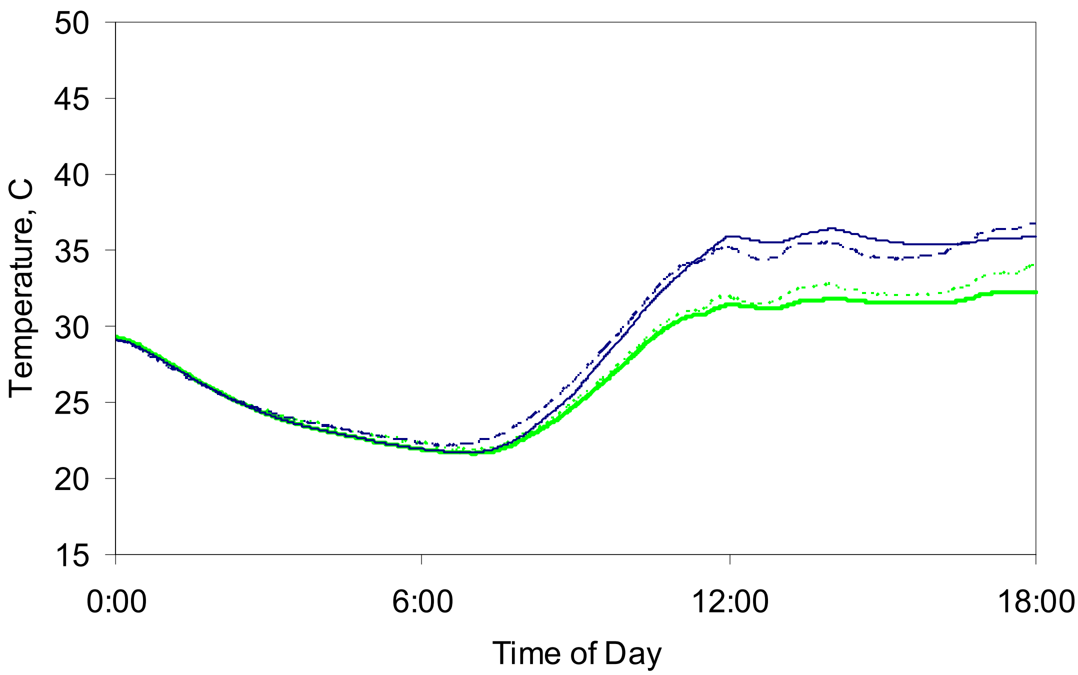

(d) Virginia creeper 1, 6/23, LAI = 2.34

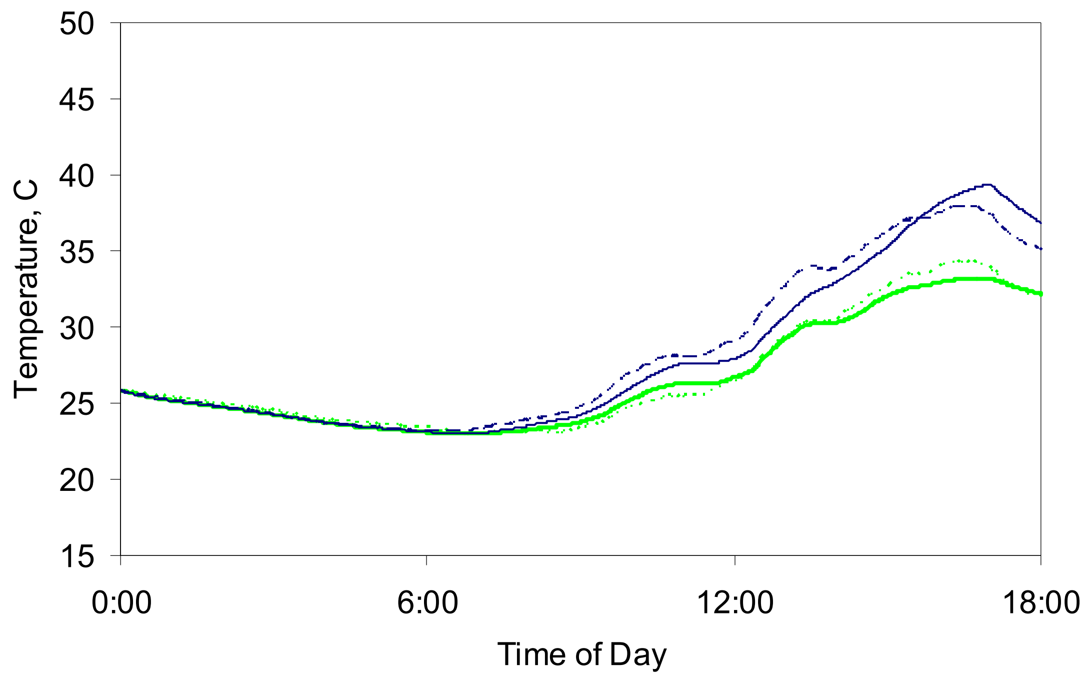

(e) Virginia creeper 1, 6/24, LAI = 2.34

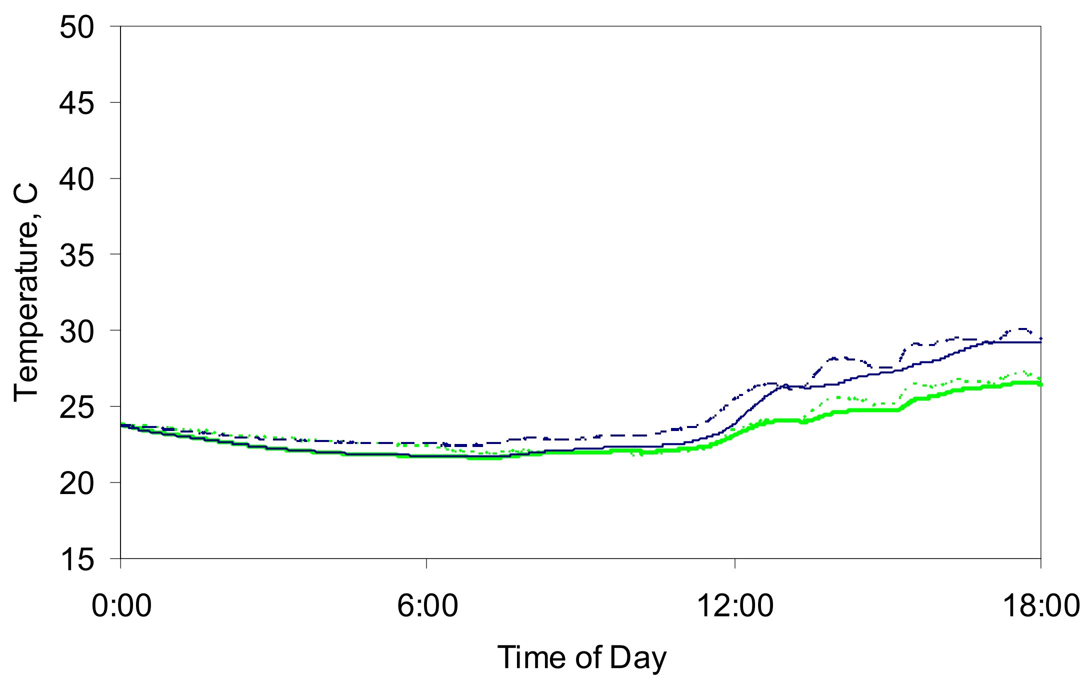

(f) Virginia creeper 1, 6/25, LAI = 2.34

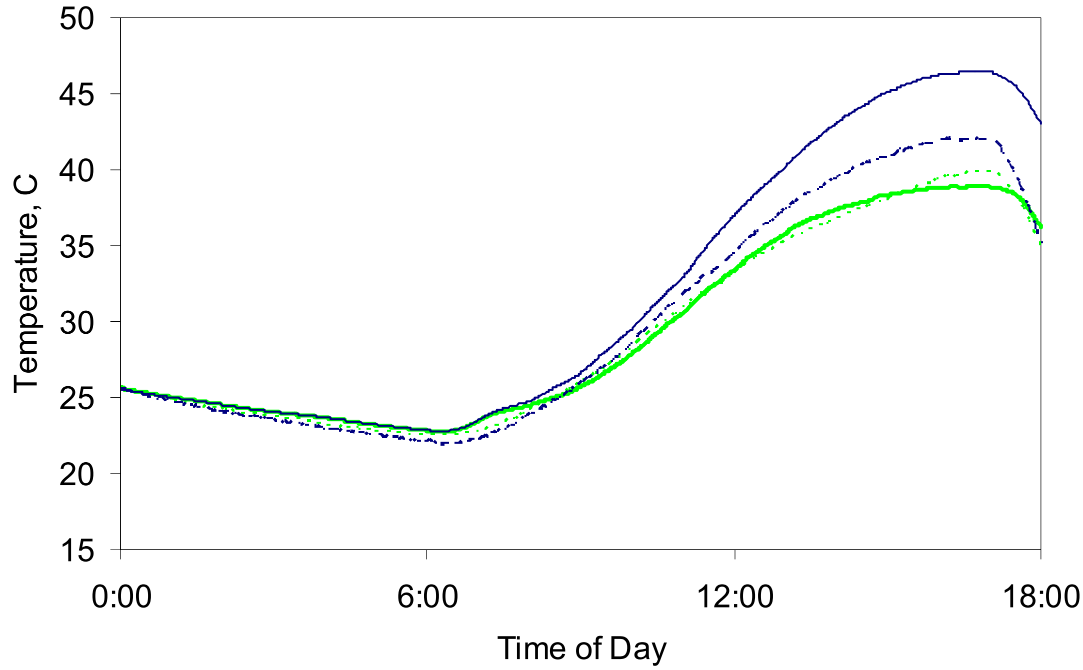

(g) Virginia creeper 2, 7/2, LAI = 1.98

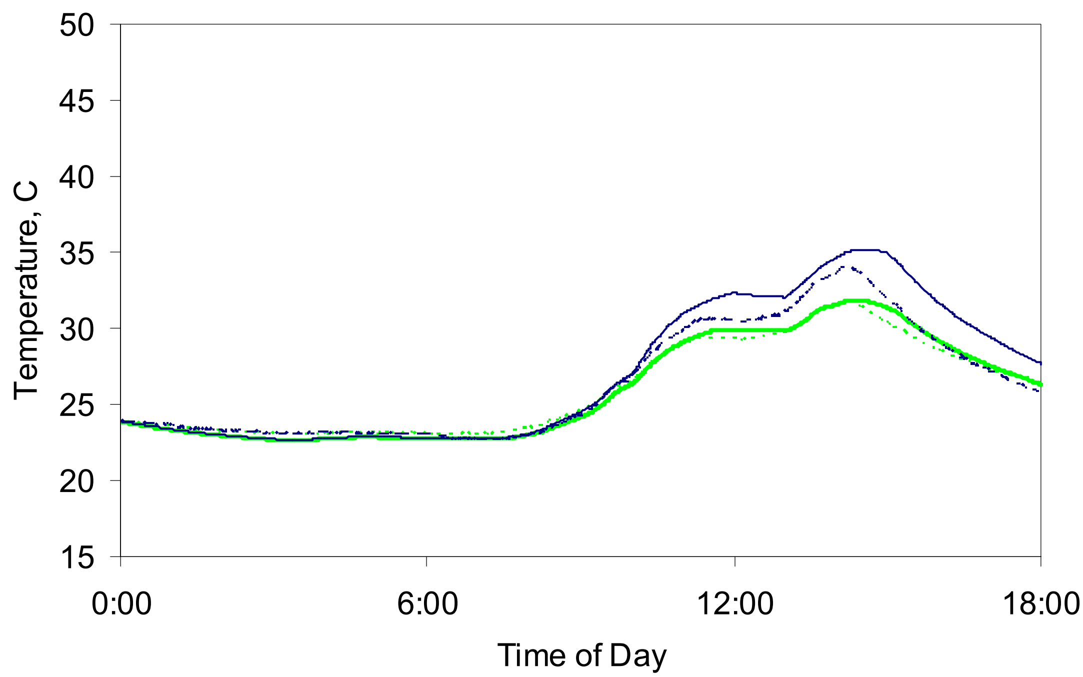

(h) Virginia creeper 2, 7/5, LAI = 1.98

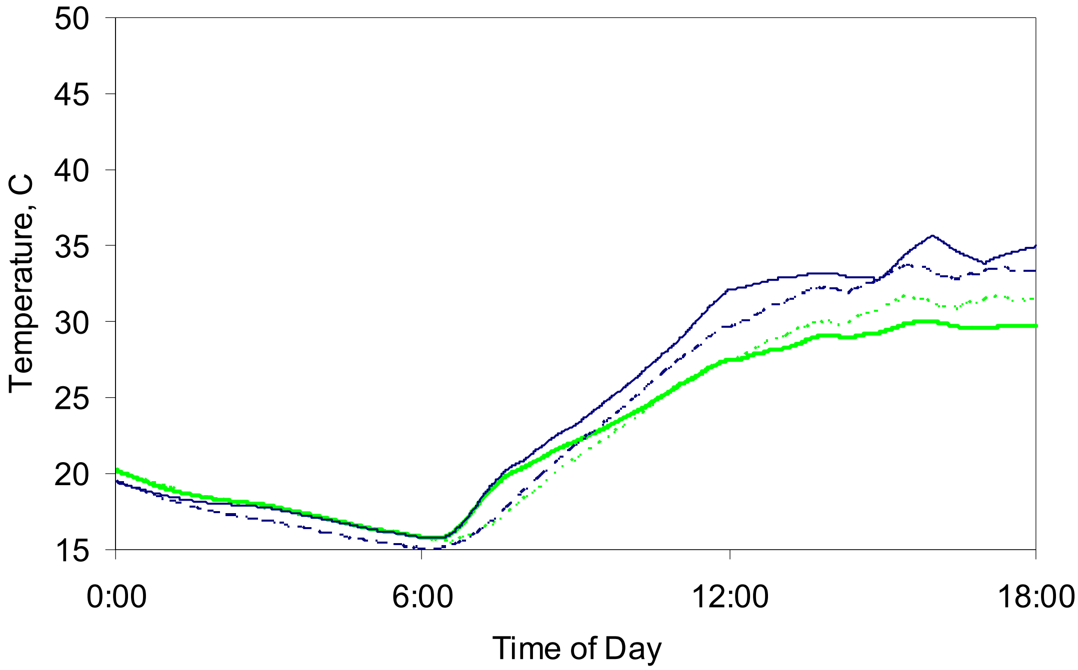

(i) Virginia creeper 2, 7/7, LAI = 1.98

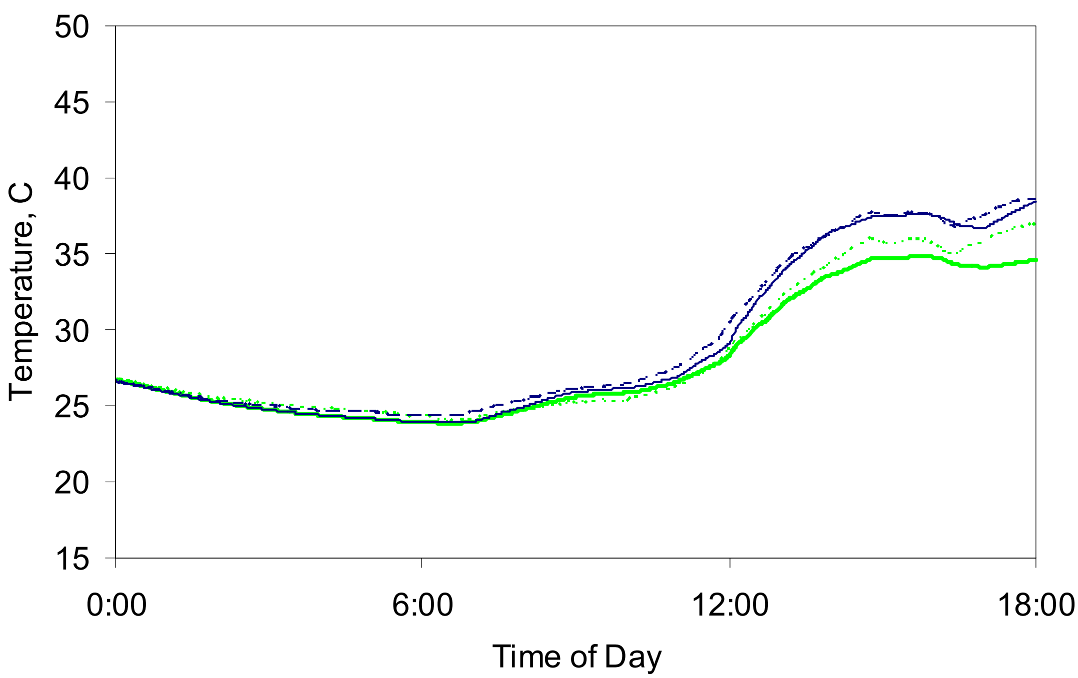

(j) Kudzu 2, 7/15, LAI = 1.78

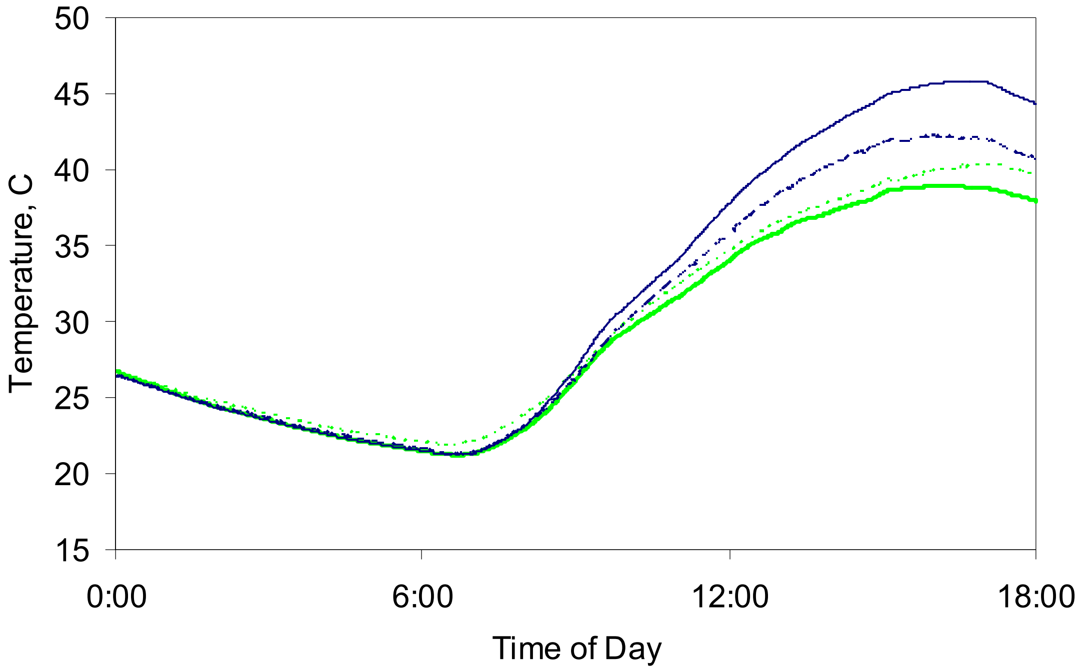

(k) Kudzu 2, 7/19, LAI = 1.78

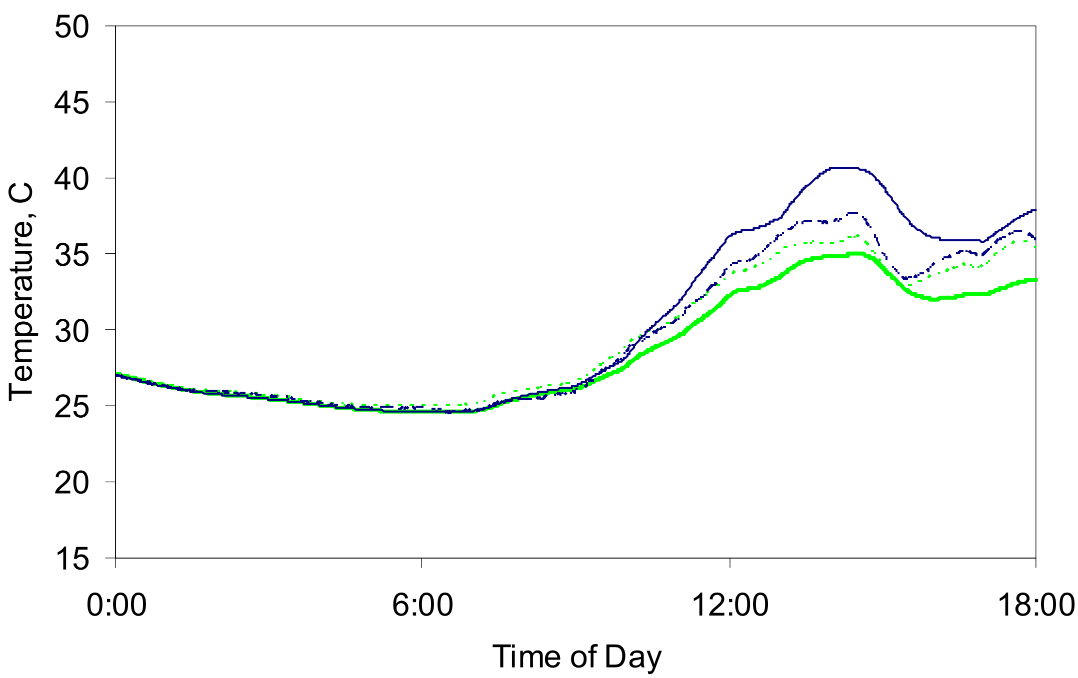

(l) Kudzu 2, 7/22, LAI = 1.78

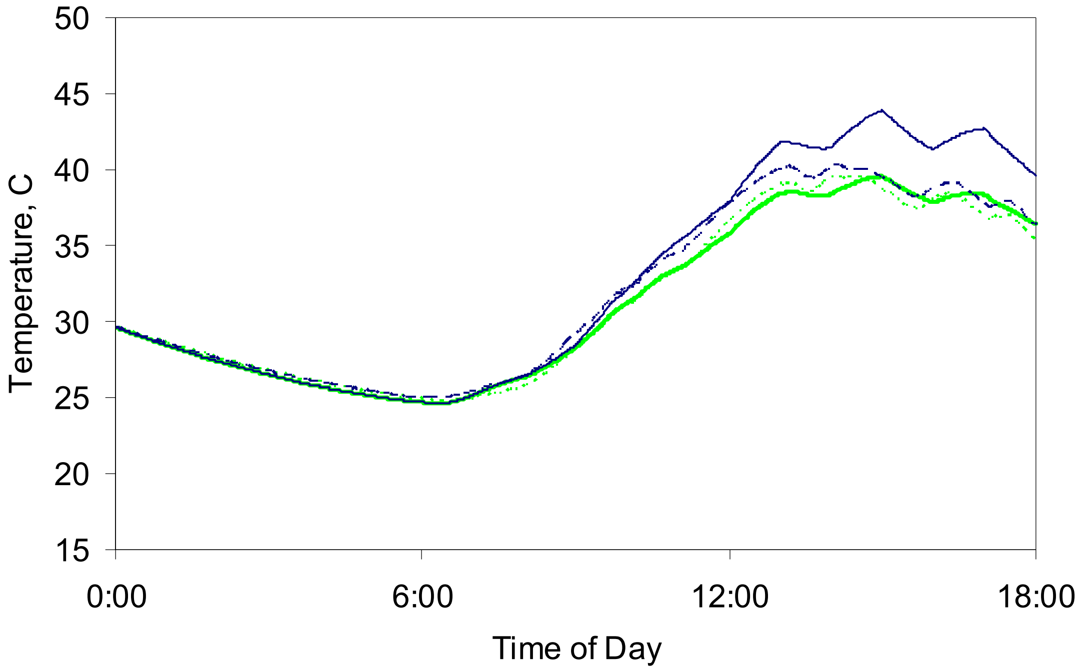

(m) Cross vine, 7/28, LAI = 0.75

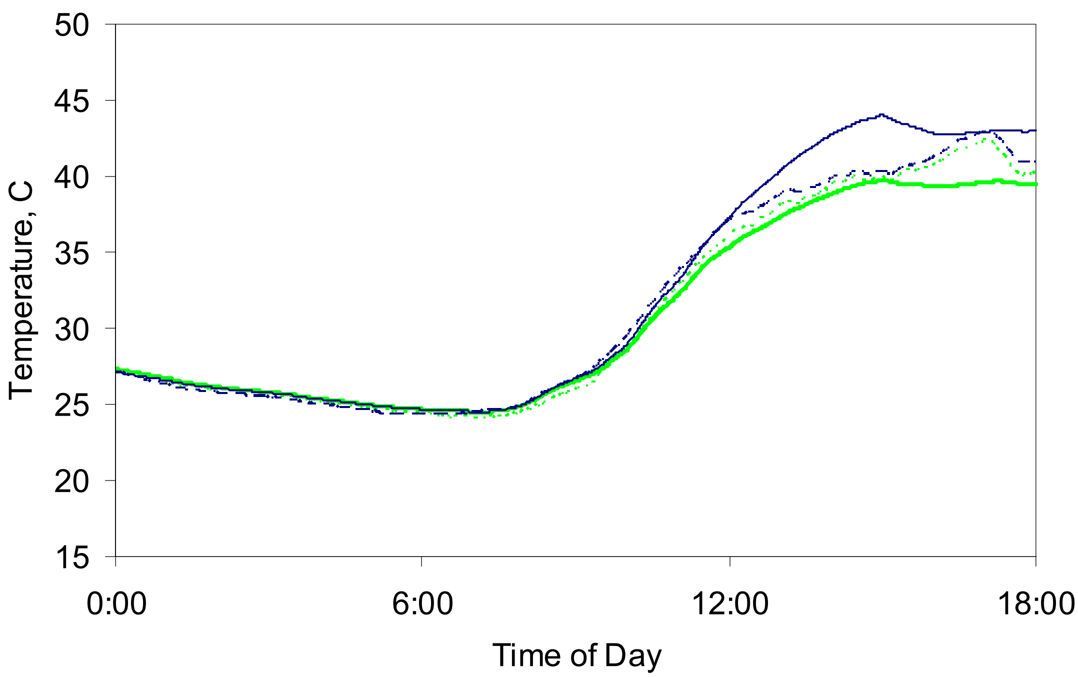

(n) Cross vine, 7/29, LAI = 0.75

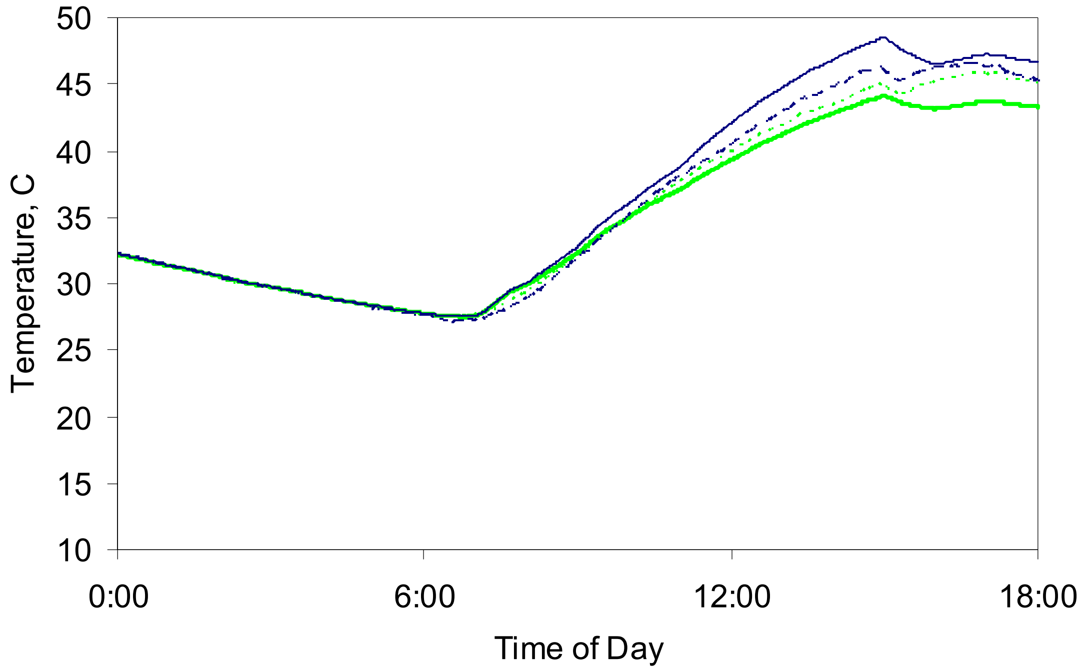

(o) Cross vine, 8/3, LAI = 0.75

Figure 4.12. Validation of temperature model using 14 days of data and several vine species with the dashed top dark line as observed control temperatures, the solid dark line is predicted control temperatures, the light dashed line is observed experimental temperatures, and the solid light line is predicted experimental temperatures.

Model Parameter Evolution

The four sets of model coefficients, R-values, and associated error are listed in Table 4.5 for each step of our model calibration and error minimization. The 2000 ft^2 house column is explained in more detail later in the section called "Model Results". Total error was unknown for the 2000 ft^2 house application since there was no validation data.

Table 4.5. Model pathway coefficients (k), resistance (R), and total error for each step of model development: calibration, error minimization and application.

Parameter	Environmental Chamber Calibration	Error Minimization	JH Outside Calibration	2000 ft^2 House
k_1	0.00133	0.001	0.005	0.005
k_2-increasing, min^{-1}	0.0201	0.028	0.1	0.1
k_2-decreasing, min^{-1}	0.121	0.059	0.045	0.045
R, °C·min/J	0.00321	0.00321	0.00411	0.000184
Total Error	12.50%	10.20%	3.60%	-

Model Bias

To determine if any model bias existed, we compared control average error, experimental average error, total control error, and total experimental error for each validation set to the leaf area index of the cloak being tested, maximum daytime temperature, and maximum solar radiation. Average experimental and average control error were the error at each minute and were determined in the following way

$$\text{Control Average Error} = [(\Sigma(((C_o - C_p)^2)^{1/2})/C_o)/1080]*100\% \quad (54)$$

where C_o was observed control temperature in °C, C_p was predicted control temperature in °C, and 1080 indicates the 1080 minutes of daily data points.

$$\text{Experimental Average Error} = [(\Sigma(((E_o - E_p)^2)^{1/2})/E_o)/1080]*100\% \quad (55)$$

where E_o was observed experimental temperature in °C and E_p was predicted experimental temperature in °C.

Total experimental and total control error were the overall daily error and were determined in the following way

$$\text{Total experimental error} = [((((\Sigma E_o) - (\Sigma E_p))^2)^{1/2})/\Sigma E_o]*100\% \quad (56)$$

$$\text{Total control error} = [((((\Sigma C_o) - (\Sigma C_p))^2)^{1/2})/\Sigma C_o]*100\% \quad (57)$$

We made regression figures to determine if there was any correlation between model error, growth characteristic, and environmental condition. Figures 4.13 through 4.18 plot average and total error versus leaf area index, maximum daily temperature, and maximum daily solar radiation along with regression lines, R^2, and p-values. All error was under 8% and bias was nonexistent. Negligible bias was indicated by regression R^2 being near zero and p-values being greater than 0.05 indicating no linear correlation between error and each growth characteristic or environmental condition. Control average and control total error were not plotted against leaf area index since they were without cloaks.

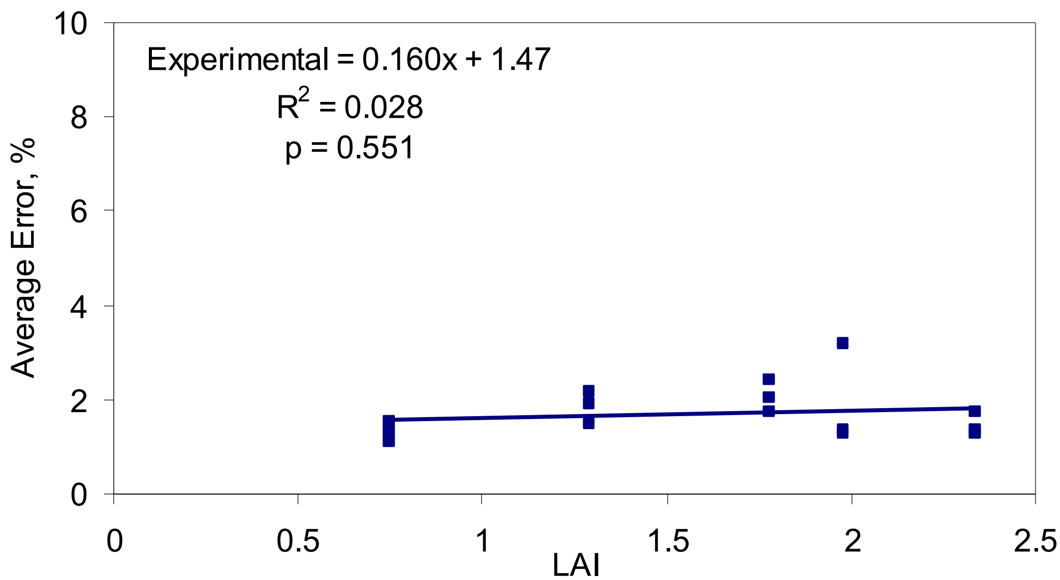

Figure 4.13. Average error of heat model as function of LAI during validation indicated negligible model bias.

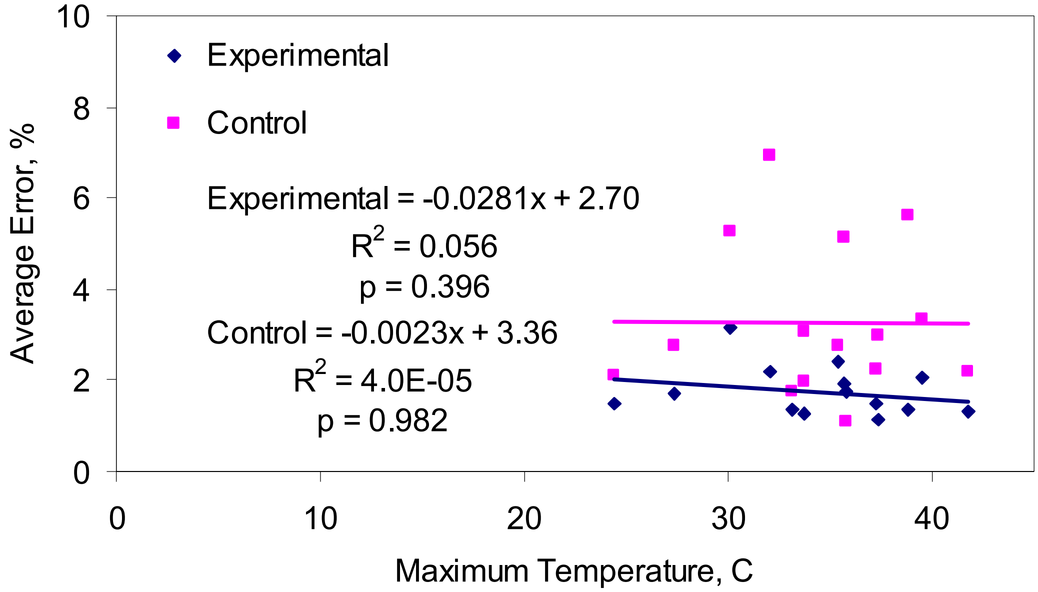

Figure 4.14. Average error of heat model as function of maximum daily temperature during validation indicating negligible model bias.

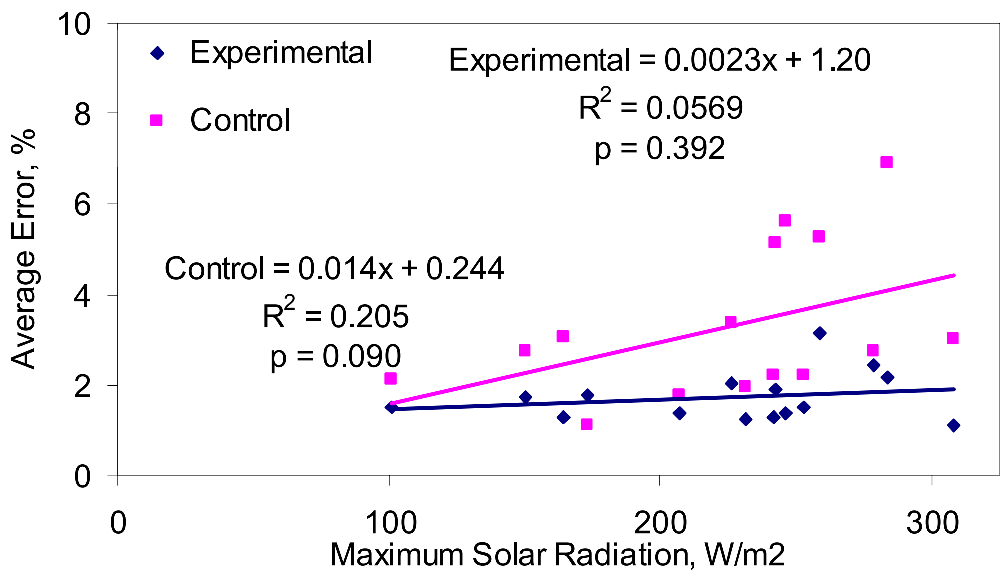

Figure 4.15. Average error of heat model as function of maximum solar radiation during validation indicating negligible model bias.

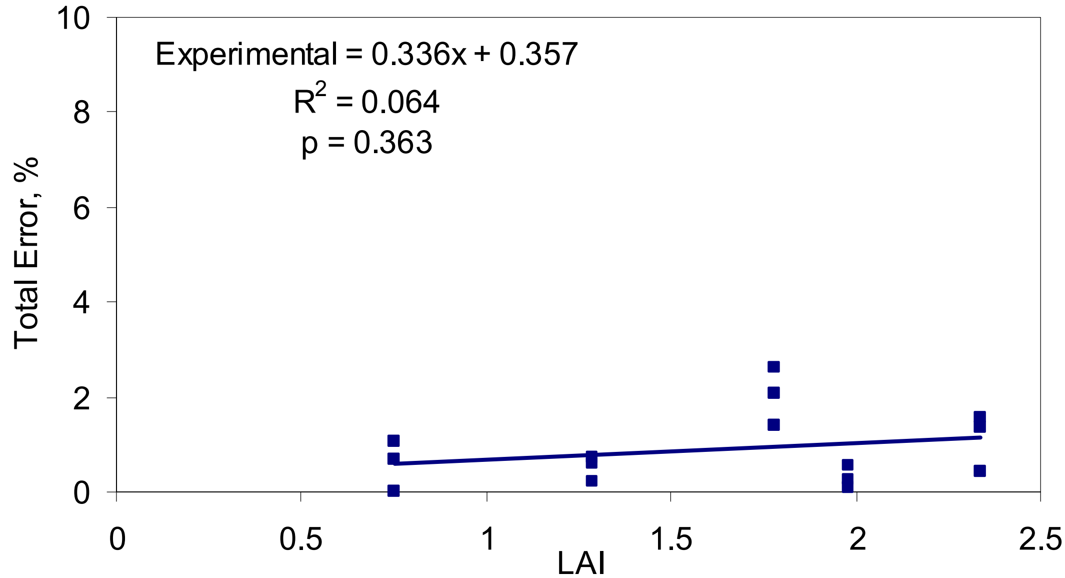

Figure 4.16. Total error of heat model as function of LAI during validation indicating negligible model bias.

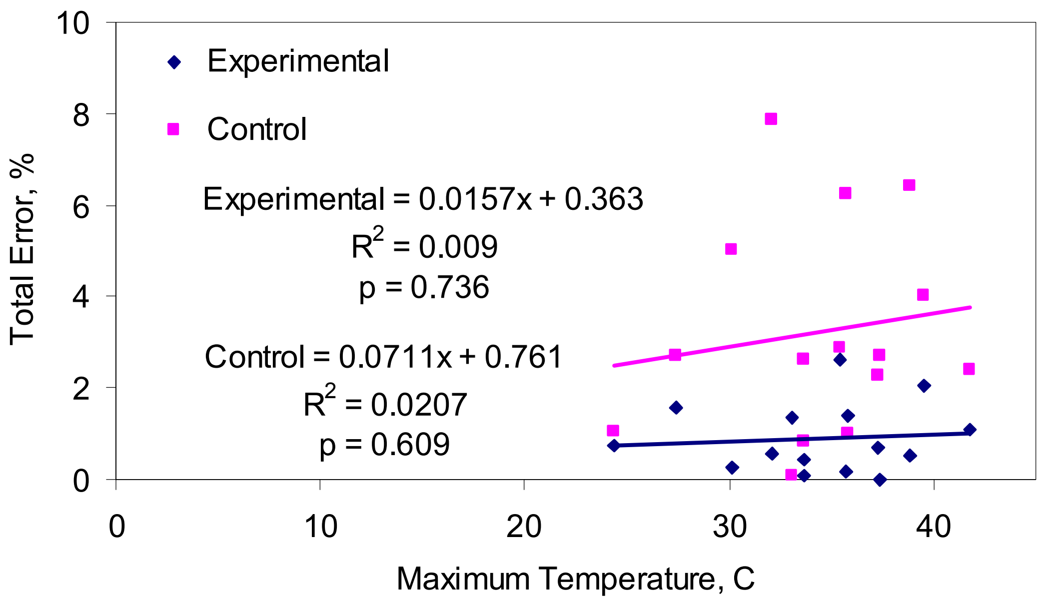

Figure 4.17. Total error of heat model as function of maximum temperature during validation indicating negligible model bias.

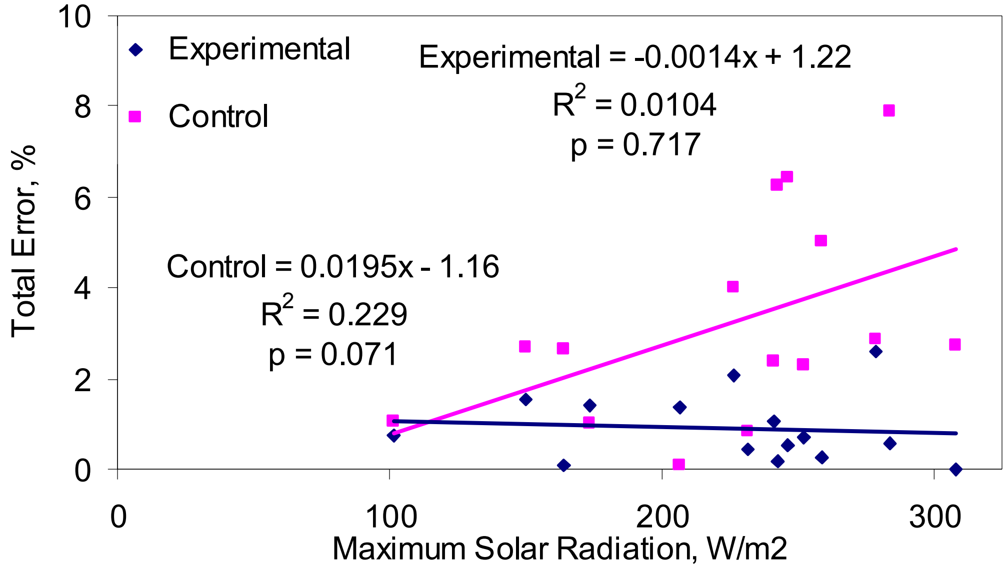

Figure 4.18. Total error of heat model as function of maximum solar radiation during validation indicating negligible model bias.

Table 4.6 displays the average date, maximum temperature, maximum solar radiation, leaf area index, average experimental error, average control error, total experimental error, and total control error for the validation data. We made this table to understand model validation conditions and associated model error. Knowing how the model was validated indicates the environmental temperatures, solar loading, and cloak leaf area indices under which we can apply the model with confidence.

Table 4.6. Validation conditions and associated model error.

	Average	Standard Deviation
Date	6-Jul	14 days
Max Temp, C	34.41	4.61
Max Sunlight, W/m2	224.38	55.96
LAI	1.63	0.57
Ave Exp Error, %	1.73	0.54
Ave Control Error, %	3.28	1.67
Total Exp Error, %	0.90	0.76
Total Control Error, %	3.21	2.28

The model was validated in the summer when annual temperature and solar radiation were highest indicating that model use may be limited at other times of the year. Also, the validation average leaf area index was 1.63 with 0.57 standard deviation meaning we were unable to validate the model against high leaf area indices. Although model bias to higher leaf area indices did not exist, we must use caution when applying the model to cloaks with higher leaf area indices than with what we validated.

The average experimental and control error was the average error in temperature estimation for each minute. This signifies the error in any model predicted temperature. We can expect 1.73% ± 0.54% in experimental temperature prediction and 3.28% ± 1.67% in control temperature prediction.

The total error indicates how the model predicts temperature over a 24-hr period rather than at each minute. This will be useful when we use daily temperature averages to make daily air conditioner energy reduction predictions. In our application of the model, temperature at each minute is less important than daily average temperature predictions. We can expect 0.90% ± 0.76% daily average experimental temperature prediction and 3.21% ± 2.28% in daily average control temperature prediction.

Additionally, bias figures showed that error was always higher for the control data than for the experimental data. The average experimental and control errors for each minute of the fifteen validation data sets were averaged to one data set so that error at each minute could be determined allowing us to see during which part of the day the model was strongest. Error between control and experimental data could also be examined (Figure 4.19).

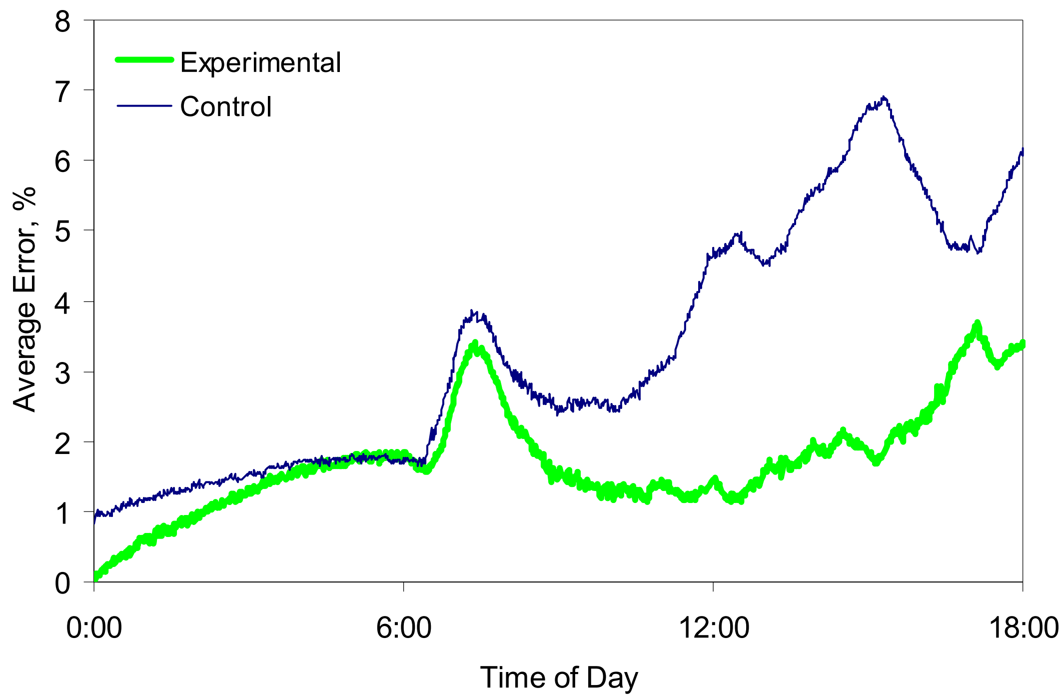

Figure 4.19. Average error of the predicted temperature for experimental and control houses based on fifteen validation runs of the model.

In compliance with bias figures, control-house error was always greater than experimental error for the 18 h validation period. We observed a spike in both sets of error data just after sunrise (0600 h). Error drops after reaching a 3 to 4% maximum, but then gradually rises throughout the day for both sets of data. Despite these differences, error for both data sets is still relatively low. The average error in the 18 h period for the experimental error was 1.73% with 0.75% standard deviation. Average control-house error average error was 3.28% with 1.74% standard deviation.

Model Results

From the fifteen days of validation data, average solar radiation and environmental temperatures were determined. The average outdoor temperature and solar energy values are plotted in Figure 4.20. The average 0000 h experimental house temperature was 25.6 °C.

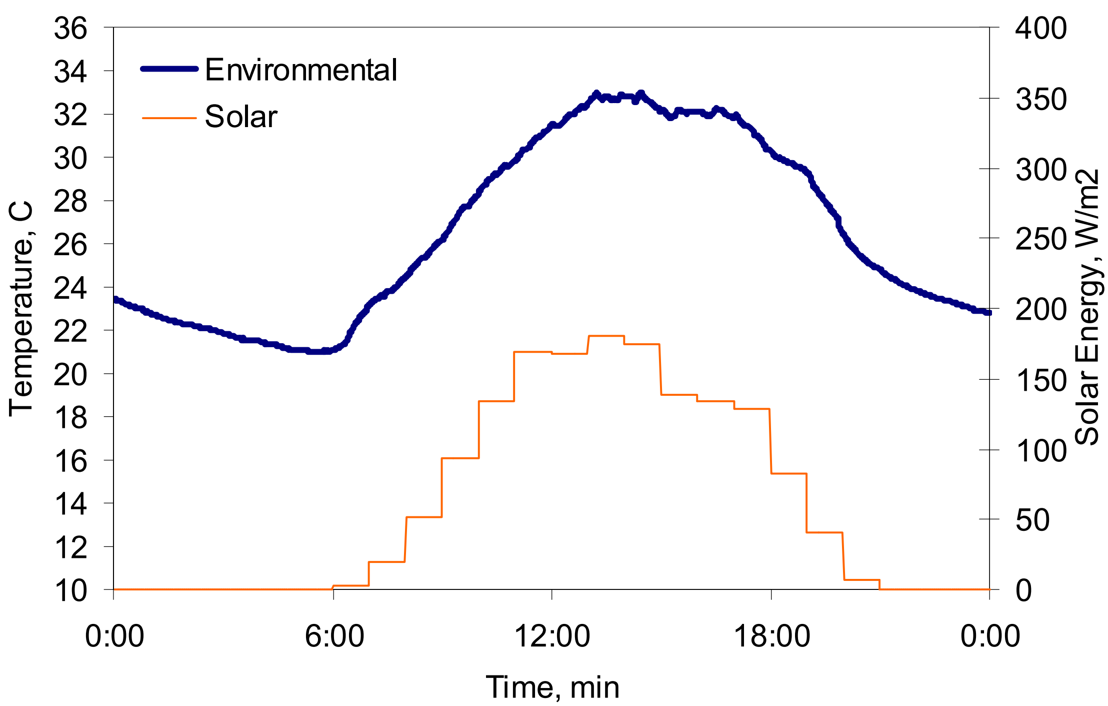

Figure 4.20. Validation data sets average environmental air temperature and solar energy.

These values were plugged into the model in Microsoft Excel using the same coefficients and model house dimensions and characteristics as in Model Validation. We found a steady state start temperature for each LAI by running the model several times changing the house temperature at 0000 h until indoor temperatures at 0000 h and 2359 h were equivalent.

We ran the model eight times with leaf area indices 0 through 7. The experimental house temperatures and environmental air temperature are shown in Figure 4.21. When we increased cloak LAI from 0 to 1, the maximum indoor air temperature decreased 3.93 °C (7.06 °F). Similarly, a cloak of LAI 2 produced a maximum indoor air temperature reduction of 5.28 °C (9.50 °F).

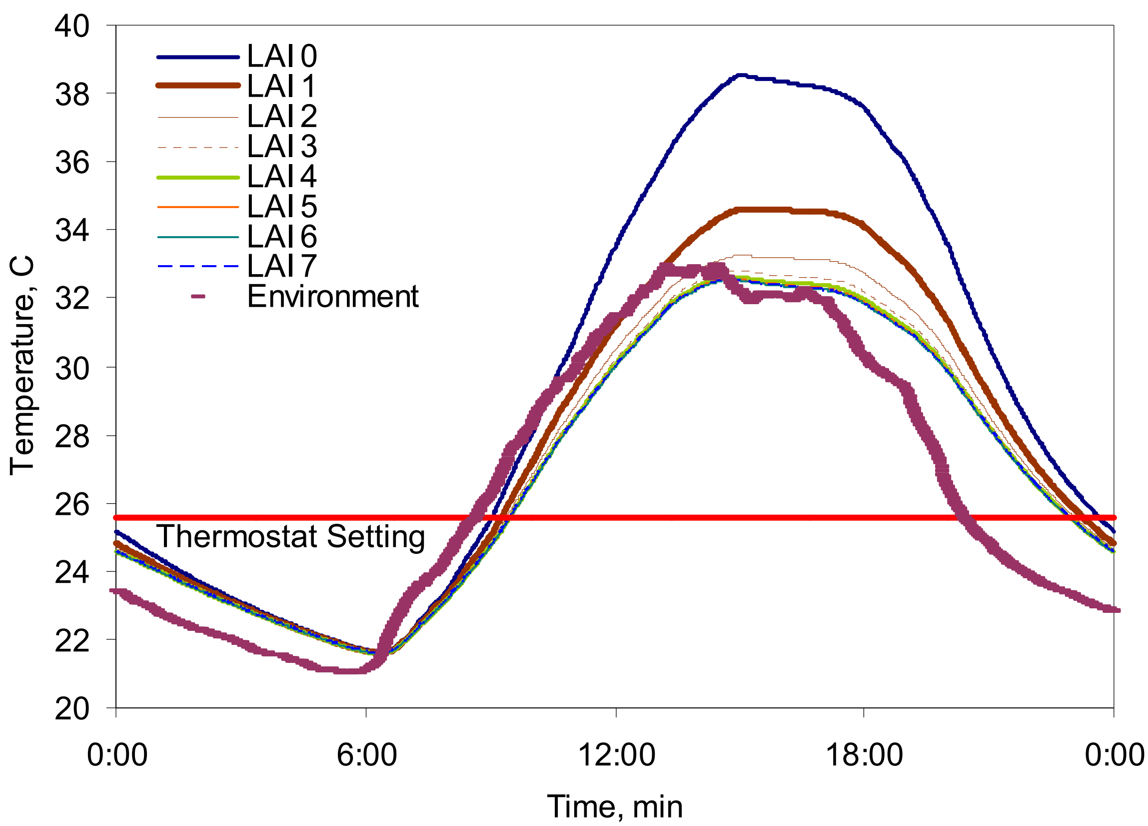

Figure 4.21. Predicted model house indoor air temperatures with cloaks that had LAI= 0 through LAI=7 with the bold horizontal line representing a typical thermostat setting.

The horizontal thick line at 25.6 °C (78 °F) was put on the graph as an example thermostat setting. No matter the particular thermostat setting, the area between the thermostat temperature and the predicted house air temperature represented the work that an air conditioning unit must perform to bring the house temperature to the thermostat setting. As we increased leaf area indices, the area between the house air temperature and thermostat temperature decreased. The decreased area signified a decrease in air conditioning energy consumption. We used this data to calculate air conditioning energy savings.

Looking at the temperature curve, we determined the average temperature reduction for cloaks with LAI 1 though 7 by

$$ATR = (\Sigma(H_{LAI = 0}))/1440 - (\Sigma(H_{LAI = X}))/1440 \qquad (56)$$

where ATR is the average temperature reduction in °C, $H_{LAI = 0}$ is the house temperature with no cloak in °C, and $H_{LAI = X}$ is the house temperature with a cloak of LAI X in °C.

Along with average temperature reduction, we calculated green cloak air conditioning energy savings finding the area between the predicted temperature curve and thermostat temperature curve for each LAI. This area is representative of the work an air conditioning unit must perform to the keep the building temperature at the thermostat setting. We calculated the percent energy savings as the percent area difference between cloaks of LAI 1 through 7 and no cloak (LAI 0).

$$B = (1 - ((\Sigma(H_{LAI = X} - 25.556))/(\Sigma(H_{LAI = 0} - 25.556))))*100\% \qquad (57)$$

where B is percent air conditioning energy reduction.

Based on the average temperature reduction of 2.03 °C (3.65 °F) for a green cloak with a leaf area index of 2 (average cloak canopy LAI was 1.73 at harvest), air conditioning energy reduction was estimated to be 40.4%. Both average temperature reduction and percent air conditioning energy reduction are plotted as a function of LAI in Figure 4.22. Additionally, both temperature reduction and energy savings were asymptotic with LAI showing that there is a limit to temperature reduction and air conditioning energy reduction.

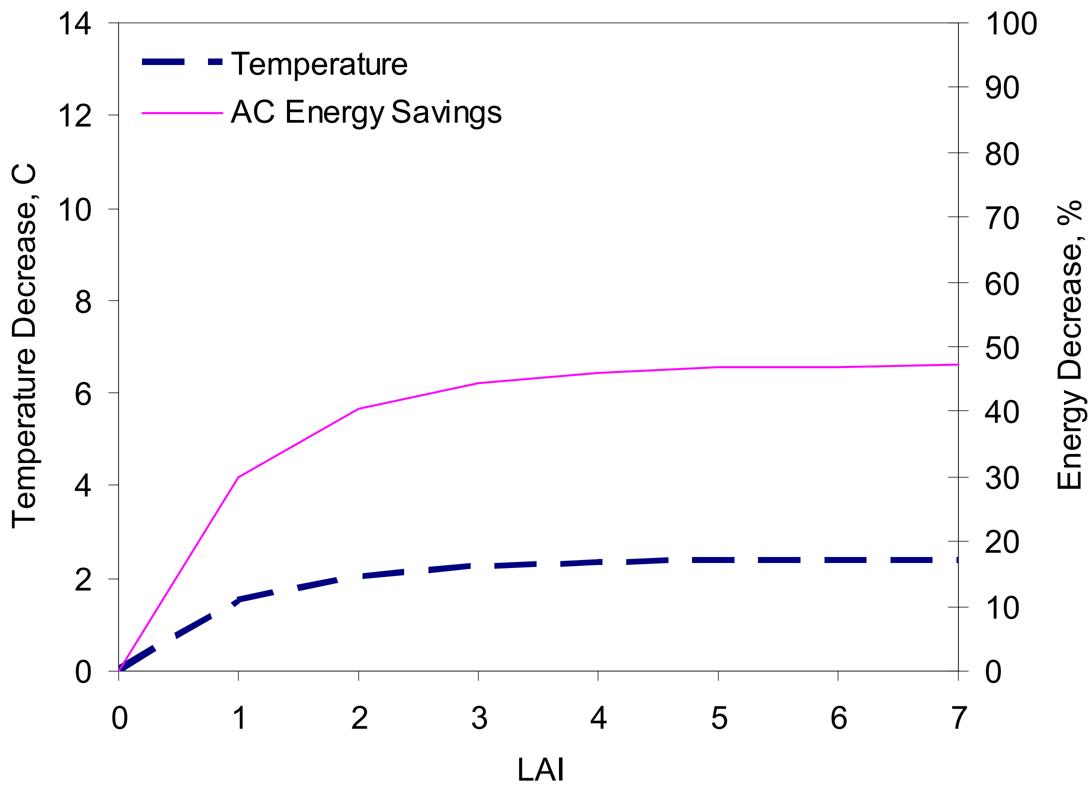

Figure 4.22. Average daily indoor house temperature reduction and air conditioning energy reduction based on cloak leaf area index given the diurnal outside air temperature and solar radiation in Figure 4.20.

Next, the model was scaled up to a 2000 ft^2 one-story (8 ft) building with three windows, a flat shingle roof, wall, roof, and floor insulation, and plywood siding and floor. With these dimensions and building materials, the roof area was 185.8 m^2, resistance value R_{total} of 0.000184 °C·min/J, and 544.14 kg mass of air in house. R_{total} for the full-scale house was an order of magnitude smaller than the model house because the wall thicknesses remained constant during scale up, but house surface area increased by one order of magnitude.

To derive R_{total} for the full scale house, we used Oak Ridge National Laboratory's (2007) website to recommend R-values for a building located in the College Park, MD area to ensure that we were using the model to simulate a typical building. The website suggested the following values for the building materials (Table 4.7).

Table 4.7. Suggested Building Material R-Values (Wikipedia, 2007) and (Desjarlais, 2007).

Insulation Location	R-Value, $ft^2·°F·h/Btu$	R-Value, $m^2·°C·min/J$
Roof, Attic	49	0.144
Floor	25	0.073
Wall	19	0.056
Window	1	0.003

Using the relative area of each building component (Table 4.8) and the total surface area (504.56 m^2) of the building, we calculated R_{total} for the scale up building (Eq. 58):

$$R_{total} = [(R_{attic})(AF_{attic}) + (R_{floor})(AF_{floor}) + (R_{wall})(AF_{wall}) + (R_{window})(AF_{window})]/SA \quad (58)$$

where AF is area fraction (relative area) of each building component and SA is total building surface area in m^2 giving:

$[(0.144)(0.368) + (0.073)(0.368) + (0.056)(0.263) + (0.003)(0.000507)]/504.56 = 0.000184$ °Cmin/J.

Table 4.8. Fraction of total building surface represented by each component 2000 ft^2 house.

Building Component	Area Fraction
Roof	0.368
Floor	0.368
Wall	0.263
Windows	0.000507

We ran the model eight times with leaf area indices 0 through 7. The full-scale house temperatures and environmental air temperature are shown in Figure 4.23. The example thermostat setting of 25.5 °C (78 °F) is plotted as a reference. When we increased cloak LAI from 0 to 1, the maximum indoor air temperature decreased by 9.87 °C (17.8 °F). Similarly, a cloak of LAI 2 produced a maximum indoor air temperature reduction of 13.1 °C (23.6 °F).

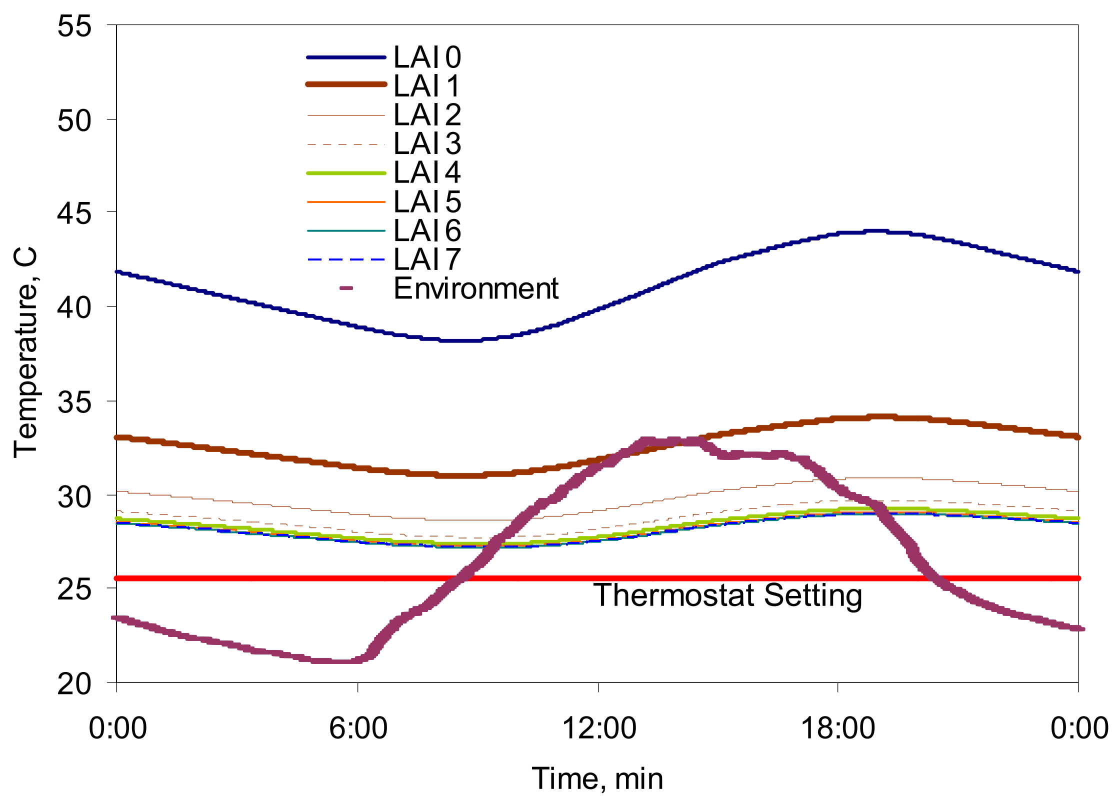

Figure 4.23. Predicted full-scale house indoor air temperatures with green cloaks having leaf areas of 0 through 7.

Again, average temperature reduction and air conditioning energy savings were computed and plotted versus leaf area index (Figure 4.24). With a green cloak of leaf area index 2, average temperature reduction was 11.3 °C (20.3 °F) and air conditioning energy reduction was estimated to be 72.9%. Both temperature reduction and energy savings were asymptotic with LAI.

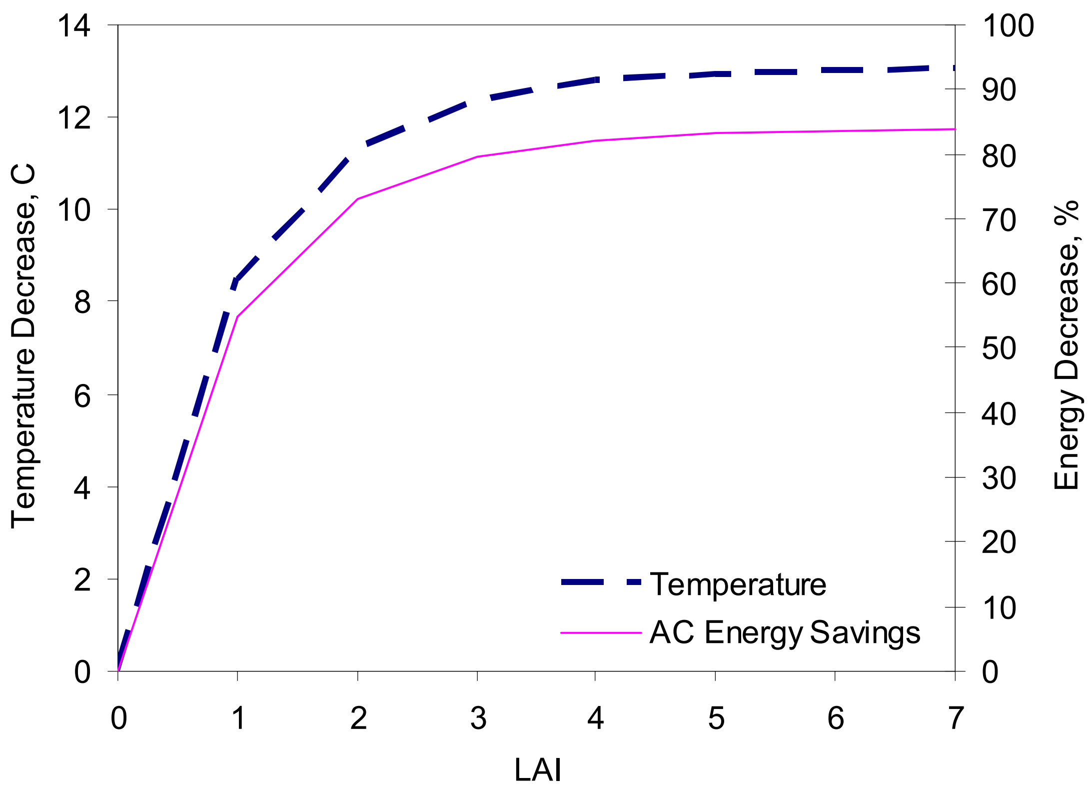

Figure 4.24. Average daily indoor house temperature reduction and air conditioning energy reduction based on cloak leaf area index given our specific diurnal outside air temperature and solar radiation shown in Figure 4.20.

Discussion

Temperature Model

We found two values of the convection coefficient k_2 were required to minimize model error—one during house warming and one during house cooling (Figures 4.8a and 4.8b). We propose that the two k_2 values were required because convective thermal energy flowed into the house differently than it flowed out of the house. In particular, since hot air rises, we suggest that energy mostly left the house through the roof, where it probably entered throughout the entire surface area of the house. The thermal resistance of the roof (and cloak) was different from the thermal resistance of the house walls and windows.

Although model error was acceptable, we are interested in the reason for the control error being greater than the experimental error (Fig. 4.19). This may be because the model only allowed house energy to be affected by the cloak through solar radiation, not through convection with the environment. In reality, the cloak added insulation to the building increasing its R-value and how thermal energy was exchanged with the environment. In our model state equation (Eq. 1), canopy leaf area index was not included in the "$k_2(E - H)/R$" term. Instead, the canopy leaf area index was only in house energy gain via solar radiation. With control error greater than experimental error, it seemed as though the model was calibrated to predict convective energy transfer with a cloak, but prediction ability was limited when no cloak was present. In the future, when applying the model to conditions where solar radiation is less making house energy gain via convection more significant than via radiation, model error may increase. This is a limitation to modeling, particularly in our simple model.

Also, we saw in the model application to the model-scale and full-scale house temperatures that there was a maximum temperature and energy consumption reduction. This was due to the cloak functioning by limiting solar radiation to the building and canopy light transmission being asymptotic with LAI. We learned that there is little energy savings advantage to a green cloak with LAI 6 or 7.

Green Cloak Energy Performance Comparison

We see significant summertime energy savings (72.9%) for the 2000 ft^2 building modeled with a canopy of leaf area index of 2. This is significant and demands pilot scale testing of the green cloak since we were unable to validate our temperature model to a full-scale building with an LAI of 2.

Given the modeled 72.9% energy consumption decrease and 11.3 °C average temperature decrease, a comparison to green roof energy savings is required. As stated in Chapter 3's Introduction, in Toronto, there was an average energy drop of 3 to 4 °C and a 5.1 °C temperature drop in India. A single story building with a grass roof saw a 25% reduction in summer cooling needs and in Pennsylvania, a 10% summer cooling energy reduction was experienced with an extensive sedum roof. Since savings are highly variable depending greatly on building size, shape, and construction, we can say our energy savings estimates are comparable to green roof energy savings and the low cost of the green cloak may make it the economic choice.

Although we did not conduct winter temperature experiments or modeling, the green cloak may be advantageous over the green roof in cold weather. Where green roofs block the warming winter sun with their layers of substrate and vegetation, the deciduous leaves of the green cloak vine community would fall off allowing the winter sun to warm building as it normally would if there was no cloak present.

Chapter 5: Effect of Green Cloak Canopy on Storm Runoff

<u>*Abstract*</u>

Increased impervious surfaces in urban areas increase stormwater runoff which can have detrimental effects on the local environment including flooding, erosion, and stream degradation. The alternative green roof retrofit, called the green cloak, was evaluated for its ability to affect runoff. The objectives of this study were to use a rainfall simulator to measure the amount of rainfall intercepted in eleven green cloak vine canopies, determine the runoff delay from the vine canopies, generate a mathematical model to estimate runoff based on rainfall simulator experiments, and compare empirical green roof runoff data to a green cloak using the model. The following measurements were made on eleven green cloaks before the rainfall simulator was used to measure the runoff from each cloak: leaf area index, canopy thickness, canopy coverage, and dead canopy. Experimental evidence indicated that LAI was a strong indicator of storm flow delay so a model was developed with LAI as a parameter to predict storm runoff from a cloak. For a 23 mm (~1 inch) rainfall event, the model estimated that a cloak with an LAI of 5 would delay the peak storm flow by at least one hour. During this event it stored 4.2 mm of rainfall (18%), which was about 33% of what an extensive green roof in North Carolina held (cite). This signified that a green cloak can significantly reduce storm flows, albeit to a lesser degree than an extensive green roof.

Introduction

Green Roof Hydrologic Service

As little as 10-15% impervious area in a watershed can degrade water quality in area streams. Often urban areas can be 10% impervious in residential neighborhoods and up to 71 to 95% impervious in industrial and commercial areas (Ferguson, 1998). As forested land is developed into built land, rainfall is no longer able to infiltrate to replenish groundwater. Instead it flows rapidly off impervious surfaces to nearby waterways. In fact, in urban areas it was estimated that 75% of total annual rainwater becomes runoff whereas in forested areas only 5% becomes runoff (Scholz-Barth, 2001).

This fast moving surge of stormwater runoff is detrimental—harming the natural and built landscape and killing biota. Local flooding and erosion are visible results of runoff. Less noticeable effects of runoff are the influx of raw sewage, particulate matter, motor oils, synthetic hydrocarbons, heavy metals, road salts, pesticides, and animal waste into local rivers. Even less obvious is the dropped water table occurring because impervious surfaces limit its recharge. Most urban areas will have their own water system and may not directly rely on groundwater as their source, but the loss of water table will negatively affect trees and crops (Dunnett and Kingsbury, 2004).

In the United States, green roofs are slowly becoming discovered for their hydrologic function. Green roofs provide valuable pervious surfaces that attempt to mimic a forested area's hydrologic function (Dunnett and Kingsbury, 2004). The affect of the green roof on stormwater runoff volumes and flow rates are recognized in Figure 5.1. Impervious surface discharge, or runoff, in an urban environment is much higher than the pervious surface discharge of a forested ecosystem. The peak flow is lower and occurs later for the pervious surface. The total volume (the area under each curve) is reduced for the pervious surface discharge because rainwater infiltrates into the ground or is intercepted by vegetation.

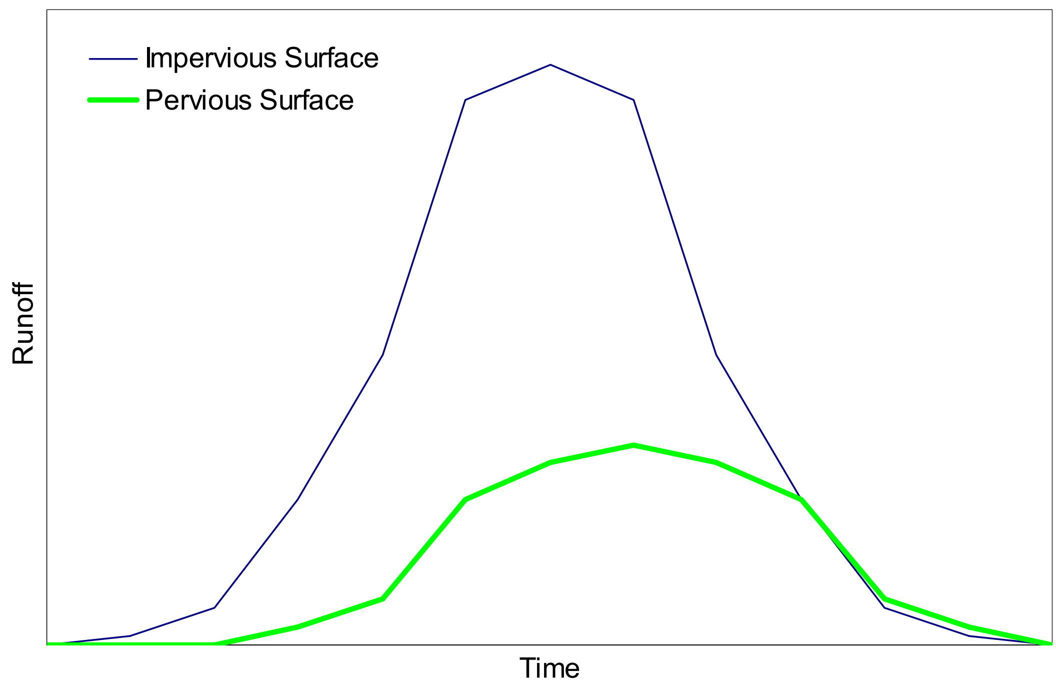

Figure 5.1. Theoretical hydrograph comparing delayed and reduced peak discharge of pervious surfaces compared to impervious surfaces.

Although green roofs are not required by law as in Germany, in some US cities there are incentives for their use. For example, in Portland for every 0.09 m^2 (1 ft^2) of installed green roof, builders are allowed 0.27 m^2 (3 ft^2) of floor space. This is advantageous to builders because they are able to build extra houses. One builder constructed six additional condominiums which earned him an estimated $1.5 million while the hydrology of the developed land was nearly unaffected (Dunnett and Kingsbury, 2004). Similarly, most towns, cities, and counties require developers to have a stormwater management plan; oftentimes, drainage basins are used to collect and hold stormwater—with green roofs, instead of using valuable land space for drainage basins builders can construct more units and have their stormwater runoff reduction strategy on the roof.

Green roofs reduce runoff by storing rainwater in substrate pore spaces, absorbing to substrate materials, being taken up by plants, being physically intercepted by plant leaves, transpired by plants to the atmosphere, or evaporating from plant and roof surfaces to the atmosphere. It is when rainfall volumes are higher than the green roof storage capacity that runoff begins to occur through the engineered green roof drainage system. Whatever the exact mechanism, runoff from green roofs occurs later and is less in volume than off of impervious surfaces. For example, in the summer when rainfall is high in temperate regions, runoff from a green roof moderately increased over a long period of time where runoff from a traditional roof massively increased over a short period of time causing damaging runoff to affect the surrounding area. See hydrograph comparison in Figure 5.1.

There are several factors that will affect the storage capacity of a green roof. For example, substrate depth, number of absorbent layers, type of layers, slope of roof, physical properties of growth media, and type of plants are all roof factors in the runoff reduction. Environmental factors that affect the performance of the green roof are the season, climate, and rainfall intensity and volume. In particular, season and climate are important because they affect green roof vegetation evapotranspiration potential (Dunnett and Kingsbury, 2004).

Researchers at Michigan State University examined the influence of vegetation in green roof runoff reduction. For six weeks in late summer and fall, runoff from a 12 cm layer gravel roof was compared to an extensive green roof with no vegetation, and an extensive green roof with sedum vegetation. The green roofs produced less runoff than the gravel roof and during times of heavier precipitation, the green roof with the vegetation produced less runoff than the green roof without vegetation (Rowe et al., 2003). The sedum and substrate on the green roof acted as sponges and offered valuable storage space that the gravel roof could not offer.

In Belgium, an increase in substrate depth showed a decrease in runoff. A standard rooftop converted 81% (665 mm) of rainfall to runoff while a 15 cm deep green roof converted only 40% (329 mm) of rainfall to runoff (Mentens et al., 2003). Runoff reduction was reduced little on roofs with substrate deeper than 15 cm indicating optimal substrate depth (Optigrün, 2002). Of course, optimal substrate depth was directly related to the region's rainfall and climate.

Optimal green roof depth in Portland, OR appeared to be close to 10 cm. This depth prevented 69% of all annual rainfall and 100% of all warm-weather storms from becoming runoff (Hutchinson et al., 2003).

Existing roof moisture content was a significant factor in the ability of a green roof to take up stormwater. If a sponge is already wet, it will have little additional water capacity. If the green roof was recently wet, its storage capacity is lower than a dry one (Rowe et al., 2003). This relates to the evapotranspiration potential in the surrounding air also. If air is humid, water will not evaporate from plants, decreasing green roof function. Similarly, if temperatures are not high enough for evaporation, evaporation will not occur. Peck et al. (1999) found 70 to 100% runoff reduction in the summer compared to in the fall when reduction was only 40 to 50% (1999). The warmer temperatures increased evaporation to the atmosphere.

Green roof hydrologic performance was highly dependent on local climate making it difficult to predict hydrologic function. According to Dr. Berghage, from the Eastern United States, a 3 to 4 inch green roof can retain about 50% of annual stormwater runoff (Berghage, 2006). Researchers estimated runoff reduction in other parts of the world. Measured during a rain event, a 3 cm sedum-moss roof in southern Sweden had runoff values that were half of precipitation rates, showing that runoff volume was essentially halved compared to a traditional impervious roof (Bengtsson, 2005).

Results of eighteen German green roof hydrology publications were used to make a model of European climate green roof hydrology. Modelers predicted cladding only 10% of buildings green roofs in Brussels, Belgium would result in a 2.7% runoff reduction for the entire city. A 54% runoff reduction was estimated for each building (Mentens, 2006).

Based on depth of rainfall, Goldsboro and Raleigh, North Carolina green roofs retained 63 and 55% of rainfall, respectively with up to 90% runoff reduction observed on the Goldsboro roof during one storm. Runoff rates from the green roofs were 87 and 57% less than the actual rainfall intensity (Moran, 2005).

Cloak Interception

Ecological inspiration for the green cloaks came partly from an understanding of forest water budgets. In forests of the eastern U.S., annual interception by canopies is between 10 and 17% of precipitation (Huff et al. 1978). Complete loss of leaf area if forests has been shown to increase their annual water yield by 20 to 29% (Huff et al. 1978). Thus, vegetated canopies can have a large impact on water budgets. It was our belief that the canopy of the green cloak could have a similar impact on urban water budgets.

For the light weight alternative green cloak design proposed in Chapter 1, the substrate and vegetation layers of the extensive green roof were replaced with a vine trellis system called the green cloak. Vines grow in the ground soil keeping the roofing system lightweight. Like a green roof, the vine canopy will intercept and store rainfall on its leaves and stems. This intercepted rainfall will eventually evaporate to the atmosphere or will be transferred below the cloak to the house gutter system. The small water storage associated with the green cloak's canopy may have a significant effect in delaying the onset of the peak storm discharge. We believe the green cloak's hydrograph will be between an impervious building surface and an extensive green roof.

Dunnett and Kingsbury (2004) only touched on the possibility of façade greening vine systems having hydrologic function. Little literature exists on the ability of the vines to affect runoff. The authors explained that this data does not exist, particularly in European research, because green roofs have been successfully proven to have a significant impact on runoff reduction. There has been little demand for the hydrologic function of façade greening ecosystems since these systems have been mostly used for aesthetic and thermal purposes (Chapters 3 and 4). Conversely, there is decades of studies on the water budget of forest canopies, which are a close analog to the green cloak. Along with rainfall interception amounts, stem flow, canopy transmission rainfall, and plant water uptake data has been published.

Table 5.1 lists several of the published canopy storage values. These values, based on leaf area index, will be used to estimate the interception abilities of vine canopies. As with green roof runoff function, it must also be realized here too that the canopy storage of each tree stand is a function of climate, canopy age, plant density, rainfall, drying cycles, and plant diversity (Link et al., 2004). In the table, we calculated the storage per LAI column using the steady state storage values and LAI values given in the water budget literature.

Table 5.1. Canopy water storage and leaf area index for various forests.

Forest type	Location	Steady State Storage, mm	LAI	Storage/ LAI, mm*	Source
Cashew trees	India	0.8	1.0-1.25	0.64-0.8	Rao, 1987
Mature rainforests	Colombian Amazonia	1.33	5.4	0.25	Marin et al., 2000
Norway spruces, Scots pine	Sweden	1.69	4.5	0.38	Lankreijer et al., 1999
Deciduous forest	Japan	1.12	2.77	0.42	Deguchi et al., 2005
Deciduous forest	Japan	0.59	4.24	0.14	Deguchi et al., 2005
Tabonco tpe forest	Puerto Rico	1.15	5.9	0.19	Schellekens et al., 1999
Temperate conifers	Pacific Northwest, US	2.7-4.3	8.6	0.31-0.5	Link et al., 2004
Temperate conifers	Na	2.4	9-13	0.18-0.27	Klaassen et al., 1998
Temperate conifers	Europe	1.1	8.55	0.15	Rutter et al., 1975
Temperate conifers	Europe	0.50-0.55	3	0.17-0.18	Loustau et al., 1992
Hardwoods	Georgia, US	1.4	na	na	Bryant et al., 2005
Mixed trees	Georgia, US	1.58	na	na	Bryant et al., 2005
Pines	Georgia, US	1.97	na	na	Bryant et al., 2005
Pines, oaks	Georgia, US	1.7	na	na	Bryant et al., 2005
Wetland trees	Georgia, US	0.98	na	na	Bryant et al., 2005
Average				*0.31*	
Standard Deviation				*0.17*	

*This column was calculated by the author using the published literature canopy storage and leaf area indices.

Table 5.1 indicates that for each unit of leaf area index, a vine canopy can be expected to hold 0.31 mm of water, but maybe as much as 0.8 mm. With a goal that the cloak canopy will have an LAI of 5 (i.e., the maximum LAI observed on vine covered barns in Chapter 2), we expect a cloak of LAI 5 to hold 1.55 mm of water, but it could hold as much as 4.0 mm. Of course this is only 16% of what a green roof is expected to hold—a 10 cm-deep green roof will hold about 25 mm with 25% porosity (Berghage, 2006). However, a small amount of storage can delay peak stormflows by hours. For example, a 24 mm rainfall event (~1 inch) that occurred over 6 hours would deliver 4 mm of rainfall per an hour. If the relationship between canopy storage, rainfall and runoff were strictly linear (which it is not), the 4 mm of canopy storage would store the first hour's rainfall and delay the beginning of runoff by one hour.

We have developed the following experimental objectives to evaluate green cloak hydrologic function compared to green roof hydrologic function.

Objectives

The objectives of this study were to:

1. Measure the amount of rainfall intercepted by green cloak vine canopies.
2. Determine the effect of a green cloak vine canopy on roof runoff.
3. Develop a hydrologic model of the green cloak to estimate roof runoff given variously sized rainfall events.
4. Compare hydrologic effects of the green cloak to an extensive green roof.

Materials and Methods

System Description

The experimental system was designed so that we could predict green cloak canopy interception and building rainfall runoff given a rain event. To this end, we used a rainfall simulator, one model plywood house, and eleven model green cloaks of varying leaf area indices to individually measure runoff volumes from the model house and each cloak. We built the model house (1.75 m x 1.5 m x 1 m) with 2” by 4” plywood framing and ¾” plywood floor, walls, and roof. We covered the plywood roof with standard black asphalt shingles (GAF Materials Corporation). The house had three plexiglass covered windows and one door. We added fiberglass insulation (Owens Corning, R-13) to the ceilings and walls and painted the outside of the house white (Figure 5.2).

Figure 5.2. Scaled model plywood houses with shingled roof. We used only one house in the rainfall experiment.

To collect runoff from both the roof and the vine cloak, a gutter system was constructed with a plywood frame and plastic sheeting. Gutters were sloped so that rainfall would collect in two diagonal corners of the house (See Figure 5.3). We use the term watershed to describe the area in which we will apply rainwater and collect runoff from—the cloak, roof, and gutters.

Figure 5.3. Construction of gutter system on model house.

We built frames for eleven green cloaks from ¾ inch (1.9 cm) diameter polyvinylchloride (PVC) tubing (Charlotte Pipe and Foundry Company). Using 16-guage wire, we constructed a grid of 6 inch (15.2 cm) squares on each frame to serve as a trellis for vine attachment (Figure 5.4). Green cloaks were designed to fit over the top of the model house with about a 20 cm gap between vegetation and the asphalt shingles (Figure 5.5).

Figure 5.4. Green cloak composed of PVC frames, wire trellis mesh, and potted vines.

Figure 5.5. Green cloak fit over model house with 20 cm gap.

We grew one vine species on each green cloak (Figure 5.6). Nine vine species were selected based on availability of local plant materials: black-eyed susan vine (*Thunbergia alata*), cross vine (*Bignonia capreolata*), kudzu (*Pueraria lobata*), Japanese honeysuckle (*Lonicera japonica*), moonflower (*Ipomoea alba*), morning glory (*Ipomoea tricolor*), porcelain berry (*Ampelopsis brevipedunculata*), Chinese trumpet vine (*Campsis grandiflora)*, and Virginia creeper (*Parthenocissus quinquefolia*). We constructed a total of eleven cloaks—two kudzu cloaks, two Virginia creeper cloaks, and seven cloaks each with one of the remaining seven vine species (Figure 5.7).

On each trellis, four individuals of each vine species were grown in potting soil in 2-gallon pots and placed at the corners of each green cloak. Cloaks were grown at the University of Maryland Research Greenhouse Complex in College Park, MD from August 2005 through mid May 2006. In May cloaks were moved outside where they remained until the end of the experiment in September 2006. In the greenhouse, cloaks were watered three times per week and fertilized (Jack's 20-10-20, Allentown, PA) once per week. While growing outside, cloaks were watered daily and fertilized (Nutricote 18-6-8, Bellevue, WA) once every 180 days.

Figure 5.6. Kudzu 2 green cloak.

Figure 5.7. Eleven green cloaks comprised of nine vine species.

Experimental Design

On September 18, 2006, after a full growing season, we measured the runoff of each cloak using a rainfall simulator. All rainfall runoff experiments were conducted in one day.

One at a time, each of the eleven canopies was placed over the model house (Figure 5.8) and a University of Maryland Department of Biological Resources Engineering constructed rainfall simulator was used to generate a 0.15 mm/min (8.5 in/day) rain event (Figure 5.9). For reference, a storm of rainfall intensity of 0.13 mm/min (7.3 in/day) is a 100-year 24-hour storm in College Park, MD (Schwab et al., 1992). Additionally, a control experiment was run collecting runoff from only the model house without a cloak.

Importantly, before each cloak trial, leaves and any remaining water were removed from the gutters and the roof and gutters were wetted with a hose so that they were equally wet (or dry) before each runoff experiment.

Figure 5.8. Cloak, house, and gutter system under rainfall simulator.

Figure 5.9. Rainfall simulator shown in place above model house.

Data Collection

Leaf area index (LAI), canopy thickness, percent canopy cover, and percent dead cover were collected from each cloak before runoff experiments were conducted.

LAI was the ratio of canopy leaf area to ground surface. An LAI of 2, for example, indicated that the area of leaves in the canopy was twice that of the horizontal surface they covered. Leaf area index was measured using the point-intercept method by inserting a meter stick perpendicular to the ground through the canopy and counting the number of times a leaf or leaflet touched a particular edge of the meter stick. A total of six subsample measurements were made on each cloak.

Canopy thickness was the entire vertical length of the canopy on the trellis. To make the measurement, a meter stick was inserted perpendicular to the canopy four times, twice on each canopy side, to measure the length the canopy consumed.

Percent canopy cover, ranging from 0 to 100%, was a measurement of the amount of horizontal vine coverage on the trellis. Percent cover was roughly estimated on each side of the trellis for a total of two measurements per trellis.

Percent canopy dead, ranging from 0 to 100%, was a measurement made to indicate the health of the canopy. Again, a measurement was made on each side of the canopy for a total of two measurements per trellis. Dead leaves were considered those that had chlorophyll loss or had senesced, either being yellow or brown in color.

Runoff was measured from the watershed comprised of the vine canopy, the shingle roof, and the plastic gutters. Runoff fell from the rainfall simulator, hit the cloak vine canopy, fell on the roof, and then ran down the gutters into two collection buckets

(Figure 5.10). The buckets were at diagonal corners of the house and their water depth was measured once per minute for a minimum of ten minutes with a meter stick.

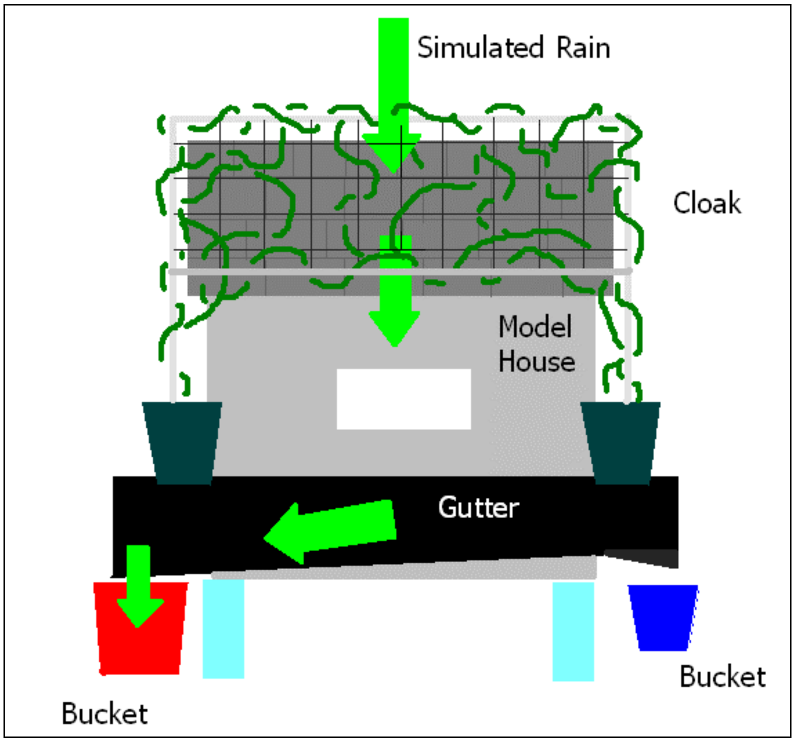

Figure 5.10. Schematic of one possible path of rainfall from rainfall simulator, through cloak to roof, off of the roof to the gutters, and down the gutters to one of the measuring buckets.

Data Analysis

We found the mean of each growth characteristic (i.e., leaf area index, thickness, percent cover, and percent dead) for each green cloak to explore their relationship to roof runoff.

We estimated roof runoff by tracking cumulative water accumulation in the two buckets for a period of at least ten minutes in each bucket. We converted the depth of water in each bucket to a runoff volume based on the dimensions of the bucket and summed the volumes from both buckets. The area of the watershed (33,912 cm^2) was measured using a meter stick and the bucket runoff volume was divided by the watershed area for a runoff depth over the entire watershed.

To perform runoff regression for each cloak and to create the hydrologic model, we required a time series plot of runoff at each minute for all of the cloaks. Since runoff measurements were cumulative, meaning each measurement included the runoff from all previous minutes, we subtracted the previous minute's runoff from that minute's runoff volume to find incremental runoff at each minute (Eq. 1).

$$I_n = M_n - M_{n-1} \qquad (1)$$

where I_n was incremental runoff during minute n, M_n was runoff measured at minute n, and M_{n-1} was measured runoff at minute n – 1.

Upon plotting the time series for each cloak, we found that runoff for each minute was highly variable and inconsistent due to the variable pooling of rainfall in the plastic gutters. To alleviate the experimental error and in an attempt to evenly distribute the pooled rainfall as runoff, the ten incremental runoff depths were smoothed using a running average of five minutes. With this smoothing technique, data points zero through four were lost to the fifth minute. To reclaim these points, points zero through four linearly increased to the fifth minute. To do this, the fourth data point was subtracted from the zero data point. This difference was divided by five. The fraction found was added to the zero point to generate the first point. The fraction was then added to the first point to make the second point, etc. until all five missing points were regenerated.

For hydrologic model genesis, we first completed linear regression to determine whether LAI, canopy thickness, percent live cover, or percent dead cover primarily controlled cloak storage (SPSS for Windows v. 13.1). A p-value of 0.05 was used to determine whether relationships were significant.

Regression Results

R^2 and p-values of each of the regression lines are displayed below in Table 5.2. It shows that runoff at minutes 6, 8, and 10 were best predicted by canopy cover. R^2 values were highest and p-values were lowest for this canopy characteristic. Alternatively, canopy dead predicted runoff the worst. R^2 values were the lowest here, while p-values were the highest showing that there was little correlation between runoff and percent dead.

Table 5.2. Effect of each cloak characteristic on storm runoff (R^2 coefficient of determination, p-significance value of relationship) at minutes 6, 8, and 10 of the experiment.

		Minute		
Characteristic	**Statistic**	**6**	**8**	**10**
Leaf Area Index	R^2	0.556	0.599	0.559
	p	0.005	0.003	0.005
Thickness	R^2	0.716	0.734	0.632
	p	0.001	0	0.002
Percent Cover	R^2	0.913	0.868	0.678
	p	0	0	0.001
Percent Dead	R^2	0.02	0.002	0
	p	0.665	0.893	0.97

From this analysis and the properties of each canopy characteristic, we determined that the runoff model would be based on leaf area index. Although regression results revealed that percent cover predicted runoff values the best, this measurement was highly qualitative. Measurements of LAI were easily made using the point intercept method, making results repeatable and easily averaged for all technicians. Additionally, it was thought that LAI was a better descriptor of the canopy because it took into account all three dimensions of the vine canopy; whereas percent cover only took two dimensions into account, ignoring thickness of the canopy. In addition, forest water budgets typically identify LAI as the key component in estimating interception.

Figures 5.12a through 5.12d are linear regressions of runoff values at minute 10 versus LAI, thickness, percent cover, and percent dead (linear regression at minutes 6 and 8 are in the Appendix). The equation of each regression line is on each figure, along with R^2 and p-values. All regression lines other than percent dead had a negative slope. The negative slopes indicated that leaf area decreased runoff. Extrapolation of the relationship indicated that there would be no runoff for the first 10 minutes if LAI = 5.5 (Figure 5.12).

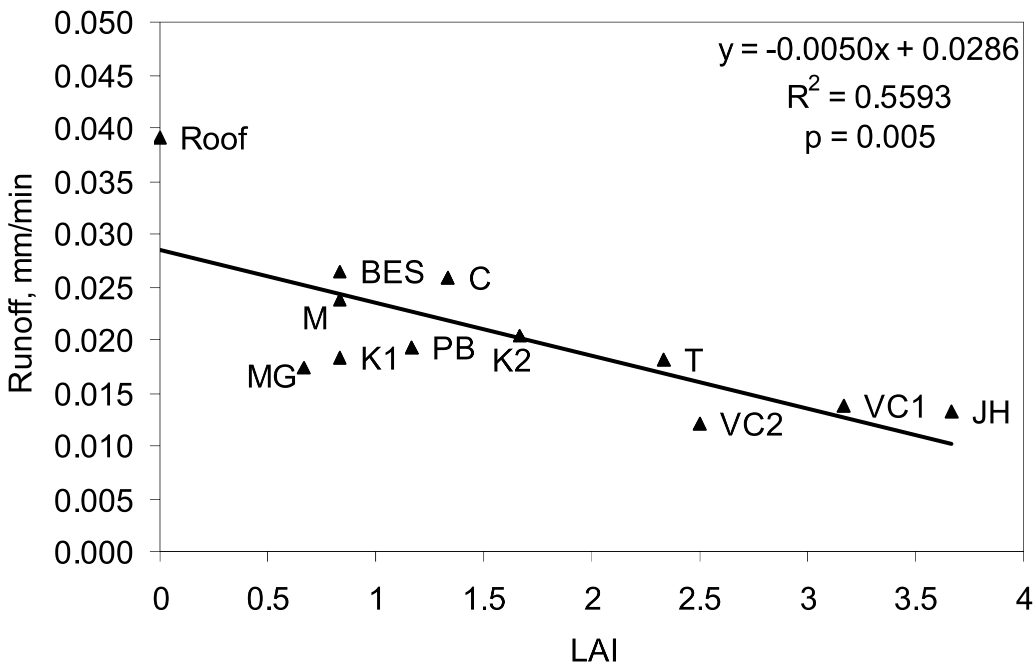

(a) LAI, p = 0.005

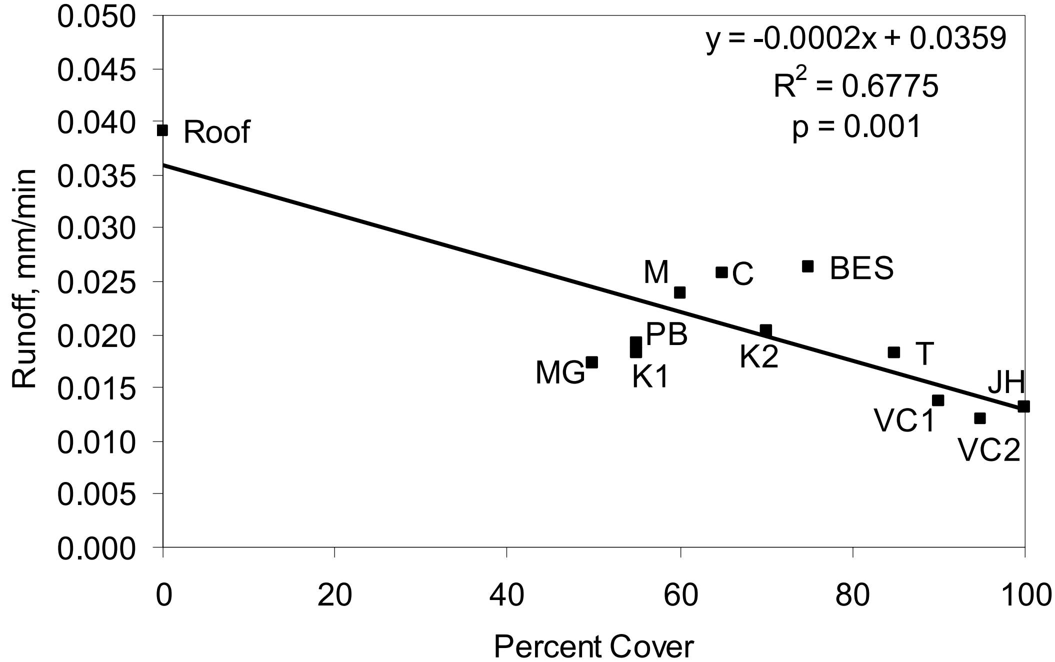

(b) Percent cover, p = 0.001

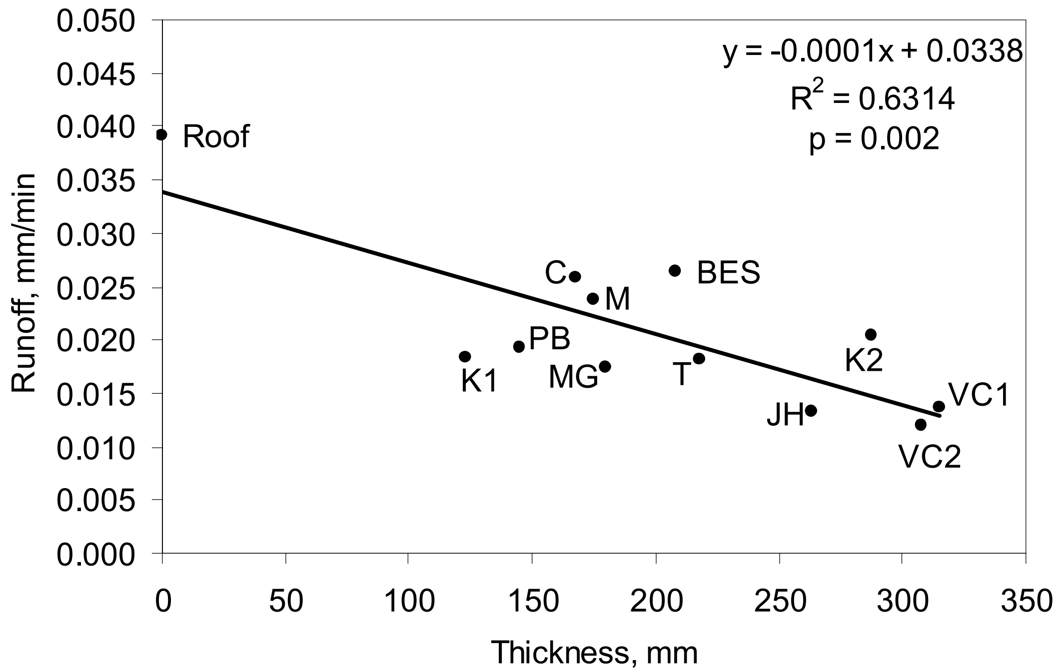

(c) Thickness, p = 0.002

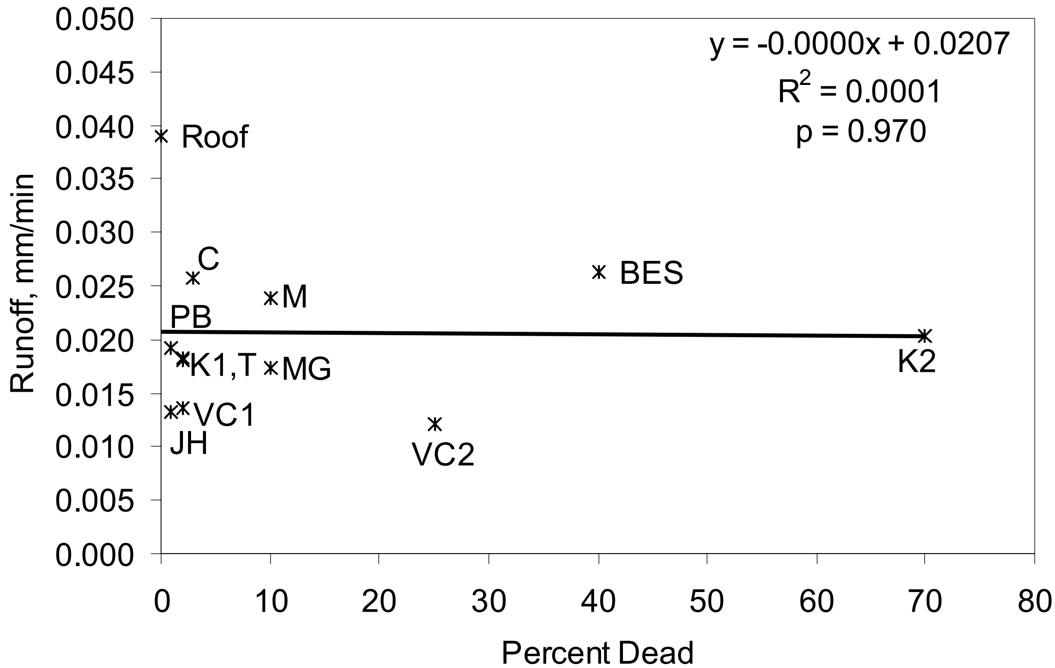

(d) Percent dead, p = 0.970

Figures 5.12. Leaf area index, canopy thickness, percent cover, and percent dead runoff regression for minute 10 runoff. Data points represent each cloak: Black Eyed Susan Vine (BESV), Porcelainberry (PB), Kudzu 2 (K2), Morning Glory (MG), Cross Vine (CV), Kudzu 1 (K1), Moonflower (M), Chinese Trumpet Creeper (CTC), Japanese Honeysuckle (JH), Virginia Creeper 2 (VC2), and Virginia Creeper 1 (VC1).

Hydrologic Model Creation

Model Development

We created a hydrologic model of the experimental green cloak system to estimate how much water the vine canopy could store and how much peak runoff was delayed. The model included rainfall as a source, canopy storage, gutter storage, and watershed outflow (Figure 5.13). Rain (J) fell on the canopy storage (Q) and then continued on to the gutter storage (G). All other losses of water from the canopy were assumed to equal zero. Runoff from the canopy was a function of canopy water and LAI (kQ/(LAI + 1)). In the experimental system we measured flow as it left the gutters. Therefore, we included gutter rainfall storage and runoff flow, so we could calibrate the model to our experimental data. Rainfall (J) was generated by the rainfall simulator. The state equation for canopy storage is given in Eq. 1, while the state equation for the gutters is given in Eq. 2. State equations are written as change in quantity stored is equal to storage inflow minus storage outflow.

$$dQ/dt = J - kQ/(LAI + 1) \qquad (1)$$

where dQ/dt was the change in cloak and roof rainfall storage over time in units mm/min, J was the rainfall intensity in mm/min, k was the cloak and roof runoff coefficient in 1/min, Q was the rainfall storage in the cloak and roof in mm, and LAI was the leaf area index which was unitless.

For the watershed state equation:

$$dG/dt = kQ/(LAI + 1) - k_G G \qquad (2)$$

where dG/dt was the change in gutter rainfall storage over time in units mm/min, k_G was the gutter runoff coefficient in 1/min, and G was the rainfall storage in the gutters in mm.

The expression "LAI + 1" controlled the amount of canopy storage based on canopy LAI. This indicated that as LAI increased, more water was held in the canopy and less water ran off to the gutters (G). The "+ 1" part of the "LAI + 1" expression accounted for water storage on the shingle roof. This assumed that the roof could store the same amount of water as a canopy with a leaf area index of 1. The "+ 1" allowed the model to account for water stored on the shingle roof if there was no cloak (LAI = 0) over the house. During model calibration, this value of 1 may be altered to minimize model error.

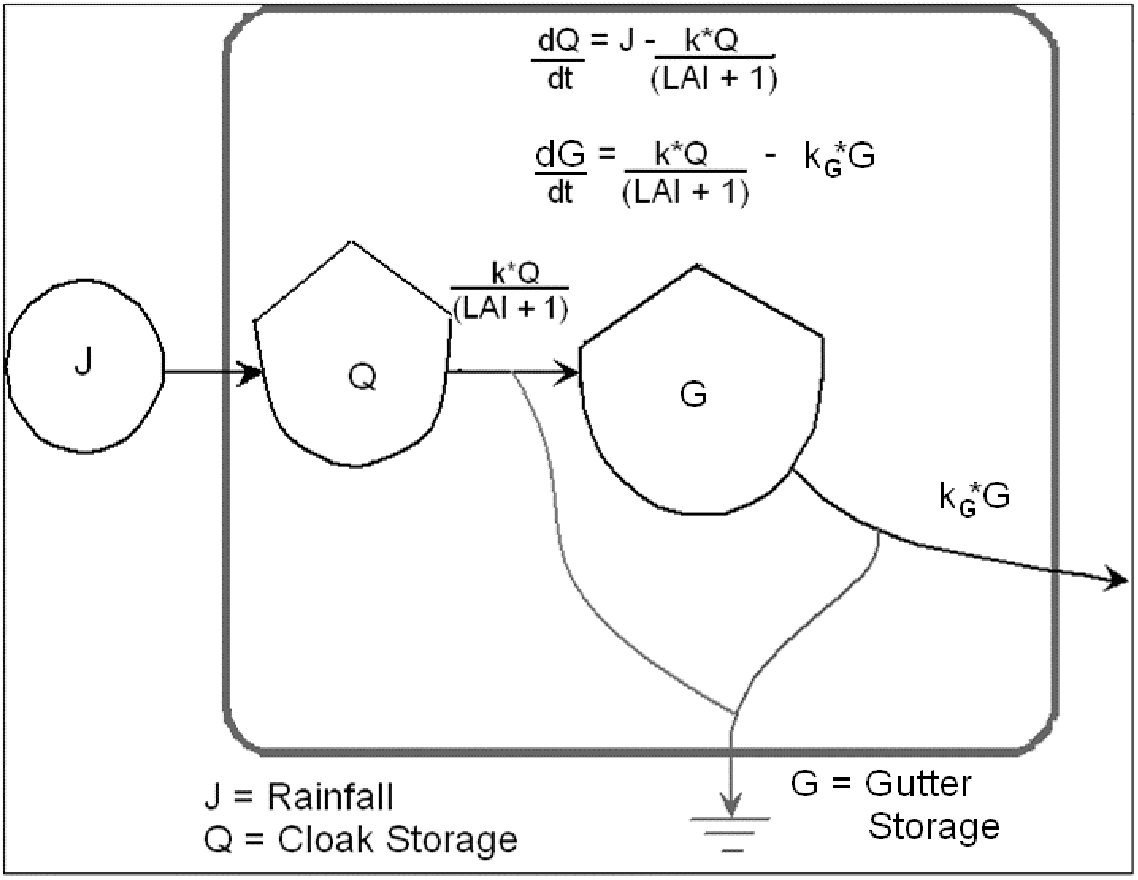

Figure 5.13. Diagram of system model with large box encompassing the entire watershed. J, rainfall source (mm/min); Q, canopy and roof water storage (mm); G, gutter storage (mm); k, canopy runoff coefficient (min^{-1}); k_G, gutter runoff coefficient (min^{-1}).

Model Calibration

To determine the pathway coefficients k and k_G, we set Equations 1 and 2 equal to zero. When dQ/dt equals zero, inflow from rainfall must equal outflow from the cloak and roof storage, which implies Eq. 3.

$$J = kQ/(LAI + 1) \quad (3)$$
$$k = J(LAI + 1)/Q$$

Substituting in J = 0.15 mm/min, LAI = 0, and Q = 0.31 mm for steady state with no green cloak in place, k was found to equal 0.48 min^{-1}. An LAI of 0 indicated there was no cloak. The roof by itself was assumed to store the same amount of water as a canopy with an LAI of 1; thus, the value of Q was the average for canopy water storage given in Table 5.1.

When dG/dt equals zero, inflow from cloak and roof must equal outflow from gutter storage, which implies Eq. 4.

$$kQ/(LAI + 1) = k_G G \qquad (4)$$
$$k_G = (kQ/(LAI + 1))/G$$

Substituting in $k = 0.48\ min^{-1}$, $Q = 0.31$ mm, LAI = 0, and G = 1 mm for steady state with no green cloak in place, k_G was found equal to $0.1488\ min^{-1}$. The G value was estimated as average depth of water stored in the gutters observed during the trials. Water pooled in gutters where there was slack in the plastic sheeting.

To test the calculated values of k and k_G, we used Microsoft Excel to run the model. First, we ran the model using the first ten minutes of runoff data for the roof alone (LAI 0) trial. Model results were compared to the observed data. Next, to avoid running the model against each of the eleven cloak data sets, we averaged the first ten minutes of all eleven cloaks' runoff data into one set of averages. We calculated the leaf area index of all eleven trials to be 1.73. We ran the model with the cloak average leaf area index (1.73) and compared predicted runoff values to the averaged observed data set.

To compare the model's performance, the model's total error per minute was calculated by finding the sum of the control and average runoff error for each of the ten minutes (Eq. 5).

$$\text{Total Error} = [(\Sigma(((C_o - C_p)^2)^{1/2})/C_o + \Sigma(((E_o - E_p)^2)^{1/2})/E_o)/10]*100\% \qquad (5)$$

where C_o = observed control runoff, C_p = predicted control runoff, E_o = observed average runoff, and E_p = predicted average runoff. The error equation is shown being divided by ten because it is based on ten minutes of runoff measurements.

Running the model with these coefficients gave a control error of 134% and an average error of 386% giving a total error of 520%. This error was much too high, since our goal was to have control and average error each under 40%. To make the total error lower, we reran the model using both the control and averaged runoff data sets while altering the values of k and k_G until we minimized model total error (Eq. 6).

$$\text{Total Error} = \min[(\Sigma(((C_o - C_p)^2)^{1/2})/C_o + \Sigma(((E_o - E_p)^2)^{1/2})/E_o)/10]*100\% \qquad (6)$$

Finally, a k value of 0.19 min^{-1} and k_G value of 0.046 min^{-1} yielded a total error of 86.6%. This gave a control (LAI = 0) error of 54.3% and average error (LAI = 1.73) of 32.3% for a total model error of 86.6%. These values were obtained using a roof LAI of 1 (from the expression "LAI + 1"). To get a smaller error, the roof LAI was altered to 0.35 giving the expression "LAI + 0.35". This gave a minimum total error of 52.8%, 22.8% and 30.0% error for control and average error, respectively. These average errors were both under the goal of 40% error.

Model Validation

The model was run twelve times—once with each of the eleven canopy LAIs and once with the control LAI of 0. The model results were compared to the gutter runoff data. Figures 5.14a through 5.14l plot the model results (solid line) and the actual measured runoff data (data points). It is seen that as the LAI of the cloak increases, the amount of runoff decreases. LAI increases more water was held in the canopy, which reduced runoff.

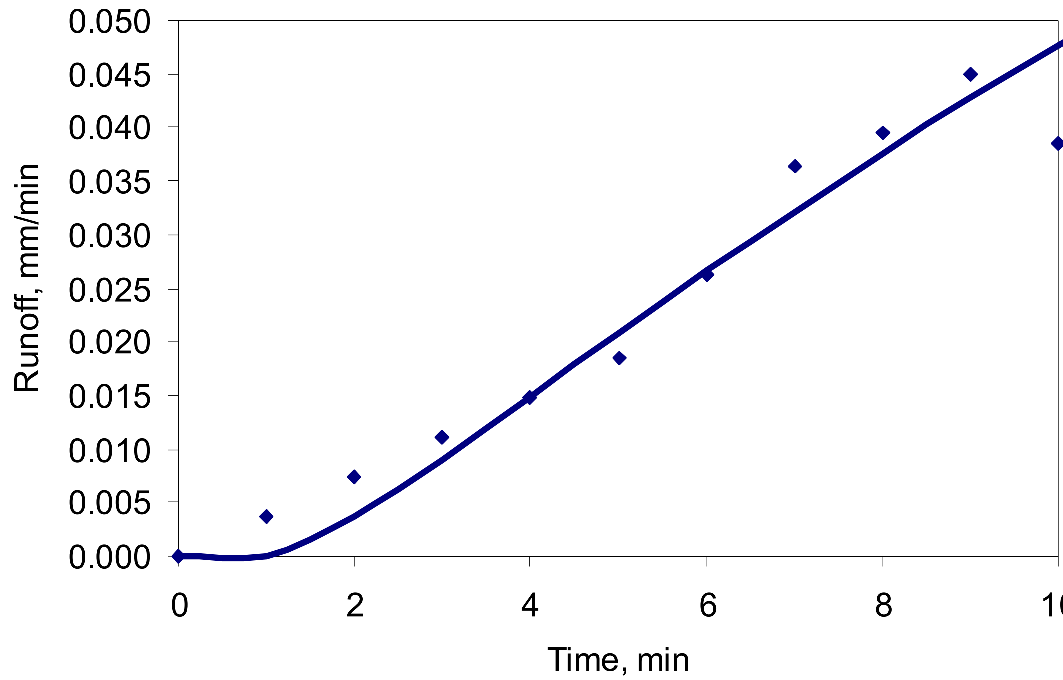

(a) Roof, LAI = 0

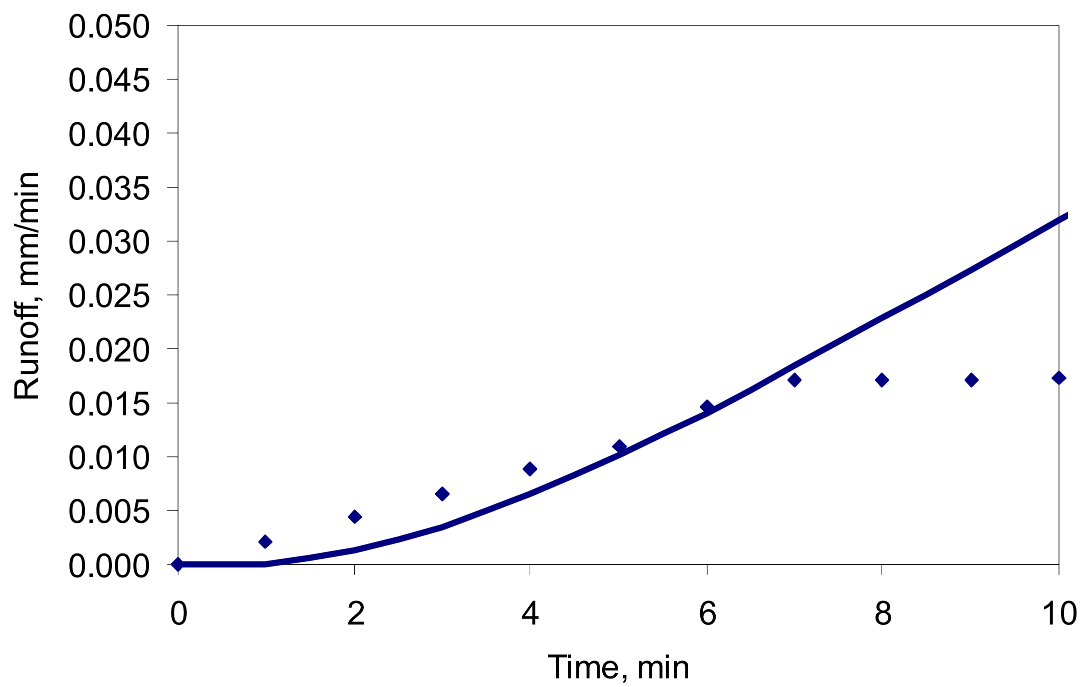

(b) Morning Glory, LAI = 0.67

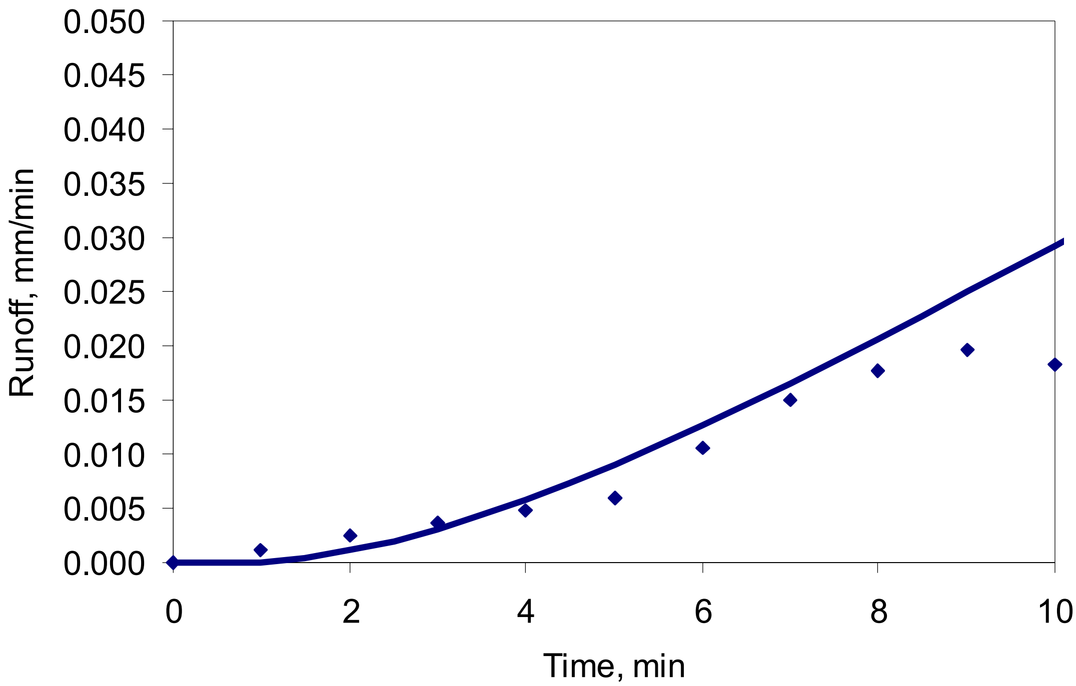

(c) Black Eyed Susan Vine, LAI = 0.83

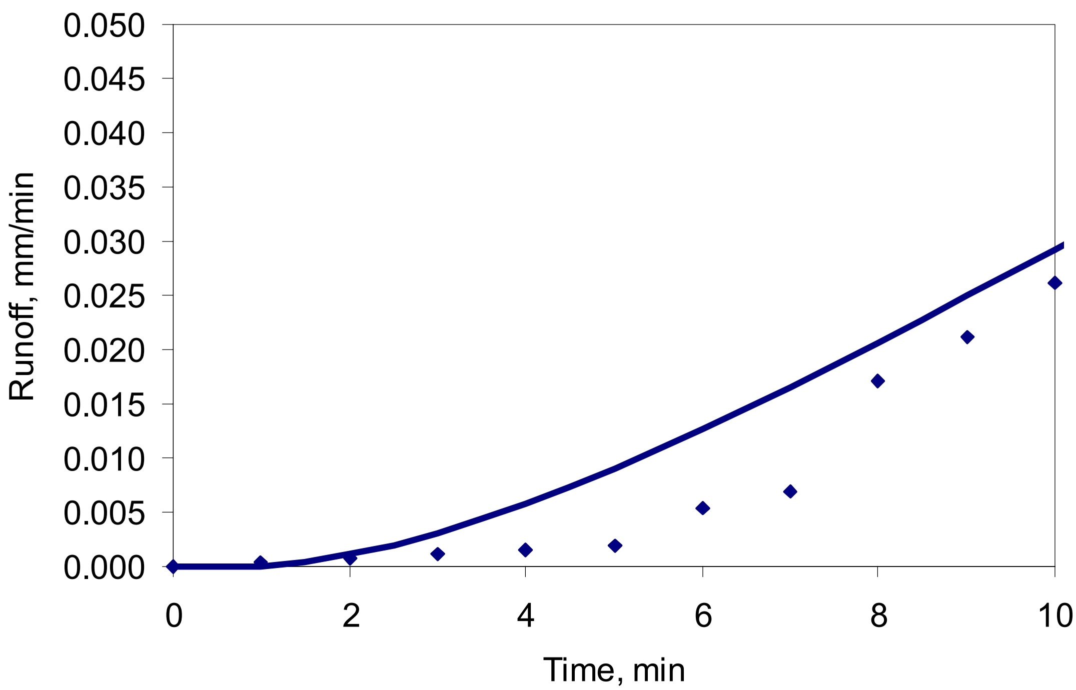

(d) Kudzu 1, LAI = 0.83

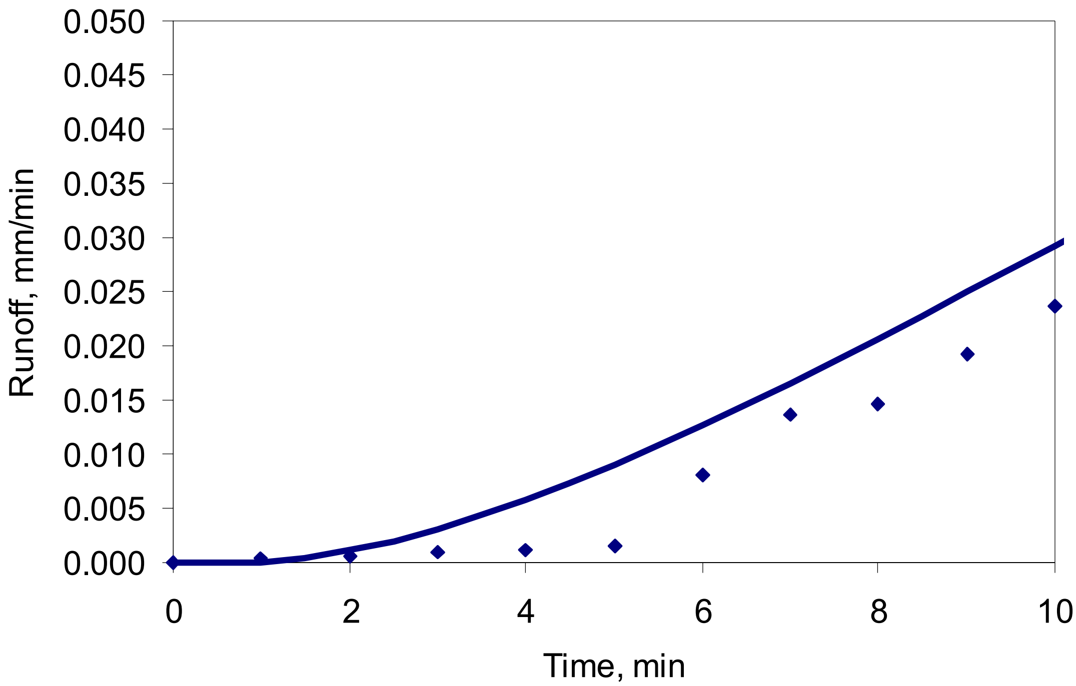

(e) Moonflower, LAI = 0.83

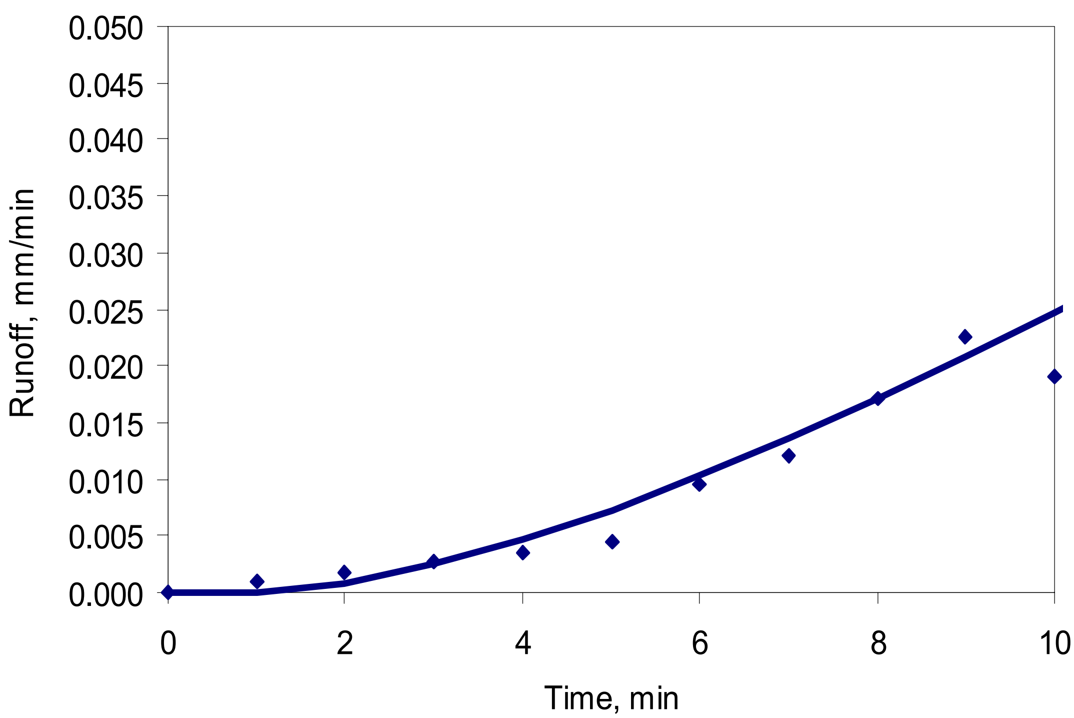

(f) Cross Vine, LAI = 1.17

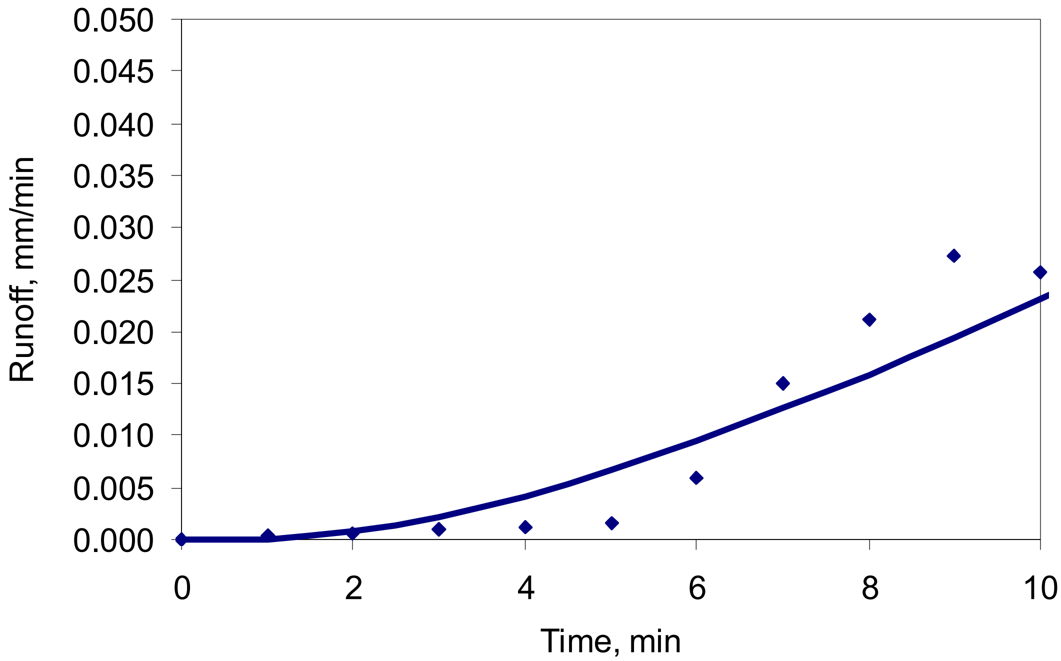

(g) Porcelainberry, LAI = 1.33

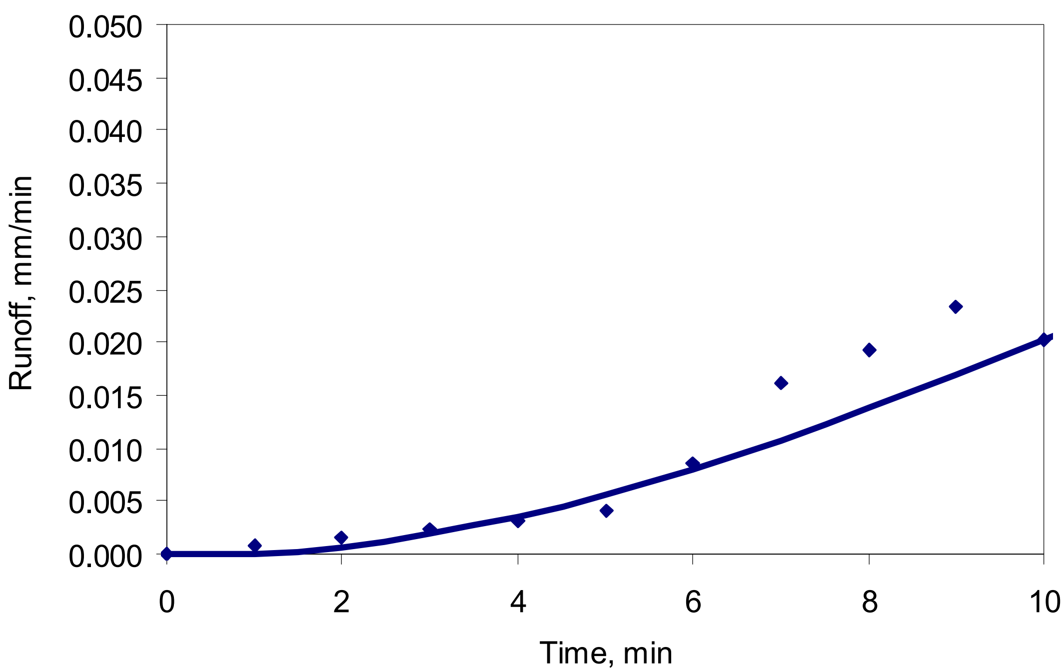

(h) Kudzu 2, LAI = 1.67

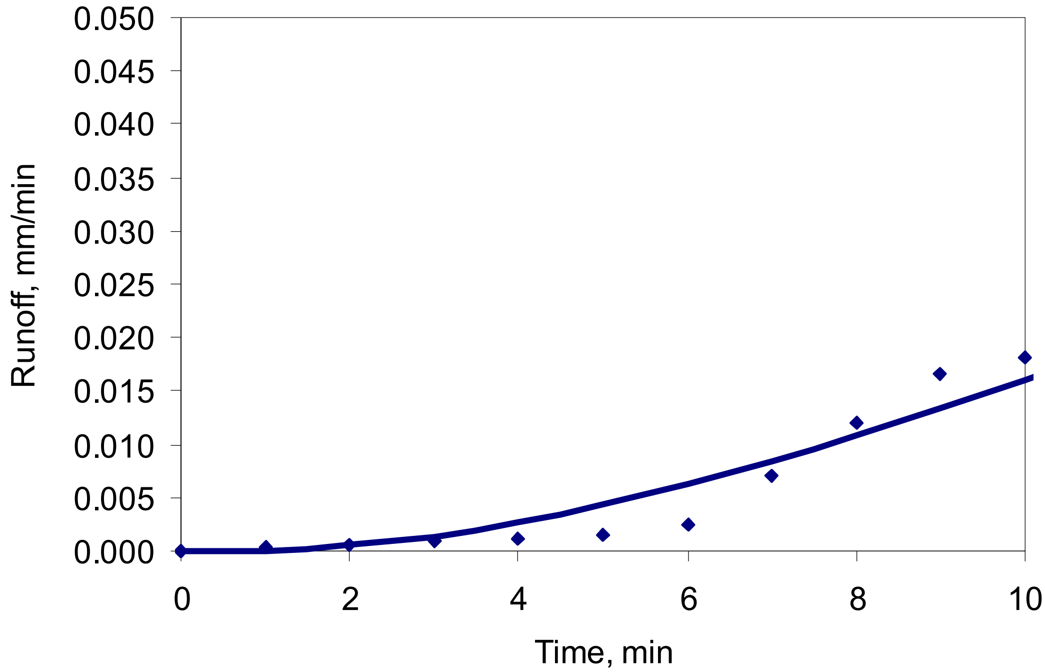

(i) Chinese Trumpet Creeper, LAI = 2.33

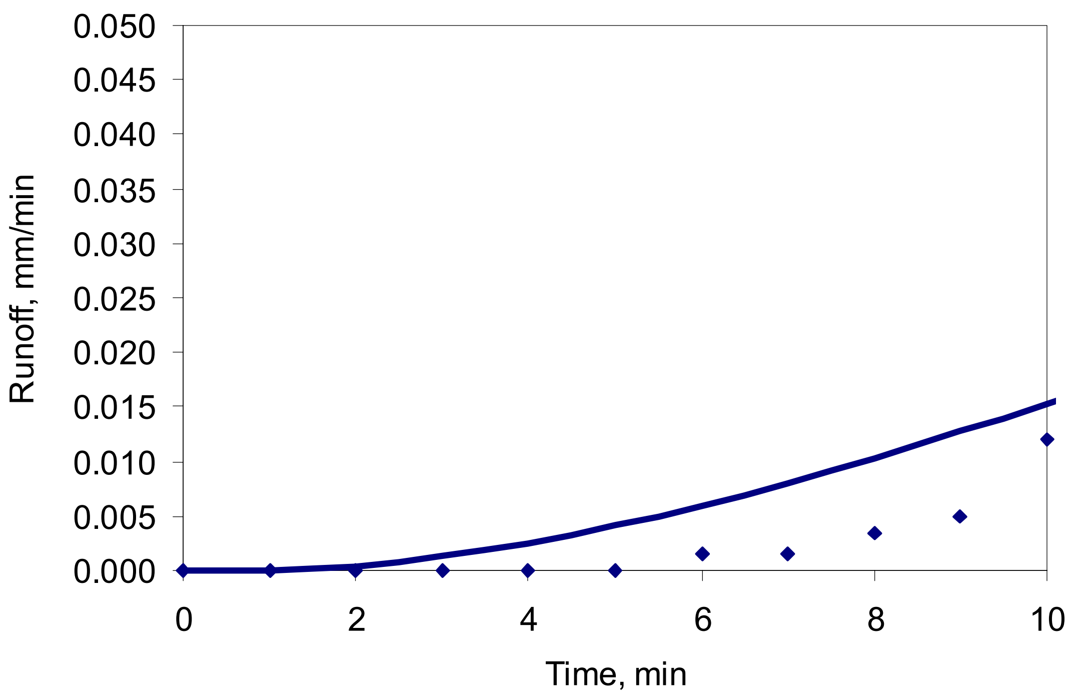

(j) Virginia Creeper 2, LAI = 2.5

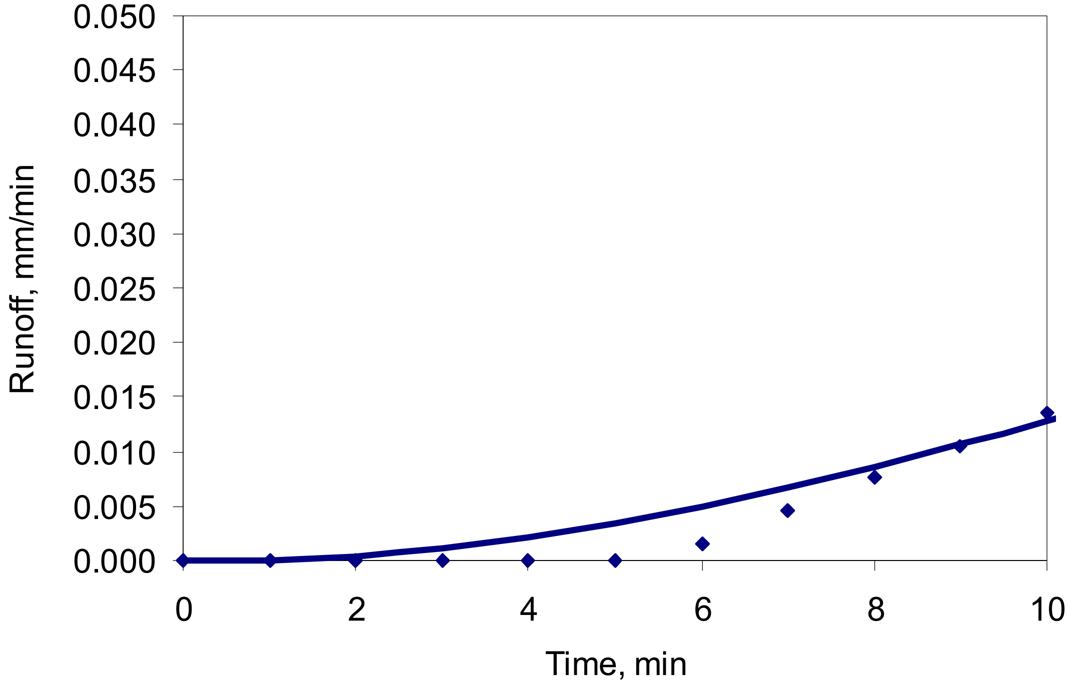

(k) Virginia Creeper 1, LAI = 3.17

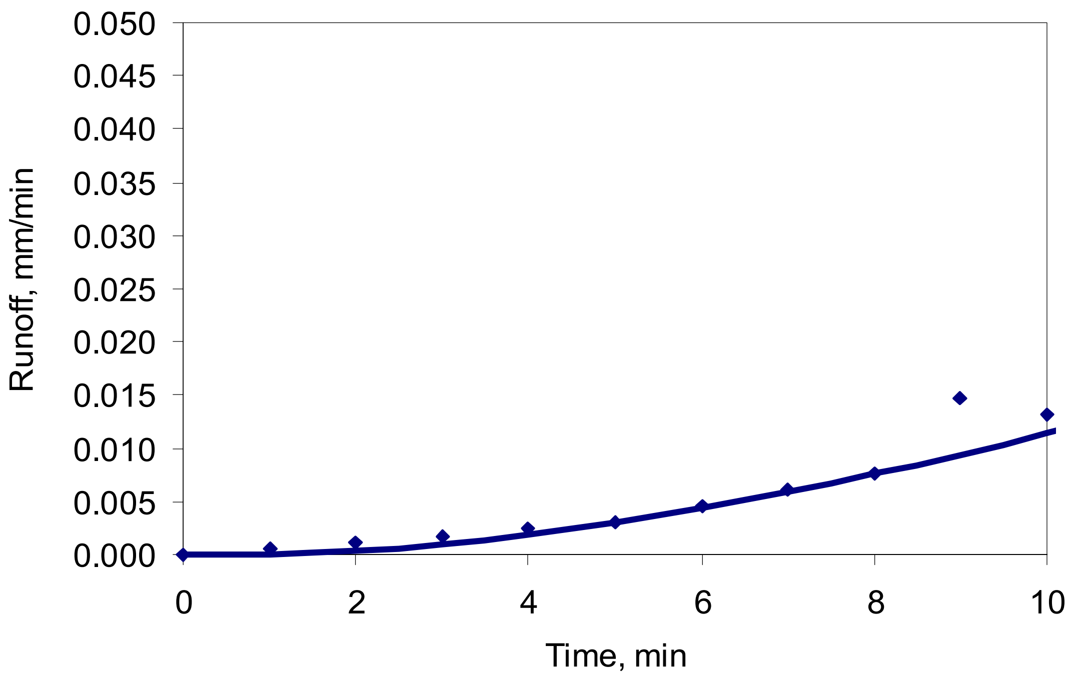

(l) Japanese Honeysuckle, LAI = 3.67

Figures 5.14. Validation of green cloak runoff model using observed runoff (diamonds).

The error per minute of each of the model validation data sets was calculated by summing error for each of the ten minutes (Eq. 7).

$$\text{Error} = [(\Sigma(((R_o - R_p)^2)^{1/2})/R_o)/10]*100\% \qquad (7)$$

where R_o is observed runoff depth and R_p is predicted runoff volume. The error equation is shown being divided by ten because it is based on ten minutes of runoff measurements. These errors are listed in Table 5.3 below.

Table 5.3. Model errors for each of the 12 runoff trials.

Cloak, LAI	Error, %
Virginia creeper 1, 3.17	58.0
Virginia creeper 2, 2.5	220.4
Kudzu 1, 0.83	123.2
Kudzu 2, 1.67	33.0
Cross, 1.17	30.9
Chinese trumpet, 2.33	70.2
Japanese honeysuckle, 3.67	30.3
Porcelainberry, 1.33	100.4
Black eyed Susan, 0.83	36.9
Moonflower, 0.83	148.1
Morning glory, 0.67	43.6
Roof, 0	22.8
Average	*76.5*
Standard Deviation	*60.8*

Figure 5.15 graphs the average errors versus the leaf area index of the data set, showing that error was not biased by leaf area index. Additionally, it is seen that 7 of the 12 validations are more than the acceptable 40% limit (shown by the solid horizontal line at 40%).

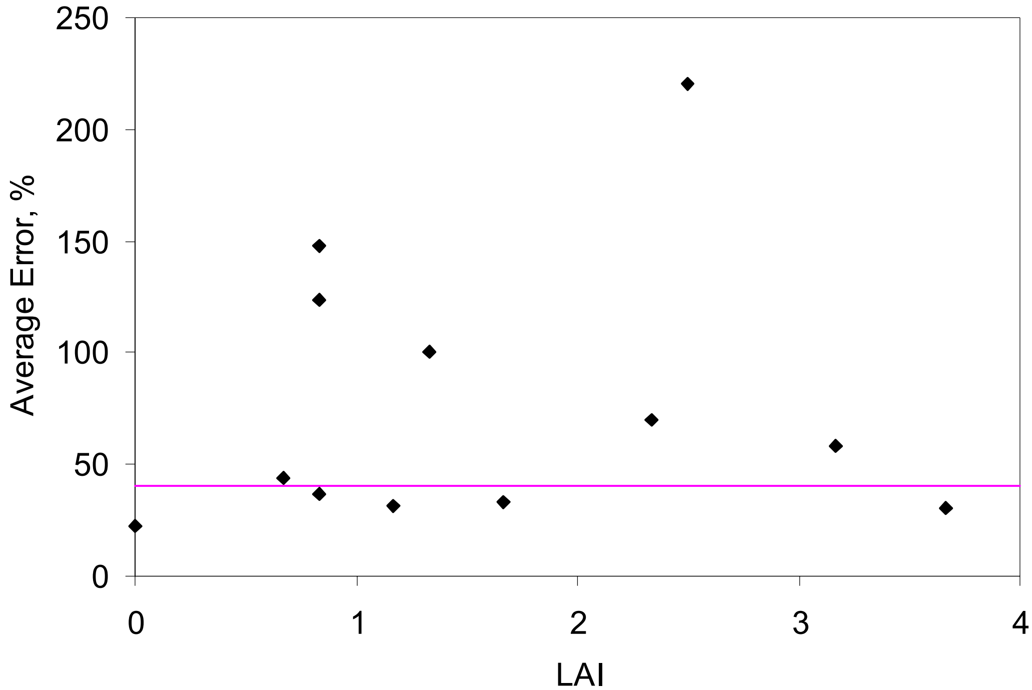

Figure 5.15. Average error of green cloak runoff model versus LAI.

Results

Model Results

With the model giving a reasonable representation of experimental data, it was applied to the green cloak to determine rainfall storage and runoff delay, which were then compared to a green roof.

Rainfall Storage. To determine the maximum storage of each LAI, the cloak and roof state equation was evaluated under steady state conditions. Maximum storage indicates that storage cannot increase anymore, meaning $dQ/dt = 0$. With $k = 0.19$, we set the cloak and roof storage equation to steady state. We calculated maximum storage Q for LAIs from 0 to 9. This was the amount of water that cloak and roof will intercept during a rain event.

$$dQ/dt = J - KQ/(LAI + 0.35) = 0$$

With $J = 0.15$ mm/min and $k = 0.19$ min^{-1}:

$$Q = 0.15*(LAI + 0.35)/0.19$$

Table 5.4 displays the amount of water stored under steady state conditions for canopies of varying LAI based on the equation given above. An LAI of 0 indicated a shingled roof with no canopy over it. All values assumed that there was a roof under the canopy.

Table 5.4. Canopy and roof storage and canopy storage alone for varying canopy LAI.

Roof LAI	Canopy LAI	Canopy and Roof Storage Q, mm	Canopy Storage, mm
0.35	0 (Roof Alone)	0.3	0
0.35	1	1.1	0.8
0.35	2	1.9	1.6
0.35	3	2.6	2.4
0.35	4	3.4	3.2
0.35	**5**	**4.2**	**3.9**
0.35	6	5.0	4.7
0.35	7	5.8	5.5
0.35	8	6.6	6.3
0.35	9	7.4	7.1

Average literature values (Table 5.1) indicated that each unit of LAI could hold 0.31 mm of water. Using our steady state Q formula, a cloak canopy should hold about 0.8 mm for each LAI (right column in Table 5.4), which was at the higher end of values reported for forest (Table 5.1). Canopy storage is based on stem and leaf morphology, leaf roughness, plant spacing, climate, canopy age, rainfall rate, drying periods, etc.

Runoff Delay. As stated in the introduction, delaying the timing of runoff is beneficial to downstream water bodies, especially stream banks. The water stored in any stormwater retention device is temporary. Constructed wetlands may hold stormwater for several days, while rain gardens may retain it for a day or two. We used the green cloak runoff model to estimate the amount of time the green cloak delayed the time to peak discharge. We tested different canopy LAI's to determine the effect of LAI on delay time. Delay was defined as the amount of time required for discharge to reach steady state given a continuous rainfall rate of 0.15 mm/min. The time elapsed between initiation of the rainfall event and the time at which discharge reached 97% of inflow (0.145 mm/min) was defined as the delay time.

Figures 5.16 displays roof discharge given canopies with leaf areas from LAI=0 to LAI=9. Without a green cloak over the roof, peak discharge was only delayed five minutes. However, a roof with a green cloak that had an LAI of 1, had the peak delayed by 23 minutes (Figure 5.16a). Cloaks with an LAI of 3 and 5 would delay peak discharge by approximately 44 and 95 minutes, respectively (Figure 5.17). Thus, green cloaks do reduce stormflows by delaying roof discharge.

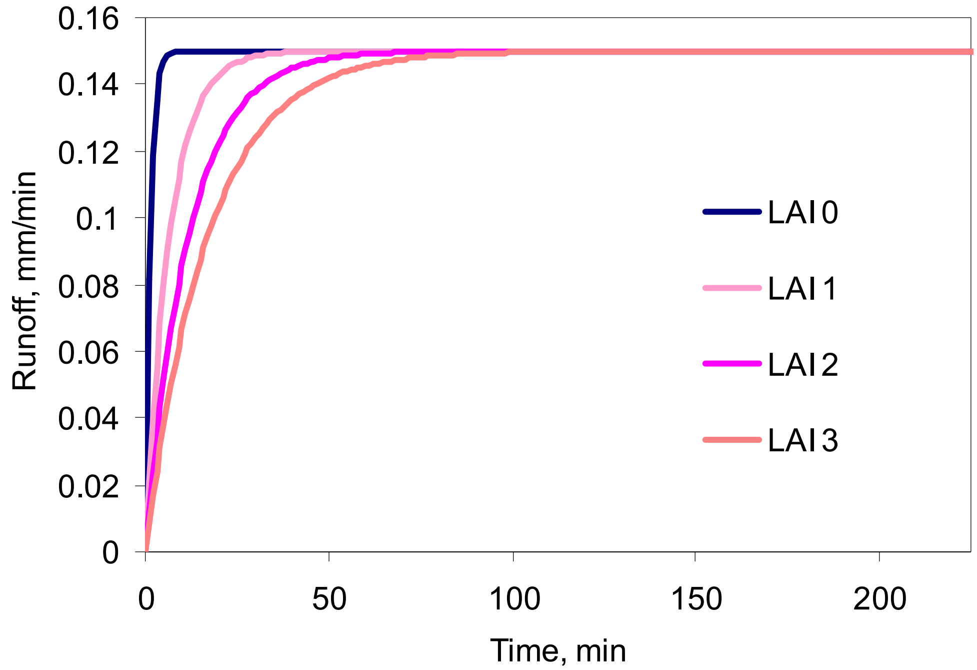

(a) LAI between 0 and 3

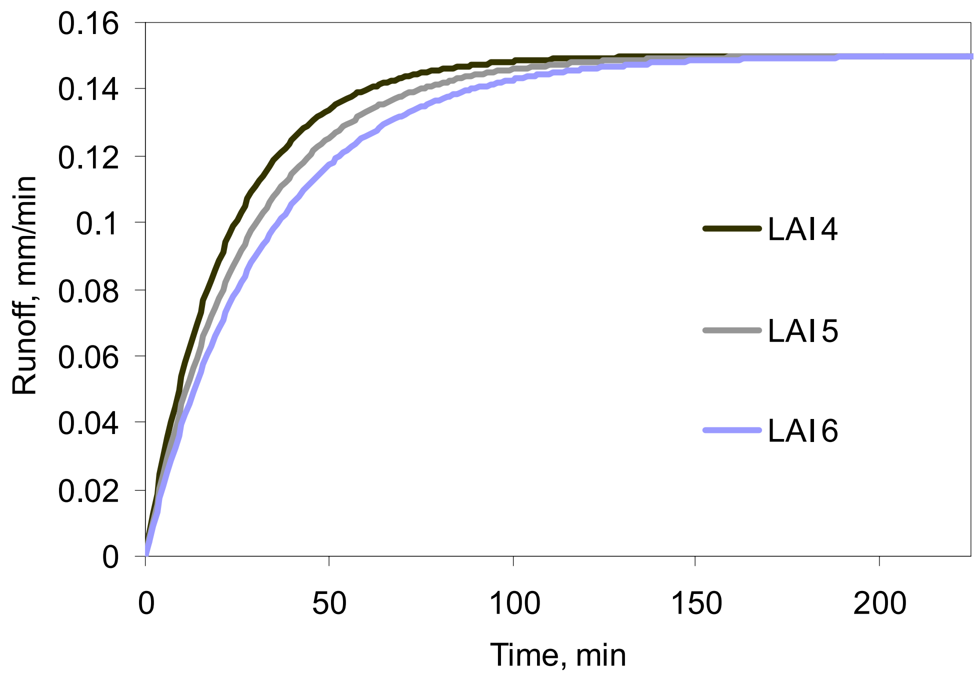

(b) LAI between 4 and 6

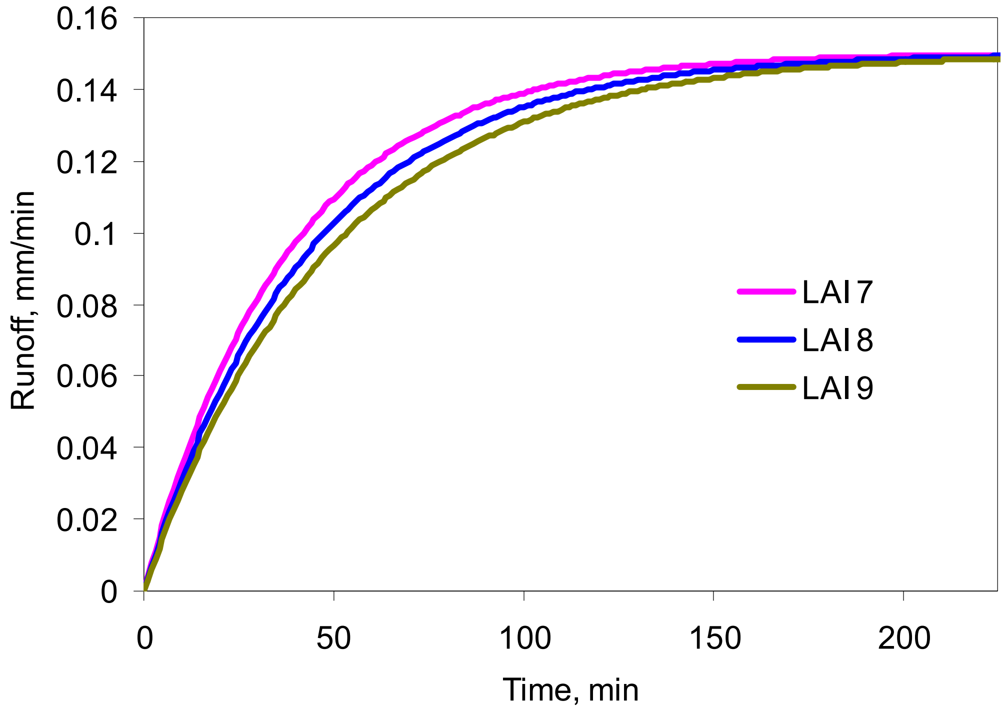

(c) LAI between 7 and 9

Figures 5.16. Modeled roof runoff for houses with green cloaks of (a) low, (b) medium, and (c) high leaf areas.

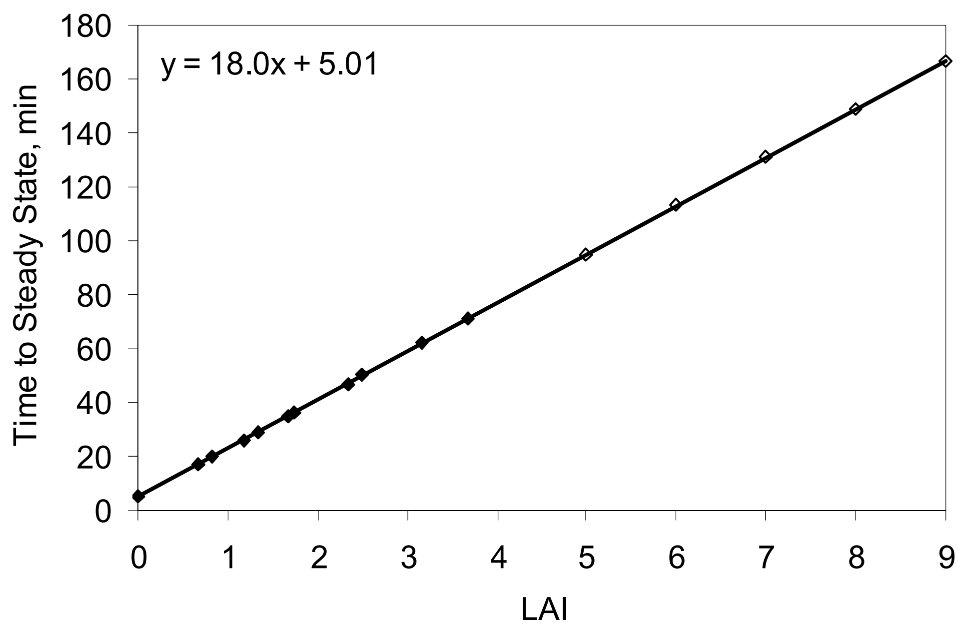

Figure 5.17. Effect of leaf area on the roof discharge rate.

Green Roof Comparison. Based on our outdoor study of vines growing naturally on buildings, mature vine canopies regularly had LAIs of 3 to 6. Using our model, this meant that a fairly mature green cloak and shingle roof system stored 2.6 to 5 mm rainfall (Table 5.4). Research on extensive green roof runoff conducted by Berghage (2006) indicated that a 102 mm (4 inches) deep media stored 25 mm (~1 inch) of rainfall. This indicated that the green cloak stored between 10 and 20% of what an extensive green roof could.

Table 5.5 performs a similar comparison, using runoff data from a 75 mm (3 inches) deep green roof in North Carolina (Moran, 2005). Six representative annual rainfall events are listed with their rainfall amounts, rainfall stored in the green roof, and percentage of rainfall stored by the green roof. We compared a green cloak of LAI of 5 to the green roof. Table 5.5 lists cloak (canopy and roof) storage (4.2 mm) and percentage of rainfall stored in green cloak. The last column quantifies what percentage of green roof storage is stored in the green cloak by dividing cloak storage by green roof storage. An average relative storage percentage of the green cloak to the green roof is 33%. Like the Berghage (2006) data, this relative storage percentage is significantly less than a green roof, but the price point of a green cloak may make it a viable option.

Table 5.5. Six rain events comparing observed storage on a North Carolina green roof to projected green cloak storage.

Rain Event	Rainfall, mm	GR Storage, mm	GR Storage, %	Cloak Storage, mm	Cloak Storage, %	$\frac{\text{Cloak Storage}}{\text{GR Storage}}$ (%)
1	7.9	7.9	100.0	4.2	53.2	53.2
2	19.6	16.3	83.1	4.2	21.4	25.8
3	19.6	16.8	85.7	4.2	21.4	25.0
4	22.6	17.0	75.3	4.2	18.6	24.7
5	25.9	11.4	44.1	4.2	16.2	36.8
6	41.4	13.2	31.9	4.2	10.1	31.8
Average	*22.8*	*13.8*	*70.0*	*4.2*	*23.5*	*32.9*

Using the model created and the rainfall intensities experienced in Moran's April 7th, 2003 storm (Rain Event No. 4 in Table 5.5), runoff volume and its timing from a shingle roof with no green cloak and a one with a green cloak that had an LAI of 5 were compared to that of the green roof. Figure 5.18 shows the results of runoff from a shingle roof (thin line) and a green cloak (broken line), Moran's green roof (thick line), and the stormwater hydrograph of rain event (gray bar graph).

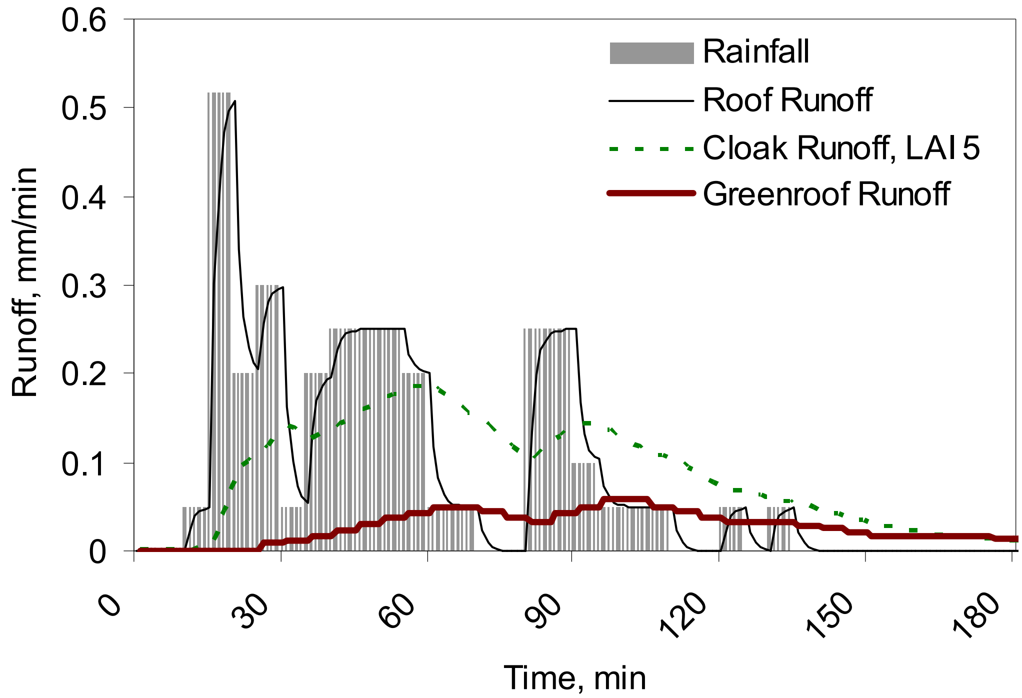

Figure 5.18. A Goldsboro, North Carolina rain event with resulting shingle roof, green cloak, and green roof runoff.

From Figure 5.18 it can be seen that both the green cloak and the green roof improved the storm hydrograph. Peak flows were delayed and greatly reduced compared to the roof alone.

We calculated the runoff reduction at 15, 30, 45, and 60 minutes for the green cloak of LAI 5 and the extensive green roof relative shingle runoff (Eq. 8).

$$RR = [(A - U)/A]*100\% \qquad (8)$$

where RR is percent runoff reduction, A is cumulative shingle roof runoff in mm, and U is cumulative runoff in mm from either the green cloak of LAI 5 or the extensive green roof. Values of percent runoff reduction from each of the two roof types are shown in Table 5.6 for minutes 15, 30, 45, and 60.

Table 5.6. Percent runoff reduction in roof, green cloak, and green roof runoff compared to rainfall intensity.

Time, min	Percent Runoff Reduction Green Cloak	Green Roof
15	77.8	100
30	70.1	98.9
45	52.7	85.6
60	43.8	91.9

After the first thirty minutes of the rain event, the green cloak reduced runoff by 70% while the green roof reduced runoff by 99%. After one hour, the green cloak reduced runoff by 44%, while the green roof reduced it by 92%. After an hour, the green cloak had reduced runoff by an amount equal to 48% of the green roof's reduction. In addition, maximum runoff from the green roof occurred at 100 minutes, whereas it occurred at 60 minutes for the green cloak.

Discussion

Similar to the ability of the canopies of natural forests to intercept rainfall and reduce storm flows, the green cloak canopy stored water from rain events, which ultimately delayed the peak discharge rate by over an hour. The leaf area index of the canopy was the most important variable in determining the green cloak's effect on roof storm discharge. The percentage of the rood surface covered by vegetation and its thickness were also significant indicators of runoff rates. For the green cloak to mitigate stormwater runoff, it is critical for it to have a high leaf area index.

The stormflow model showed that a green cloak with a canopy that had a lead area of 5 could hold 4.2 mm of water, or an average of 0.8 mm/LAI-unit. After 30 minutes of a 25 mm (1 inch) rain event, the green cloak reduced runoff volume by 66% compared to the shingle roof. When compared to Moran's extensive green roof runoff data, green cloak runoff reduction was approximately 45% of the extensive green roof runoff reduction and had approximately 60% the green roof's runoff maxima delay. We feel that these green cloak characteristics may be quite reasonable and acceptable once green cloak costs are compared to green roof costs.

The green cloak offers a new and promising stormwater management device that can improve urban hydrology, returning it close to its pre-development state. As improvements are made to the green cloak (e.g., high diversity canopies) it should be able to store more water and reduce stormflows beyond what this inaugural design revealed.

Chapter 6: Cost-Benefit Analysis of Green Cloak

Abstract

We performed a cost-benefit analysis of the green cloak to compare with a conventional shingle roof and an extensive green roof. We designed a green cloak for a 2000 ft^2 building for costing purposes only. We evaluated the costs of materials and installation and the benefits from energy savings, roof lifetime extension, and tax credits to estimate the payback period and benefit-cost ratio of the green cloak in three climatically different locations—College Park, MD, central TX, and south FL assuming two different electricity rates (\$0.10 and \$0.20/kWh). Given an average peak daytime temperature reduction of 11.3 °C, we found that the payback period for all locations was less than the predicted green cloak lifetime of 30 years with a maximum benefit-cost ratio of 8.11 for south Florida. Additionally, we found the cost of the green cloak to be 38% less than an extensive green roof. These results indicate that the green cloak could be both a yielding investment, which justifies further exploring its potential in a pilot-scale experiment.

Introduction

Background

We were inspired to design the alternative green roof retrofit, called the *green cloak,* to overcome the drawbacks of extensive green roofs including their high installation costs, structural load requirements, and flat roof specificity. The green cloak uses a vine trellis system suspended above a building to limit the need for heavy soil media substrate and structural support. Additionally, vines are inexpensive and fast growing. As previous chapters showed, the vines intercepted rainfall to slow down peak storm discharge and provide energy savings similar to that of the extensive green roof making them a competitive green technology.

We compared the runoff detention and energy savings of the green cloak to extensive green roofs and conventional roof tops. To study runoff detention and retention, energy savings, and vine growth rates, we conducted experiments using scaled down trellises and plywood buildings. We used the methodology of Ecological Engineering to study vines growing on dilapidated tobacco barns as an ecological analogue to the green cloak. Growth characteristics of the barn vine community were compared to the green cloak trellis vines. We generated mathematical models to determine green cloak runoff and energy performance at leaf area indices not observed in the field. In the following section, we will use the major findings of this thesis to generate a rough pilot scale green cloak design so that a cost benefit analysis can be performed.

For example, we learned with four vines planted per square meter, vines were able to cover the trellis system quickly with most having 100% coverage within one year of growth (Chapter 2). We learned that increased leaf area index correlated well with increased runoff reduction, roof temperature reduction, and indoor building temperature reduction (Chapters 3 and 5). Barns with the highest leaf area indices had trumpet creeper growing on them (Ch. 2). Most barns had multiple species which increased their leaf area index. Maximum barn LAI was 5. We recommended the use of two to three vine species per cloak to increase leaf area index and cover (Ch. 2). The barns with the highest LAI's had trumpet creeper (*Campsis radicans*), and Virginia creeper (*Parthenocisus quinquefolia*) as species.

Vine Information

Expecting trumpet vine and Virginia creeper to grow well on a pilot scale green cloak since they grew vigrously on the barns, we found literature containing information specific to these species' growth characteristics. Table 6.1 lists vine height, profile or thickness, solar needs, climbing mechanism, vigor, support required, optimal plant spacing, and proper spacing from walls (Dunnett and Kingsbury, 2004). We used these characteristics to shape the pilot scale green cloak design.

Table 6.1. Trumpet vine and Virginia creeper growth characteristics (Dunnett and Kingsbury, 2004).

Species	Trumpet vine (*Campsis radicans*)	Virginia creeper (*Parthenocissus quinquefolia*)
Height	10 m (33 ft)	15 m (49.5 ft)
Profile	0.9 m (3 ft)	0.3 m (1 ft)
Aspect	Full sun	Light shade to sun
Climbing mechanism	Aerial roots	Suckers, but not always reliable
Vigor	Strong	Strong
Support	Horizontal supports or trellis (right-angle or diagonal mesh).	Self-clinging, but some supporting trellis (preferably diagonal mesh) is advisable.
Optimal plant spacing	4 m (13.2 ft)	-
Distance from wall	0.15 m (0.5 ft)	-
Notes	Despite aerial roots, support is recommended.	Often confused with Boston ivy (*Parthenocissus tricuspidata*).

Costs and Benefits of Green Roofs

Roof Costs. We conducted a literature review of costs and benefits of conventional and extensive green roofs as a basis for comparing the green cloak's costs and benefits. According to Dunnett and Kingsbury (2004), 2002 prices for conventional shingle roofs ranged from \$4 to \$8.50/ft^2 (\$43.06 to \$91.50/m^2) including the materials and installation costs of framing, plywood, tarpaper, and shingles. The lower cost is for a roof with a lifetime of less than 15 to 20 years, while the higher price is for a roof with a lifetime of thirty to fifty years. Extensive green roofs cost between \$10 and \$20/ft^2 (\$107.64 and \$215.28/m^2) and intensive green roofs cost between \$20 to \$40/ft^2 (\$215.28 to \$430.56/m^2). The lifetime of a green roof is fifty to one hundred years (Dunnett and Kingsbury, 2004).

Increased Building Footprint. In addition to green roofs lowering energy consumption and reducing runoff, they provide builders a means to gain stormwater credits for swapping imperviousness for perviousness, which allows builders to develop a larger fraction of a land parcel. A builder that installs a green roof at an apartment complex qualifies and can build more apartment units, which increases revenue and the value of the building.

Energy Savings. Building heating and cooling energy savings is another benefit of green roofs. In summer months, green roofs are used to shade the building's roof from the hot sun's rays. In winter months, green roofs are thought of as an extra layer of insulation of the building's roofing system. A computer simulation program has been used to examine the indoor air temperatures of buildings with and without green roofs during both the summer and winter. For example, in July at three in the afternoon, indoor air temperature was reduced by at least 10 ºC in a building with a green roof compared to a building with a traditional non-vegetated roof (Ferrante and Mihalakakou, 2001).

These drops in indoor air temperature translate directly to air conditioning energy savings. Peck et al. (1999) saw a 3 to 4 °C (6 to 8 °F) lower temperature under a green roof compared to a building without a green roof when outdoor temperatures were 25 to 30 °C (77 to 86 °F). In Toronto, every 0.5 °C (0.9 °F) degree drop in indoor air temperature reduced air conditioning demand by 8% indicating that there could be a 48% to 64% reduction in energy use (Peck et. al, 1999). Similarly in Maryland, the local power company estimated that summertime energy demand dropped by 5% for each 1 °F (0.56 °C) increase on the thermostat (Pepco, 2005). Peck (2003) found a 25% reduction in summer cooling demand for a one story building covered with a grass roof of 10 cm (4 in.) substrate in Canada. In Rock Springs, Pennsylvania, Berghage (2006) determined that model buildings covered with extensive green roofs demanded 10% less electricity than uncovered buildings.

Using Indian green roof building temperature data, a model was produced showing that a green roof of leaf area index 4.5 would reduce indoor air temperatures by an average of 5.1 °C over a 24 hour period. This translated to a 3.02 kWh (10300 Btu) reduction in energy demand per day. Additionally, air temperatures were most reduced in the green roof building during the afternoon when energy demand from power utilities peaks and is problematic (Kumar and Kaushik, 2005).

Indirect Benefits. There are several additional indirect benefits of green roofs that should be considered when performing a cost-benefit analysis. Some effects, like roof lifetime extension, may not be apparent until long after a green roof has been installed. On the other hand, some benefits may not be apparent for a single building, but when the additive effects of several green roofs are evaluated for a city, these effects become more visible. For example, green roofs can contain large volumes of rain alleviating the need to replace old sewer systems which are likely to overflow into river systems due to large rain events. Also, property values and marketability may be increased given the market and public green roof opinion (Peck et al., 1999).

Some benefits are enjoyed due to the specific use of a building. For an apple cider factory in Germany, a roof meadow cools water required for the operation of their business (Peck et al., 1999). Building operators can harvest retained rainwater and use in toilet flushing and irrigation (Thomas, 1998). Evidence also suggests that in hospitals, patients exposed to nature heal faster due to the peaceful environment plants provide—not only does this make people healthier, but decreases the expenses of long hospital stays (Ulrich, 1999).

Taking these direct and indirect benefits and the high installation costs of green roofs into consideration, researchers conducted life cycle cost analyses. Peck and Kuhn (2000) and Scholz-Barth (2001) estimated that a green roof can double or triple the lifetime of the roof below paying for itself in the long-term. In fact, the green roof on Derry and Toms department store in England has had the same roof membrane since 1938 (Peck et al., 1999). Wong et al. (2003) performed a life cycle cost analysis of rooftop gardens in Singapore and found that without consideration of runoff and energy savings benefits, extensive green roofs will pay for themselves in the long run based on roof lifetime extension. Conversely, intensive roofs will not pay for themselves upon consideration of energy saving value. The value of the usable added square footage must be considered to make intensive green roofs worthwhile.

Objectives

Our aim in this chapter was to:

1. Estimate the installation and maintenance costs and energy savings for a simulated green cloak covered building.
2. Compare these costs and savings of green cloak with conventional asphalt shingled roof construction and an extensive green roof.

Methods

Costs

To estimate installation and maintenance costs of a simulated green cloak, we developed a green cloak design for a one story 2000 ft^2 flat roof building. We used this design to generate a list of construction expenses (e.g., materials and labor) and maintenance expenses. The simulated green cloak design, including vine species, spacing, and structural materials, were based on our findings reported in Chapter 2, cost effectiveness, and weather durability. It was assumed that the building had conventional roof construction. The design was developed for costing purposes only. The design was not evaluated by a professional engineer for structural soundness.

We obtained costs data from a major building supply retailer (Home Depot, 2007), plant costs from Seedland.com (Seedland, 2007), and labor costs from a Maryland green buildings contractor (Michael Furbish of Furbish Company, pers. comm.). Conventional shingle roof and extensive green roof costs were taken from Dunnett and Kingsbury (2004).

We explored the sensitivity of the total cost of the green cloak to major parts costs, including tubing, wire mesh, labor, and plant materials. We compared the materials and installation costs of the green cloak to the materials and installation costs of an extensive green roof and a conventional shingle roof.

Benefits

As we described in the Introduction, there are many indirect and direct benefits of green roofs, however we only quantified energy savings, roof lifetime extension value, and green building tax credit for our cost-benefit analysis of the green cloak. These were the three benefits that we could evaluate with known dollar values. Indirect benefits are listed in the Results section but we did not estimate their monetary value.

To calculate annual energy savings, we first determined typical annual air conditioning costs for a one story 2000 ft^2 house in three locations (College Park, MD, central Texas, and south Florida) with two energy prices. We used Nebraska Public Power District's online air conditioning cost calculator which uses the following equation to predict air conditioning energy cost (Nebraska, 2007) (Eq. 1).

$$A = H_X \cdot T_X \cdot C/(1000 \cdot E) \qquad (1)$$

where A is annual air conditioning energy cost in dollars, H_X is heat gain in Btu/hr, T_X is cooling time in hours, C is energy cost in \$/kWh, and E is air conditioning unit efficiency in SEER (Btu/W·h). SEER is an acronym for seasonal energy efficiency ratio comparing the cooling output in Btu to total electricity input in W·h. The higher the SEER value, the more efficient the air conditioning unit.

Heat gain for an average 2000 ft^2 house in eastern Nebraska was estimated to be 42,000 Btu/hr (Zach, 2007). Heat gain was derived from several equations that take into account solar power, building dimensions, air tightness, number of windows, insulation type, etc. (Zach, 2007). We assumed the same building in College Park, Maryland, central Texas, and south Florida, with the only difference in heat gain being solar power due to geographical location. We used the U.S. Department of Energy's national solar power distribution figure to derive heat gain for buildings in College Park, Maryland, central Texas, and south Florida proportionally (Concentrating, 2006) (Eq 2).

$$H_X = (H_{EN}/SP_{EN})SP_X \qquad (2)$$

where H_X is heat gain in either Maryland, central Texas, or south Florida in units Btu/hr, H_{EN} is heat gain in eastern Nebraska in units Btu/hr, SP_{EN} is solar power in eastern Nebraska in $W{\cdot}h/m^2{\cdot}d$, and SP_X is solar power in either Maryland, central Texas, or south Florida in units $W{\cdot}h/m^2{\cdot}d$. Table 6.2 lists values of solar power and heat gain in each location.

Table 6.2. Solar power and heat gain for eastern Nebraska, central Texas, south Florida, and College Park, MD.

Location	Solar Power, $W{\cdot}h/m^2{\cdot}d$	Heat Gain, Btu/hr
Eastern Nebraska	4250	42000
Central Texas	4750	46941
South Florida	4250	42000
College Park, Maryland	3750	37059

Annual cooling hours in College Park, MD were 900 hours, in central Texas were 1800 hours, and in south Florida were 2800 hours (Air-Conditioning, 2007). We assumed energy prices to be either \$0.10/kWh or \$0.20/kWh to estimate the net benefits under present and future energy prices. We assumed a 13 SEER air conditioning unit efficiency for all annual cost estimates.

To determine the percentage of energy savings offered by the green cloak, we applied our temperature model from Chapter 3 to the one story 2000 ft^2 house. We estimated indoor temperature for a 24-hour period for the house with and without the green cloak. In this case we assumed the green cloak had an LAI of 2. Outdoor temperature and solar radiation were taken from observational data collected at the University of Maryland College Park campus in the summer of 2006.

To estimate energy savings (Chapter 3), we used the heat model generated temperature curves for cloaks of LAI 0 and LAI 2 given that LAI 0 represents a house with no cloak. For each of the cloaks, we found the area between each modeled temperature curve and the thermostat setting of 25.6 °C. This area represented work performed by an air conditioning unit to keep the indoor air temperature at the thermostat setting. We calculated the percent difference in area of the LAI 2 and LAI 0 cloak. To predict each location's annual air conditioning savings, we multiplied the predicted percentage air conditioning energy savings by annual air conditioning costs (Eq. 3).

$$S = A \cdot B / 100\% \qquad (3)$$

where S is annual air conditioning savings in dollars, A is annual air conditioning energy cost in dollars, and B is percent air conditioning energy demand drop.

In addition to annual air conditioning energy savings, we predicted that a green cloak could at least double the lifetime of a shingle roof given the estimation that green roofs can double or triple the lifetime of a roof given their shading and temperature swing reducing abilities (Scholz-Barth, 2001). During outside temperature measurements (Ch. 3), the maximum heat of day roof temperature difference measured was 23.4 °C on a building covered with the Virginia creeper 2 cloak with 90% canopy cover and an LAI of 2.34. We evaluated the annual value of a doubling a conventional shingle roof's lifetime of 15 years and installation cost of \$4.50/ft^2.

Even though there is no specific green cloak tax credit yet, we factored a tax credit into the benefits analysis of the green cloak. We used the cool metal roof tax credit of \$500 (Investment, 2007) as an estimated tax credit for a green cloak since both types of roofs are used for energy savings that act to limit heat gain to the building below.

Green Cloak Cost Benefit Analysis

By using the predicted energy savings of the green cloak, we found the net annual benefit of the green cloak (Eq. 4).

$$NAB = S + ARS + TC - M \qquad (4)$$

where NAB is net annual benefit in dollars, S is the annual air conditioning savings in dollars, ARS is annual roof savings in dollars, TC is annual value of tax credit in dollars, and M is annual maintenance in dollars.

We calculated the payback period of the green cloak for each of the three locations (Eq. 5).

$$P = CIC/NAB \qquad (5)$$

where P is the payback period in years, CIC is the initial construction and installation costs in dollars. Using the estimated lifetime of a green cloak to be 30 years, we evaluated which of our locations would be most suitable for a green cloak given energy prices. The NAB will be enjoyed after the payback period is over. Prior to the end of the of payback period, the NAB will go towards construction and installation costs.

We calculated the annual benefit cost ratio of the green cloak (Eq. 6).

$$BCR = (30 \cdot S + 30 \cdot ARS + 30 \cdot TC)/(CIC + 30 \cdot M) \qquad (6)$$

where BCR is the benefit-cost ratio. The BCR indicates money saved relative to costs. A BCR of 2 indicates that the benefit of the cloak is twice that of the cost. For example, if the cloak cost \$100, the benefit would be \$200 meaning the \$100 investment would be doubled. A minimum BCR of 1 is required to break even.

Results

Simulated Green Cloak Design

Top and side views of the simulated green cloak are shown in Figures 1a and 1b. The frame will be constructed using galvanized steel tubing and steel wire mesh to support the vine canopy. Guide wires were attached to each corner to stabilize the steel frame. One of two vines species, trumpet vine or Virginia creeper, will be planted at each vertical support.

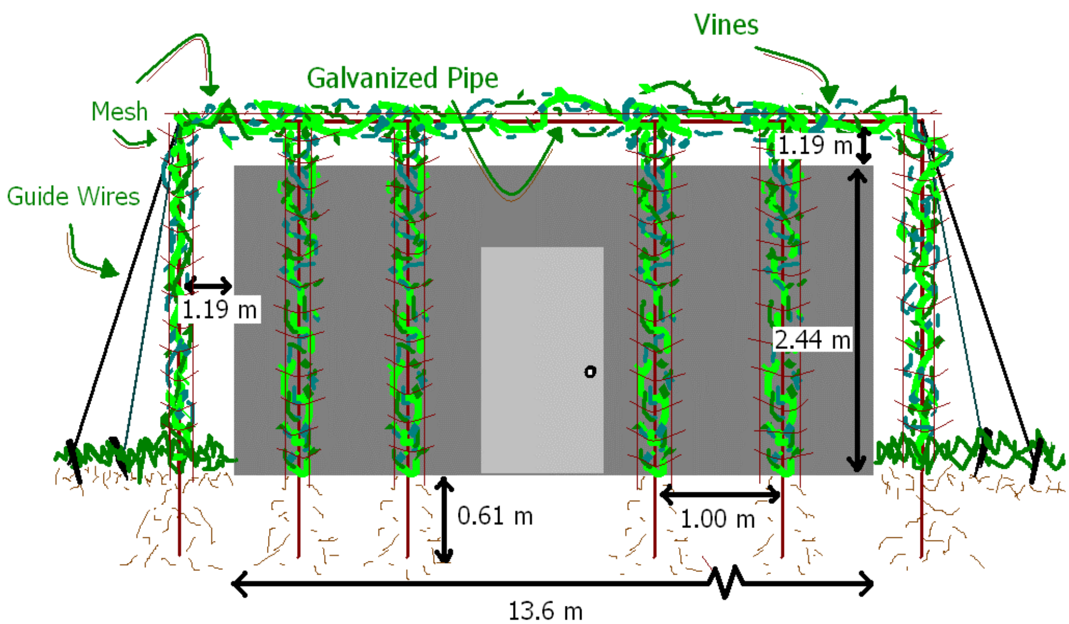

(a)

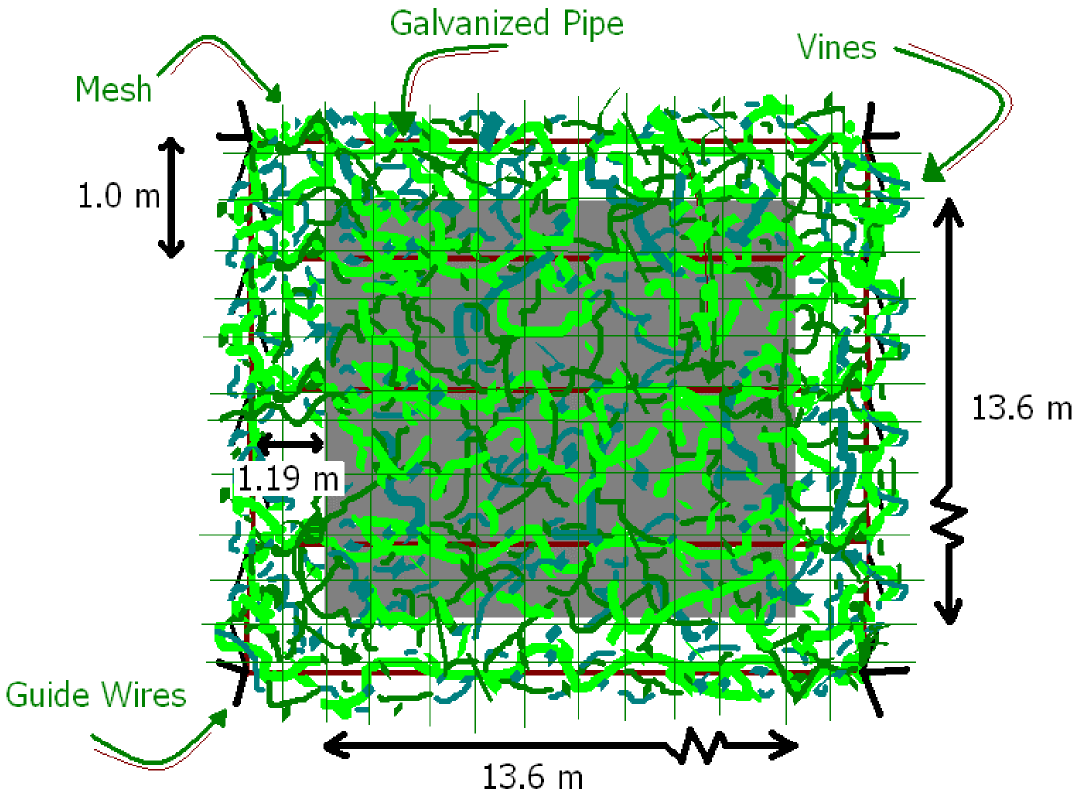

(b)

Figure 1a and 1b. Schematics of the side and top view of simulated 2000 ft^2 building with green cloak.

Frame. We chose 1" diameter galvanized tube as a maintenance free, weather resistant, structurally supportive, and cost effective material for the cloak frame. Galvanized steel has a lifetime of 20 to 40 years (Big Top Manufacturing, 2007). Given the correct structural design, a structure can be made from galvanized tube to withstand 120 mph winds and have zone four earthquake compliance (Big, 2007). Since optimal vine plant spacing is 4 m (Table 6.1), we designed the cloak structure to have vertical galvanized support structures every 4 m giving a total number of vertical supports of 24. Supports will be a total of 4.24 m (13.9 ft) long since they will be buried 0.61 m (2 ft) below ground, the building is 2.44 m (8 ft) tall, and there is a 1.19 m (3.9 ft) building protection clearance between the cloak and the building roof (Ch. 2). This design will require 101.8 m (334 ft) of galvanized tube.

Additionally, we used the same galvanized tube to run horizontally connecting the vertical supports. There will be four horizontal supports running along the perimeter of the building. Five more supports will run parallel over the building roof at approximately 4 m spacing. These nine horizontal supports total 192.9 m (633 ft). Including both vertical and horizontal supports, this gives a required amount of galvanized tubing of 294.7 m (967 ft).

Galvanized tube is threaded so that pieces can be screwed to one another. Additionally, galvanized tube fittings are available to attach tubes at angles to produce structures. Given the 24 vertical supports, 24 fittings will be required to construct the cloak frame.

Guide Wires. Two staked 3/16" guide wires will be used at each corner of the building for added stability for a total of 8 guide wires and 16" stakes. Since the cloak will be 3.63 m (11.9 ft) tall and the guide wire will be a 45° angle from the ground, we found the required length of guide wire. Each guide wire will be 5.12 m (16.8 ft) long for a total of 41.1 m (135 ft) of guide wire.

Wire Mesh. There will be a 0.61 m wide by 3.63 m (2 ft by 11.9 ft) tall piece of galvanized steel mesh (2" by 4" rectangles) attached to each support for each plant to grow on. Twenty-four vertical supports will require 53.1 m^2 (571 ft^2) of mesh. The same mesh will be attached to the horizontal supports of the cloak frame. The top of the cloak will be 256.3 m^2 (2759 ft^2) requiring a total of 309.4 m^2 (3330 ft^2) galvanized steel mesh.

Zip Ties. UV-resistant zip ties will be used to secure the mesh to the galvanized tubing and to itself at 1 foot intervals. Given that the mesh is 1.22 m (4 ft) wide and the cloak is 16 m (52.5 ft) wide, this means that there will be 14 widths of mesh across the cloak roof. Including the zip ties required to tie the mesh to itself, the horizontal galvanized supports and the vertical galvanized supports, a total of 1441 zip ties will be required to attach the mesh to the cloak frame.

Plants. Given 24 vertical supports with one plant growing up each support, 24 plants will be required. Vine species should be alternated at every support so that at least 2 vine species will be used in the cloak design. At planting, fertilizer and water will be given to each of the 24 plants.

Installation. Installation requires one supervisor and a team of 6 skilled workers. A supervisor was paid $25/hour and a skilled laborer was paid $15/hour. Including overhead, insurance, and taxes for these employees, these rates were doubled to $50 and $30 per hour (Furbish, 2007b). Labor-hours for installation were assumed similar to large outdoor tents (Anchor Industries 2007). We used their recommendation of 22.8 man hours to set up a 15.2 m by 18.3 m (50' by 60') tent (Anchor, 2007), which was approximately the same size as our simulated green cloak (16.0 m by 16.0 m or 52.5' by 52.5').

Operation and Maintenance. Operation and Maintenance costs included a skilled worker managing vine growth and inspecting the metal frame. We assumed two site visits per year, which would costs $60 annually. We did not include watering or fertilizing of the vines in Operation and Maintenance category because we assumed the plants will be rain-fed and will not need supplemental nutrients once established in the soil.

Cost Analysis

Costs of the Simulated Green Cloak. For the 2000 ft^2 one story building, the required quantities of materials and their related costs are listed in Table 6.3. Unit prices were from the Home Depot as of June 2007. Price discounts available to contractors or large purchasers would lower our cost estimate.

Table 6.3. Itemized cost estimate for installing and maintaining the simulated green cloak on a one-story 2000 ft^2 building.

Item	**Unit Price**	**No. Units**	**Total Cost**
Construction & Installation			
Materials			
Galvanized Tube, 1" diameter	\$1.70/ft[1]	967 ft	\$1,643.90
Tube Fittings, 1” diameter	\$2.00/fitting[1]	24 fittings	\$ 48.00
Guide Wire, 3/16" diameter	\$0.27/ft[1]	135 ft	\$ 36.45
Stakes, 16" length	\$3.10/stake[1]	8 stakes	\$ 24.80
Galvanized Wire Mesh, 14°	\$0.15/ft^2[1]	3330 ft^2	\$ 499.50
Zip Ties, 4" length	\$0.06/tie[1]	1441 ties	\$ 86.46
Vines	\$3.26/plant[2]	24 plants	\$ 78.24
Fertilizer, 40 lb bag	\$7.18/bag[1]	1 bag	\$ 7.18
Water	\$0.002/gal[3]	24 gal	\$ 0.05
Installation			
Supervisory Labor	\$50/hr[4]	22.8 hours[4]	\$1,140.00
Skilled Labor	\$30/hr[4]	22.8 hours[5]	\$ 684.00
Total Capital Costs			**\$4,248.58**
Maintenance & Operation	\$30/hr[4]	2 hours/yr[6]	\$ 60.00

All cost information was collected in June 2007 from the following sources: [1]Home Depot (Home, 2007), [2]Seedland.com (Seedland, 2007), [3]EPA (EPA, 2007), [4]Michael Furbish (Furbish, 2007b), [5]Anchor Industries (Anchor, 2007), and [6]estimate.

The construction and installation costs were \$4249 for the 2000 ft^2 (185.8 m^2) building. On a per area basis this was:

$$\text{CIC/Building Roof Area} = \$4{,}248.58/2000 \text{ ft}^2 = \$2.12/\text{ft}^2.$$

Operation and Maintenance costs were \$60.00/year.

<u>Model Sensitivity</u>. We explored the sensitivity of the cost estimate by altering the prices of the main components of the design to determine how the cost of the green cloak would change. First, we increased the tube diameter to 2" for increased stability. According to Home Depot pricing, 2" galvanized tube was \$3.50 per foot (1" tubing was \$1.70 per foot). Additionally, 2" tube fittings were \$3.00 each (1" fittings were \$2.00 each). Two inch tubes required longer zip ties. The longer zip ties (11") were \$0.10 each. These changes brought the Construction and Installation costs to \$6,070.82 which was \$3.04/ft^2. Operation and Maintenance costs remained at \$60.00/year.

Second, we determined the sensitivity of the cost-estimate to a lower wire mesh price because the mesh available in Home Depot had 2" by 4" spacing, which was less than we required. Assuming that mesh with larger spacing would cost less since it would require less galvanized steel, we cut the cost of the mesh from \$0.15/ft^2 to \$0.08/ft^2. With this the Construction and Installation costs were \$4,015.48 which was \$2.01/ft^2. Operation and Maintenance costs remained at \$60.00/year.

Third, we assumed that installation would take twice as long as the recommended time from Anchor Industries. We doubled installation time from 22.8 hours to 45.6 hours. This increased the Construction and Installation costs to \$6,072.58 which was \$3.04/ft^2. Operation and Maintenance costs remained at \$60.00/year.

Finally, we increased the plant density to one plant every meter around the building instead of 1 plant every 4 m. Galvanized guide wire and stakes would be used around the building. Twenty-four plants would remain on the 24 vertical supports, but three more plants would be added between each support since each support was about 4 m apart. This would require an increase of 72 plants for a total of 96 plants. Seventy-two extra plants would require 72 more stakes and 1212 ft more of guide wire increasing the Construction and Installation costs to \$5,033.74 which was \$2.52/ft^2. Operation and Maintenance costs remained at \$60.00/year.

Roof Comparison. The green cloak was less expensive to install than a green roof. In all cost estimates, the green cloak was no more than \$3.04/ft^2. Combining its costs with the costs of a new shingle roof (\$4.50 to \$8.00/ft^2) gives a total roofing cost of \$7.54 to \$11.04/ft^2. An extensive green roof costs \$10 to \$20/ft^2 which does include first re-roofing with a root-repelling membrane. Taking the averages of the green cloak and green roof price ranges (\$9.29 and \$15/ft^2, respectively), the green cloak construction and installation costs are 38% less expensive than an extensive green roof.

Benefit Analysis

Energy Savings. The green cloak reduced peak daytime temperature of the inside of the house by a maximum of 13.1 °C (23.6 °F) and an average 24-hour temperature difference of 11.3 °C (20.3 °F) compared to the house with no green cloak (Figure 6.2). We used Figure 6.2 to find the potential daily summertime energy savings by calculating the area between the modeled temperature curve and thermostat setting for each cloak. The percent energy savings, 72.9%, was the percentage area difference of a cloak with LAI 0 and LAI 2.

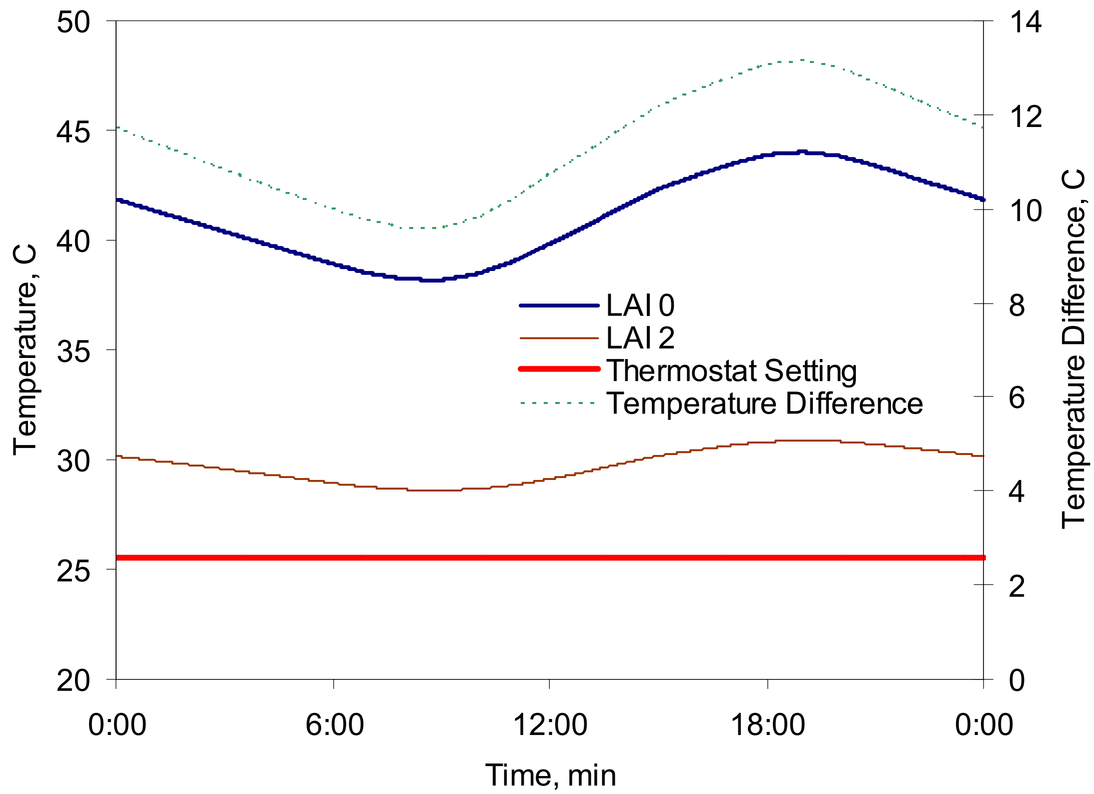

Figure 6.2. Indoor house temperature for a roof with no green cloak (solid thick line), with a green cloak of LAI equal to 2 (solid thin line), their difference (broken line, right axis), and house thermostat setting (horizontal solid line).

We generated Table 6.4 with annual energy costs and savings for each location. We will show an example calculation for Annual Energy Cost (A) and Annual Energy Savings (S) in College Park, MD with an energy cost of \$0.10/kWh and 13 SEER air conditioning unit using Equations 1 and 3.

$$A = [(37059 \text{ Btu/hr})\cdot(900 \text{ hrs})\cdot(\$0.10/\text{kWh})]/[(13 \text{ Btu/Wh})\cdot(1000 \text{ Wh/kWh})] = \$256.56$$

$$S = (\$256.56)\cdot(72.9\%)/100\% = \$187.03$$

We found that the green cloak could save \$187 per year in energy costs in Maryland, but as much as \$659 per year in South Florida when electricity prices were assumed to be \$0.10/kWh (Table 6.4). At \$0.20/kWh annual energy savings doubled to \$374 and \$1,319 for Maryland and Florida, respectively.

Table 6.4. Cost savings from reduced cooling load for Maryland, Florida and Texas.

Location	Heat Gain (H_X) (Btu/hr)	Cooling Time (T) (hr)	Energy Cost (C) ($/kWh)	Annual Energy Cost (A) ($)	Energy Savings (B) (%)	Annual Energy Savings (S) ($)
College Park, MD	37059	900	$0.10	$ 256.56	72.9	$ 187.03
Central Texas	46941	1800	$0.10	$ 649.95	72.9	$ 473.81
South Florida	42000	2800	$0.10	$ 904.62	72.9	$ 659.47
College Park, MD	37059	900	$0.20	$ 513.12	72.9	$ 374.06
Central Texas	46941	1800	$0.20	$1,299.90	72.9	$ 947.63
South Florida	42000	2800	$0.20	$1,809.23	72.9	$1,318.93

Roof Lifetime Extension. To determine the annual value of roof lifetime extension of a green roof, we assumed a green cloak with a lifetime of 30 years, a green cloak doubling the lifetime of the shingle roof below, and a shingle roof with an installation price of $4.50/ft^2. Given a shingle roof lifetime of 15 years, this would mean that over the lifetime of one green cloak, a building owner would be saved the costs of one shingle roof. In our cost analysis, this was a value of $300 annually (Eq. 7).

$$ARS = RCIC \cdot RA/GCL = \qquad (7)$$
$$ARS = (\$4.50/ft^2) \cdot (2000\ ft^2)/30\ yrs = \$300$$

where ARS is annual roof savings in dollars, RCIC is shingle roof construction and installation cost in $/ft^2, RA is roof area in ft^2, and GCL is green cloak lifetime in years.

Green Building Tax Credit. We found an annual tax credit value of $16.67 based on a $500 tax credit and a 30 year green cloak lifetime Eq. 8.

$$TC = TTC/GCL =$$

$$TC = \$500/30\ years = \$16.67$$

where TTC is total tax credit in dollars.

Table 6.5 lists the direct and indirect benefits of the green cloak, but we only estimated savings value for reduced cooling load, extended life for asphalt shingles, and projected green building tax credit. Estimating the savings of the other items was beyond the scope of our work. We listed benefits for College Park, MD, central Texas, and south Florida with current energy prices ($0.10/kWh) in the table along with other unknown benefits of the green cloak.

Table 6.5. Potential direct and indirect benefits of green cloak.

	Annual Value		
Benefit	**College Park, MD**	**Central Texas**	**South Florida**
Direct Benefit			
Energy Savings	$187.03	$473.81	$659.47
Indirect Benefit			
Roof lifetime extension	$300.00	$300.00	$300.00
Tax credit	$ 16.67	$ 16.67	$ 16.67
Stormwater mediation	?	?	?
Property values	?	?	?
Aesthetics	?	?	?
Building unique benefits	?	?	?

We calculated the net annual benefit of the cloak for each location (Table 6.6). We will show an example calculation for Net Annual Benefit (NAB) for a green cloak in College Park, MD at $0.10/kWh energy cost using Equation 4.

$$\text{NAB} = \$187.03 + \$300.00 + \$16.67 - \$60.00 = \$443.70$$

Net annual benefit was greater, when energy prices were higher and in locations in which cooling hours were greater. The NAB in College Park, MD with current energy prices was about $444. In south Florida, with $0.20/kWh, NAB was $1,576. Net annual benefit did not account for installation and construction costs, therefore, a payback period was determined to calculate when the NAB was first enjoyed.

Table 6.6. Net annual benefit of green cloak for Maryland, Florida and Texas.

Location	Energy Cost (C) ($/kWh)	Annual Energy Savings (S) ($)	Annual Roof Savings (ARS) ($)	Annual Tax Credit (TC) ($)	Annual Maintenance (M) ($)	Net Annual Benefit (NAB) ($)
College Park, MD	$0.10	$ 187.03	$300.00	$16.67	$60.00	$ 443.70
Central Texas	$0.10	$ 473.81	$300.00	$16.67	$60.00	$ 730.48
South Florida	$0.10	$ 659.47	$300.00	$16.67	$60.00	$ 916.14
College Park, MD	$0.20	$ 374.06	$300.00	$16.67	$60.00	$ 630.73
Central Texas	$0.20	$ 947.63	$300.00	$16.67	$60.00	$1,204.30
South Florida	$0.20	$1,318.93	$300.00	$16.67	$60.00	$1,575.60

We calculated the payback period of the cloak for each location (Table 6.7). We will show an example calculation for Payback period (P) for a green cloak in College Park, MD at $0.10/kWh energy cost using Equation 5.

$$P = \$4,248.58/\$443.70 = 9.6 \text{ years}$$

Payback period was less when energy prices were higher and in locations in which cooling hours were greater. For a green cloak to be feasible, the payback period must be less than 30 years—the projected lifetime of a green cloak. Once the payback period is reached, benefits are enjoyed. At current energy prices, a green cloak in Maryland would take 9.6 years to pay for itself. With energy prices at $0.20/kWh, we estimated that a green cloak in south Florida paid for itself the soonest in 2.70 years.

Table 6.7. Payback period of green cloak for Maryland, Florida and Texas.

Location	Energy Cost (C) ($/kWh)	Construction and Installation Costs (CIC) ($)	Net Annual Benefit (NAB) ($)	Payback Period (P) (yrs)
College Park, MD	$0.10	$4,248.58	$ 443.70	9.60
Central Texas	$0.10	$4,248.58	$ 730.48	5.82
South Florida	$0.10	$4,248.58	$ 916.14	4.64
College Park, MD	$0.20	$4,248.58	$ 630.73	6.70
Central Texas	$0.20	$4,248.58	$1,204.30	3.53
South Florida	$0.20	$4,248.58	$1,575.60	2.70

We calculated the benefit cost ratio of the cloak for each location (Table 6.8). We will show an example calculation for benefit cost ratio (BCR) for a green cloak in College Park, MD at $0.10/kWh energy cost using Eq. 6.

$$BCR = (30\cdot 187.03 + 30\cdot 300.00 + 30\cdot 16.67)/(4248.58 + 30\cdot 60) = 2.50$$

Benefit cost ratio was greatest when energy prices were higher and in locations in which cooling hours were greater. In College Park, MD, with current energy prices, the benefit cost ratio was only 2.50. In south Florida, with higher energy prices, the benefit cost ratio was 8.11.

Table 6.8. Benefit cost ratio of green cloak for Maryland, Florida and Texas.

Location	Energy Cost (C) ($/kWh)	Annual Energy Savings (S) ($)	Annual Roof Savings (ARS) ($)	Annual Tax Credit (TC) ($)	Const. and Install. Costs (CIC) ($)	Annual Maint. (M) ($)	Benefit Cost Ratio (BCR)
College Park, MD	$0.10	$ 187.03	$300.00	$16.67	$4,248.58	$60.00	2.50
Central Texas	$0.10	$ 473.81	$300.00	$16.67	$4,248.58	$60.00	3.92
South Florida	$0.10	$ 659.47	$300.00	$16.67	$4,248.58	$60.00	4.84
College Park, MD	$0.20	$ 374.06	$300.00	$16.67	$4,248.58	$60.00	3.43
Central Texas	$0.20	$ 947.63	$300.00	$16.67	$4,248.58	$60.00	6.27
South Florida	$0.20	$1,318.93	$300.00	$16.67	$4,248.58	$60.00	8.11

Discussion

The cost of a green cloak for a 2000 ft^2 building was estimated to be \$4249 (\$2.12/ft^2) for installation plus \$60/y for maintenance. After performing a sensitivity analysis on the green cloak installation and construction costs, we found that the green cloak cost should remain less than \$3.05/ft^2 for construction and installation. Together with a new shingle roof (\$4.50 to \$8/ft^2), a green cloak would cost a total of \$7.55 to \$11.05/ft^2. This is approximately 38% less than the cost of an extensive green roof. Assuming that energy savings, green tax credit, roof lifetime extension, other indirect benefits, and maintenance costs are equivalent for green cloaks and green roofs, green cloaks are cheaper. Given the results of Ch. 4, a green roof can retain more runoff than a green cloak giving a green roof a higher rainfall mitigation value. If rainfall mitigation function is important for a roofing project, a green roof may be a worthwhile alternative after considering the runoff mitigation benefit. If rainfall mitigation is not important, like in a rural environment, a green cloak may be a better green technology choice.

We predicted a 73% air conditioning energy savings with a green cloak of LAI 2. Considering current and possible future energy prices in College Park, MD, central Texas, and south Florida, this led to a \$187 to \$1319 annual air conditioning costs savings. We estimated the green cloak to double the lifetime of the shingle roof below due to its building shading and roof temperature reduction properties. We estimated a \$500 tax credit for green cloak construction and installation. Given these costs and benefits, we estimated the green cloak under all conditions to pay for itself within the 30 year lifetime of the green cloak (between 9.60 and 2.70 years) proving the green cloak to be a cost effective technology.

Not only does a green cloak make sense, we have modeled the green cloak to be a yielding investment. Given the conditions of our analysis, we calculated the benefit cost ratio of the green cloak to be between 2.50 and 8.11 suggesting that over a 30 year lifetime a green cloak of LAI 2 investment returns could be more than eight-fold.

As a novel, inexpensive, and lightweight alternative to green roofs, the green cloak should provide many benefits, such as energy savings, roof lifetime extension, aesthetics, habitat, runoff mitigation, increased mental wellbeing, and possible property value increase. While we only estimated the monetary benefits offered as energy savings, extending the life of asphalt shingles, and green building tax incentives, it will be interesting to see more complete economic analyses conducted on the green cloak in the future.

Chapter 7: Conclusion

Green roofs are becoming popular in the United States for their rainfall retention and energy saving abilities. However, current green roof designs have high installation costs, heavy load-bearing requirements, and restrictions to low-sloped roofs. We designed a novel green roof retrofit technology, called the *green cloak*, which uses fast-growing vine species and a trellis to suspend vegetation above a roof. Green cloak vegetation is able to shade and insulate the building below while remaining lightweight, inexpensive, and non-slope specific. This thesis examined the practicality of the green cloak studying vine growth rates and characteristics, summer indoor temperature reduction, canopy runoff reduction, and associated costs through field experiments, prototype testing, mathematical modeling, and benefit-cost analysis.

We compared growth characteristics of vines cultivated on engineered PVC trellises (green cloak) to naturally occurring vine communities colonizing dilapidated tobacco barns to inform green cloak design (Chapter 2). We found 100% coverage on the engineered trellises and comparable barn leaf areas in less than one year of growth (Figures 2.6 and 2.8). These results imply that the barns' maximum leaf area index of 5 is an achievable green cloak leaf area index (Table 2.3). Barn ecosystems typically had higher species diversity and leaf area indices than green cloaks (Table 2.3). Trumpet creeper and Virginia creeper were species found on barns with high leaf area indices indicating their potential use in future green cloak design (Table 2.5). Through leaf area index regression, we found that high leaf area indices can be achieved in immature ecosystems without extensive woody material growth as found in the mature barn vine communities (Figures 2.10 through 2.12). Green cloaks had lower light transmission for equivalent barn LAI indicating the benefit of even an immature green cloak (Figures 2.13 and 2.16). These results suggest that the benefits of a green cloak can be enjoyed within the first year of installation.

Based on our findings in Chapter 2, we learned that green cloak vines have potential to provide significant coverage to a building roof early in development. In Chapter 3, we determined if the green cloak would be a suitable alternative energy saving technology by comparing green cloak effects and related growth characteristics on indoor model building and roof temperature. Specifically, we found a maximum temperature decrease of 3.1 °C with the Porcelainberry (PB) and Virginia Creeper 1 (VC1) cloaks, a roof temperature reduction of 23 °C (Tables 3.1 and 3.2), and a significant correlation between canopy cover and LAI with indoor building temperature reduction (Figures 3.12 and 3.13).

In Chapter 4, we developed a mathematical model to determine the ability of the green cloak to lower indoor building temperature and energy consumption in a full-scale building. We developed a model to successfully predict indoor building temperature based on environmental air temperature, solar radiation, building dimensions, and cloak leaf area index. We calibrated and validated the model with temperature data recorded during the outdoor temperature experiments reported in Chapter 3. We applied the model to a one story 2000 ft^2 (185.8 m^2) house with a green cloak of LAI 2 to find a potential average daily air temperature decrease of 11.3 °C, a maximum temperature decrease of 13.1 °C, and an air conditioning energy consumption decrease of 72.9% (Figures 4.23 and 4.24). These results indicate that the green cloak is a comparable technology to green roofs from an energy savings standpoint and green cloak costs and benefits must be evaluated further.

As green roofs are primarily used for rainfall retention, we used Chapter 5 to evaluate runoff reduction abilities of the green cloak. We used a rainfall simulator to measure the amount of rainfall intercepted in eleven green cloak vine canopies and to determine the runoff delay from the vine canopies. We compared rainfall interception relative to cloak growth characteristics determining that increases in leaf area index significantly decreased rainfall runoff. We generated a mathematical model to estimate runoff based on rainfall simulator experiments and leaf area index. For an average storm of 22.8 mm, model results showed that a cloak of LAI 5 stored 4.2 mm of water and about 33% of the water that an extensive green roof in North Carolina held (Table 5.4 and 5.5). The green cloak delayed the peak storm runoff from a 0.15 mm/min storm by 100 minutes (Figure 5.18). This signified that although a green cloak holds less water than the extensive green cloak, its still may be a valid choice for builders if it costs less.

Since indoor building temperature and rainfall runoff reduction results indicated the similarities of a green cloak and green roof, we evaluated the benefits and costs of the green cloak relative to an extensive green roof (Chapter 6). We estimated the cost of installing a green cloak for a 2000 ft^2 building to be \$9.29/ft^2—38% less than an extensive green roof (\$15/ft^2) (Table 6.3). We further evaluated the costs, energy savings, roof lifetime extension, and green building tax benefit to find the payback periods and benefit-cost ratios in three geographically different locations—College Park, MD, central TX, and south FL with two different energy rates (\$0.10 and \$0.20/kWh). We estimated that the green cloak, with a 30 year lifetime, would double the lifetime of the conventional shingle roof below. We estimated a onetime $500 tax credit. Based on roof location, energy costs, and an average peak daytime temperature reduction of 11.3 °C, we found net annual benefit ranging from $444 to $1576, payback periods less than the predicted green cloak lifetime (2.7 to 9.6 years), and benefit-cost ratios ranging from 2.5 to 8.11 (Tables 6.7 and 6.8). We predict that maximum green cloak benefit will be experienced in locations where annual cooling costs are greatest; in our model this was south Florida with the most annual cooling hours. These results indicated that the green cloak could be both a yielding investment and a smart alternative green roof technology.

Taking into consideration the quick growth rates of vines, rainfall runoff detention and retention, indoor building temperature moderation, and reduced installation costs, we see the green cloak being a beneficial ecologically inspired technology. These exciting results show that we were able to maintain green roof benefits while eliminating drawbacks at a lower cost and lighter weight. Since the green cloak payback period was shorter in hotter climates, we believe that the green cloak would be most successful in the southern US and with its low installation costs possibly in Latin America to keep livestock alive, healthy, and cool. With such vast potential, we hope to see a pilot-scale green cloak study in which indoor building temperature and runoff reduction can be studied under real, rather than simulated, conditions.

Chapter 8: Future Work

Maryland poultry farmers produced over 1.3 billion pounds of chicken in 2004 valued at $628 million representing about 33% of Maryland's farm income (Delmarva, 2005). For poultry farming to remain competitive and environmentally friendly, rising energy costs must be mitigated because buildings must be heated in winter and cooled in summer to maintain ideal temperature and humidity for healthy bird growth (Fairchild, 2005). At cold temperatures, birds must divert metabolic energy to heat and away from growth, while at hot temperatures birds must be kept cool to maintain proper rates of weight gain (Bucklin, 2003).

In the mid-Atlantic, propane and natural gas are the fuels used to heat broiler facilities (Fairchild, 2005). Recently, some farmer's have seen annual increases in winter fuel bills of $1500 per house, which is a 30% increase (Van Hoy, 2005). In the summer in the Southeast US, the high solar load can easily increase roof temperatures to 66º C (150º F), which adds unwanted radiant heat to the flock (Donald, 1999). Donald (1999) found that houses with insulated ceilings had maximum temperatures of 33º C (92º F) and 0.5% mortality, while those without insulation experienced 37º C (99º F) and 14.3% mortality, which highlights the importance of controlling the solar heat load. Currently, tunnel ventilation and evaporative cooling systems are widely used to remove summer heat (Winchell, 1994). Tunnel ventilation uses fans on each end of the house to push air through at velocities of 4 to 5 mph which causes a cooling effect of up to 5.5º C (10º F) (Bucklin, 2003). To obtain temperatures lower than outside air, evaporative cooling and fogging are used to cool incoming air (Bucklin, 2003).

With energy prices at all time highs and little reprieve in sight, research is needed to identify ways in which farmers can substitute renewable energy for non-renewable forms to promote their financial and environmental sustainability (Feenstra, 1997). Using the positive findings of this thesis, we propose that our design for a novel green roof technology be explored as a means to lower energy consumption and associated fuel expenditures in poultry housing. In the summer, the green cloak can cool the building (1) by reflecting solar irradiance and (2) through evaporative cooling provided by water transpired from leaf surfaces. If planted with deciduous vines, in the winter sunlight will not be blocked from entering poultry houses and what branches remain will insulate the building retarding the convective heat loss due to cold winter winds. The green cloak will have low installation and maintenance costs and will decrease the use of nonrenewable fuels for heating and cooling, which will save the farmer money, especially as the price of energy remains at historic highs.

We recommend the next generation of green cloak research be focused on a pilot scale trial on a poultry building using a similar design to the one outlined in Chapter 6. The site for the green cloak pilot scale project should be one in which there are two nearly identical agricultural buildings where a green cloak could be installed on one of the buildings and the other could be left as a control. Before starting the experiment, the two buildings should be measured for solar radiation, neighboring vegetation, energy consumption, and building construction. Importantly, there should be sufficient space around the building for supports and guide wires along with the building owner's full consent to the project and understanding that there could be building damage due to vines.

The scale up experiment can be used to answer questions that were raised but left unanswered in this experiment. For example, temperature data and building information should be collected to validate the ability of the model for building scale up application. The 73% energy consumption reduction prediction was collected from the temperature model, but not validated since there was no full scale data with which to validate it. Runoff from the experimental building should be collected during storms and compared to the control building for extended understanding of its abilities. The errors for the runoff model were high limiting our confidence in the model results. Runoff may be especially important on a farm in which animal waste can quickly become runoff.

Temperatures of buildings should be constantly monitored and compared to canopy leaf area indices. Coverage and thickness should be measured and compared to plant spacing. As an added potential benefit, we also recommend that roof temperatures be recorded and compared to bird mortality as in Donald's 1999 study. Maintenance with respect to keeping vines on trellises should be evaluated and added into green cloak costs. Wintertime questions including snow, wind, and leaf litter can also be answered along with the ability of vines to come back in the spring with improved coverage for the next summer season.

Appendix A

Appendix A lists raw data from Chapter 2: Cloak and Barn Vine Growth and Comparison Using Ecological Engineering Theory. Table A.a lists the growth in LAI of the cloaks over the one year growing period. Define a

Table A.a. LAI of the eleven cloaks over the one year growing period where VC1 is Virginia Creeper 1, VC2 is Virginia Creeper 2, PB is Porcelainberry, K1 is Kudzu 1, K2 is Kudzu 2, JH is Japanese Honeysuckle, CTC is Chinese Trumpet Creeper, MG is Morning Glory, BESV is Black Eyed Susan Vine, MF is Moonflower, and CV is Cross Vine.

	VC1	VC2	PB	K1	K2	JH	CTC	MG	BESV	MF	CV
8/25/2005	0.00	0.00									
9/12/2005	0.77	0.29									
9/27/2005	1.23	1.13	0.99								
1/9/2006	2.24	1.22	2.58	1.37							
2/7/2006	1.64	1.47	3.78	0.64	0.68						
2/15/2006	1.60	2.16	3.90	1.20	0.49	0.00					
2/23/2006	1.36	1.78	4.33	0.00	0.00	0.32					
3/2/2006	1.72	2.94	5.03	1.52	0.71	0.00					
3/10/2006	1.39	1.36	2.39	0.80	1.94	1.22					
3/16/2006	1.58	2.75	3.47	1.43	0.54	0.00					
3/23/2006											
3/31/2006											
4/6/2006	1.04		3.21	0.85	0.41	0.54					
4/13/2006	1.11	4.22	2.87	1.68	0.42	0.70	0.78				
4/20/06		0.69	2.70		0.55	0.89					
4/25/06	1.75	0.85	2.26	1.12	0.00	0.61	0.00				
4/27/2006	1.98	1.00	1.71	1.99	0.70	1.14	0.77				
5/4/2006	2.03	0.85	2.72	2.44	0.78	1.29	0.98				
5/11/2006	2.95	0.98	3.70	1.17	1.42	1.83	1.49				
5/19/2006	2.62	2.32	2.65	1.05	0.86	2.96	1.08	0.00	0.00	0.00	0.00
5/25/2006	1.77	1.78		0.00	0.76	1.13	0.83				
6/2/2006	1.90	1.94	0.11	0.22	0.34	1.96	0.49				
6/8/2006	1.72	2.02	0.72	0.37	0.56	0.50	0.42				
6/15/2006	1.93	1.58	1.41	1.37	0.39	2.83	1.19				
6/29/2006	2.57	1.98	0.22	0.00	0.91	2.07	0.29	0.07			
7/6/2006	2.74	4.01	1.60	0.13	1.23	2.01	0.52	0.18			
7/13/2006											
7/21/2006											
7/28/2006	4.67	3.17	1.50	2.33	2.33	3.33	2.50	1.17	1.67	1.17	1.00
8/10/2006	3.00	2.17	1.17	0.67	1.00	2.00	1.67	0.33	1.00	1.67	0.50

Table A.b lists the growth in canopy coverage of the cloaks over the one year growing period.

Table A.b. Percent canopy coverage of the eleven cloaks over the one year growing period where VC1 is Virginia Creeper 1, VC2 is Virginia Creeper 2, PB is Porcelainberry, K1 is Kudzu 1, K2 is Kudzu 2, JH is Japanese Honeysuckle, CTC is Chinese Trumpet Creeper, MG is Morning Glory, BESV is Black Eyed Susan Vine, MF is Moonflower, and CV is Cross Vine.

	VC1	VC2	PB	K1	K2	JH	CTC	MG	BESV	MF	CV
8/25/2005	61	42	6								
9/12/2005	78	50	44								
9/27/2005	89	56	50	17							
1/9/2006											
2/7/2006	95	80	100	35	25						
2/15/2006	95	80	100	40	25	5					
2/23/2006	95	95	100	50	30	10					
3/2/2006	99	95	100	70	40	12					
3/10/2006	100	100	100	80	50	15					
3/16/2006	100	95	100	75	40	25					
3/23/2006											
3/31/2006											
4/6/2006	100		100	70	45	30					
4/13/2006	98		100	97	30	25	7				
4/20/06		94	90	85	45	58	15				
4/25/06											
4/27/2006	99	90	98	50	55	85	30				
5/4/2006	100	95	99	90	45	85	30				
5/11/2006	100	90	100	70	45	85	45				
5/19/2006	95	80	100	50	20	90	55	0	0	0	0
5/25/2006	85	85		5	30	95	65				
6/2/2006	95	85	5	5	30	100	40				
6/8/2006	92	92	5	10	30	100	60				
6/15/2006	95	95	7	10	50	100	50				
6/29/2006	100	100	7	7	60	100	50	3			
7/6/2006	100	100	10	10	65	100	55	10			
7/13/2006	100	99	17	13	65	99	55	25	7		2
7/21/2006	100	100	20	15	80	100	60	30	10		5
7/28/2006	100	100	25	45	85	100	85	50	15	7	10
8/10/2006	100	100	60	75	75	95	60	40	50	40	45

Table A.c lists the growth in canopy dead of the cloaks over the one year growing period.

Table A.c. Percent canopy dead of the eleven cloaks over the one year growing period where VC1 is Virginia Creeper 1, VC2 is Virginia Creeper 2, PB is Porcelainberry, K1 is Kudzu 1, K2 is Kudzu 2, JH is Japanese Honeysuckle, CTC is Chinese Trumpet Creeper, MG is Morning Glory, BESV is Black Eyed Susan Vine, MF is Moonflower, and CV is Cross Vine.

	VC1	VC2	PB	K1	K2	JH	CTC	MG	BESV	MF	CV
8/25/2005											
9/12/2005											
9/27/2005											
1/9/2006											
2/7/2006											
2/15/2006	0.5	0.5	0	1	0	0					
2/23/2006	0	0	0	1	0	0					
3/2/2006	0	0	3	5	1	0					
3/10/2006	0	0	1	5	2	1					
3/16/2006	0	0.5	0	5	1	0					
3/23/2006											
3/31/2006											
4/6/2006	0		0	5	5	0					
4/13/2006	1		12	3	2	1	1				
4/20/06		2	10	15	15	1	0				
4/25/06											
4/27/2006	2	1	5	17	3	0	0				
5/4/2006	3	1	3	90	27	0	0				
5/11/2006	1	1	5	90	2	0	0				
5/19/2006	1	1	50	97	12	0	0				
5/25/2006	1	1		90	10	0	0				
6/2/2006	1	1	2	60	5	2	90				
6/8/2006	2	2	7	2	5	3	99				
6/15/2006	0	0	2	5	7	0	10				
6/29/2006	0	0	0	0	0	2	0	10			
7/6/2006	1	1	0	0	1	5	0	10			
7/13/2006	0	0	0	3	1	3	1	5	0		0
7/21/2006	1	1	0	2	1	2	0	7	0		0
7/28/2006	0	0	0	2	2	3	0	7	1	2	0
8/10/2006	1	1	0	1	3	0	1	0	0	1	0

Table A.d lists the growth in canopy thickness above trellis of the cloaks over the one year growing period.

Table A.d. Canopy thickness above trellis (mm) of the eleven cloaks over the one year growing period where VC1 is Virginia Creeper 1, VC2 is Virginia Creeper 2, PB is Porcelainberry, K1 is Kudzu 1, K2 is Kudzu 2, JH is Japanese Honeysuckle, CTC is Chinese Trumpet Creeper, MG is Morning Glory, BESV is Black Eyed Susan Vine, MF is Moonflower, and CV is Cross Vine.

	VC1	VC2	PB	K1	K2	JH	CTC	MG	BESV	MF	CV
8/25/2005	75	60	40								
9/12/2005	130	100	90								
9/27/2005	100	80	100	50							
1/9/2006											
2/7/2006	150	170	260	190	150						
2/15/2006	160	140	260	140	90	30					
2/23/2006	140	120	140	110	110	15					
3/2/2006	170	200	180	200	150	15					
3/10/2006	130	200	130	160	100	10					
3/16/2006	250	230	230	220	250	50					
3/23/2006											
3/31/2006											
4/6/2006	200		170	210	170	20					
4/13/2006	110		140	240	230	50	30				
4/20/06		125	125	250	150	40	40				
4/25/06											
4/27/2006	200	140	160	200	180	70	110				
5/4/2006	230	120	120	120	290	150	110				
5/11/2006	100	90	100	70	45	85	45				
5/19/2006	200	110	120	100	160	70	110				
5/25/2006	170	160		140	170	120	150				
6/2/2006	150	240	50	100	240	110	30				
6/8/2006	170	100	70	130	150	100	40				
6/15/2006	150	150	80	120	150	110	70				
6/29/2006	110	100	30	70	110	150	70	50			
7/6/2006	100	120	60	150	140	85	100	30			
7/13/2006	90	120	90	80	160	75	60	100	50		30
7/21/2006	150	85	100	120	150	155	100	110	50		70
7/28/2006	160	150	130	140	240	240	180	110	60	110	45
8/10/2006	200	140	180	200	160	230	160	90	130	130	30

Table A.e lists the growth in canopy maximum thickness above trellis of the cloaks over the one year growing period.

Table A.e. Canopy maximum thickness above trellis (mm) of the eleven cloaks over the one year growing period where VC1 is Virginia Creeper 1, VC2 is Virginia Creeper 2, PB is Porcelainberry, K1 is Kudzu 1, K2 is Kudzu 2, JH is Japanese Honeysuckle, CTC is Chinese Trumpet Creeper, MG is Morning Glory, BESV is Black Eyed Susan Vine, MF is Moonflower, and CV is Cross Vine.

	VC1	VC2	PB	K1	K2	JH	CTC	MG	BESV	MF	CV
8/25/2005	85	110	90								
9/12/2005	170	140	180								
9/27/2005	140	140	160	120							
1/9/2006											
2/7/2006	250	270	350	360	260						
2/15/2006	280	270	330	410	170	30					
2/23/2006	190	210	220	220	150	20					
3/2/2006	260	250	280	250	180	20					
3/10/2006	260	240	190	270	230	30					
3/16/2006	300	270	275	600	400	140					
3/23/2006											
3/31/2006											
4/6/2006	250		180	310	310	60					
4/13/2006	150		280	350	320	120	40				
4/20/06		150	180	300	210	120	50				
4/25/06											
4/27/2006	260	180	220	250	380	120	110				
5/4/2006	230	150	250	260	400	150	150				
5/11/2006	200	130	170	120	200	80	70				
5/19/2006	240	260	250	300	400	300	170				
5/25/2006	230	220		270	470	350	330				
6/2/2006	200	240	120	200	355	410	100				
6/8/2006	230	110	100	170	300	220	150				
6/15/2006	300	250	120	230	480	300	220				
6/29/2006	200	270	230	170	220	240	200	50			
7/6/2006	120	310	60	310	490	330	180	110			
7/13/2006	230	250	150	210	300	280	230	130	60		110
7/21/2006	220	260	190	250	300	270	160	400	110		150
7/28/2006	260	300	170	240	370	350	270	230	130	300	210
8/10/2006	320	300	330	440	540	440	450	450	220	440	340

Table A.f lists the observations made on each plot at Barn 1.

Table A.f. Observations at each plot at Barn 1.

	Plot	**1**	**2**	**3**
Site details	road	rt 4	rt 4	rt 4
	Date	14-Jul	14-Jul	14-Jul
	location	Wilkerson Baseball Field	Wilkerson Baseball Field	Wilkerson Baseball Field
	nickname	1	2	3
	Orientation (degrees)	90	90	90
	Elevation (cm)	220	220	220
	Growth notes	vines hanging on roof, not growng along wall		
Thickness	Thick 1 (cm)	92	117	56
	Thick 2 (cm)	79	98	56
	Thick 3 (cm)	79	104	72
	Ave Thick (cm)	83.33	106.33	61.33
LAI	LAI 1	7	2	3
	LAI 2	3	3	2
	LAI 3	5	6	2
	LAI 4	5	2	2
	LAI 5	4	4	4
	Avg LAI	4.8	3.4	2.6
Light	Under 1	38	48	31
	Under 2	35	43	33
	Under 3	23	42	26
	Under 4	26	15	18
	Under 5	27	33	23
	Under Avg	29.8	36.2	26.2
	Over 1	135	125	133
	Over 2	116	109	152
	Over Avg	125.5	117	142.5
	% Transmittance	0.237	0.309	0.184
	Shade/Sun	Shade	Shade	Shade
Biomass	Poison, nonwoody	29.238	14.817	
	Poison, woody	15.174	244.280	
	Va creeper, nonwoody	3.4	107.314	148.158
	Va creeper, woody		12.094	

	Smilax, nonwoody	152.952	161.895
	Grape, nonwoody		
	Grape, woody		
	Trumpet, nonwoody		
	Trumpet, woody		
	Black, nonwoody		
	Black, woody		
	Honeysuckle, nonwoody		
	Honeysuckle, woody		
	Hydrangea, nonwoody		
	Hydrangea, woody		
Other vine species	NA		

Table A.g lists the observations made on each plot at Barn 2.

Table A.g. Observations at each plot at Barn 2.

	Plot	1	2	3
Site details	road	rt 4	rt 4	rt 4
	Date	14-Jul	14-Jul	14-Jul
	location	Wilkerson House	Wilkerson House	Wilkerson House
	nickname	4	5	6
	Orientation (degrees)	96	96	96
	Elevation (cm)	220	220	220
	Growth notes	hanging off roof, more gowing on side than barn 1		
Thickness	Thick 1 (cm)	103	110	91
	Thick 2 (cm)	80	125	85
	Thick 3 (cm)	75	130	123
	Ave Thick (cm)	86	121.667	99.667
LAI	LAI 1	4	3	2
	LAI 2	3	4	4
	LAI 3	1	3	6
	LAI 4	4	6	3
	LAI 5	5	4	4
	Ave LAI	3.4	4	3.8
Light	Under 1	24	16	11
	Under 2	18	25	33
	Under 3	21	22	30
	Under 4	25	15	24
	Under 5	21	24	11
	Under Ave	21.8	20.4	21.8
	Over 1	165	169	143
	Over 2	172	165	142
	Over Ave	168.5	167	142.5
	% Transmittance	0.129	0.122	0.153
	Shade/Sun	Shade	Shade	Shade
Biomass	Poison, nonwoody	39.903	74.763	135.634
	Poison, woody	148.323		216.628
	Va creeper, nonwoody		24.365	
	Va creeper, woody			
	Smilax, nonwoody	60.679	74.815	

	Grape, nonwoody		59.297	18.725
	Grape, woody	51.554	301.910	7.441
	Trumpet, nonwoody			
	Trumpet, woody			
	Black, nonwoody			
	Black, woody			
	Honeysuckle, nonwoody			
	Honeysuckle, woody			
	Hydrangea, nonwoody			
	Hydrangea, woody			
Other vine species	Honeysuckle			

Table A.h lists the observations made on each plot at Barn 3.

Table A.h. Observations at each plot at Barn 3.

	Plot	1	2	3
Site details	road	rt 268	rt 268	rt 268
	Date	21-Jul	21-Jul	21-Jul
	location	Behind Howard Pond	Behind Howard Pond	Behind Howard Pond
	nickname	A	B	C
	Orientation (degrees)	120	120	120
	Elevation (cm)	300	300	300
	Growth notes	growing both on wall and hanging from roof		
Thickness	Thick 1 (cm)	94	32	34
	Thick 2 (cm)	71	41	36
	Thick 3 (cm)	73	33	46
	Ave Thick (cm)	79.333	35.333	38.667
LAI	LAI 1	3	4	3
	LAI 2	2	4	1
	LAI 3	5	1	1
	LAI 4	4	2	2
	LAI 5	2	2	3
	Ave LAI	3.2	2.6	2
Light	Under 1	2	3	3
	Under 2	1	6	1
	Under 3	2	2	2
	Under 4	3	9	2
	Under 5	5	7	9
	Under Ave	2.6	5.4	3.4
	Over 1	37	45	26
	Over 2	39	33	46
	Over Ave	38	39	36
	% Transmittance	0.068	0.138	0.094
	Shade/Sun	Shade	Shade	Shade
Biomass	Poison, nonwoody			
	Poison, woody			
	Va creeper, nonwoody			
	Va creeper, woody			

	Smilax, nonwoody			
	Grape, nonwoody	71.255	25.970	
	Grape, woody	13.969	27.400	
	Trumpet, nonwoody	33.533	64.875	50.379
	Trumpet, woody	35.200	65.953	59.492
	Black, nonwoody			
	Black, woody			
	Honeysuckle, nonwoody			
	Honeysuckle, woody			
	Hydrangea, nonwoody			
	Hydrangea, woody			
Other vine species	Honeysuckle			
	Small red morning glory			

Table A.i lists the observations made on each plot at Barn 4.

Table A.i. Observations at each plot at Barn 4.

	Plot	1	2	3
Site details	road	rt 268	rt 268	rt 268
	Date	21-Jul	21-Jul	21-Jul
	location	Howard Fruitstand	Howard Fruitstand	Howard Fruitstand
	nickname	D	E	F
	Orientation (degrees)	271	271	271
	Elevation (cm)	120	120	120
	Growth notes	growing along side of barn from ground. Not hanging.		
Thickness	Thick 1 (cm)	28	27	33
	Thick 2 (cm)	26	24	26
	Thick 3 (cm)	26	31	35
	Ave Thick (cm)	26.66666667	27.33333333	31.33333333
LAI	LAI 1	1	1	1
	LAI 2	3	4	3
	LAI 3	2	1	1
	LAI 4	1	1	1
	LAI 5	1	0	1
	Ave LAI	1.6	1.4	1.4
Light	Under 1	619	338	56
	Under 2	234	134	60
	Under 3	366	111	150
	Under 4	1625	60	136
	Under 5	1108	209	225
	Under Ave	790.4	170.4	125.4
	Over 1	973	1249	1605
	Over 2	837	898	1658
	Over Ave	905	1073.5	1631.5
	% Transmittance	0.873370166	0.158733116	0.076861784
	Shade/Sun	Sun	Sun	Sun
Biomass	Poison, nonwoody	38.1315534	96.15552632	67.80655172
	Poison, woody		45.4	11.4
	Va creeper, nonwoody			

	Va creeper, woody Smilax, nonwoody Grape, nonwoody Grape, woody Trumpet, nonwoody Trumpet, woody Black, nonwoody Black, woody Honeysuckle, nonwoody Honeysuckle, woody Hydrangea, nonwoody Hydrangea, woody
Other vine species	Honeysuckle Small red morning glory Grape

Table A.j lists the observations made on each plot at Barn 5.

Table A.j. Observations at each plot at Barn 5.

	Plot	**1**	**2**	**3**
Site details	road	rt 778	rt 778	rt 778
	Date	21-Jul	21-Jul	21-Jul
	location	At entrance to Subdivision	At entrance to Subdivision	At entrance to Subdivision
	nickname	G	H	I
	Orientation (degrees)	210	210	210
	Elevation (cm)	323	323	323
	Growth notes	growing on side of barn		
Thickness	Thick 1 (cm)	69	32	35
	Thick 2 (cm)	51	35	43
	Thick 3 (cm)	59	33	34
	Ave Thick (cm)	59.667	33.333	37.333
LAI	LAI 1	3	1	3
	LAI 2	4	3	1
	LAI 3	4	2	5
	LAI 4	5	5	2
	LAI 5	3	2	1
	Ave LAI	3.8	2.6	2.4
Light	Under 1	62	27	29
	Under 2	29	59	35
	Under 3	46	18	9
	Under 4	21	69	8
	Under 5	45	9	26
	Under Ave	40.6	36.4	21.4
	Over 1	1608	791	411
	Over 2	1350	443	451
	Over Ave	1479	617	431
	% Transmittance	0.027	0.059	0.050
	Shade/Sun	Sun	Sun	Sun
Biomass	Poison, nonwoody			
	Poison, woody			
	Va creeper, nonwoody			

	Va creeper, woody			
	Smilax, nonwoody			
	Grape, nonwoody			
	Grape, woody			
	Trumpet, nonwoody	110.697	103.048	87.224
	Trumpet, woody	105.694	23.700	19.570
	Black, nonwoody			
	Black, woody			
	Honeysuckle, nonwoody			
	Honeysuckle, woody			
	Hydrangea, nonwoody			
	Hydrangea, woody			
Other vine species	NA			

Table A.k lists the observations made on each plot at Barn 6.

Table A.k. Observations at each plot at Barn 6.

	Plot	**1**	**2**	**3**
Site details	road	jewell rd	jewell rd	jewell rd
	Date	4-Aug	4-Aug	4-Aug
	location	Back Barn at Strawberry Stand	Back Barn at Strawberry Stand	Back Barn at Strawberry Stand
	nickname	1	2	3
	Orientation (degrees)	172	172	172
	Elevation (cm)	300	300	300
	Growth notes	hanging from roof and growing wall ?		
Thickness	Thick 1 (cm)	59	66	76
	Thick 2 (cm)	38	64	71
	Thick 3 (cm)	72	88	94
	Ave Thick (cm)	56.3333333	72.666667	80.333333
LAI	LAI 1	6	5	2
	LAI 2	2	9	4
	LAI 3	5	4	3
	LAI 4	4	6	5
	LAI 5	3	4	3
	Ave LAI	4	5.6	3.4
Light	Under 1	103	39	163
	Under 2	110	62	45
	Under 3	109	70	37
	Under 4	106	123	34
	Under 5	31	88	39
	Under Ave	91.8	76.4	63.6
	Over 1	1200	1178	1172
	Over 2	1330	825	816
	Over Ave	1265	1001.5	994
	% Transmittance	0.07256917	0.0762856	0.0639839
	Shade/Sun	Sun	Sun	Sun
Biomass	Poison, nonwoody			
	Poison, woody			
	Va creeper, nonwoody			
	Va creeper, woody			

	Smilax, nonwoody			
	Grape, nonwoody			
	Grape, woody			
	Trumpet, nonwoody	319.410901	211.94464	162.63749
	Trumpet, woody	152.377673	98.410019	193.66974
	Black, nonwoody			15.06899
	Black, woody		7.8432277	
	Honeysuckle, nonwoody			
	Honeysuckle, woody			
	Hydrangea, nonwoody			
	Hydrangea, woody			
Other vine species	Honeysuckle			

Table A.l lists the observations made on each plot at Barn 7.

Table A.l. Observations at each plot at Barn 7.

	Plot	1	2	3
Site details	road	jewell rd	jewell rd	jewell rd
	Date	4-Aug	4-Aug	4-Aug
	location	Little Barn at Strawberry Stand	Little Barn at Strawberry Stand	Little Barn at Strawberry Stand
	nickname	4	5	6
	Orientation (degrees)	86	86	86
	Elevation (cm)	220	220	220
	Growth notes	hanging from roof ?		
		wasps!, ants, lots of bugs around.		
		First time weve seen a lot of bugs		
Thickness	Thick 1 (cm)	41	62	28
	Thick 2 (cm)	45	32	26
	Thick 3 (cm)	43	44	21
	Ave Thick (cm)	43	46	25
LAI	LAI 1	4	1	2
	LAI 2	3	3	1
	LAI 3	0	2	2
	LAI 4	2	1	1
	LAI 5	2	2	0
	Ave LAI	2.2	1.8	1.2
Light	Under 1	59	48	96
	Under 2	32	43	104
	Under 3	56	46	69
	Under 4	44	83	153
	Under 5	28	18	86
	Under Ave	43.8	47.6	101.6
	Over 1	302	202	180
	Over 2	261	216	169
	Over Ave	281.5	209	174.5
	% Transmittance	0.156	0.228	0.582
	Shade/Sun	Shade	Shade	Shade
Biomass	Poison, nonwoody		0.6	
	Poison, woody			
	Va creeper, nonwoody	165.346	196.664	94.142
	Va creeper, woody		8.200	15.489

	Smilax, nonwoody Grape, nonwoody Grape, woody Trumpet, nonwoody Trumpet, woody Black, nonwoody Black, woody Honeysuckle, nonwoody Honeysuckle, woody Hydrangea, nonwoody Hydrangea, woody
Other vine species	Grape

Table A.m lists the observations made on each plot at Barn 8.

Table A.m. Observations at each plot at Barn 8.

	Plot	8a	8b	8c
Site details	road	fairhaven rd	fairhaven rd	fairhaven rd
	Date	25-Aug	25-Aug	25-Aug
	location	right/east	right/east	right/east
	nickname	1	2	3
	Orientation (degrees)	180	180	180
	Elevation (cm)	325	325	325
	Growth notes	growing on wall, got hatchet to get biomass off with		
Thickness	Thick 1 (cm)	125	134	115
	Thick 2 (cm)	140	140	127
	Thick 3 (cm)	122	138	136
	Ave Thick (cm)	129	137.3333333	126
LAI	LAI 1	5	4	6
	LAI 2	6	5	8
	LAI 3	6	4	8
	LAI 4	6	4	5
	LAI 5	3	1	4
	Ave LAI	5.2	3.6	6.2
Light	Under 1	88	26	41
	Under 2	43	85	35
	Under 3	48	123	36
	Under 4	94	26	34
	Under 5	32	53	20
	Under Ave	61	62.6	33.2
	Over 1	434	681	1705
	Over 2	446	1454	458
	Over Ave	440	1067.5	1081.5
	% Transmittance	0.139	0.059	0.031
	Shade/Sun	Sun	Sun	Sun
Biomass	Poison, nonwoody	191.7		
	Poison, woody	152.9		
	Va creeper, nonwoody			
	Va creeper, woody			
	Smilax, nonwoody			

	Grape, nonwoody			
	Grape, woody			
	Trumpet, nonwoody	506.3		
	Trumpet, woody	87.6		
	Black, nonwoody			
	Black, woody			
	Honeysuckle, nonwoody	68.8	152.4	
	Honeysuckle, woody		82.7	
	Hydrangea, nonwoody		259.0	262.1
	Hydrangea, woody		379.4	593.0
Other vine species	Va creeper			

Table A.n lists the observations made on each plot at Barn 9.

Table A.n. Observations at each plot at Barn 9.

	Plot	1	2	3
Site details	road	fairhaven rd	fairhaven rd	fairhaven rd
	Date	25-Aug	25-Aug	25-Aug
	location	left/west	left/west	left/west
	nickname	4	5	6
	Orientation (degrees)	90	90	90
	Elevation (cm)	300	300	300
	Growth notes	grape hanging pi growing on barn. Wood popping out		
Thickness	Thick 1 (cm)	116	67	40
	Thick 2 (cm)	105	97	33
	Thick 3 (cm)	122	95	39
	Ave Thick (cm)	114.333	86.333	37.333
LAI	LAI 1	2	4	2
	LAI 2	3	3	2
	LAI 3	4	6	3
	LAI 4	3	0	2
	LAI 5	4	2	3
	Ave LAI	3.2	3	2.4
Light	Under 1	20	30	27
	Under 2	20	37	28
	Under 3	22	26	17
	Under 4	22	24	9
	Under 5	22	16	46
	Under Ave	21.2	26.6	25.4
	Over 1	134	147	116
	Over 2	106	188	97
	Over Ave	120	167.5	106.5
	% Transmittance	0.177	0.159	0.238
	Shade/Sun	Shade	Shade	Shade
Biomass	Poison, nonwoody	188.9	76.2	
	Poison, woody	15.5	17.6	
	Va creeper, nonwoody			
	Va creeper, woody			
	Smilax, nonwoody			

	Grape, nonwoody		115.3	349.5
	Grape, woody	40.4	2.7	
	Trumpet, nonwoody			
	Trumpet, woody			
	Black, nonwoody			
	Black, woody			
	Honeysuckle, nonwoody			
	Honeysuckle, woody			
	Hydrangea, nonwoody			
	Hydrangea, woody			
Other vine species	Morning glory			
	Blackberry			

Table A.o lists the regression barn data.

Table A.o. Barn regression data.

Barn	LAI	Biomass g/m2	Nonwoody, g/m2	Woody, g/m2	Average Thickness, cm	Light Trans, %	Species Count
1	3.6	1185.6	823.6	543.2	83.67	24.357	3
2	3.73	1618.8	650.8	968	102.44	13.484	4
3	2.6	597.2	328	269.2	51.11	10.044	2
4	1.47	345.2	269.6	113.6	28.44	36.966	1
5	2.93	600	401.2	198.8	43.4	4.537	1
6	4.33	1548.4	945.6	603.2	69.78	7.095	2
7	1.73	640.4	609.2	47.2	38	32.186	2
8	5	3647.6	1920.4	1727.2	130.78	7.599	4
9	2.87	1074.8	973.2	152.4	79.33	19.132	2

Table A.p lists the regression cloak data.

Table A.p. Cloak regression data.

Name	LAI	Biomass, g/m2	Average Thickness, cm	Cover, %	Dead, %	Light Trans
Kudzu 1	0.83	344.4	20.8	75	40	25.313
Kudzu 2	1.67	513.6	28.8	70	70	33.526
Va Creeper 1	3.17	1048	31.5	90	2	3.384
Va Creeper 2	2.5	1685.6	30.8	95	25	6.569
Morning Glory	0.67	313.2	18	50	10	30.888
Cross Vine	1.17	162.4	14.5	55	1	26.934
Moonflower	0.83	540.4	17.5	60	10	19.121
Black Eyed	0.83	96.8	12.3	55	2	72.454
Porcelain Berry	1.33	240	16.8	65	3	48.585
Honeysuckle	3.67	714	26.3	100	1	8.212
Trumpet Vine	2.33	354	21.8	85	2	19.495

Appendix B

The following Figures Ba though Bi are from Chapter 5: Effect of Green Cloak Canopy on Water Runoff.

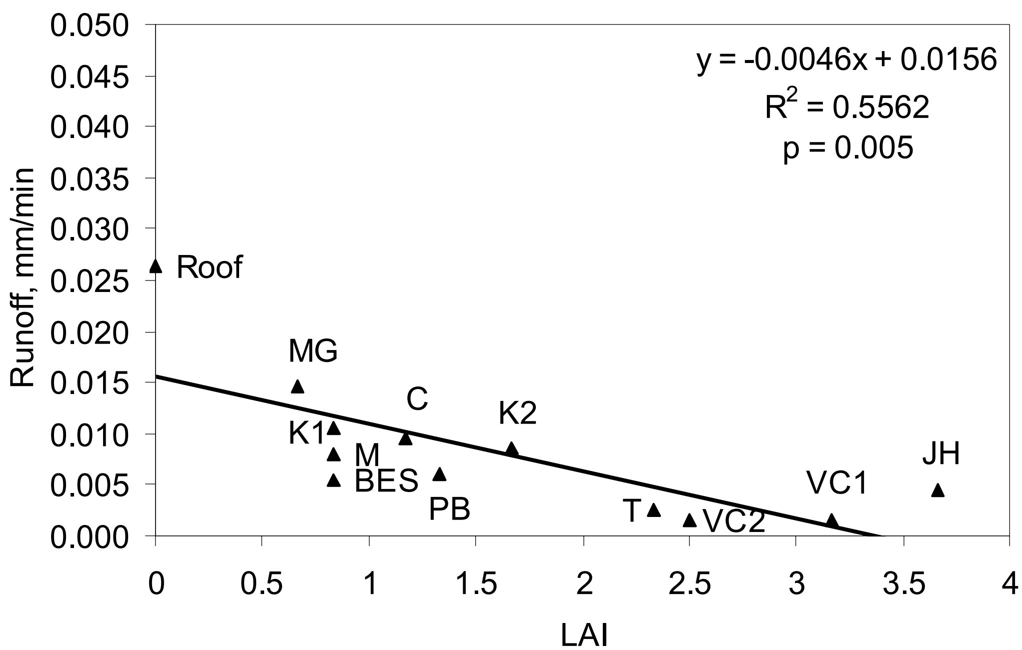

(a) Minute 6. p = 0.005

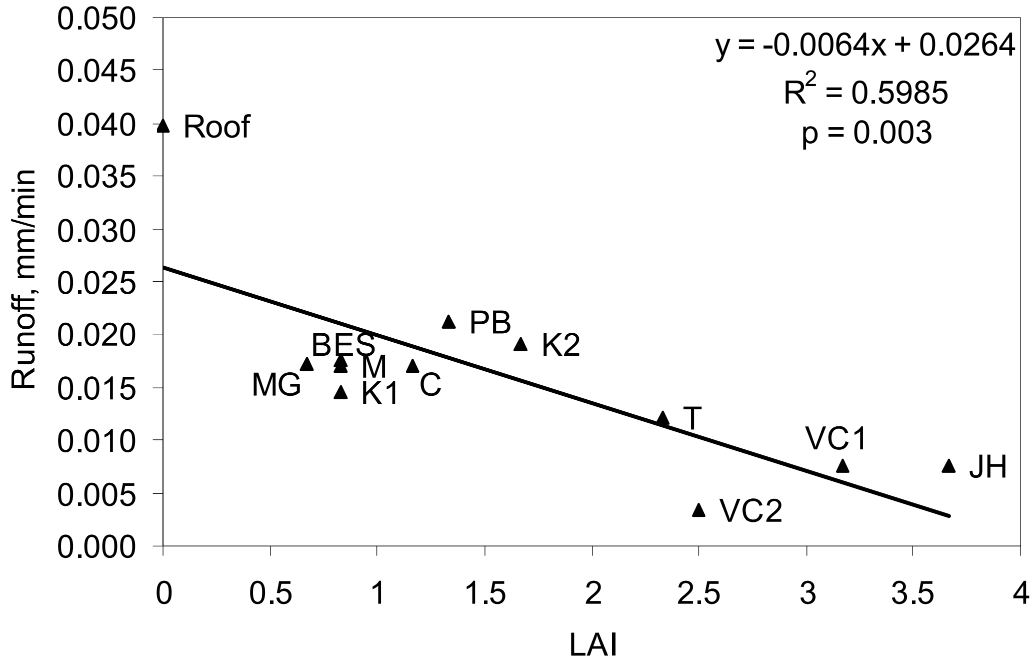

(b) Minute 8. p = 0.003

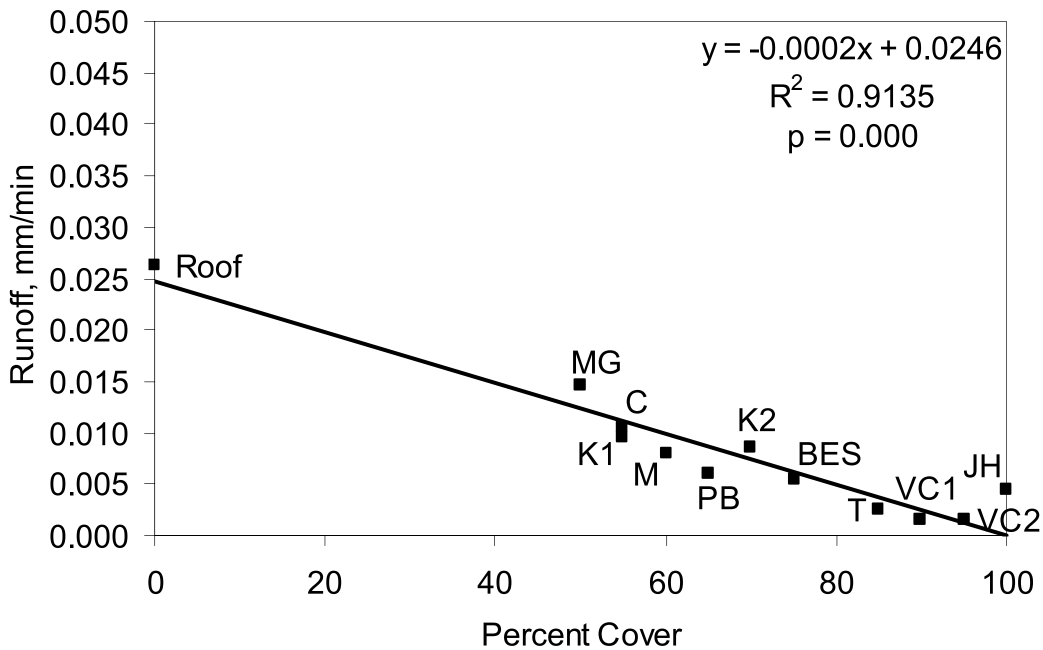

(c) Minute 6. p = 0.000

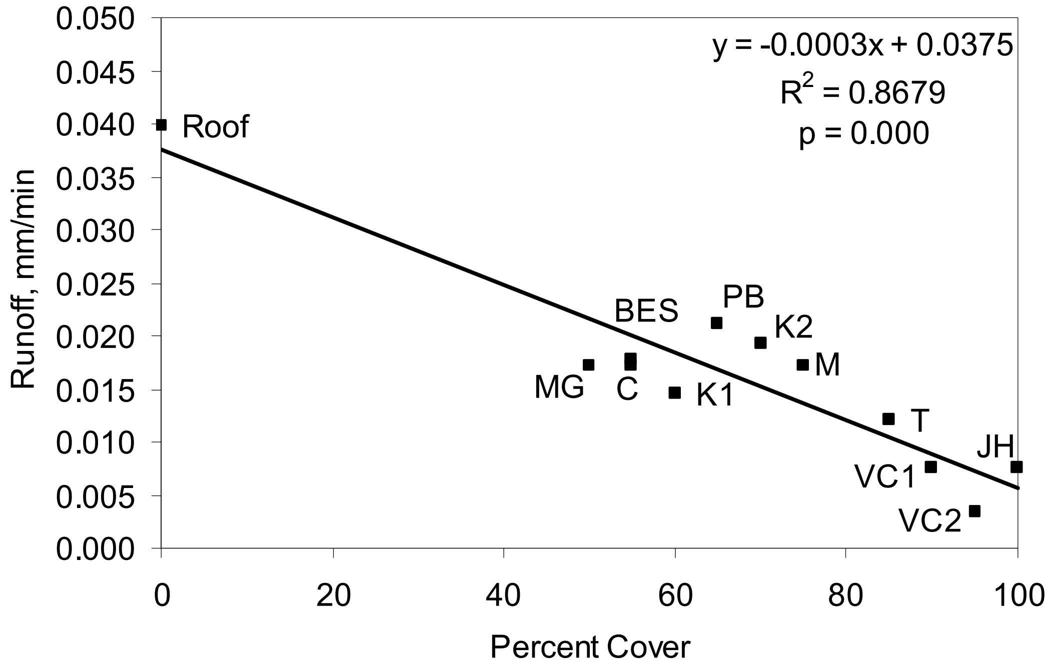

(d) Minute 8, p = 0.000

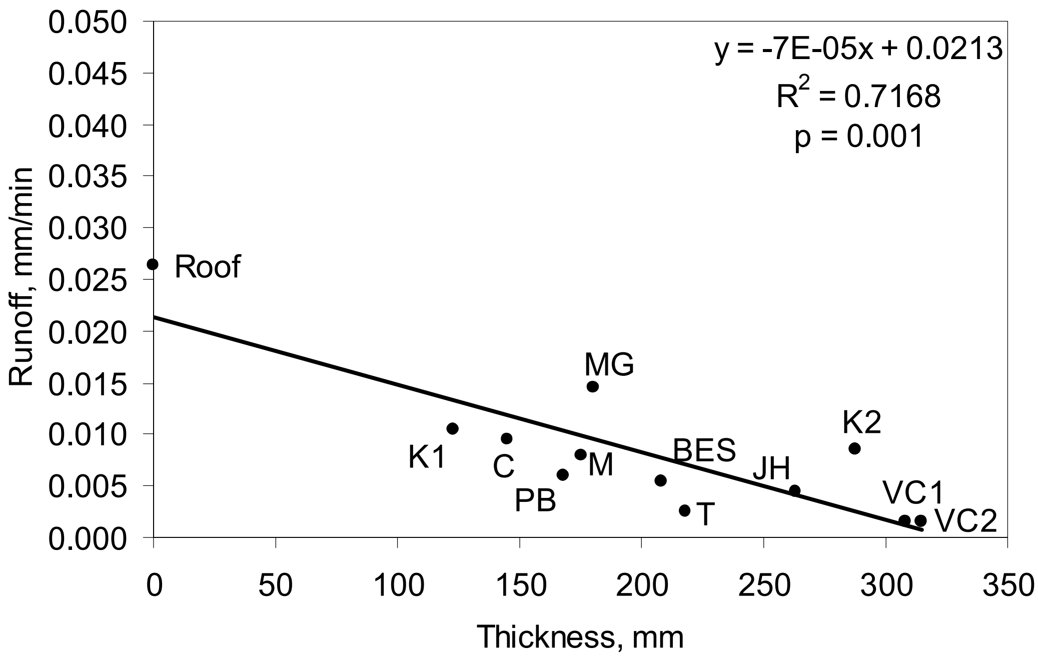

(e) Minute 6. p = 0.001

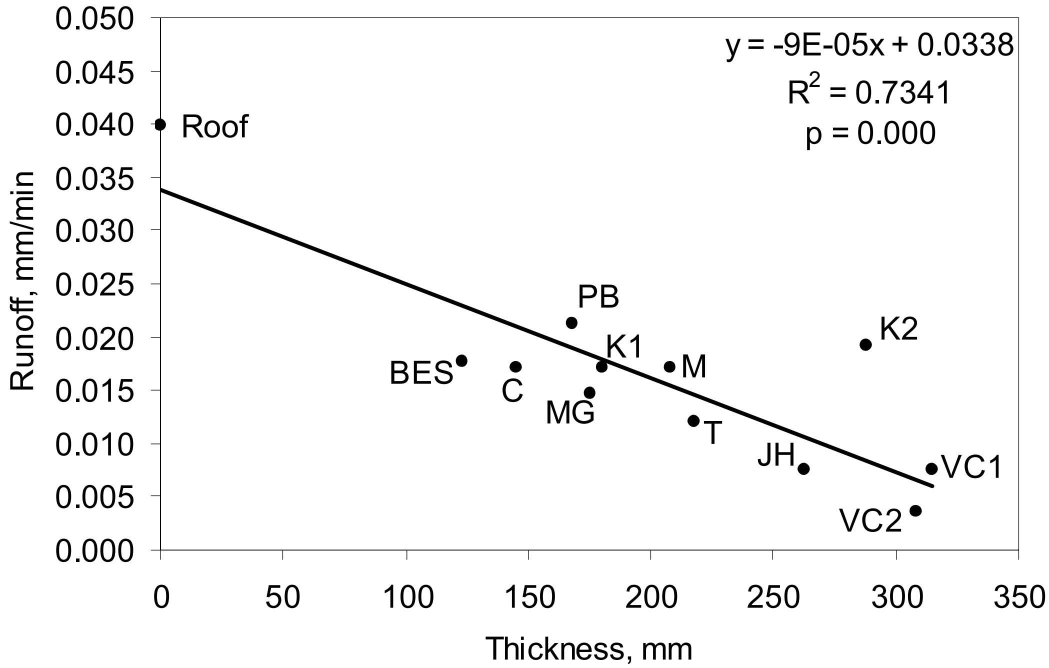

(f) Minute 8. p = 0.000

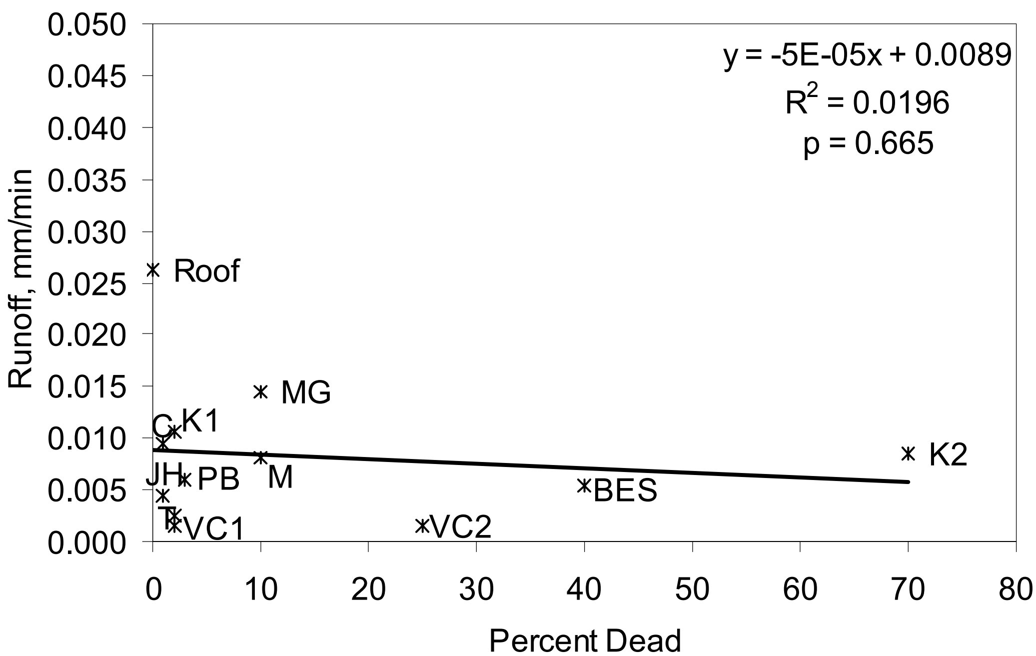

(g) Minute 6, p = 0.665

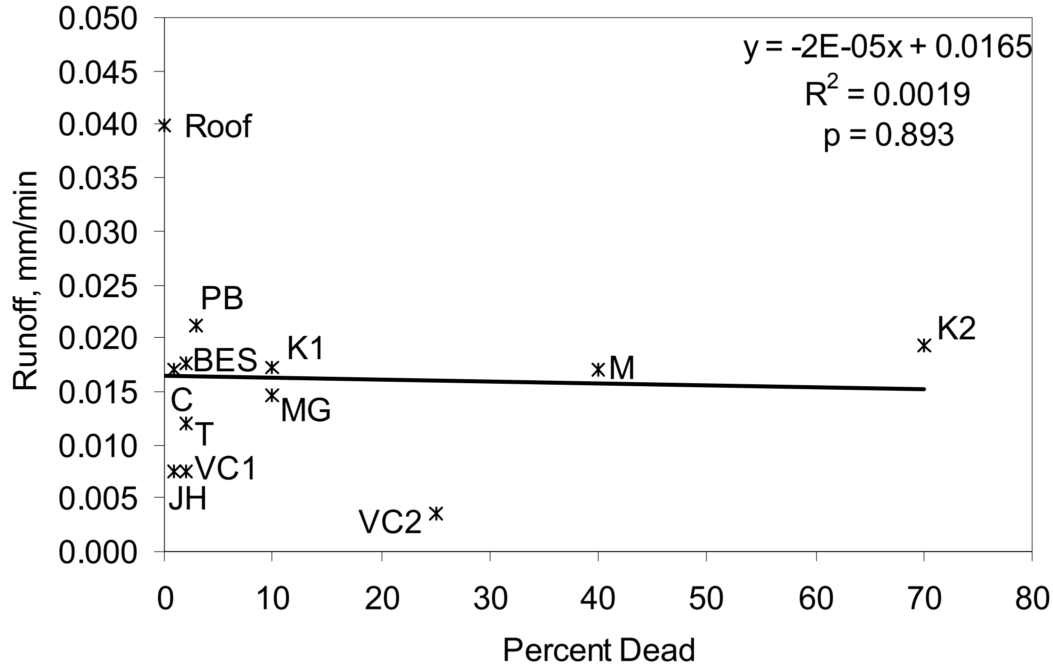

(h) Minute 8, p = 0.893

Figures Ba through Bh. Leaf area index, canopy thickness, percent cover, and percent dead runoff regression for minute 6 and 8 runoff. Data points represent each cloak: Black Eyed Susan Vine (BESV), Porcelainberry (PB), Kudzu 2 (K2), Morning Glory (MG), Cross Vine (CV), Kudzu 1 (K1), Moonflower (M), Chinese Trumpet Creeper (CTC), Japanese Honeysuckle (JH), Virginia Creeper 2 (VC2), and Virginia Creeper 1 (VC1).

Table B.i lists cloak runoff in mm for each minute.

Table B.i. Cloak runoff from rainfall simulator experiment (mm).

Time, min	VC1	VC2	K1	K2	CV	CTC
0	0.0000	0.0000	0.0000	0.0000	0.0000	0.0000
1	0.0000	0.0000	0.0000	0.0000	0.0000	0.0000
2	0.0000	0.0000	0.0000	0.0000	0.0000	0.0000
3	0.0000	0.0000	0.0000	0.0000	0.0000	0.0000
4	0.0000	0.0000	0.0099	0.0200	0.0224	0.0075
5	0.0075	0.0075	0.0175	0.0227	0.0251	0.0050
6	0.0151	0.0000	0.0075	0.0379	0.0126	0.0227
7	0.0152	0.0099	0.0506	0.0154	0.0253	0.0252
8	0.0153	0.0075	0.0204	0.0205	0.0280	0.0227
9	0.0154	0.0354	0.0360	0.0050	0.0051	0.0154
10	0.0077	0.0127	0.0310	0.0206	0.0257	0.0101
11	0.0050	0.0231	0.0555	0.0258	0.0258	0.0232
12	0.0205	0.0077	0.0234	0.0260	0.0312	0.0207
13	0.0206	0.0537	0.0211	0.0530	0.0078	0.0078
14	0.0000	0.0157	0.0320	0.0132	0.0315	0.0129
15	0.0157	0.0102	0.0164	0.0162	0.0264	0.0181
Time, min	JH	PB	BESV	MF	MG	ROOF
0	0.0000	0.0000	0.0000	0.0000	0.0000	0.0000
1	0.0000	0.0000	0.0000	0.0000	0.0000	0.0000
2	0.0000	0.0000	0.0000	0.0000	0.0125	0.0099
3	0.0075	0.0000	0.0075	0.0000	0.0251	0.0250
4	0.0075	0.0075	0.0227	0.0075	0.0176	0.0582
5	0.0076	0.0227	0.0225	0.0326	0.0177	0.0384
6	0.0076	0.0452	0.0229	0.0279	0.0127	0.0517
7	0.0076	0.0305	0.0127	0.0050	0.0127	0.0261
8	0.0433	0.0307	0.0178	0.0231	0.0256	0.0528
9	0.0000	0.0000	0.0155	0.0306	0.0180	0.0265
10	0.0050	0.0051	0.0257	0.0156	0.0258	0.0430
11	0.0177	0.0207	0.0646	0.0129	0.0156	0.0620
12	0.0000	0.0468	0.0210	0.0259	0.0209	0.0496
13	0.0206	0.0131	0.0052	0.0181	0.0183	0.0470
14	0.0101	0.0210	0.0344	0.0131	0.0079	0.0310
15	0.0078	0.0343	0.0505	0.0239	0.0343	0.0677

Literature Cited

Akbari, H., 2003. Measured energy savings from the application of reflective roofs in two small non-residential buildings. Energy 28:953-967.

Air-Conditioning and Refrigeration Institute. Cooling System Calculator. Last viewed 28 May 2007. http://www.energyexperts.org/ac_calc.

Anchor Industries. Clearspan Fabric Structures. Last viewed 1 June 2007. www.anchorindustries.com/instructions/A_Aspn.pdf.

Bengtsson, L., L. Grahn, J. Olsson, 2005. Hydrological function of a thin extensive green roof in southern Sweden. Nordic Hydrology 36(3):259-268.

Berghage, R., 2006. Designing Green Roof Growing Media. Green Roof Symposium. Brookside Gardens, Wheaton, MD. November 16, 2006.

Bryant, M., S. Bhat, J. Jacobs, 2005. Measurements and modeling of throughfall variability for five forest communities in the southeastern US. Journal of Hydrology 312:95-108.

Big Top Manufacturing. Last viewed 1 June 2007. www.bigtopshelters.com.

Bucklin, R. Tunnel Ventilation of Broiler Houses. University of Florida IFAS Extension 2003.

Clearspan Fabric Structures. Anchor Industries, Inc. Last viewed 1 June 2007. www.anchorindustries.com/instructions/A_Aspn.pdf.

Concentrating Solar Power. U.S. Department of Energy-Energy Efficiency and Renewable Energy. Last viewed 29 June 2007. http://www.eere.energy.gov/states/alternatives/csp.cfm?print.

Deguchi, A., S. Hattori, H. Park, 2005. The influence of seasonal changes in canopy structure on interception loss: Application of the revised Gash model. Journal of Hydrology xx:1-23.

Delmarva Poultry Industry, Inc. Facts About Maryland's Broiler Chicken Industry. May 2005. www.dpichicken.com.

Desjarlais, A., 2007. R-Value Recommendations for New Buildings. Building Envelope Research. Oak Ridge National Laboratory. Last viewed 7 August 2007. http://www.ornl.gov/cgi-bin/cgiwrap?user=roofs&script=ZipTable/ins_fact.pl.

Donald, J. Need for Insulation in Warm-Climate Poultry Housing. Poultry Ventilation Pointers Series 1999.

Dunnett, N., N. Kingsbury, 2004. Planting Green Roofs and Living Walls. Timber Press, Portland, Oregon.

Eco Tecture. Last viewed 3 May 2007. http://www.ecotectureblog.com/?p=55.

EPA. Safe Drinking Water Act. Last viewed 19 June 2007. www.epa.gov/safewater/sdwa/30th/factsheets/costs_funding.html.

Fairchild, B. Basic Introduction to Broiler Housing Environmental Control. Cooperative Extension Service/The University of Georgia College of Agricultural and Environmental Sciences Bulletin 2005;1264.

Feenstra, G. What is Sustainable Agriculture? University of California Sustainable Agriculture Research & Education Program. December 1997. www.sarep.ucdavis.edu.

Ferguson, B. K., 1998. Introduction to Stormwater: Concept, Purpose, Design. John Wiley & Sons, Inc. New York, NY.

Ferrante, A., G. Mihalakakou, 2001. The influence of water, green and selected passive techniques on the rehabilitation of historical industrial buildings in urban areas. Solar Energy 70(3):245-253.

Furbish Company. Last viewed 3 May 2007a. http://www.furbishco.com.

Furbish, M. Furbish Company. Email from Michael Furbish. Received on 9 June 2007b.

Green Roofs Infrastructure Monitor, 2001. 3(2).

Greenscreen. Last viewed 10 August 2007. http://www.greenscreen.com.

Hanson, P., 2006. Walker Branch Throughfall Displacement Experiment (TDE) hourly weather data. Oak Ridge National Laboratory, Oak Ridge, TN. http://tde.ornl.gov/hourly.html.

Home Depot. Ocean City, MD. June 2007.

Huff, D.D., W.T. Swank, C.A. Troendle, G.S. Henderson, J.B. Waide, and T. Hanes, 1978. Elemental cycles and water budget analyses applied to forest management in the Eastern United States. Proceedings of the Society of American Foresters. Available at: http://cwt33.ecology.uga.edu/publications/819.pdf.

Hutchinson, D., P. Abrams, R. Retzlaff, T. Liptan, 2003. Stormwater monitoring of two ecoroofs in Portland, Oregon, USA. Greening Rooftops for Sustainable Communities, Proceedings of the First North American Green Roofs Conference, Chicago, IL, May 2003. http://www.greenroofs.org/index.php?option=com_content&task=view&id=32&Itemid=46.

Incropera, F., D. De Witt, 1990. Fundamentals of Heat and Mass Transfer. John Wiley & Sons, Inc. New York, NY.

Investment Grade Roofing. 2006 Energy Tax Credits for Metal Roofing Purchasing. Last viewed 4 July 2007. http://www.metalroofing.com/v2/content/news/energy-tax-incentive.cfm.

Johnson, A., 1999. Biological Process Engineering. John Wiley & Sons, Inc. New York, NY.

Kangas, P., 2004. Ecological Engineering. CRC Press LLC. Boca Raton, FL.

Kim, Y., J. Baik, 2005. Spatial and temporal structure of the urban heat island in Seoul. Journal of Applied Meteorology 44:591-604.

Klassen W., F. Bosveld, E. de Water, 1998. Water storage and evaporation as constituents of rainfall interception. Journal of Hydrology 212/213:36-50.

Kolb, W., T. Schwarz, 1986. Zum Klimatisierungseffekt von Pflanzenbeständen auf Dächern, Teil I. Zeitschrift fur Vegetationstechnik 9. Republished in Veitshoechheimer Berichte, Heft 39, Dachbegrünung.

Kumar, R. S.C. Kaushik, 2005. Performance evaluation of green roof and shading for thermal protection of buildings. Building and Environment 40:1505-1511.

Lankreijer, H., A. Lundberg, A. Grelle, A. Lindroth, J. Seibert., 1999. Evaporation and storage of intercepted rain analyzed by comparing two models applied to a boreal forest. Agricultural and Forest Meteorology 98/99:595-604.

Link, T., M. Unsworth, D. Marks. 2004. The dynamics of rainfall interception by a seasonal temperature rainforest. Agricultural and Forest Meteorology 12:171-191.

Liu, K., B. Baskaran., 2003. Thermal performance of green roofs through field evaluation. Greening Rooftops for Sustainable Communities, Proceedings of the First North American Green Roofs Conference, Chicago, IL, May 2003. http://www.greenroofs.org/index.php?option=com_content&task=view&id=32&Itemid=46.

Local Climatological Data Unedited, 2006. NOAA Satellite and Information Service. National Climate Data Center. U.S. Department of Commerce. http://cdo.ncdc.noaa.gov/ulcd/ULCD.

Loustau, D., P. Berbigier, A. Granier, 1992. Interception loss, throughfall and stemflow in a maritime pine stand. II. An application of Gash's analytical model of interception. Journal of Hydrology 138:469-485.

Low-Impact Development Design Strategies, 1999. Programs and Planning Division, Department of Environmental Resources, Prince George's County, Maryland.

Marin, C., W. Bouten, J. Sevink, 2000. Gross rainfall and its partitioning into throughfall, stemflow and evaporation of intercepted water in four forest ecosystems in western Amazonia. Journal of Hydrology 237:40-57.

McQuiston, F., J. Parker, 1982. Heating, Ventilation, and Air Conditioning. John Wiley & Sons, New York, New York.

Mentens, J., D. Raes, M. Hermy, 2006. Green roofs as a tool for solving the rainwater runoff problem in the urbanized 21st century? Landscape and Urban Planning 77:217-226.

Mentens, J., D. Raes, M. Hermy, 2003. Effect of orientation on the water balance of green roofs. Greening Rooftops for Sustainable Communities, Proceedings of the First North American Green Roofs Conference, Chicago, IL, May 2003. http://www.greenroofs.org/index.php?option=com_content&task=view&id=32&Itemid=46.

Moran, A., B. Hunt, J. Smith, 2005. Hydrologic and water quality performance from greenroofs in Goldsboro and Raleigh, North Carolina. Green Roofs for Healthy Cities 2005 Conference Proceedings CD, Washington, DC, May 2005. http://www.greenroofs.org/index.php?option=com_content&task=view&id=32&Itemid=46.

Nebraska Public Power District. Air Conditioning Cost Calculator. Last viewed 28 May 2007. http://www.nppd.com/My_Home/Services/Additional_Files/airconditioning_calculator.asp.

NPDES Storm Water Sampling Document. United States Environmental Protection Agency. Office of Water. July 1992. Last viewed on 1 July 2007. http://www.epa.gov/npdes/pubs/owm0093.pdf.

Optigrün, 2002. Catalogue. Optigrün. Krauchenwies-Goggingen, Germany.

Owens, M., 1999. Impervious Surfaces. Critical Area Act and Criteria. Critical Area Commission for the Chesapeake and Atlantic Coastal Bays, Annapolis, MD.

Peck, S., 2003. Private benefits, public benefits. Available via http://www.peck.ca/grhcc.

Peck, S. P., C. Callaghan, M. E. Kuhn, B. Bass, 1999. Greenbacks from Greenroofs: Forging a New Industry in Canada. Canada Mortgage and Housing Corporation. Toronto, CA.

Peck, S. and M. Kuhn, 2000. Design Guidelines for Green Roofs. Environment Canada. Toronto, CA.

Pepco. 85 Ways to Save Energy Brochure. April 2005.

Rao, A., 1987. Interception losses of rainfall from Cashew trees. Journal of Hydrology 90(3-4):293-301.

Rowe, D., 2007. Michigan State University. The Green Roof Program at MSU. Last viewed 2 August 2007. http://www.hrt.msu.edu/faculty/Rowe/Green_roof.htm.

Rowe, D., R. Clayton, N. Van Woert, M. Monterusso, D. Russell, 2003. Green roof slope, substrate depth and vegetation influence runoff. Greening Rooftops for Sustainable Communities, Proceedings of the First North American Green Roofs Conference, Chicago, IL, May 2003. http://www.greenroofs.org/index.php?option=com_content&task=view&id=32&Itemid=46.

Rutter, A., A. Morten, P. Robbins, 1975. A predictive model of rainfall interception in forests. II. Generalization of the model and comparison with observations in some coniferous and hardwood stands. Journal of Applied Ecology 12:367-380.

Schellekens, J., F. Scatena, L. Bruijnzeel, A. Wickel, 1999. Modeling rainfall interception in a lowland tropical rainforest in northeastern Puerto Rico. Journal of Hydrology 225:168-184.

Scholz-Barth, K., 2001. Green Roofs: Stormwater Management from the Top Down. Environmental Design and Construction Magazine 15 January 2001. Last viewed 12 December 2005. http://www.edcmag.com/CDA/ArticleInformation/features/BNP_features_item/0,4120,18769,00.html.

Schwab, G., D. Fangmeier, W. Elliot, R. Frevert, 1992. Soil and Water Conservation Engineering. John Wiley & Sons, Inc. New York, NY.

Seedland. Last visited 8 June 2007. http://www.seedland.com.

Thomas, T., 1998. Domestic water supply using rainwater harvesting. Building Research and Information 26(2):94-101.

Theodosiou, G., 2003. Summer period analysis of the performance of a planted roof as a passive cooling technique. Energy and Buildings 35:909-917.

Ulrich, R., 1999. Effects of gardens on health outcomes: Theory and research. Chapter in C. C. Marcus and M. Barnes (Eds.), *Healing Gardens: Therapeutic Benefits and Design Recommendations.* New York: John Wiley, 27-86.

Van Hoy, S., 2005. Tyson to Help Farmers with Energy Costs. The Morning News. Stephens Media Publication. Last viewed 17 December 2005. http://www.nwaonline.com.

Wikipedia. R-value (insulation). Last viewed 7 August 2007. http://en.wikipedia.org/wiki/R-value_%28insulation%29.

Winchell, W., 1994. Broiler Housing. Canada Plan Service Leaflet M-5310. Last viewed 16 December 2005. http://www.cps.gov.on.ca/English/plans/E5000/5310/M-5310L.pdf.

Wong, N., Y. Chen, C. Ong, A. Sia, 2002. Investigation of thermal benefits of rooftop garden in the tropical environment. Building and Environment 38:261-270.

Wong, N., S. Tay, R. Wong, C. Ong, A. Sia, 2003. Life cycle cost analysis of rooftop gardens in Singapore. Building and Environment 38:499-509.

Zach, S. Nebraska Public Power District. Email from Steven Zach. Received on 18 June 2007.